Ghent University

Faculty of Science

Department of Plant Biotechnology and Bioinformatics

VIB, Plant Systems Biology

# Identification of molecular components affecting root architecture

**Ianto Roberts**

Promoter: **Prof. Dr. Tom Beeckman**

Co-promoter: **Prof. Dr. Ive De Smet**

Thesis submitted as partial fulfillment of the requirements for obtaining the degree of Doctor of Philosophy (Ph.D.) in Science: Biochemistry and Biotechnology

Academic year: 2015-2016

# Examination commission

## Promoters:

Prof. Dr. Tom Beeckman

Department of Plant Biotechnology and Bioinformatics, Faculty of Science, Ghent University
Department of Plant Systems Biology, VIB

Prof. Dr. Ive De Smet

Department of Plant Biotechnology and Bioinformatics, Faculty of Science, Ghent University
Department of Plant Systems Biology, VIB

## Chair:

Prof. Dr. Frank Van Breusegem

Department of Plant Biotechnology and Bioinformatics, Faculty of Science, Ghent University
Department of Plant Systems Biology, VIB

## Secretary:

Prof. Dr. Sofie Goormachtig

Department of Plant Biotechnology and Bioinformatics, Faculty of Science, Ghent University
Department of Plant Systems Biology, VIB

## Members of the commission:

Prof. Dr. Bruno Cammue

Department of Plant Fungi Interactions, Faculty of Bioscience Engineering, University of Leuven
Department of Plant Biotechnology and Bioinformatics, Faculty of Science, Ghent University
Department of Plant Systems Biology, VIB

Prof. Dr. Danny Geelen

Department of Plant Production, Faculty of Bioscience Engineering, Ghent University

Prof. Dr. Reidunn Aalen

Department of Biosciences, Genetics and Evolutionary Biology, University of Oslo

Dr. Bert De Rybel

Department of Plant Biotechnology and Bioinformatics, Faculty of Science, Ghent University
Department of Plant Systems Biology, VIB

## SUMMARY

The growing world population, global climate changes and shrinking arable land demand for an increase in the yield of crops to cope with these challenges. Engineering the root system of plants might allow obtaining a more efficient uptake of water and growth-limiting nutrients from the soil, and thereby increase yield. The efficiency of the root system depends on its three-dimensional structure, which is termed root system architecture (RSA) and is mainly determined by root length, root branching and the growth angle of lateral roots. Therefore, knowledge about the regulation of the lateral root development process will be crucial for engineering a better root system. The highly coordinated cell divisions and cell specification events during lateral root development are tightly regulated by cell-to-cell communication, to a large degree mediated by signaling peptide ligand – receptor-kinase pairs. In the 'Root Development Group' from Prof. Dr. Tom Beeckman, the CEP5 signaling peptide was identified in a transcriptomics study as a potential regulator of lateral root development in the model plant *Arabidopsis thaliana*.

The CEP5 signaling peptide is a member of the C-TERMINALLY ENCODED PEPTIDE (CEP) family, which belongs to the class of small secreted post-translationally modified signaling peptides that are derived from a non-functional precursor prepropetide. The CEP prepropeptides contain an N-terminal secretory signal peptide with a predicted conserved arginine residue as cleavage site, and contain one to five C-terminally conserved sequence regions of 15 amino acid residues, termed CEP domains. The active mature CEP peptides are derived from conserved CEP domains after proteolytic processing. The proline residues of these mature CEP peptides can undergo a post-translational modification to form hydroxyproline (HyP) residues, and potentially be further modified with (tri)arabinosylation on the HyP residue. The CEP peptides are perceived by the leucine-rich repeat receptor-like kinase (LRR-RLK) proteins CEP RECEPTOR 1/XYLEM INTERMIXED WITH PHLOEM 1 (CEPR1/XIP1) and CEP RECEPTOR 2 (CEPR2).

In this thesis, the CEP peptide family was functionally characterized in more detail. An evolutionary phylogenetic study revealed that CEP peptides originated from the seed plant lineage onwards, correlating with the emergence of novel plant structures, such as seed development, nodule formation and lateral root formation from the pericycle. By performing an *in silico* analysis on the *Arabidopsis* genome, we identified an additional ten members in addition to the previously identified five members, bringing the total to 15 members. Based on the sequence of the mature CEP peptides, the CEP family was divided into two groups: group I (CEP1 to CEP12) and group II (CEP13 to CEP15), in which group I members typically contain three prolines (at position 3, 7 and 11), whereas group II members only have two prolines (at position 9 and 11).

Through a gain-of-function analysis using overexpression lines for all 15 *CEP* genes, clear differences in the effect on plant growth were found between group I and group II members. And notably, group I CEP peptides could be further subdivided into three functional subgroups based on a correlation between gain-of-function phenotypes and the amino acid at position 3 in the mature CEP peptides. Subgroup Ia CEP peptides, encoded by *CEP2*, *CEP9* and *CEP10*, generally contain a hydrophobic alanine residue at position 3, and their overexpression has no drastic impact on root and shoot growth. Subgroup Ib CEP peptides, encoded by *CEP1*, *CEP3*, *CEP4*, *CEP5*, *CEP7*, *CEP8*, *CEP11* and *CEP12*, all contain a positively charged hydrophilic arginine residue at position 3, and their overexpression leads to a drastic reduction in root and shoot growth. Subgroup Ic only consists of the

CEP6a and CEP6b peptides, which contain a hydrophobic glycine and a negatively charged hydrophilic glutamic acid residue at position 3 respectively, and their overexpression leads to intermediate reduced root and shoot growth. This suggested that the amino acid at position 3 might possibly be an important contributor to different activity in the CEP I subgroups. On the other hand, group II CEP peptides, encoded by *CEP13*, *CEP14* and *CEP15*, contain multiple differences in conserved amino acid residues at the N-terminal part compared to group I CEP peptides, and their overexpression leads to an increase in the size of the root system, opposite to most group I members. This suggests that group II CEP peptides form a separate functional class compared to group I CEP peptides, and group I CEP peptides can be subdivided into three functional subgroups.

Expression analysis of all 15 *CEP* genes showed that some members have very specific expression patterns, but in most cases there were large overlaps in expression of *CEP* genes from each (sub)group, mainly in the flower organs, in the shoot apical meristem region, in the leaf- and root vasculature, in the pericycle and during lateral root development. Interestingly, only *CEP14* showed expression in the primary- and lateral root apical stem cell niche. Expression analysis of *CEPR1*/*XIP1* and *CEPR2* revealed that the receptors are expressed in tissues overlapping with *CEP* expression; however, the two receptors themselves are never expressed in the same tissues. *CEPR1*/*XIP1* is expressed in the flower receptacle and petal veins, in the leaf venation, in the basal meristem in the phloem pole-associated pericycle cells, and in the phloem companion cells in the differentiation zone of the root. In contrast, *CEPR2* is expressed in the pistil and stamen of the flowers, in the shoot apical meristem, in the leaves, in the metaxylem, in the (xylem pole-associated) pericycle cells, and in the primary- and lateral root tips in the apical stem cell niche and columella. Considering the non-overlapping expression patterns of the proposed CEP receptors, they probably regulate different developmental processes and are likely not functionally redundant. In agreement with this, loss-of-function mutants for *CEPR1*/*XIP1* and *CEPR2* revealed opposite phenotypes, with the *xip1-1* mutant showing a drastic reduction in primary root length and number of lateral roots, while the *cepr2-4* mutant showed a slight increase in the primary root length and number of lateral roots. While gain-of-function analysis showed that overexpression of *CEP* Ib genes drastically reduces the size of the root system through a gradual consumption of the root apical meristem, higher-order loss-of-function mutants of the *CEP* Ib genes showed an increase in the size of the root system, suggesting that these peptides might function as root growth control regulators.

The CEP5 peptide, belonging to subgroup Ib, was shown to be expressed during the entire lateral root developmental process, from lateral root priming in the basal meristem to lateral root emergence. However, CEP5 is not expressed in the xylem pole-associated pericycle cells, from which lateral root are formed, but instead is expressed specifically in the phloem pole-associated pericycle cells that are associated with the sites of lateral root formation. Synthetic CEP5 peptide treatments, *CEP5* overexpression and *CEP5* RNAi knock-down analysis, suggested that CEP5 negatively regulates lateral root initiation. Expression of *CEPR1*/*XIP1* was shown to overlap with *CEP5* expression, and was proposed to function as its receptor. The *xip1-1* mutant showed a reduction in lateral root initiation, similar to *CEP5* overexpression or CEP5 synthetic peptide treatments. This suggests that CEP5 might negatively regulate CEPR1/XIP1 activity. Further analysis on the mode-of-action of CEP5 activity revealed that it might influence the auxin response by stabilization of the AUXIN/INDOLE-3-ACETIC ACID INDUCIBLE (Aux/IAA) proteins, which repress the AUXIN RESPONSE FACTOR (ARF) transcriptional activators, and thereby influence lateral root development.

In parallel with the characterization of CEP peptides as regulators of root growth, an EMS-mutagenesis screen revealed three other molecular components regulating root system architecture. A loss-of-function mutant in the *CELLULOSE SYNTHASE 6* (*CESA6*) gene was shown to generate a shallow dense root system, with a shorter primary root and an increased density of horizontally growing lateral roots. Such a shallow dense root system is potentially better suited for phosphate uptake in the top-soil layer. A loss-of-function mutant in the *CULLIN-ASSOCIATED AND NEDDYLATION-DISSOCIATED 1* (*CAND1*) gene leads to a narrow dense root system, with lateral roots growing under a very steep angle along the primary root. This root system is potentially better suited for tapping deeper regions of the soil, which might be better for water and nitrate uptake. And a new gain-of-function mutant allele for the *IAA12*/*BODENLOS* (*BDL*) gene was identified, which was found to be severely disturbed in lateral root spacing and formed clusters of lateral roots. This might potentially be used to engineer plants with induced lateral root clusters in regions of high nutrient content for increased uptake. The root system architecture phenotypes of these mutants observed on *in vitro* 1/2 MS Petri plates were shown to be retained in more natural conditions in the soil, using mini-rhizotrons. Rhizotrons will take on an important role in future studies on root development, bringing our research one step closer to engineering crops with an improved root system in soil, and higher yield.

## SAMENVATTING

Met de steeds toenemende wereldbevolking, de globale klimaatsveranderingen en de slinkende landbouw oppervlakte, is er nood aan een toename van opbrengst van landbouwgewassen om tegemoet te komen aan deze uitdagingen. Het modificeren van het wortelstelsel van de planten zou kunnen zorgen voor een betere opname van water en nutriënten uit de grond, en hierdoor de opbrengst verhogen. De efficiëntie van het wortelstelsel wordt bepaald door z'n driedimensionale structuur, en wordt de wortel architectuur genoemd. Deze wordt bepaald door de lengte van de wortels, de vertakkingscapaciteit van zijwortels en de hoek waaronder de zijwortels groeien langs de hoofdwortel. Kennis over de regulatie van het zijwortel ontwikkelingsproces is dus cruciaal voor het bekomen van een efficiënter wortelstelsel. Zijwortelontwikkeling gaat gepaard met strikt gecoördineerde celdelingen en celspecificatie die gereguleerd worden via cel-cel communicatie, bijvoorbeeld door peptide ligand – receptor kinase signalisatie. In de 'Root Development Group' van Prof. Dr. Tom Beeckman werd het CEP5 peptide geïdentificeerd in een transcriptoom analyse als een mogelijke regulator van zijwortelontwikkeling in de modelplant *Arabidopsis thaliana* (de zandraket).

Het CEP5 peptide behoort tot de C-TERMINALLY ENCODED PEPTIDE (CEP) peptide familie van de klasse van kleine gesecreteerde post-translationeel gemodificeerde signaliserende peptiden die afkomstig zijn van niet-functionele prepropeptiden. Deze CEP prepropeptiden bevatten een N-terminaal secretie signaal peptide die ertoe leidt dat de peptiden gesecreteerd worden, en bevatten aan de C-terminale kant één tot vijf sterk geconserveerde regio's van 15 aminozuren lang, welke de CEP domeinen genoemd worden. De functionele signaliserende CEP peptiden zijn afkomstig van deze geconserveerde CEP domeinen na uitgeknipt te worden door proteases. De prolines in deze mature CEP peptiden kunnen verder gemodificeerd worden tot hydroxyprolines, en mogelijks nog verder gemodificeerd worden met (tri-)arabinosyl-ketens aan deze hydroxyprolines. De CEP peptiden treden op als liganden voor de 'leucine-rich repeat receptor-like kinase (LRR-RLK)' receptoren CEP RECEPTOR 1/XYLEM INTERMIXED WITH PHLOEM 1 (CEPR1/XIP1) en CEP RECEPTOR 2 (CEPR2).

In deze thesis werden de CEP peptiden en hun receptoren verder functioneel gekarakteriseerd. Uit een phylogenetische evolutie analyse bleek dat de oorsprong van CEP peptiden samenvalt met het ontstaan van de tak van zaadplanten in het plantenrijk, en dus gepaard ging met de ontwikkeling van nieuwe plantenorganen, zoals zaadontwikkeling, nodule vorming en zijwortelvorming uit de pericyclus. Een *in silico* analyse van het *Arabidopsis* genoom leidde tot het identificeren van tien nieuwe *CEP* genen bovenop de vijf eerder geïdentificeerde leden, waardoor het totaal aantal 15 *CEP* genen bedraagt. Gebaseerd op de sequentie van de mature CEP peptiden werd de CEP family opgesplitst in twee groepen: groep I (CEP1 tot CEP12) en groep II (CEP13 tot CEP15), waarbij leden van group I gekenmerkt werden door drie geconserveerde prolines (op positie 3, 7 en 11) en group II leden door twee geconserveerde prolines (op positie 9 en 11).

Uit een 'gain-of-function' analyse met overexpressie lijnen voor alle 15 *CEP* genen werd een duidelijk verschil gezien tussen groep I en groep II leden op basis van het effect op plantengroei. Daarnaast werd groep I verder opgesplitst in drie functionele subgroepen, gebaseerd op een correlatie tussen het fenotype en het aminozuur op positie 3 in het mature CEP peptide. Subgroep Ia CEP peptiden, gecodeerd door de *CEP2*, *CEP9* en *CEP10* genen, bevatten een hydrofobe alanine op positie 3, en overexpressie heeft geen drastische impact op de wortel of het bovengronds gedeelte van de plant. Daartegenover bevatten subgroep Ib CEP peptiden, gecodeerd door *CEP1*, *CEP3*, *CEP4*, *CEP5*, *CEP7*,

*CEP8*, *CEP11* en *CEP12* genen, steeds een positief geladen hydrofiel arginine op positie 3, en zorgt overexpressie voor een drastische reductie in de groei van het wortelstelsel en het bovengronds gedeelte van de plant. Verder bestaat subgroep Ic enkel uit de peptiden CEP6a en CEP6b, beide gecodeerd door het *CEP6* gen, en bevatten respectievelijk een hydrofobe glycine en negatief geladen hydrofiel glutaminezuur op positie 3, waarbij overexpressie leidt tot een intermediaire reductie in wortel en scheut groei. Dit suggereerde dat het aminozuur op positie 3 mogelijks een belangrijke rol speelt voor de verschillende activiteit van de CEP I subgroepen. In contrast, groep II CEP peptiden, gecodeerd door de *CEP13*, *CEP14* en *CEP15* genen, bevatten meerdere verschillen in geconserveerde aminozuren in het N-terminale gedeelte van het CEP peptide ten opzichte van groep I leden, en hun overexpressie zorgde voor een toename in grootte van het wortelstelsel, het tegenovergestelde van het fenotype bij de meeste leden van groep I. Samengevat kunnen groep II CEP peptiden gezien worden als een afzonderlijke functionale klasse ten opzichte van groep I CEP peptiden, en kan groep I verder opgesplitst worden in drie functionele subgroepen.

Expressie analyse van alle 15 *CEP* genen toonde aan dat sommige een zeer specifiek expressie patroon vertoonden, maar dat in de meeste gevallen er een sterke overlap in expressie was voor leden van elke (sub)groep, en voornamelijk voorkwam in de bloemorganen, de regio van het apicale scheutmeristeem, in het vasculair weefsel van bladeren en wortels, in de pericyclus en tijdens zijwortelontwikkeling. Opmerkelijk was dat enkel *CEP14* tot expressie kwam in de apicale stamcel regio van de hoofdwortel en van de zijwortels. Expressie analyse van de receptoren *CEPR1*/*XIP1* en *CEPR2* toonde aan de deze tot expressie komen in weefsels overlappend met *CEP* expressie, maar dat de receptoren onderling zelf nooit tot expressie komen in hetzelfde weefsel. *CEPR1*/*XIP1* komt tot expressie in de vruchtbodem en kroonblad nervatuur van de bloemen, in de nervatuur van de bladeren, in het basale meristeem in de floëem pool-geassocieerde pericyclus cellen, in de floëem zustercellen hogerop in het vasculair weefsel van de wortel, en aan de basis van ontwikkelende zijwortels. Daartegenover komt *CEPR2* tot expressie in de stamper en meeldraden van de bloemen, in het scheut apicaal meristeem, in de bladeren, in de meta-xyleem cellen in het vasculair weefsel van de wortel, in de (xyleem pool-geassocieerde) pericyclus cellen, en in de apicale stamcel regio van de hoofdwortel en zijwortels. Gezien de niet-overlappende expressie patronen worden waarschijnlijk afzonderlijke ontwikkelingsprocessen gereguleerd door deze receptoren, waardoor ze niet functioneel redundant zijn aan elkaar. Overeenstemmend hiermee hadden 'loss-of-function' mutanten van de receptoren verschillende fenotypes: een kortere hoofdwortel en minder zijwortels in de *xip1-1* mutant, en geen opmerkelijk verschil in wortelarchitectuur voor de *cepr2* mutanten. Verder toonden hogere orde 'loss-of-function' mutanten van *CEP* Ib genen een toename in de grootte van het wortelstelsel, een fenotype tegenovergesteld aan de sterke reductie van wortelgroei in de overeenstemmende 'gain-of-function' overexpressie lijnen. Dit suggereert dat CEP peptiden mogelijk dienst doen als regulatoren die de mate van wortelgroei controleren.

De rol van het CEP5 peptide, dat opgepikt werd in een transcriptoom analyse van zijwortelinitiatie, werd verder in detail bestudeerd in functie van zijn mogelijke rol in zijwortelontwikkeling. Expressie analyse toonde aan dat *CEP5*, behorende tot subgroep Ib, tot expressie komt gedurende het hele zijwortelontwikkelingsproces, van zijwortelpriming in het basale meristeem tot de uitgroei van de zijwortel. Maar, *CEP5* komt niet tot expressie in de xyleem pool-geassocieerde pericyclus cellen waaruit de zijwortel gevormd wordt, maar specifiek in de floëem pool-geassocieerde pericyclus cellen grenzend aan het weefsel waaruit zijwortels ontstaan. Behandelingen met synthetisch CEP5 peptide en *CEP5* overexpressie leidden tot een reductie in zijwortelinitiatie, terwijl *CEP5*

neerregulatie zorgde voor het toename van zijwortelinitiatie, waaruit blijkt dat het *CEP5* peptide een negatieve invloed heeft op zijwortelinitiatie. Expressie analyse van *CEPR1*/*XIP1* toonde aan dat deze sterk overlappend is met *CEP5* expressie en werd op basis van een genetische analyse als mogelijke receptor van CEP5 aangeduid. Opmerkelijk was dat de *xip1-1* mutant een reductie vertoonde in zijwortelinitiatie, hetzelfde als in synthetisch CEP5 peptide behandelingen en *CEP5* overexpressie. Dit suggereert dat CEP5 mogelijks als negatieve regulator van CEPR1/XIP1 activiteit optreedt. Verdere analyse van het effect van CEP5 signalisatie toonde aan dat CEP5 mogelijks een invloed heeft op de auxine respons door het stabiliseren van de AUXIN/INDOLE-3-ACETIC ACID INDUCIBLE (Aux/IAA) eiwitten, die optreden als repressoren van de AUXIN RESPONSE FACTOR (ARF) transcriptionele activatoren van auxine geïnduceerde respons genen. Dus, mogelijks reguleert het CEP5 peptide zijwortelontwikkeling door het controleren van de auxine respons.

In parallel met het karakteriseren van de CEP peptiden als regulatoren van wortelgroei, werden via een EMS-mutagenese screen drie andere moleculaire regulatoren van de wortel architectuur geïdentificeerd. Een 'loss-of-function' mutatie in het *CELLULOSE SYNTHASE 6* (*CESA6*) gen zorgde voor een kortere hoofdwortel met een denser netwerk van zijwortels die horizontaler uitgroeiden ten opzichte van de hoofdwortel. Dit leidde tot een ondiep dens wortelstelsel dat mogelijks beter aangepast is voor de opname van fosfaat, aangezien dit meer in de oppervlakkige regio's van de bodem voorkomt. Een 'loss-of-function' mutatie in het *CULLIN-ASSOCIATED AND NEDDYLATION-DISSOCIATED 1* (*CAND1*) gen zorgde voor een dens netwerk van zijwortels dat onder een scherpe hoek uitgroeiden langsheen de hoofdwortel. Dit leidde tot een wortelstelsel dat mogelijks beter aangepast zou zijn voor de opname van water en nitraat die voornamelijk dieper in de bodem terug te vinden zijn. En een nieuw 'gain-of-function' mutant allel voor het *IAA12*/*BODENLOS* (*BDL*) gen zorgde voor een sterke verstoring in de zijwortel verdeling over de hoofdwortel, en zorgde voor de vorming van clusters van zijwortels. Een gecontroleerde inductie van zijwortel clusters in regio's met hoge concentraties aan nutriënten zou een mogelijke manier zijn om een efficiënter wortel systeem te verkrijgen. Verder werd voor het eerst aangetoond dat de wortel architectuur fenotypes die bekomen werden via *in vitro* groei op Petri platen met ½ MS groei medium, behouden bleven in meer natuurlijke groeicondities in aarde, door gebruik te maken van mini-rhizotrons. Rhizotron onderzoek zal een belangrijke rol spelen in toekomstig onderzoek naar wortelontwikkeling, en zal ons terug een stapje dichter brengen bij gewassen met een efficiënter wortelstel en een hogere opbrengst.

# TABLE OF CONTENTS

Examination Commission

Summary - Samenvatting

List of abbreviations

**PART I. INTRODUCTION** ..... **1**

**Chapter 1.**

Root development in *Arabidopsis* ..... **3**

**Chapter 2.**

Peptide signaling in *Arabidopsis* ..... **27**

**Scope and outline** ..... **63**

**PART II. RESULTS** ..... **67**

**Chapter 3.**

The CEP family in land plants: evolutionary analyses, expression studies, and a role in *Arabidopsis* shoot development ..... **69**

**Chapter 4.**

Functional characterization of the CEP family and their proposed receptors ..... **89**

**Chapter 5.**

CEP5 and XIP1/CEPR1 regulate lateral root initiation in *Arabidopsis* ..... **129**

**Chapter 6.**

The small signaling peptide CEP5 attenuates the dynamic AUX/IAA equilibrium ..... **153**

**Chapter 7.**

An EMS-screen to identify molecular components controlling root system architecture ..... **171**

**PART III. GENERAL CONCLUSIONS AND PERSPECTIVES** ..... **201**

***Curriculum vitae*** ..... **223**

## LIST OF ABBREVIATIONS

A-loop = activation loop
AFB = AUXIN-RELATED F-BOX PROTEIN
AD = ancillary domain
ALE1 = ABNORMAL LEAF SHAPE 1
AP-2 = adaptor protein complex-2
ARE = auxin responsive element
ARF = AUXIN RESPONSE FACTOR
ASA = azidosalicylic acid
ASK1 = Arabidopsis S-PHASE KINASE-ASSOCIATED PROTEIN 1 (SKP1)-HOMOLOGUE 1
ASL = ASYMMETIC LEAVES2-LIKE
AtD14 = ARABIDOPSIS DWARF 14
ATP = adenosine triphosphate
AtPep = Arbaidopsis PROPEP
AtSBT = Arabidopsis subtilisin-like serine protease
AtSK = ARABIDOPIS SHAGGY-RELATED PROTEIN KINASE
AUX1 = AUXIN RESISTANT 1
Aux/IAA = INDOLE-3-ACETIC ACID INDUCIBLE
AuxRe = auxin responsive element
AXL1 = AXR1-LIKE 1
AXR1 = AUXIN RESISTANT 1
BAK1 = BRI1-ASSOCIATED RECEPTOR KINASE 1
BAM = BARELY ANY MERISTEM
BBM = BABYBOOM
BDL = BODENLOS
BES1 = *bri1* EMS SUPPRESSOR 1
BIK1 = BOTRYTIS-INDUCED KINASE 1
BIN2 = BRASSINOSTEROID INSENSITIVE 2
BIR2 = BAK1-INTERACTING RECEPTOR-LIKE KINASE 2
BKI1 = BRI1 KINASE INHIBITOR 1
BKK1 = BAK1-LIKE 1
BL = brassinolide
BP = BREVIPEDICELLUS
BR = brassinosteroid
BRI1 = BRASSINOSTEROID-INSENSITIVE 1
BRL = BRI1-LIKE
BSK = BR-SIGNALING KINASES
BSL = BSU1-LIKE
BSU1 = *bri1* SUPPRESSOR 1
BZR1/2 = BRASSINAZOLE RESISTANT ½
CaMV = cauliflower mosaic virus
CAND1 = CULLIN-ASSOCIATED AND NEDDYLATION-DISSOCIATED 1
CCP = circumferential cell proliferation
CDG1 = CONSTITUTIVE DIFFERENTIAL GROWTH 1
CDL1 = CDG1-LIKE1
CEP = C-TERMINALLY ENCODED PEPTIDE
CEPR = CEP RECEPTOR
CESA = CELLULOSE SYNTHASE
CLE = CLAVATA/EMBRYO SURROUNDING REGION-RELATED PROTEIN

CLEL = CLE-LIKE
CLV = CLAVATA
COI1 = CORONATINE INSENSITIVE 1
CRN = CORYNE
CSC = cellulose synthase complex
CSI1 = CELLULOSE SYNTHASE INTERACTING 1
CSN = COP9 SIGNALOSOME
CSR = class-specific region
CST = CAST AWAY
CTD = C-terminal domain
CUL1 = CULLIN HOMOLOGUE 1
CWR = cell wall remodeling
CYC = CYCLIN
DAMP = damage-associated molecular pattern
DBD = DNA binding domain
DD = dimerization domain
DUB = de-ubiquitination enzyme
DVL1 = DEVIL 1
EAR = ETHYLENE RESPONSE FACTOR (ERF)-associated amphiphilic repressor
ECR1 = E1-C-TERMINAL-RELATED 1
EE = early endosome
elf18 = EF-Tu-derived elf18 peptide
EFR = EF-Tu RECEPTOR
EMS = ethylmethanesulfonate
ENDO40 = EARLY NODULIN GENE 40
EPF = EPIDERMAL PATTERNING FACTOR
EPFL = EPF-LIKE
ER = ERECTA
ERL = ERECTA-LIKE
ESR = EMBRYO SURROUNDING REGION
ETA = ENHANCER OF TIR1-1 AUXIN RESISTANCE 2
EVR = EVERSHED
flg22 = flagellin-derived flg22 peptide
FLS2 = FLAGELLIN SENSING 2
GAI = GIBBERELLINIC ACID-INSENSITIVE
GH3 = Gretchen Hagen 3
GID1 = GIBBERELLIN INSENSITIVE DWARF 1
GLV = GOLVEN
GMC = guard mother cell
GN = GNOM
GRIp = GRIM REAPER PEPTIDE
GSK = GLYCOGEN SYNTHASE KINASE 3 (GSK3)-LIKE KINASE
HEAT = huntingtin-elongation-A-subunit-TOR
HyP = hydroxyproline
IAA = indole-3-acetic acid
IBA = indole-3-butyric acid
IC = initial cell
ID = island domain
IDA = INFLORESCENCE DEFICIENT IN ABSCISSION
IDL = IDA-LIKE

IKU2 = HAIKU2
INDEL = insertion deletion
IRX1 = IRREGULAR XYLEM 1
IXR2 = ISOXABEN RESISTANT 2
JA = jasmonic acid
JAZ = JASMONATE ZIM-DOMAIN PROTEIN
FC = founder cell
FER = FERONIA
GA = gibberellinic acid
GT-2 = Glycosyl-Transferase family 2
HAE = HAESA
HCS = highly conserved segment
HPAT = HYDROXYPROLINE O-ARABINOSYLTRANSFERASE
HSL = HAESA-LIKE
HVE = HEMIVENATA
KNAT = KNOTTED-LIKE FROM ARABIDOPSIS THALIANA
KOD = KISS OF DEATH
LAX = LIKE AUX1
LBD = LATERAL ORGAN BOUNDARIES-DOMAIN
L*er* = Landsberg *erecta*
LEW2 = LEAF WILTING 2
LR = lateral root
LRD = lateral root development
LRI = lateral root initiation
LRIS = lateral root inducible system
LRMC = lateral root mother cell
LRP = lateral root primordium/lateral root primordia
LRR = leucine-rich repeat
LRRCT = leucine-rich repeat C-terminal domain
LRRNT = leucine-rich repeat N-terminal domain
MAKR4 = MEMBRANE-ASSOCIATED KINASE REGULATOR 4
MAMP = microbe-associated molecular pattern
MAP = MITOGEN ACTIVATED PROTEIN
MAPK = MAP KINASE
MAPKK = MAP KINASE KINASE
MAPKKK = MAP KINASE KINASE KINASE
MAX2 = MORE AXXILARY GROWTH 2
MMC = meristemoid mother cell
MP = MONOPTEROS
MR = middle region
NAA = 1-naphthaleneacetic acid
NEDD8 = Neural Precursor Cell Expressed, Developmentally Down-Regulated 8
NEV = NEVERSHED
NPA = 1-N-naphthylphthalamic acid
NRT = NITRATE TRANSPORTER
NTD = N-terminal domain
OSIP108 = OXIDATIVE STRESS-INDUCED PEPTIDE 108
OZ = organizing center
P4H = PROLYL-4-HYDROXYLASE
PAMP = pathogen-associated molecular pattern

PAPS = 3’-phosphoadenosine 5’-phosphosulfate
PB1 = Phox/Bem1p
PBL = PBS1-LIKE
PBS1 = avrPphB SUSCEPTIBLE 1
PCD = programmed cell death
PCR = plant specific region
PCR = polymerase chain reaction
PDF = plant defensing
PEP = PLANT ELLICITOR PEPTIDE
PEPR = PEP RECEPTOR
PIN = PIN FORMED
PIP = PAMP-INDUCED SECRETED PEPTIDE
PIPL = PIP-LIKE
PLL1 = POL-LIKE 1
PLS = POLARIS
PLT = PLETHORA
POL = POLTERGEIST
PP2A = PROTEIN PHOSPHATASE 2A
PPP = phloem-pole-associated pericycle
PR = primary root
PRC1 = PROCUSTE 1
PRR = pattern recognition receptor
PSK = PHYTOSULFOKINE
PSKR = PSK-RECEPTOR
PSY1 = PLANT PEPTIDE CONTAINING SULFATED TYROSINE 1
PSYR1 = PSY1-RECEPTOR 1
PXL = PXY-LIKE
PXY = PHLOEM INTERCALATED XYLEM
RALF = RAPID ALKALINIZATION FACTOR
RALFL = RALF-LIKE
RAM = root apical meristem
RBX1 = RING-BOX PROTEIN 1
RCE1 = RUB1 CONJUGATING ENZYME 1
RGA = REPRESSOR OF GA1-3
RGF = ROOT GROWTH FACTOR
RGFR = RGF RECEPTOR
RGL = RGA-LIKE
RLK = receptor-like kinase
RLK7 = RECEPTOR-LIKE KINASE 7
RLP = receptor-like protein
RSA = root system architecture
ROT4 = ROTUNDIFOLIA FOUR
RPK2 = RECEPTOR-LIKE PROTEIN KINASE 2
QC = quiescent center
SAM = shoot apical meristem
SCF = ASK1-CUL1-F-box protein E3 ligase complex
SCR/SP11 = S-LOCUS CYSTEIN RICH PROTEIN/S-LOCUS PROTEIN 11
SDD1 = STOMATA DENSITY AND DISTRIBUTION 1
SERK = SOMATIC EMBRYOGENESIS RECEPTOR-LIKE KINASE
SKP1 = S-PHASE KINASE-ASSOCIATED PROTEIN 1

SL = strigolactone
SLGG = stomatal-lineage ground cell
SLY1 = SLEEPY 1
SMXL = SUPPRESSOR OF MAX2 1 (SMAX1)-LIKE
SOBIR1 = SUPPRESSOR OF BIR1-1
SOL1 = SUPRESSOR OF LIGAND-LIKE PROTEIN 1
SOL2 = SUPRESSOR OF LIGAND-LIKE PROTEIN 2
sORF = small open reading frame
SPCH = SPEECHLESS
SRM = Selected Reaction Monitoring
SUS = SUCROSE SYNTHASE
SYS = SYSTEMIN
TaP = tri-arabinosylation
TDIF = TRACHEARY DIFFERENTIATION INHIBITORY FACTOR
TDR = TDIF-RECEPTOR
TE = tracheary element
TGN = trans-Golgi network
TIR1 = TRANSPORT INHIBITOR RESPONSE 1
TMH = transmembrane helix
TMM = TOO MANY MOUTHS
TOAD2 = TOADSTOOL 2
TPD = TOPLOSS domain
TPL = TOPLESS
TPR = TOPLESS-RELATED
TPST = TYROSYLPROTEIN SULFOTRANSFERASE
UFO = UNUSUAL FLORAL ORGANS
VH1 = VASCULAR HIGHWAY 1
VS = variable segment
WOX = WUSCHEL-RELATED HOMEOBOX
WUS = WUSCHEL
XIP1 = XYLEM INTERMIXED WITH PHLOEM1
XPP= xylem-pole-associated pericycle
YDA = YODA

# PART I:
# Introduction

# Chapter 1:

## Root development in *Arabidopsis*

# 1. General introduction

About 460-700 million years ago, plants started colonizing land (Heckman et al, 2001). A major challenge for this was to free themselves from an aquatic environment, in which water and nutrient uptake posed little problem, and make the transition to a relatively dry terrestrial environment. To overcome this challenge, plants evolved roots. The major functions of roots are a firm anchorage and the acquisition of nutrients and water from the soil. In order to efficiently fulfill these functions, plants rely on the plasticity of the root system architecture (RSA) to respond to their dynamic environment (Lynch, 1995). RSA can be modulated in several ways: promotion or inhibition of primary root growth, density of lateral root formation along the root axis and the angle of the LR growth direction along the main root axis. Other functions of plant roots include interactions with both beneficial and pathogenic organisms, gravity perception, photoassimilate storage (*e.g.* starch), water storage, phytohormone synthesis and clonal propagation.

With the exponentially growing world population, less arable land available for agriculture, the effects of climate change (*e.g.* drought) and higher costs for energy, fertilizers and water, researches in plant biotechnology received the important task to increase crop productivity to overcome these challenges. Considering the functions of the root system, engineering RSA might allow designing crops with higher yield under dryer and nutrient-poor conditions, and thereby partly meet these challenges. Designing a more efficient RSA can be achieved by marker-assisted breeding or by genetically engineering the crops in a more targeted manner. Therefore however, the molecular regulators of root formation need to be identified first.

Research in plant (root) development has mainly been conducted in *Arabidopsis thaliana* (*Arabidopsis*), the model plant for dicotyledonous plants. It was chosen as a model plant for several reasons: its small size, short generation time (6 to 9 weeks), it is a self-fertilizer, easy to transform by floral dipping with *Agrobacterium tumefaciens*, it produces a large number of seeds per plant, it is easily mutagenized and has a small genome (~130 Mb), which is fully sequenced (Arabidopsis Genome, 2000). And interestingly, it has a relatively simple (root)morphology and anatomy, with most of the developmental processes well-studied and documented.

# 2. The hidden half of *Arabidopsis*

## 2.1 Root morphology and anatomy

There are two major types of roots in the plant kingdom: the allorhizic or taproot-system and the homorhizic or fibrous-system. The taproot-system is characteristic for dicotyledonous species, such as *Arabidopsis*, whereas the fibrous-system is characteristic for monocotyledonous species, such as maize (Smith & De Smet, 2012; Orman-Ligeza et al, 2013). The root system of *Arabidopsis* is characterized by the formation of the embryonic primary root, which remains dominant during its whole life cycle, from which post-embryonic lateral roots emerge later in development (Malamy & Benfey, 1997) .

The *Arabidopsis* root is composed of single radial concentric tissue layers of epidermis, cortex and endodermis (from outside to inside), which surround the stele. The stele consists of the pericycle surrounding the vascular bundle. The diarch vascular bundle with bilateral symmetry contains two xylem poles and two phloem poles with procambium in between. The xylem is composed of tracheids and vessel elements, while the phloem is composed of sieve-tube cells and companion cells. The pericycle can be subdivided in two populations: phloem-pole-associated pericycle (PPP) cells and xylem-pole-associated pericycle (XPP) cells, from which lateral roots are formed. At the root tip, there is an additional tissue called the root cap, which is composed of central columella cells and lateral root cap cells (Dolan et al, 1993; Schiefelbein et al, 1997) **(Figure 1)**.

## 2.2 Root growth

The root is composed of four sequential developmental zones. In the root apical meristem (RAM) zone, formative divisions in the stem cell niche generate the different cell types for each tissue, followed by multiple rounds of proliferative divisions in cell files. The basal meristem is a transition zone of combined proliferative cell division and elongation. In the elongation zone, cell division ceases and the cells rapidly expand longitudinally. Finally, in the maturation or differentiation zone, cells differentiate and acquire their specialized features **(Figure 1)**.

Thus, post-embryonic root growth is supported by the stem cell niche in the RAM. This stem cell niche is a population of stem cells or initials that generates every tissue layer in the root. Initials divide asymmetrically to give rise to two distinct daughter cells, a copy of the original initial and a daughter cell programmed for generating a cell file with a different cell fate. The initials are situated around a group of mitotically less active cells, called the quiescent centre (QC). The major function of the QC is the maintenance of the stem cell niche by suppressing differentiation of the initials. There are five sets of meristematic initials in the *Arabidopsis* RAM: one forms the epidermis and lateral root cap, one forms the columella root cap, one produces both the cortex and endodermal layers, one produces the cells of the stele, and ones gives rise to the pericycle (Dolan et al, 1993; Perilli et al, 2012; Sozzani & Iyer-Pascuzzi, 2014) **(Figure 1)**.

# 3. Lateral roots

## 3.1 Morphology and anatomy of lateral root formation

The root system requires the formation of lateral roots along its main root axis for more efficient scanning of the soil for water and nutrients. Lateral roots emerge in an acropetal order and are ordered along the main axis in a regular left-right alternating pattern (De Smet et al, 2007). Lateral roots are initiated post-embryonically from patches of XPP cells along the primary root (Dolan et al, 1993). These cells are called the pericycle founder cells. A lateral root primordium (LRP) is established from the founder cells through several rounds of coordinated anticlinal and periclinal divisions, and can be divided into seven consecutive developmental stages (stage I to VII). After that, the LRP emerges from the main root and its growth is maintained by its own independent functional RAM (Malamy & Benfey, 1997; Lucas et al, 2013; von Wangenheim et al, 2016) **(Figure 1)**.

## 3.2 The pericycle

The pericycle is not a concentric homogenous tissue, but instead a heterogeneous tissue consisting of two populations: XPP and PPP cells. An obvious reason for this statement is that lateral roots are only formed from XPP cells. However, there are other examples of differences between these two cell populations. Differential gene expression patterns suggest two populations of pericycle cells (Beeckman et al, 2001; Laplaze et al, 2005; Brady et al, 2007; Parizot et al, 2008). Differences at the cytological level are present, with XPP cells exhibiting meristematic features, such as large nuclei, small vacuoles and dense cytoplasm, whereas PPP cells do not (Parizot et al, 2008). Cell length measurements have indicated that the pericycle cells at the xylem poles are shorter than those at the phloem poles (Dubrovsky et al, 2000; Beeckman et al, 2001). And finally, differences in cell division competence are apparent, with PPP cells remaining in the G1-phase after exiting the RAM, whereas XPP cells advance to the G2-phase of the cell cycle and are in a mitosis-competent state (Beeckman et al, 2001). Taken together, the PPP cells are quiescent, whereas XPP cells remain competent to divide and form lateral root primordia (LRP), and can be regarded as an extended meristem (Dubrovsky et al, 2000; Casimiro et al, 2003). A recent transcriptional study suggested the two populations of pericycle cells originate from their close association with their underlying vascular tissue. Thus, XPP cells are intimately linked with the underlying xylem, whereas PPP cells with the underlying phloem, instead of forming a separate independent concentric uniform layer surrounding the vasculature (Parizot et al, 2012).

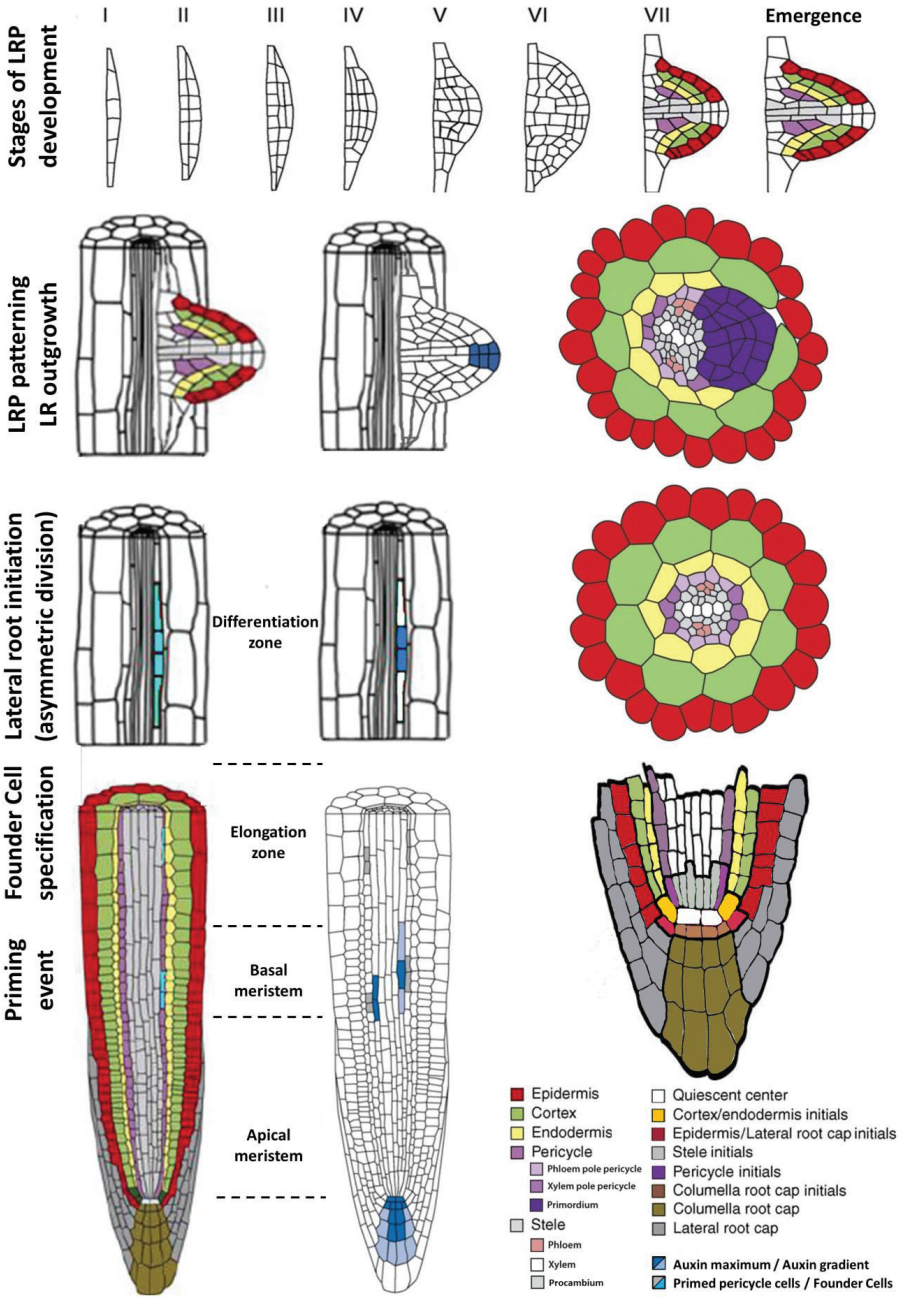


**Figure 1.** ***Arabidopsis*** **root development.** The root is composed of sequential developmental zones with different tissue types, which are formed through formative divisions by initials in the RAM stem cell niche. Lateral roots (LRs) are formed from xylem-pole pericycle cells in several consecutive steps: priming in the basal meristem after a periodic auxin response pulse, founder cell (FC) specification in the auxin minimum zone, the first asymmetric formative division of the FCs triggered by an auxin maximum response, lateral root primordium (LRP) patterning regulated by an auxin gradient, and finally LR outgrowth and elongation. LRP development is divided into seven stages (stage I to VII) formed by several rounds of controlled anticlinal and periclinal divisions, after which the LR emerges with its own functional meristem. (Figure adapted from Peret et al, 2009a; Peret et al, 2009b)

## 3.3 Lateral root development

Lateral root development can be divided into several steps. In the basal meristem, small groups of XPP cells undergo 'priming' after a periodic auxin response pulse, and acquire the potential to move to the next step. Afterwards, a few of these primed XPP undergo cell specification to become founder cells in the auxin minimum zone. This is followed by a first round of asymmetric formative divisions of the founder cells, which is triggered by an auxin maximum response. Then, a LRP is formed through a series of coordinated anticlinal and periclinal divisions driven by an auxin gradient. The lateral root emerges from the main root after penetrating the overlaying tissue layers, which is also an auxin-dependent process. And finally, the lateral root continues growing with its own functional RAM. Thus, auxin plays a crucial role during the entire process of lateral root formation. Therefore, a profound knowledge of the auxin signaling pathway is required first to understand the underlying mechanisms at play during lateral root development **(Figure 1)**.

### 3.3.1 Auxin signaling and its key molecular players

#### 3.3.1.1 The ARF proteins

The auxin response factors (ARFs) are transcription factors that mediate auxin-dependent transcriptional regulation. The *Arabidopsis* genome encodes 23 ARFs (Ulmasov et al, 1999). They have an N-terminal DNA binding domain (DBD), a variable middle region (MR) and a C-terminal Phox/Bem1p (PB1) domain. The DBD is composed of a plant-specific B3-type domain, two dimerization domains (DD), and an ancillary domain (AD). The B3-domain binds two everted TGTCTC auxin-responsive element (ARE or AuxRE) motifs separated by 7 bp (ER7), which is a consensus sequence found in promoters of auxin-inducible genes (Ulmasov et al, 1997). The DD-domains are involved in dimerization interactions between two ARFs, each binding at one of the everted ARE motifs (Boer et al, 2014). Five ARFs (ARF5, 6, 7, 8 and 19) contain a variable glutamine (Q)-rich MR and are transcriptional activators, whereas the other ARFs with an S, P, L/G-rich MR are thought to act as transcriptional repressors (Tiwari et al, 2003). The C-terminal part contains the conserved domains III and IV, together forming a PB1 domain with a β-grasp fold. This PB1 domain serves as a platform for homo- and hetero-dimerization (and oligomerization) with other ARFs and Aux/IAAs (Kim et al, 1997; Guilfoyle & Hagen, 2007; Korasick et al, 2014; Nanao et al, 2014).

#### 3.3.1.2 The Aux/IAA proteins

The Aux/IAA transcription factors are believed to act as transcriptional repressors by hetero-dimerizing with the ARF transcriptional activators and thereby preventing these ARFs from activating transcription of downstream target-genes (Abel et al, 1994; Farcot et al, 2015). The *Arabidopsis* genome encodes 29 different Aux/IAAs (Abel & Theologis, 1996). The proteins have four highly conserved domains. Domain I contains an EAR-motif (ETHYLENE RESPONSE FACTOR (ERF)-associated amphiphilic repressor) that recruits the transcriptional co-repressor TOPLESS (TPL), and its homologs TPL-RELATED 1 to 4 (TPR1-4). The EAR-motif interacts with the N-terminal TOPLESS domain (TPD) that stimulates tetramerization of TPL/TPR proteins, while their C-terminal WD40 domains induce transcriptional repression by sequestering chromatin-modifying enzymes (Tiwari et al, 2004; Szemenyei et al, 2008; Kagale & Rozwadowski, 2011; Ke et al, 2015). Domain II is essential for auxin-stimulated Aux/IAA proteolysis (see below) (Gray et al, 2001). Domain III and IV form a PB1 domain, similar to ARFs, and is involved in homo- and heterodimerization with other Aux/IAAs and ARFs (Kim et al, 1997; Korasick et al, 2014).

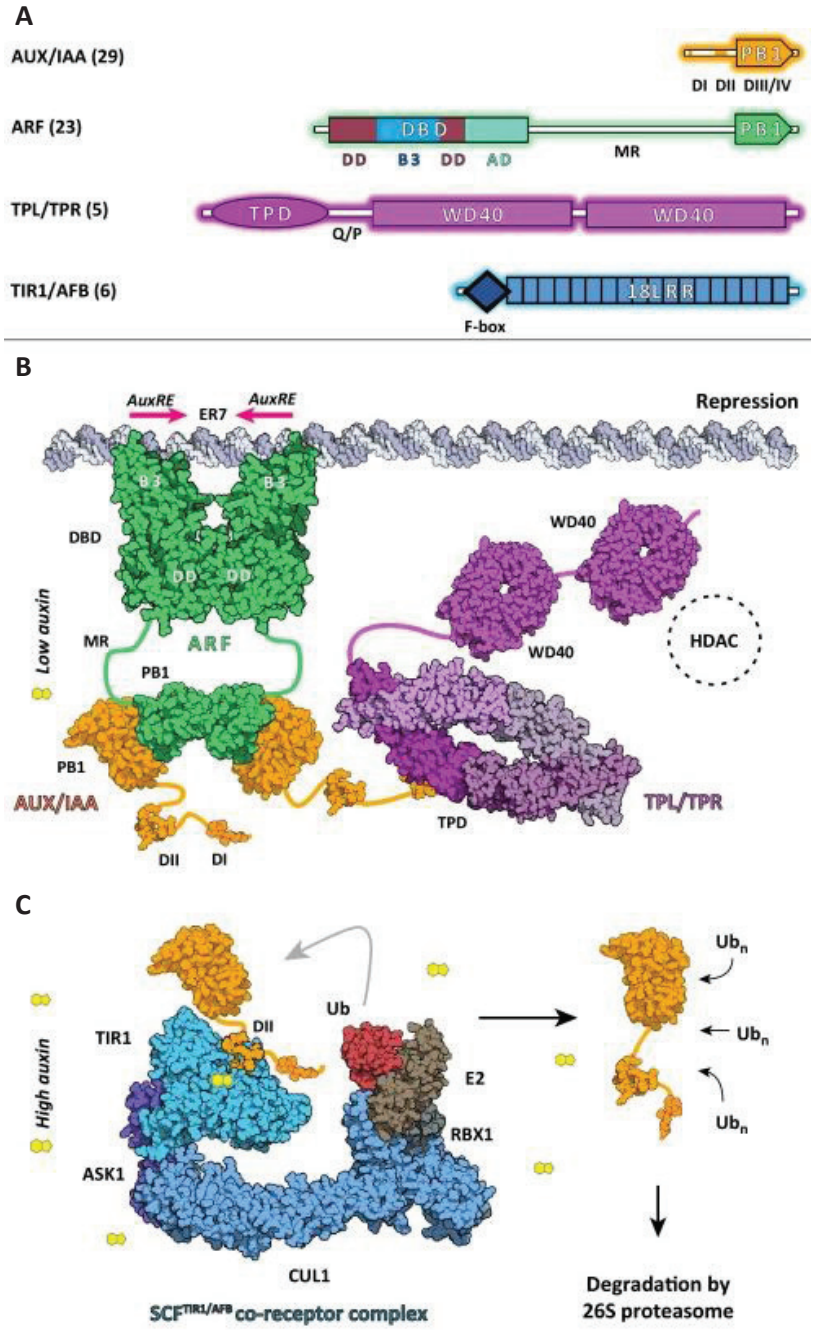


**Figure 2. Auxin signaling. (A)** Domain structure of ARFs, AUX/IAAs, TPL/TPR co-repressors, and TIR1/AFB F-box proteins. **(B)** ARFs form dimers that interact through their DD-domains, while their B3-domain binds to ARE motifs in the promoter of auxin responsive genes. At low auxin concentrations, ARFs dimerize through their PB1 domain with Aux/IAAs. The EAR motif in domain I of Aux/IAAs recruits TPL/TPR co-repressors, which leads to transcriptional repression. **(C)** At higher auxin concentrations, auxin serves as molecular glue between domain II of Aux/IAAs and TIR1/AFB F-box proteins. This stimulates Aux/IAA ubiquitination by the $SCF^{TIR1/AFB}$ E3 ligase complex and subsequent targeting for proteolysis mediated by the 26S proteasome. Degradation of Aux/IAAs derepresses the ARF activity on transcription. (Figure from Dinesh et al., 2016)

#### 3.3.1.3 The $SCF^{TIR1/AFB}$ auxin receptor and the auxin signaling mechanism

When IAA enters the nucleus, it binds the leucine-rich repeat (LRR) domain of its receptor TRANSPORT INHIBITOR RESPONSE 1 (TIR1) or a member of the closely related AUXIN-RELATED F-BOX PROTEIN 1-5 (AFB1-5) auxin receptor proteins. TIR1 contains 18 LRRs of various lengths (from 22 to 35 residues) forming a right-handed superhelix of one full turn. The top surface contains three long intra-repeat loops (loop 2 in LRR2, loop 12 in LRR12 and loop 14 in LRR14), with loop 2 playing an important role in creating the auxin binding pocket (Dharmasiri et al, 2005a; Dharmasiri et al, 2005b; Kepinski & Leyser, 2005; Tan et al, 2007).

TIR1 and AFB1-5 are F-box proteins that also bind Aux/IAA proteins, and are part of the $SCF^{TIR1/AFB}$ E3 ubiquitin ligase complex, which consists of *Arabidopsis* S-PHASE KINASE-ASSOCIATED PROTEIN 1 (SKP1)-HOMOLOGUE 1 (ASK1), CULLIN HOMOLOGUE 1 (CUL1), RING-BOX PROTEIN 1 (RBX1) and the F-box protein TIR1/AFB1-5. ASK1 is essential in the recognition and binding of the F-box and acts as a bridging protein between CUL1 and the F-box protein. CUL1 forms the major structural scaffold of the SCF-complex that links the ASK1 domain with the RBX1 domain, together forming a horseshoe-shaped complex. RBX1 contains a small zinc-binding domain called the RING finger, to which the E2-ubiquitin conjugating enzyme binds, allowing the transfer of ubiquitin residues to a lysine residue on the target Aux/IAA protein that is bound by the F-box protein. The F-box protein (TIR1/AFB1-5) dictates the specificity of SCF-complex by aggregating to Aux/IAA target proteins independently of the complex and then binding to the ASK1 component. It is believed that auxin functions as a molecular glue between the TIR1/AFB F-box protein and the conserved domain II of the Aux/IAA transcriptional regulators, thereby forming a TIR1/AFB – AUX/IAA co-receptor complex for binding auxin (Calderon Villalobos et al, 2012). This brings the Aux/IAA protein into close proximity with the functional E2 enzyme for ubiquitination, and subsequently targets it for proteasomal degradation (Dharmasiri et al, 2005a; Kepinski & Leyser, 2005; Dinesh et al, 2015).

Thus, in the absence of auxin, Aux/IAAs interact with ARFs and this leads to transcriptional repression. While in the presence of auxin, Aux/IAAs are targeted for proteasomal degradation, which leads to subsequent release of the ARF transcription factors from inhibition, and thereby inducing the auxin transcriptional response.

Considering the core parts of the auxin signaling module can contain 23 ARFs, 29 Aux/IAAs, 5 TPL/TPRs and 6 TIR1/AFBs, the theoretical number of possible different complexes is huge (>20,000 possible combinations). In general it is believed that specific pairs of Aux/IAA and ARF proteins are formed in different tissues and at different times and places in development, thus allowing a wide variety of auxin effects (Piya et al, 2014).

### 3.3.2 Lateral root priming

Root biologists long wondered if lateral roots can be formed from any XPP cells along the main root, or whether there already exist fixed patches of XPP cells that can develop into lateral roots, while cells outside these patches are not able to do so. Recent evidence suggests that the latter is the more plausible scenario for regulating lateral root spacing. This is known as the prepatterning model and involves an oscillatory lateral root priming event in the basal meristem, which marks the first step in lateral root formation. Lateral root priming is regulated by a complex regulatory mechanism in which auxin transport, oscillations in gene expression and auxin signaling, auxin homeostasis and cell cycle regulation play important roles.

#### 3.3.2.1 Auxin transport

Auxin is mainly synthesized in the leaves and transported from the shoot to the root apex. Bulk transport occurs through the phloem and once near the root tip region this is followed by local polar auxin transport mediated by the auxin efflux carriers PIN FORMED 1 (PIN1) and PIN4 (Geldner et al, 2001; Friml et al, 2002). This flow of auxin, together with locally synthesized auxin (Ljung et al, 2005; Petersson et al, 2009), is transported through 'the inverse fountain auxin transport pathway' back into the basal meristem region just above the root apical meristem. This is mediated by polar auxin transport through the action of the PIN3 and PIN7 auxin efflux carriers in the columella cells (Benkova et al, 2003; Dubrovsky et al, 2011), the PIN2 auxin efflux carrier in the lateral root cap and epidermal cells (Chen et al, 1998; Luschnig et al, 1998; Muller et al, 1998) and the AUXIN RESISTANT 1 (AUX1) auxin influx carrier in the lateral root cap cells and the epidermal cells (De Smet et al, 2007). This reflux of auxin in the basal meristem region has been shown to be important for the priming of XPP cells (De Smet et al, 2007; Lucas et al, 2008a; Lucas et al, 2008b).

#### 3.3.2.2 Oscillations in gene expression and auxin signaling during lateral root priming

The regular spacing of lateral roots is controlled by an oscillatory endogenous mechanism controlled by thousands of oscillating genes, which ensures that only a limited number of XPP cells acquire the competence to form lateral roots in a well-defined spatiotemporal manner. This lateral root priming process occurs in the basal meristem, also referred to as the oscillation zone (De Smet et al, 2007; De Rybel et al, 2010; Moreno-Risueno et al, 2010). The oscillating priming event in the basal meristem is strongly correlated with periodic auxin signaling pulses, which can be visualized by *DR5* auxin response marker lines (De Smet et al, 2007; Moreno-Risueno et al, 2010). It was revealed that the oscillations lead to local auxin responses in the protoxylem strands, which triggers priming in the neighboring XPP cells (De Smet et al, 2007). The patches of XPP cells that are primed then become 'prebranch sites' higher up in the root, marked by an increased static *DR5* auxin response signal (Moreno-Risueno et al, 2010). The priming events seem to occur at regular time intervals of approximately 4 hours under standard *in vitro* growth conditions (Xuan et al, 2015). Interestingly, it was found that not all prebranch sites necessarily lead to formation of a lateral root, but only in beneficial environmental conditions will they further develop into lateral roots. This leaves the plant with a large pool of cells that are competent to adapt the root architecture, thereby ensuring its high plasticity in a changing environment.

Based on several observations, auxin signaling in the basal meristem seems to play an important role in lateral root priming. A recent study showed that local auxin perception in the basal meristem by TIR1 and AFB2 is required to surpass a certain threshold in the intensity of the local auxin response, which is needed to translate the oscillation signal into a prebranch site (Xuan et al, 2015).

A functional auxin response during priming depends on an Aux/IAA28 – ARF7 signaling module that induces the expression of the GATA23 transcription factor, a positive regulator for founder cell specification (De Rybel et al, 2010; Moreno-Risueno et al, 2010). Interestingly, *ARF7* expression was shown to rhythmically pulse with the same period as the *DR5* auxin response in the basal meristem (Moreno-Risueno et al, 2010). However, these are most likely not the only auxin signaling proteins that are involved in the priming event, since *Aux/IAA8* and *Aux/IAA19* are also expressed in the basal meristem region and their mutant lines show defects in lateral root formation (Groover et al, 2003; Tatematsu et al, 2004; Moreno-Risueno et al, 2010; Arase et al, 2012). It has been shown that *Aux/IAA8* and *ARF7* expression is auxin-insensitive (Dreher et al, 2006; Moreno-Risueno et al, 2010), while *Aux/IAA28* expression is reduced by auxin (Rogg et al, 2001), and *Aux/IAA19* expression is ARF7-dependent (Tatematsu et al, 2004). This suggests that some auxin signaling modules are auxin-dependent and act sequential, while others are not directly regulated by the auxin response triggered by auxin influx in the basal meristem but rather depend on the overall oscillatory gene expression. Together, this indicates a complex interplay between multiple auxin signaling modules that are controlled by auxin influx pulses from the basal meristem and an internal clock of periodic oscillations in gene expressions in the basal meristem region.

#### 3.3.2.3 Auxin homeostasis

Although indole-3-butyric acid (IBA) has long been used as a compound to stimulate lateral root formation (IBA is the active ingredient in rooting powder used in horticulture), its precise mode of action remained elusive. Using a chemical compound called naxillin, it was discovered that IBA is converted to IAA in the lateral root cap and contributes to the free IAA pool that follows the transport route towards the basal meristem, thereby stimulating lateral root priming. Mutants defective in the IBA-to-IAA conversion pathway (e.g. *ibr1/ibr3/ibr10* mutants) are insensitive to the IBA-stimulatory effect on the auxin response in the basal meristem and show a significant reduction in lateral root formation. Using the sensitive *pDR5::LUCIFERASE* auxin response reporter, it was shown that the IBA-to-IAA conversion is required to reach a certain threshold in the auxin response intensity in the basal meristem to translate the oscillation signals into a prebranch site (De Rybel et al, 2012; Xuan et al, 2015). A transcriptome profiling on Col-0 and *ibr1ibr3ibr10* triple mutant root tips after IBA treatment revealed upregulation of the *Gretchen Hagen3* genes *GH3.3* and *GH3.6*, which encode for auxin conjugating enzymes. These were hypothesized to control the amount of free IAA that is released from the IBA-to-IAA conversion in the root cap (Xuan et al, 2015). Thus, it seems that a tight control on auxin homeostasis regulates lateral root priming.

#### 3.3.2.4 The driving force for the oscillations in the basal meristem

Recently, researchers finally uncovered the underlying mechanism responsible for the oscillatory gene expression in the basal meristem. The oscillations in auxin response in the basal meristem were shown to occur with the same periodicity as the recurring programmed cell death (PCD) of senescent lateral root cap cells, which are continuously sloughed off during root growth. Using an *in-silico* auxin-transport model, it was suggested that the most distal lateral root cap cells build up high auxin concentrations by local IBA-to-IAA conversion, followed by active auxin transporter-dependent re-allocation of IAA from these cells towards the basal meristem. These auxin influx pulses in the basal meristem likely trigger the local oscillatory gene expression behavior. Based on these observations, the authors assumed that during root growth, the root tip senses the local environment (*e.g.* water and nutrient content) and affects the timing of the PCD program accordingly to act on lateral root priming and thereby contributes to shaping root system architecture (Xuan et al, 2016) **(Figure 3)**.

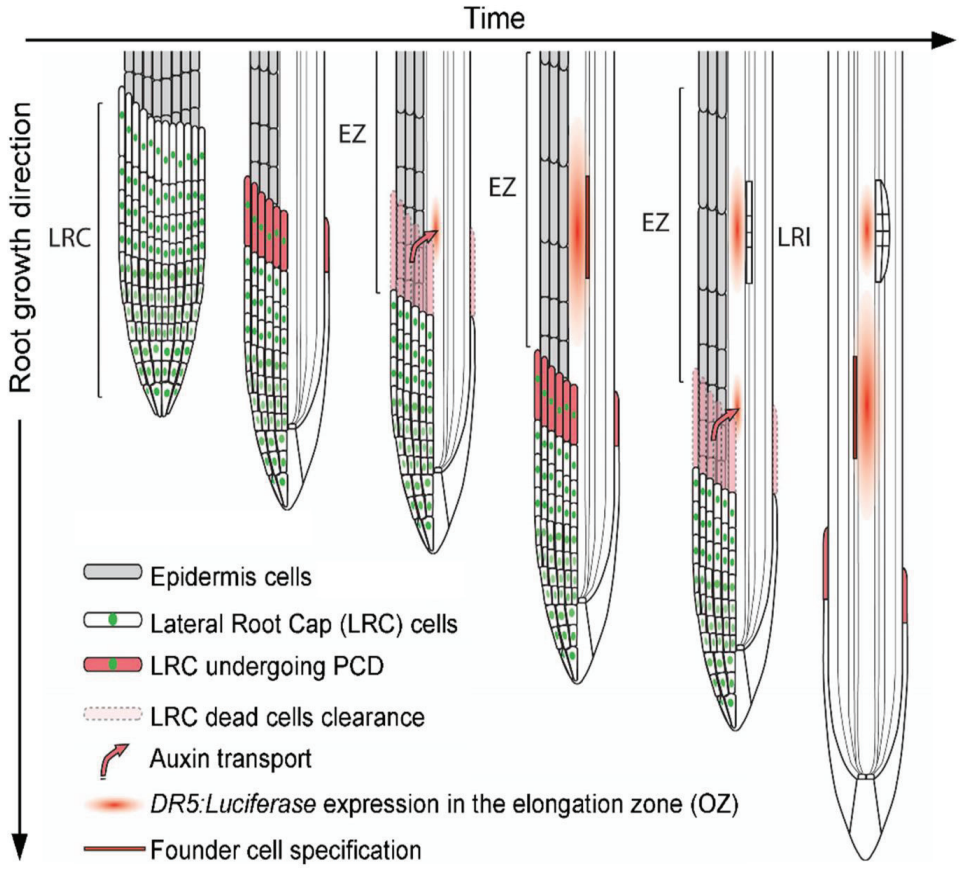


**Figure 3. Lateral root priming.** Periodic programmed cell death of lateral root cap cells (LRC) triggers a re-allocation of auxin (partly derived from local IBA to IAA conversion) towards the basal meristem, and thereby triggers the oscillatory gene expression pattern and priming of XPP cells. (Figure from Xuan et al., 2016)

#### 3.3.2.5 Cell cycle regulation

Regulation of the cell cycle determines the availability of sufficient XPP cells in the basal meristem region and is also an important factor for lateral root priming. Recently, the role of *CYCLIN D4;1* (*CYCD4;1*) during the lateral root priming event was described. While the primary root length was unaffected, *cycd4;1* mutants showed a significant decrease in lateral root formation. Expression analysis of *CYCD4;1* revealed its specific expression in the XPP cells in a decreasing gradient from the apical meristem to the basal meristem region. Loss of *CYCD4;1* function resulted in an earlier transition of XPP cells from cell division to cell elongation, resulting in a larger average length of pericycle cells in the basal meristem region. This leads to reduced XPP cell density in this region, and therefore also less cells that can undergo priming. Thus, the CYCD4;1 protein affects the XPP cell flux through the basal meristem by controlling their rate of cell division, and thereby has an impact on the number of XPP cells that can become lateral roots (Nieuwland et al, 2009).

### 3.3.3 Lateral root founder cell specification

Following the priming event, founder cell specification occurs within a developmental window that is located in a well-defined zone in the early-differentiation zone above the basal meristem where auxin content and response are minimal. This was termed the auxin minimum zone and is believed to sensitize the two flanking primed XPP cells for a local auxin accumulation, which can be visualized by a *DR5* auxin response signal. This auxin response is required for founder cell specification (Dubrovsky et al, 2008; Dubrovsky et al, 2011). So far, the GATA23 transcription factor, which acts downstream of the ARF7 – Aux/IAA28 module during priming, is one of the few regulators identified to play a role during founder cell specification (De Rybel et al, 2010). Recently, MEMBRANE-ASSOCIATED KINASE REGULATOR 4 (MAKR4) was identified in a transcriptome profiling analysis on lateral root priming as another candidate regulator of founder cell specification. The MAKR4 protein was shown to localize to the plasma membrane of founder cells just before lateral root initiation and was demonstrated to be involved in converting a prebranch site into a lateral root (Xuan et al, 2015).

### 3.3.4 Lateral root initiation

Almost immediately after the local auxin response in the two flanking founder cells, their nuclei start to migrate towards the common cell wall. Quickly following thereafter occurs an anticlinal asymmetric formative cell division, generating two small radially swollen daughter cells flanked by two longer daughter cells (De Rybel et al, 2010; Dubrovsky et al, 2011). This process is defined as the lateral root initiation event and is the first cytological visual sign of the site of lateral root formation.

The nuclear migration event and the onset of the asymmetric cell division are controlled by an Aux/IAA14 – ARF7/ARF19 auxin signaling module that induces the expression of the *LATERAL ORGAN BOUNDARIES-DOMAIN 16/ASYMMETIC LEAVES2-LIKE 18* (*LBD16/ASL1*8) transcription factor in the founder cells (Fukaki et al, 2002; Fukaki et al, 2005; Okushima et al, 2005; Wilmoth et al, 2005; De Rybel et al, 2010; Goh et al, 2012a). Four other members of the class I LBD subfamily have also been reported to act downstream of ARF7 and ARF19 during lateral root initiation: *LBD17/ASL15*, *LBD18/ASL20*, *LBD29/ASL16* and *LBD33* (Okushima et al, 2007; Berckmans et al, 2011; Feng et al, 2012a; Feng et al, 2012b; Goh et al, 2012a; Kang et al, 2013). The cell cycle E2Fa transcription factor is a direct transcriptional downstream target of these LBD transcription factors and is required for initiating the asymmetric cell division, thereby linking auxin signaling to cell cycle activation (Berckmans et al, 2011). Other downstream targets are the auxin efflux transport proteins PIN1, PIN3, PIN7 and the auxin influx transport protein AUX1. These will lead to an increased influx of auxin in the divided cells to activate later signaling pathways during LRP development. It has been shown that ARF7 and ARF19 might also interact with other Aux/IAA proteins during lateral root initiation, such as Aux/IAA1, Aux/IAA3 and Aux/IAA18 (Tian & Reed, 1999; Yang et al, 2004; Uehara et al, 2008; Goh et al, 2012b). This indicates that probably multiple ARF – Aux/IAA modules regulate the lateral root initiation process.

### 3.3.5 Lateral root primordium development

After lateral root initiation, the first asymmetric cell division is followed by another round of anticlinal asymmetric cell division, generating a central core of four small radially enlarged XPP cells flanked by two larger daughter cells. This single layer of cells is termed stage I of LRP development. A LRP further develops from this central core exclusively through a series of coordinated periclinal and anticlinal divisions, passing through seven stages of LRP development before emerging from the parent root (Malamy & Benfey, 1997) **(Figure 1)**.

During LRP development, an auxin gradient is created by active auxin transport (PIN1, PIN3 and AUX1). This starts with an auxin maximum in the central core cells after the first asymmetric divisions, followed by a gradual shift over time of a strong auxin response to the tip of older LRP stages (Benkova et al, 2003). Auxin has previously been described to act as a morphogen during LRP development (Benkova et al, 2009). Recent evidences finally allowed explaining the possible mechanism behind this process. Some Aux/IAAs have been demonstrated to interact stronger with certain ARFs than with others, leading to auxin signaling modules (*e.g.* Aux/IAA14 interacts strongly with ARF7 and ARF19, while Aux/IAA12 interacts strongly with ARF5) (Weijers et al, 2005). Furthermore, it was shown that each Aux/IAA protein has a different sensitivity for auxin binding (*e.g.* Aux/IAA14 is very sensitive to auxin binding, while Aux/IAA12 is much less sensitive) (Calderon Villalobos et al, 2012). Altogether, during lateral root initiation the auxin sensitive Aux/IAA14 is degraded during the moderate auxin response in the founder cells and releases ARF7 and ARF19 to activate the expression of downstream regulators that trigger lateral root initiation (*e.g.* LBDs, E2Fa and the auxin transporters). Afterwards, an auxin maximum is created in the inner core cells by the induced auxin transporters, which leads to the degradation of the less sensitive Aux/IAA12 and releases ARF5 to trigger the expression of ARF6 followed by ARF8 during further LRP development (De Smet et al, 2010). These induce expression of *PLETHORA* genes (*PLT1*, *PLT2* and *BABYBOOM* (*BBM*)) to ensure proper LRP organogenesis and create a meristematic region at the LRP tip. On the other hand, the cells at the flanks and base of the LRP never reach the threshold of auxin content for the degradation of Aux/IAA12 and therefore the expression of the *PLT* root genes is never induced (Lavenus et al, 2015). In these cells, the transcription factor PUCHI represses cell divisions, thereby maintaining the dome-shaped developing LRP (Hirota et al, 2007).

However, the above described Aux/IAA – ARF modules are by no means the only modules that are involved during lateral root development. A role for ARF2, ARF3 and ARF4 (Marin et al, 2010; Yoon et al, 2010), Aux/IAA16 (Rinaldi et al, 2012) and Aux/IAA17 (Kim et al, 2006), during lateral root development have also been described, illustrating that lateral root formation is controlled by multiple overlapping and sequential Aux/IAA – ARF signaling modules **(Figure 4)**.

### 3.3.6 Lateral root emergence

During lateral root emergence, several parental tissues have to be penetrated and this requires cell separation in the endodermal, cortical and epidermal cell layers adjacent to the developing LRP. Again, auxin appears to be a key player in this process. An Aux/IAA3 – ARF7 signaling module in the overlaying endodermal cells induces the expression of cell wall remodeling (CWR) enzymes, which lead to cell separation (Neuteboom et al, 1999; Laskowski et al, 2006; Goh et al, 2012b). Auxin, originating from developing lateral root primordium, later acts as a local inductive signal through an Aux/IAA14 - ARF7/ARF19 module to induce the expression of the auxin influx carrier LIKE AUX1 3 (LAX3) in cortical and epidermal cells directly overlaying the LRP and thereby reinforces the auxin-dependent induction of the CWR enzymes (Swarup et al, 2008). The INFLORESCENCE DEFICIENT IN ABSCISSION (IDA)/IDA-LIKE (IDL) signaling peptide family and their receptors HAESA (HAE) and HAESA-LIKE 2 (HSL2) *(see Introduction on peptide signaling)* were also described to play a role in these cell separation processes and act downstream of the Aux/IAA – ARF modules (Kumpf et al, 2013) **(Figure 4)**. Once the lateral root emerges from the parent root, it acquires its own functional meristem, supporting its independent growth (Malamy & Benfey, 1997).

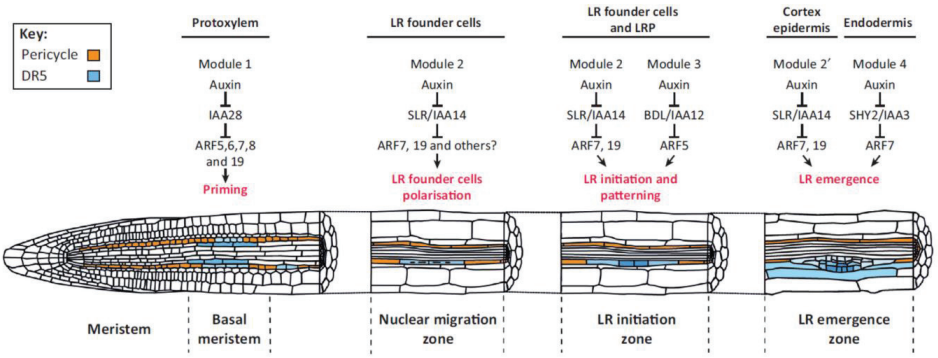


**Figure 4. LR formation is controlled by multiple sequential Aux/IAA - ARF auxin signaling modules.** Priming is controlled by an IAA28 – ARF5, 6, 7, 8 and 19 (mainly ARF7) module. Founder cell specification is controlled by an IAA14/SLR1 – ARF7, 19 module. Lateral root initiation is controlled by an IAA14/SLR1 – ARF7, ARF19 module followed by an IAA12/BDL – ARF5 module. Lateral root primordium emergence is controlled by an IAA14/SLR – ARF7, 19 module and an IAA3/SHY2 – ARF7 module. Additional Aux/IAA – ARF modules (not depicted in this figure) are involved during the different steps of LR formation. (Figure from Lavenus et al, 2013)

# 4. Lateral root inducible system

Considering lateral root initiation is spatially and temporally asynchronous and involves only a limited number of cells, it is very difficult to efficiently follow this process in detail with molecular techniques. To overcome these problems, a system was developed that allows synchronization of the pericycle and enhances the activation of lateral root initiation (Himanen et al, 2002). This lateral root inducible system (LRIS) is based on seed germination in the presence of the auxin transport inhibitor 1-N-naphthylphthalamic acid (NPA), which prevents pericycle activation, followed by a transfer to the synthetic auxin 1-naphthaleneacetic acid (NAA), which induces synchronous lateral root initiation. Targeted broad-scale transcript profiling experiments using the LRIS were used to identify important candidate genes involved in lateral root formation (Himanen et al, 2002; Vanneste et al, 2005; De Smet et al, 2008; Parizot et al, 2010). This system can also be applied to other plant species to study lateral root formation, like for example the monocot maize (Jansen et al, 2013a; Jansen et al, 2013b; Crombez et al, 2016).

# 5. Root system architecture

## 5.1 Definition and parameters

The root system is responsible for anchorage and uptake of water and nutrients from the soil. The efficiency of the root system is determined by its three dimensional distribution pattern in the soil, referred to as the root system architecture (RSA). During evolution, plant species acquired different forms of RSA, each one adapted to their environment **(Figure 5)**.

RSA is dependent on several parameters: (1) the growth rate of the main root and lateral roots (long or short roots); (2) the branching capacity (more or less lateral roots); (3) the angle of the lateral root growth direction compared to the main root axis (horizontally or vertically oriented lateral roots); and (4) selective positioning and outgrowth of lateral roots along the main root axis (regions with dense lateral root network versus regions with a less dense lateral root network) (Lynch, 1995; Kong et al, 2014; Tian et al, 2014) **(Figure 6)**.

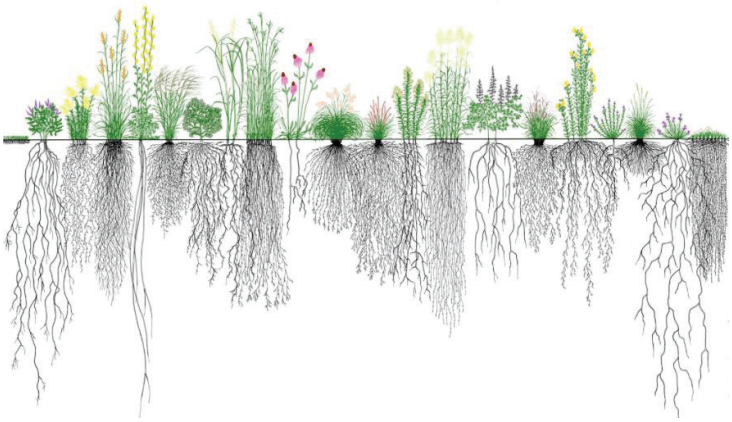

**Figure 5. Root system architecture in different plant species**. (Figure from McNear, 2013)

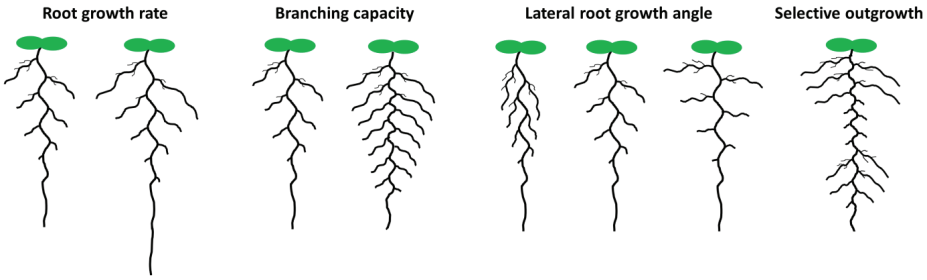


**Figure 6. The main parameters of root system architecture (RSA).**

## 5.2 The impact of environmental conditions

RSA is not solely determined by the genetic background of the plant, but is to a large degree also shaped by environmental conditions. The root system architecture shows a remarkable plasticity, necessary for responding to different situations of (heterogeneous) nutrient availability in the soil (Lopez-Bucio et al, 2003; Malamy, 2005; Giehl et al, 2014) **(Figure 7)**. Some forms of root architecture are better adapted to a certain situation than others. An increased growth rate can lead to longer roots that are able to scan a larger volume of soil for nutrients. An increased number of LRs increases the potential of the root system to scan the soil more thoroughly and therefore allows for a higher uptake of water and nutrients (Gaudin et al, 2014) **(Figure 8A)**. The angle of the lateral roots along the main root axis can also be beneficial for certain conditions. The combination of a long deep primary root with lateral roots that grow out under a sharp angle (steep and deep), leads to a root system that is better adapted for water and nitrogen uptake in deeper regions of the soil (Lynch, 2013; Uga et al, 2013; Uga et al, 2015) **(Figure 8B)**. In contrast, in the case of a shallow root system with lateral roots that grow almost horizontally near the soil surface, the root system is better adapted for phosphate uptake, since this is mainly found near the soil surface (Lynch, 1995; Hammond et al, 2009; Niu et al, 2013) **(Figure 8C)**. Selective positioning or outgrowth of LRs along the main root ensures that the plant only invests energy in lateral root development in regions of nutrient availability **(Figure 8D)**. Thus, adopting a specific type of root system architecture for different environmental conditions will allow the plant to achieve optimal uptake of water and nutrients. Identifying regulators that affect root system architecture might therefore allow engineering the hidden half of crops to improve yield (Kong et al, 2014; Tian et al, 2014).

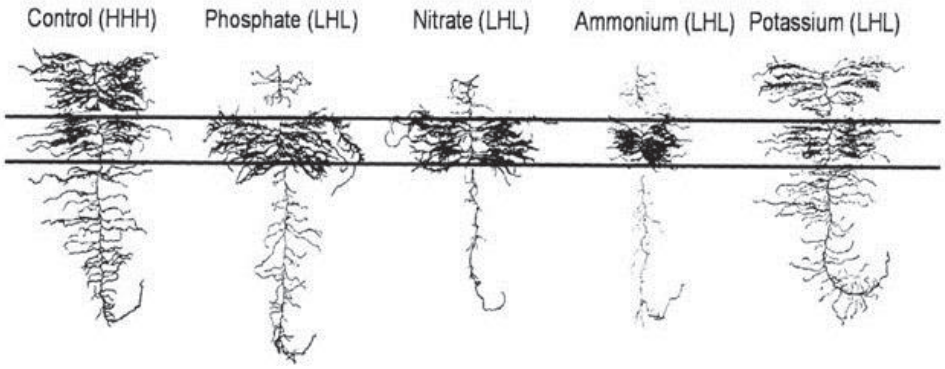


**Figure 7.** Root system architecture is shaped by local environmental differences (H: high concentration of nutrient; L: low concentration of nutrient). (Figure from McNear, 2013)

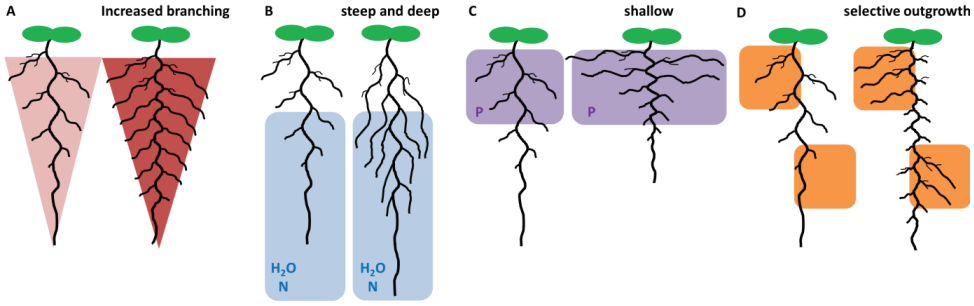


**Figure 8. The plasticity of RSA under different conditions of nutrient availability. (A)** Increased root branching leads to increased uptake of nutrients. **(B)** The steep and deep ideotype is better for water and nitrate uptake deeper in the soil. **(C)** A shallow root system is more suited for phosphate uptake close to the surface. **(D)** Selective outgrowth of lateral roots in regions of high nutrient concentration.

# 6. References


Abel S, Oeller PW, Theologis A (1994) Early auxin-induced genes encode short-lived nuclear proteins. *Proc Natl Acad Sci U S A* **91:** 326-330

Abel S, Theologis A (1996) Early genes and auxin action. *Plant Physiol* **111:** 9-17

Arabidopsis Genome I (2000) Analysis of the genome sequence of the flowering plant Arabidopsis thaliana. *Nature* **408:** 796-815

Arase F, Nishitani H, Egusa M, Nishimoto N, Sakurai S, Sakamoto N, Kaminaka H (2012) IAA8 involved in lateral root formation interacts with the TIR1 auxin receptor and ARF transcription factors in Arabidopsis. *PloS one* **7:** e43414

Beeckman T, Burssens S, Inze D (2001) The peri-cell-cycle in Arabidopsis. *J Exp Bot* **52:** 403-411

Benkova E, Ivanchenko MG, Friml J, Shishkova S, Dubrovsky JG (2009) A morphogenetic trigger: is there an emerging concept in plant developmental biology? *Trends Plant Sci* **14:** 189-193

Benkova E, Michniewicz M, Sauer M, Teichmann T, Seifertova D, Jurgens G, Friml J (2003) Local, efflux-dependent auxin gradients as a common module for plant organ formation. *Cell* **115:** 591-602

Berckmans B, Vassileva V, Schmid SP, Maes S, Parizot B, Naramoto S, Magyar Z, Alvim Kamei CL, Koncz C, Bogre L, Persiau G, De Jaeger G, Friml J, Simon R, Beeckman T, De Veylder L (2011) Auxin-dependent cell cycle reactivation through transcriptional regulation of Arabidopsis E2Fa by lateral organ boundary proteins. *Plant Cell* **23:** 3671-3683

Boer DR, Freire-Rios A, van den Berg WA, Saaki T, Manfield IW, Kepinski S, Lopez-Vidrieo I, Franco-Zorrilla JM, de Vries SC, Solano R, Weijers D, Coll M (2014) Structural basis for DNA binding specificity by the auxin-dependent ARF transcription factors. *Cell* **156:** 577-589

Brady SM, Orlando DA, Lee JY, Wang JY, Koch J, Dinneny JR, Mace D, Ohler U, Benfey PN (2007) A high-resolution root spatiotemporal map reveals dominant expression patterns. *Science* **318:** 801-806

Calderon Villalobos LI, Lee S, De Oliveira C, Ivetac A, Brandt W, Armitage L, Sheard LB, Tan X, Parry G, Mao H, Zheng N, Napier R, Kepinski S, Estelle M (2012) A combinatorial TIR1/AFB-Aux/IAA co-receptor system for differential sensing of auxin. *Nature chemical biology* **8:** 477-485

Casimiro I, Beeckman T, Graham N, Bhalerao R, Zhang H, Casero P, Sandberg G, Bennett MJ (2003) Dissecting Arabidopsis lateral root development. *Trends Plant Sci* **8:** 165-171

Chen R, Hilson P, Sedbrook J, Rosen E, Caspar T, Masson PH (1998) The arabidopsis thaliana AGRAVITROPIC 1 gene encodes a component of the polar-auxin-transport efflux carrier. *Proc Natl Acad Sci U S A* **95:** 15112-15117

Crombez H, Roberts I, Vangheluwe N, Motte H, Jansen L, Beeckman T, Parizot B (2016) Lateral Root Inducible System in Arabidopsis and Maize. *Journal of visualized experiments : JoVE*

De Rybel B, Audenaert D, Xuan W, Overvoorde P, Strader LC, Kepinski S, Hoye R, Brisbois R, Parizot B, Vanneste S, Liu X, Gilday A, Graham IA, Nguyen L, Jansen L, Njo MF, Inze D, Bartel B, Beeckman T (2012) A role for the root cap in root branching revealed by the non-auxin probe naxillin. *Nature chemical biology* **8:** 798-805

De Rybel B, Vassileva V, Parizot B, Demeulenaere M, Grunewald W, Audenaert D, Van Campenhout J, Overvoorde P, Jansen L, Vanneste S, Moller B, Wilson M, Holman T, Van Isterdael G, Brunoud G, Vuylsteke M, Vernoux T, De Veylder L, Inze D, Weijers D, Bennett MJ, Beeckman T (2010) A novel aux/IAA28 signaling cascade activates GATA23-dependent specification of lateral root founder cell identity. *Current biology : CB* **20:** 1697-1706

De Smet I, Lau S, Voss U, Vanneste S, Benjamins R, Rademacher EH, Schlereth A, De Rybel B, Vassileva V, Grunewald W, Naudts M, Levesque MP, Ehrismann JS, Inze D, Luschnig C, Benfey PN, Weijers D, Van Montagu MC, Bennett MJ, Jurgens G, Beeckman T (2010) Bimodular auxin response controls organogenesis in Arabidopsis. *Proc Natl Acad Sci U S A* **107:** 2705-2710

De Smet I, Tetsumura T, De Rybel B, Frei dit Frey N, Laplaze L, Casimiro I, Swarup R, Naudts M, Vanneste S, Audenaert D, Inze D, Bennett MJ, Beeckman T (2007) Auxin-dependent regulation of lateral root positioning in the basal meristem of Arabidopsis. *Development* **134:** 681-690

De Smet I, Vassileva V, De Rybel B, Levesque MP, Grunewald W, Van Damme D, Van Noorden G, Naudts M, Van Isterdael G, De Clercq R, Wang JY, Meuli N, Vanneste S, Friml J, Hilson P, Jurgens G, Ingram GC, Inze D, Benfey PN, Beeckman T (2008) Receptor-like kinase ACR4 restricts formative cell divisions in the Arabidopsis root. *Science* **322:** 594-597

Dharmasiri N, Dharmasiri S, Estelle M (2005a) The F-box protein TIR1 is an auxin receptor. *Nature* **435:** 441-445

Dharmasiri N, Dharmasiri S, Weijers D, Lechner E, Yamada M, Hobbie L, Ehrismann JS, Jurgens G, Estelle M (2005b) Plant development is regulated by a family of auxin receptor F box proteins. *Dev Cell* **9:** 109-119

Dinesh DC, Villalobos LI, Abel S (2016) Structural Biology of Nuclear Auxin Action. *Trends Plant Sci* **21:**302-316

Dolan L, Janmaat K, Willemsen V, Linstead P, Poethig S, Roberts K, Scheres B (1993) Cellular organisation of the Arabidopsis thaliana root. *Development* **119:** 71-84

Dreher KA, Brown J, Saw RE, Callis J (2006) The Arabidopsis Aux/IAA protein family has diversified in degradation and auxin responsiveness. *Plant Cell* **18:** 699-714

Dubrovsky JG, Doerner PW, Colon-Carmona A, Rost TL (2000) Pericycle cell proliferation and lateral root initiation in Arabidopsis. *Plant Physiol* **124:** 1648-1657

Dubrovsky JG, Napsucialy-Mendivil S, Duclercq J, Cheng Y, Shishkova S, Ivanchenko MG, Friml J, Murphy AS, Benkova E (2011) Auxin minimum defines a developmental window for lateral root initiation. *The New phytologist* **191:** 970-983

Dubrovsky JG, Sauer M, Napsucialy-Mendivil S, Ivanchenko MG, Friml J, Shishkova S, Celenza J, Benkova E (2008) Auxin acts as a local morphogenetic trigger to specify lateral root founder cells. *Proc Natl Acad Sci U S A* **105:** 8790-8794

Farcot E, Lavedrine C, Vernoux T (2015) A modular analysis of the auxin signalling network. *PloS one* **10:** e0122231

Feng Z, Sun X, Wang G, Liu H, Zhu J (2012a) LBD29 regulates the cell cycle progression in response to auxin during lateral root formation in Arabidopsis thaliana. *Ann Bot* **110:** 1-10

Feng Z, Zhu J, Du X, Cui X (2012b) Effects of three auxin-inducible LBD members on lateral root formation in Arabidopsis thaliana. *Planta* **236:** 1227-1237

Friml J, Benkova E, Blilou I, Wisniewska J, Hamann T, Ljung K, Woody S, Sandberg G, Scheres B, Jurgens G, Palme K (2002) AtPIN4 mediates sink-driven auxin gradients and root patterning in Arabidopsis. *Cell* **108:** 661-673

Fukaki H, Nakao Y, Okushima Y, Theologis A, Tasaka M (2005) Tissue-specific expression of stabilized SOLITARY-ROOT/IAA14 alters lateral root development in Arabidopsis. *Plant journal* **44:** 382-395

Fukaki H, Tameda S, Masuda H, Tasaka M (2002) Lateral root formation is blocked by a gain-of-function mutation in the SOLITARY-ROOT/IAA14 gene of Arabidopsis. *Plant journal* **29:** 153-168

Gaudin AC, McClymont SA, Soliman SS, Raizada MN (2014) The effect of altered dosage of a mutant allele of Teosinte branched 1 (tb1-ref) on the root system of modern maize. *BMC genetics* **15:** 23

Geldner N, Friml J, Stierhof YD, Jurgens G, Palme K (2001) Auxin transport inhibitors block PIN1 cycling and vesicle trafficking. *Nature* **413:** 425-428

Giehl RF, Gruber BD, von Wiren N (2014) It's time to make changes: modulation of root system architecture by nutrient signals. *J Exp Bot* **65:** 769-778

Goh T, Joi S, Mimura T, Fukaki H (2012a) The establishment of asymmetry in Arabidopsis lateral root founder cells is regulated by LBD16/ASL18 and related LBD/ASL proteins. *Development* **139:** 883-893

Goh T, Kasahara H, Mimura T, Kamiya Y, Fukaki H (2012b) Multiple AUX/IAA-ARF modules regulate lateral root formation: the role of Arabidopsis SHY2/IAA3-mediated auxin signalling. *Philosophical transactions of the Royal Society of London Series B, Biological sciences* **367:** 1461-1468

Gray WM, Kepinski S, Rouse D, Leyser O, Estelle M (2001) Auxin regulates SCF(TIR1)-dependent degradation of AUX/IAA proteins. *Nature* **414:** 271-276

Groover AT, Pattishall A, Jones AM (2003) IAA8 expression during vascular cell differentiation. *Plant Mol Biol* **51:** 427-435

Guilfoyle TJ, Hagen G (2007) Auxin response factors. *Curr Opin Plant Biol* **10:** 453-460

Hammond JP, Broadley MR, White PJ, King GJ, Bowen HC, Hayden R, Meacham MC, Mead A, Overs T, Spracklen WP, Greenwood DJ (2009) Shoot yield drives phosphorus use efficiency in Brassica oleracea and correlates with root architecture traits. *J Exp Bot* **60:** 1953-1968

Heckman DS, Geiser DM, Eidell BR, Stauffer RL, Kardos NL, Hedges SB (2001) Molecular evidence for the early colonization of land by fungi and plants. *Science* **293:** 1129-1133

Himanen K, Boucheron E, Vanneste S, de Almeida Engler J, Inzé D, Beeckman T (2002) Auxin-mediated cell cycle activation during early lateral root initiation. *Plant Cell* **14:** 2339-2351

Hirota A, Kato T, Fukaki H, Aida M, Tasaka M (2007) The auxin-regulated AP2/EREBP gene PUCHI is required for morphogenesis in the early lateral root primordium of Arabidopsis. *Plant Cell* **19:** 2156-2168

Jansen L, Hollunder J, Roberts I, Forestan C, Fonteyne P, Van Quickenborne C, Zhen RG, McKersie B, Parizot B, Beeckman T (2013a) Comparative transcriptomics as a tool for the identification of root branching genes in maize. *Plant biotechnology journal* **11:** 1092-1102

Jansen L, Parizot B, Beeckman T (2013b) Inducible system for lateral roots in Arabidopsis thaliana and maize. *Methods in molecular biology* **959:** 149-158

Kagale S, Rozwadowski K (2011) EAR motif-mediated transcriptional repression in plants: an underlying mechanism for epigenetic regulation of gene expression. *Epigenetics* **6:** 141-146

Kang NY, Lee HW, Kim J (2013) The AP2/EREBP gene PUCHI Co-Acts with LBD16/ASL18 and LBD18/ASL20 downstream of ARF7 and ARF19 to regulate lateral root development in Arabidopsis. *Plant Cell Physiol* **54:** 1326-1334

Ke J, Ma H, Gu X, Thelen A, Brunzelle JS, Li J, Xu HE, Melcher K (2015) Structural basis for recognition of diverse transcriptional repressors by the TOPLESS family of corepressors. *Science advances* **1:** e1500107

Kepinski S, Leyser O (2005) The Arabidopsis F-box protein TIR1 is an auxin receptor. *Nature* **435:** 446-451

Kim H, Park PJ, Hwang HJ, Lee SY, Oh MH, Kim SG (2006) Brassinosteroid signals control expression of the AXR3/IAA17 gene in the cross-talk point with auxin in root development. *Bioscience, biotechnology, and biochemistry* **70:** 768-773

Kim J, Harter K, Theologis A (1997) Protein-protein interactions among the Aux/IAA proteins. *Proc Natl Acad Sci U S A* **94:** 11786-11791

Kong X, Zhang M, De Smet I, Ding Z (2014) Designer crops: optimal root system architecture for nutrient acquisition. *Trends Biotechnol* **32:** 597-598

Korasick DA, Westfall CS, Lee SG, Nanao MH, Dumas R, Hagen G, Guilfoyle TJ, Jez JM, Strader LC (2014) Molecular basis for AUXIN RESPONSE FACTOR protein interaction and the control of auxin response repression. *Proc Natl Acad Sci U S A* **111:** 5427-5432

Kumpf RP, Shi CL, Larrieu A, Sto IM, Butenko MA, Peret B, Riiser ES, Bennett MJ, Aalen RB (2013) Floral organ abscission peptide IDA and its HAE/HSL2 receptors control cell separation during lateral root emergence. *Proc Natl Acad Sci U S A* **110:** 5235-5240

Laplaze L, Parizot B, Baker A, Ricaud L, Martiniere A, Auguy F, Franche C, Nussaume L, Bogusz D, Haseloff J (2005) GAL4-GFP enhancer trap lines for genetic manipulation of lateral root development in Arabidopsis thaliana. *J Exp Bot* **56:** 2433-2442

Laskowski M, Biller S, Stanley K, Kajstura T, Prusty R (2006) Expression profiling of auxin-treated Arabidopsis roots: toward a molecular analysis of lateral root emergence. *Plant Cell Physiol* **47:** 788-792

Lavenus J, Goh T, Guyomarc'h S, Hill K, Lucas M, Voss U, Kenobi K, Wilson MH, Farcot E, Hagen G, Guilfoyle TJ, Fukaki H, Laplaze L, Bennett MJ (2015) Inference of the Arabidopsis lateral root gene regulatory network suggests a bifurcation mechanism that defines primordia flanking and central zones. *Plant Cell* **27:** 1368-1388

Lavenus J, Goh T, Roberts I, Guyomarc'h S, Lucas M, De Smet I, Fukaki H, Beeckman T, Bennett M, Laplaze L (2013) Lateral root development in Arabidopsis: fifty shades of auxin. *Trends Plant Sci* **18:** 450-458

Ljung K, Hull AK, Celenza J, Yamada M, Estelle M, Normanly J, Sandberg G (2005) Sites and regulation of auxin biosynthesis in Arabidopsis roots. *Plant Cell* **17:** 1090-1104

Lopez-Bucio J, Cruz-Ramirez A, Herrera-Estrella L (2003) The role of nutrient availability in regulating root architecture. *Curr Opin Plant Biol* **6:** 280-287

Lucas M, Godin C, Jay-Allemand C, Laplaze L (2008a) Auxin fluxes in the root apex co-regulate gravitropism and lateral root initiation. *J Exp Bot* **59:** 55-66

Lucas M, Guedon Y, Jay-Allemand C, Godin C, Laplaze L (2008b) An auxin transport-based model of root branching in Arabidopsis thaliana. *PloS one* **3:** e3673

Lucas M, Kenobi K, von Wangenheim D, Vobeta U, Swarup K, De Smet I, Van Damme D, Lawrence T, Peret B, Moscardi E, Barbeau D, Godin C, Salt D, Guyomarc'h S, Stelzer EH, Maizel A, Laplaze L, Bennett MJ (2013) Lateral root morphogenesis is dependent on the mechanical properties of the overlaying tissues. *Proc Natl Acad Sci U S A* **110:** 5229-5234

Luschnig C, Gaxiola RA, Grisafi P, Fink GR (1998) EIR1, a root-specific protein involved in auxin transport, is required for gravitropism in Arabidopsis thaliana. *Genes & development* **12:** 2175-2187

Lynch J (1995) Root Architecture and Plant Productivity. *Plant Physiol* **109:** 7-13

Lynch JP (2013) Steep, cheap and deep: an ideotype to optimize water and N acquisition by maize root systems. *Ann Bot* **112:** 347-357

Malamy JE (2005) Intrinsic and environmental response pathways that regulate root system architecture. *Plant, cell & environment* **28:** 67-77

Malamy JE, Benfey PN (1997) Organization and cell differentiation in lateral roots of Arabidopsis thaliana. *Development* **124:** 33-44

Marin E, Jouannet V, Herz A, Lokerse AS, Weijers D, Vaucheret H, Nussaume L, Crespi MD, Maizel A (2010) miR390, Arabidopsis TAS3 tasiRNAs, and their AUXIN RESPONSE FACTOR targets define an autoregulatory network quantitatively regulating lateral root growth. *Plant Cell* **22:** 1104-1117

McNear DH (2013) The Rhizosphere - Roots, Soil and Everything In Between. *Nature Education Knowledge* **4(3):**1

Moreno-Risueno MA, Van Norman JM, Moreno A, Zhang J, Ahnert SE, Benfey PN (2010) Oscillating gene expression determines competence for periodic Arabidopsis root branching. *Science* **329:** 1306-1311

Muller A, Guan C, Galweiler L, Tanzler P, Huijser P, Marchant A, Parry G, Bennett M, Wisman E, Palme K (1998) AtPIN2 defines a locus of Arabidopsis for root gravitropism control. *The EMBO journal* **17:** 6903-6911

Nanao MH, Vinos-Poyo T, Brunoud G, Thevenon E, Mazzoleni M, Mast D, Laine S, Wang S, Hagen G, Li H, Guilfoyle TJ, Parcy F, Vernoux T, Dumas R (2014) Structural basis for oligomerization of auxin transcriptional regulators. *Nature communications* **5:** 3617

Neuteboom LW, Veth-Tello LM, Clijdesdale OR, Hooykaas PJ, van der Zaal BJ (1999) A novel subtilisin-like protease gene from Arabidopsis thaliana is expressed at sites of lateral root emergence. *DNA Res* **6:** 13-19

Nieuwland J, Maughan S, Dewitte W, Scofield S, Sanz L, Murray JA (2009) The D-type cyclin CYCD4;1 modulates lateral root density in Arabidopsis by affecting the basal meristem region. *Proc Natl Acad Sci U S A* **106:** 22528-22533

Niu YF, Chai RS, Jin GL, Wang H, Tang CX, Zhang YS (2013) Responses of root architecture development to low phosphorus availability: a review. *Ann Bot* **112:** 391-408

Okushima Y, Fukaki H, Onoda M, Theologis A, Tasaka M (2007) ARF7 and ARF19 regulate lateral root formation via direct activation of LBD/ASL genes in Arabidopsis. *Plant Cell* **19:** 118-130

Okushima Y, Overvoorde PJ, Arima K, Alonso JM, Chan A, Chang C, Ecker JR, Hughes B, Lui A, Nguyen D, Onodera C, Quach H, Smith A, Yu G, Theologis A (2005) Functional genomic analysis of the AUXIN RESPONSE FACTOR gene family members in Arabidopsis thaliana: unique and overlapping functions of ARF7 and ARF19. *Plant Cell* **17:** 444-463

Orman-Ligeza B, Parizot B, Gantet PP, Beeckman T, Bennett MJ, Draye X (2013) Post-embryonic root organogenesis in cereals: branching out from model plants. *Trends Plant Sci* **18:** 459-467

Parizot B, De Rybel B, Beeckman T (2010) VisuaLRTC: a new view on lateral root initiation by combining specific transcriptome data sets. *Plant Physiol* **153:** 34-40

Parizot B, Laplaze L, Ricaud L, Boucheron-Dubuisson E, Bayle V, Bonke M, De Smet I, Poethig SR, Helariutta Y, Haseloff J, Chriqui D, Beeckman T, Nussaume L (2008) Diarch symmetry of the vascular bundle in Arabidopsis root encompasses the pericycle and is reflected in distich lateral root initiation. *Plant Physiol* **146:** 140-148

Parizot B, Roberts I, Raes J, Beeckman T, De Smet I (2012) In silico analyses of pericycle cell populations reinforce their relation with associated vasculature in Arabidopsis. *Philosophical transactions of the Royal Society of London Series B, Biological sciences* **367:** 1479-1488

Peret B, De Rybel B, Casimiro I, Benkova E, Swarup R, Laplaze L, Beeckman T, Bennett MJ (2009a) Arabidopsis lateral root development: an emerging story. *Trends Plant Sci* **14:** 399-408

Peret B, Larrieu A, Bennett MJ (2009b) Lateral root emergence: a difficult birth. *J Exp Bot* **60:** 3637-3643

Perilli S, Di Mambro R, Sabatini S (2012) Growth and development of the root apical meristem. *Curr Opin Plant Biol* **15:** 17-23

Petersson SV, Johansson AI, Kowalczyk M, Makoveychuk A, Wang JY, Moritz T, Grebe M, Benfey PN, Sandberg G, Ljung K (2009) An auxin gradient and maximum in the Arabidopsis root apex shown by high-resolution cell-specific analysis of IAA distribution and synthesis. *Plant Cell* **21:** 1659-1668

Piya S, Shrestha SK, Binder B, Stewart CN, Jr., Hewezi T (2014) Protein-protein interaction and gene co-expression maps of ARFs and Aux/IAAs in Arabidopsis. *Frontiers in plant science* **5:** 744

Rinaldi MA, Liu J, Enders TA, Bartel B, Strader LC (2012) A gain-of-function mutation in IAA16 confers reduced responses to auxin and abscisic acid and impedes plant growth and fertility. *Plant Mol Biol* **79:** 359-373

Rogg LE, Lasswell J, Bartel B (2001) A gain-of-function mutation in IAA28 suppresses lateral root development. *Plant Cell* **13:** 465-480

Schiefelbein JW, Masucci JD, Wang H (1997) Building a root: the control of patterning and morphogenesis during root development. *Plant Cell* **9:** 1089-1098

Smith S, De Smet I (2012) Root system architecture: insights from Arabidopsis and cereal crops. *Philosophical transactions of the Royal Society of London Series B, Biological sciences* **367:** 1441-1452

Sozzani R, Iyer-Pascuzzi A (2014) Postembryonic control of root meristem growth and development. *Curr Opin Plant Biol* **17:** 7-12

Swarup K, Benkova E, Swarup R, Casimiro I, Peret B, Yang Y, Parry G, Nielsen E, De Smet I, Vanneste S, Levesque MP, Carrier D, James N, Calvo V, Ljung K, Kramer E, Roberts R, Graham N, Marillonnet S, Patel K, Jones JD, Taylor CG, Schachtman DP, May S, Sandberg G, Benfey P, Friml J, Kerr I, Beeckman T, Laplaze L, Bennett MJ (2008) The auxin influx carrier LAX3 promotes lateral root emergence. *Nat Cell Biol* **10:** 946-954

Szemenyei H, Hannon M, Long JA (2008) TOPLESS mediates auxin-dependent transcriptional repression during Arabidopsis embryogenesis. *Science* **319:** 1384-1386

Tan X, Calderon-Villalobos LI, Sharon M, Zheng C, Robinson CV, Estelle M, Zheng N (2007) Mechanism of auxin perception by the TIR1 ubiquitin ligase. *Nature* **446:** 640-645

Tatematsu K, Kumagai S, Muto H, Sato A, Watahiki MK, Harper RM, Liscum E, Yamamoto KT (2004) MASSUGU2 encodes Aux/IAA19, an auxin-regulated protein that functions together with the transcriptional activator NPH4/ARF7 to regulate differential growth responses of hypocotyl and formation of lateral roots in Arabidopsis thaliana. *Plant Cell* **16:** 379-393

Tian H, De Smet I, Ding Z (2014) Shaping a root system: regulating lateral versus primary root growth. *Trends Plant Sci* **19:** 426-431

Tian Q, Reed JW (1999) Control of auxin-regulated root development by the Arabidopsis thaliana SHY2/IAA3 gene. *Development* **126:** 711-721

Tiwari SB, Hagen G, Guilfoyle T (2003) The roles of auxin response factor domains in auxin-responsive transcription. *Plant Cell* **15:** 533-543

Tiwari SB, Hagen G, Guilfoyle TJ (2004) Aux/IAA proteins contain a potent transcriptional repression domain. *Plant Cell* **16:** 533-543

Uehara T, Okushima Y, Mimura T, Tasaka M, Fukaki H (2008) Domain II mutations in CRANE/IAA18 suppress lateral root formation and affect shoot development in Arabidopsis thaliana. *Plant Cell Physiol* **49:** 1025-1038

Uga Y, Kitomi Y, Ishikawa S, Yano M (2015) Genetic improvement for root growth angle to enhance crop production. *Breeding science* **65:** 111-119

Uga Y, Sugimoto K, Ogawa S, Rane J, Ishitani M, Hara N, Kitomi Y, Inukai Y, Ono K, Kanno N, Inoue H, Takehisa H, Motoyama R, Nagamura Y, Wu J, Matsumoto T, Takai T, Okuno K, Yano M (2013) Control of root system architecture by DEEPER ROOTING 1 increases rice yield under drought conditions. *Nat Genet* **45:** 1097-1102

Ulmasov T, Hagen G, Guilfoyle TJ (1999) Activation and repression of transcription by auxin-response factors. *Proc Natl Acad Sci U S A* **96:** 5844-5849

Ulmasov T, Murfett J, Hagen G, Guilfoyle TJ (1997) Aux/IAA proteins repress expression of reporter genes containing natural and highly active synthetic auxin response elements. *Plant Cell* **9:** 1963-1971

Vanneste S, De Rybel B, Beemster GT, Ljung K, De Smet I, Van Isterdael G, Naudts M, Iida R, Gruissem W, Tasaka M, Inze D, Fukaki H, Beeckman T (2005) Cell cycle progression in the pericycle is not sufficient for SOLITARY ROOT/IAA14-mediated lateral root initiation in Arabidopsis thaliana. *Plant Cell* **17:** 3035-3050

von Wangenheim D, Fangerau J, Schmitz A, Smith RS, Leitte H, Stelzer EH, Maizel A (2016) Rules and Self-Organizing Properties of Post-embryonic Plant Organ Cell Division Patterns. *Current biology : CB* **26:** 439-449

Weijers D, Benkova E, Jager KE, Schlereth A, Hamann T, Kientz M, Wilmoth JC, Reed JW, Jurgens G (2005) Developmental specificity of auxin response by pairs of ARF and Aux/IAA transcriptional regulators. *The EMBO journal* **24:** 1874-1885

Wilmoth JC, Wang S, Tiwari SB, Joshi AD, Hagen G, Guilfoyle TJ, Alonso JM, Ecker JR, Reed JW (2005) NPH4/ARF7 and ARF19 promote leaf expansion and auxin-induced lateral root formation. *Plant journal* **43:** 118-130

Xuan W, Audenaert D, Parizot B, Moller BK, Njo MF, De Rybel B, De Rop G, Van Isterdael G, Mahonen AP, Vanneste S, Beeckman T (2015) Root Cap-Derived Auxin Pre-patterns the Longitudinal Axis of the Arabidopsis Root. *Current biology : CB* **25:** 1381-1388

Xuan W, Band LR, Kumpf RP, Van Damme D, Parizot B, De Rop G, Opdenacker D, Moller BK, Skorzinski N, Njo MF, De Rybel B, Audenaert D, Nowack MK, Vanneste S, Beeckman T (2016) Cyclic programmed cell death stimulates hormone signaling and root development in Arabidopsis. *Science* **351:** 384-387

Yang X, Lee S, So JH, Dharmasiri S, Dharmasiri N, Ge L, Jensen C, Hangarter R, Hobbie L, Estelle M (2004) The IAA1 protein is encoded by AXR5 and is a substrate of SCF(TIR1). *Plant journal* **40:** 772-782

Yoon EK, Yang JH, Lim J, Kim SH, Kim SK, Lee WS (2010) Auxin regulation of the microRNA390-dependent transacting small interfering RNA pathway in Arabidopsis lateral root development. *Nucleic acids research* **38:** 1382-1391

# Chapter 2:

## Peptide signaling in *Arabidopsis*

# 1. General introduction on secreted signaling peptides

Over the years, it has become increasingly clear that secreted signaling peptides play an important role in cell-cell communication processes during plant growth and development, and are also involved in defense response and symbiosis (Marshall et al, 2011; Czyzewicz et al, 2013; Okamoto et al, 2013; Hou et al, 2014; Tavormina et al, 2015).

Secreted signaling peptides generally act as ligands for receptor(-like) kinase (RLK) proteins (Butenko et al, 2009; Murphy et al, 2012). The large group of RLK proteins in the plant lineage evolved independently from the two large groups of receptor tyrosine kinases and receptor serine/threonine kinases in the metazoan lineage, and originated from a common ancestral protein family from which the Pelle receptor kinases in animals also evolved (Shiu & Bleecker, 2001; Cock et al, 2002). Many structural differences between the plant and metazoan receptor kinase groups exist, although some basic features (*e.g.* auto-phosphorylation upon ligand binding, the formation of large receptor complexes with cytoplasmic kinases and phosphatases and downstream kinase cascade signaling) are similar through convergent evolution (Cock et al, 2002).

RLKs in plants typically have an N-terminal extracellular receptor domain connected via a transmembrane region to a C-terminal cytoplasmic kinase domain. Binding of the secreted peptide ligand to the extracellular receptor domain often triggers (auto)phosphorylation activity in the intracellular kinase domain and subsequently triggers a phosphorylation cascade of cytoplasmic protein kinases. Recent evidence suggests that RLKs often interact with a co-receptor upon binding of the peptide ligand to the receptor domain, in which the peptide ligand acts as molecular glue between both receptor domains. This leads to an interaction between both intracellular domains and subsequently triggers a cytoplasmic phosphorylation cascade (Hothorn et al, 2011; Santiago et al, 2013; Sun et al, 2013a) **(Figure 1)**.

Considering their involvement in such a wide array of biological processes, a large number of different secreted peptides and RLKs are expected. Based on genome-wide *in silico* sequence analysis, it is estimated that there are over 1000 secreted peptides and 600 RLKs encoded in the *Arabidopsis* genome, which can be divided into many different families based on their sequence homology (Shiu & Bleecker, 2001; Lease & Walker, 2006; Ghorbani et al, 2015). The often highly conserved peptide sequences accompanied by the sometimes large numbers of peptides within a family (some families count more than 30 members) frequently results in functional redundancy. This explains why so few secreted peptides have been identified through classical forward genetics, in which the knock-out of a single peptide gene resulted in a clear mutant phenotype (Clark et al, 1996; Matsubayashi & Sakagami, 1996; Pearce et al, 2001; Butenko et al, 2003). As a consequence, most currently known peptide families were identified through *in silico* studies based on several known features of previously identified secreted signaling peptides. Although, it is likely that additional types of signaling peptides, with different features, will be identified in future proteome studies (such as peptides derived from functional precursor proteins).

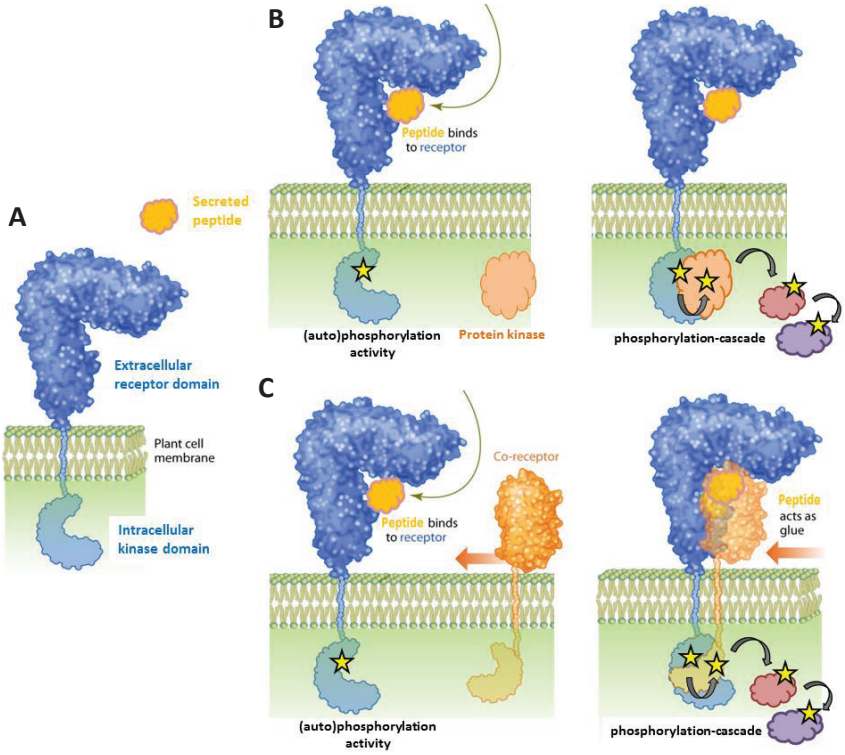


**Figure 1. Peptide – receptor binding. (A)** Structure of a receptor-like kinase (RLK) protein. **(B)** Binding of the peptide ligand to the RLK induces (auto)phosphorylation activity and triggers an intracellular protein kinase phosphorylation cascade. **(C)** A co-receptor interacts with the RLK upon peptide ligand binding, triggering an intracellular phosphorylation cascade. (Figure adapted from NSF press release 11-119, June 14 2011)

# 2. Features of signaling peptides

## 2.1 Classification of signaling peptides

Recently a new classification system for signaling peptides based on their features was suggested, dividing them into two major groups: precursor-derived and non-precursor-derived peptides (Tavormina et al, 2015) **(Figure 2)**. Peptides from the latter group are only just emerging on the scene and are directly translated from small open reading frames (sORFs) (<100 amino acids) located in the 5' region of a gene, in primary transcripts of miRNAs or in other transcript encoding sORFs, leading to the production of peptides such as POLARIS (PLS), EARLY NODULIN GENE 40 (ENOD40), ROTUNDIFOLIA FOUR (ROT4), KISS OF DEATH (KOD), DEVIL 1 (DVL1) and OXIDATIVE STRESS-INDUCED PEPTIDE 108 (OSIP108) (Tavormina et al, 2015). However, most well-characterized signaling peptides belong to the precursor-derived group. This group can be divided into two subgroups: peptides derived from a non-functional precursor and those derived from a functional precursor (the peptide originates from a functional protein with a different activity than the derived peptide). To date secreted signaling peptides derived from a nonfunctional precursor were studied most intensively. These can be further subdivided into three classes: small post-translationally modified peptides, cysteine-rich peptides and finally peptides that are neither post-translationally modified nor contain cysteine-rich regions.

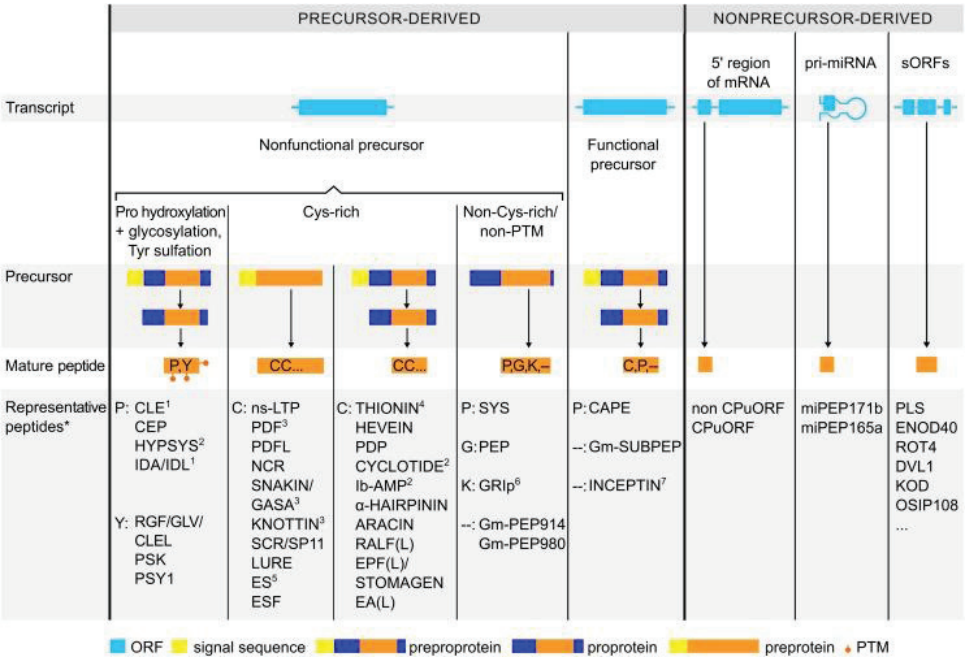


**Figure 2. Classification system of signaling peptides based on features.** (Figure from Tavormina et al, 2015)

### 2.1.1 Small post-translationally modified peptides

Small post-translationally modified peptides are translated as a nonfunctional precursor preproprotein/prepropeptide with an N-terminal signal peptide sequence that targets the peptide to the secretion pathway and is later cleaved to form a proprotein/propeptide. The proprotein/propeptide contains a variable region likely involved in processing of the mature peptide and a conserved C-terminal domain that is proteolytically processed into a small mature peptide of usually less than 20 amino acid residues. The mature peptide generally undergoes at least one type of post-translational modification, such as tyrosine sulfation, proline hydroxylation, or hydroxyproline arabinosylation (Matsubayashi, 2014).

The best known small post-translationally modified peptides include the PHYTOSULFOKINE (PSK) family (Matsubayashi & Sakagami, 1996; Yang et al, 1999; Yang et al, 2000; Yang et al, 2001), PLANT PEPTIDE CONTAINING SULFATED TYROSINE1 (PSY1) (Amano et al, 2007), ROOT GROWTH FACTOR / GOLVEN / CLE-LIKE (RGF/GLV/CLEL) family (Matsuzaki et al, 2010; Whitford et al, 2012; Fernandez et al, 2013a; Fernandez et al, 2013b), CLAVATA(CLV)/EMBRYO SURROUNDING REGION (ESR)-RELATED PROTEIN (CLE) family (Fletcher et al, 1999; Cock & McCormick, 2001), INFLORESCENCE DEFICIENT IN ABSCISSION (IDA) and IDA-LIKE (IDL) family (Butenko et al, 2003), PAMP-INDUCED SECRETED PEPTIDE (PIP) and PIP-LIKE (PIPL) family (Hou et al, 2014; Vie et al, 2015), and the C-TERMINALLY ENCODED PEPTIDE (CEP) family (Ohyama et al, 2008; Delay et al, 2013; Roberts et al, 2013).

Post-translational modifications have been shown to alter the conformation and physicochemical properties of the secreted peptides and increase the binding affinity and specificity for their receptor protein (Ohyama et al, 2009; Shinohara & Matsubayashi, 2013).

Until now, tyrosine sulfation has been identified in the PSK (Matsubayashi & Sakagami, 1996), PSY1 (Amano et al, 2007) and RGF/GLV/CLEL family (Matsuzaki et al, 2010; Whitford et al, 2012) and is mediated by the *cis*-Golgi-localized transmembrane TYROSYLPROTEIN SULFOTRANSFERASE (TPST). TPST catalyzes the transfer of a sulfate group from 3'-phosphoadenosine 5'-phosphosulfate (PAPS) to the phenolic group of a tyrosine residue which has an N-terminally adjacent aspartic acid residue (DY motif) and is often accompanied by multiple acidic amino acids nearby (Komori et al, 2009).

Proline hydroxylation occurs in the PSY (Amano et al, 2007), RGF/GLV/CLEL (Matsuzaki et al, 2010), CLE (Ito et al, 2006; Kondo et al, 2006) and CEP (Ohyama et al, 2008) peptide families and is mediated by PROLYL-4-HYDROXYLASE (P4H). P4H is an endoplasmic reticulum (ER)/Golgi-localized transmembrane 2-oxoglutarate-dependent dioxygenase (Yuasa et al, 2005).

In the PSY, CLE and CEP family, some of the hydroxyproline (hyp) residues have been shown to be further modified with an β-1-,2-linked tri-arabinoside chain mediated by the Golgi-localized transmembrane HYDROXYPROLINE O-ARABINOSYLTRANSFERASE (HPAT) (Amano et al, 2007; Ohyama et al, 2009; Ogawa-Ohnishi et al, 2013; Mohd-Radzman et al, 2015).

### 2.1.2 Cysteine-rich peptides

The class of cysteine-rich peptides can be further subdivided into two subclasses. Peptides from the first subclass are synthesized as a prepeptide with a conserved N-terminal signal peptide domain targeting them to the secretion pathway. The mature peptide is formed after signal peptide cleavage and intramolecular disulfide bond formation between (4 to 16) cysteine residues (Marshall et al, 2011). This subclass includes among others the plant defensin (PDF) family (Thomma et al, 2002), the LURE family (Okuda et al, 2009) and the S LOCUS CYSTEIN RICH PROTEIN / S LOCUS PROTEIN 11 (SCR/SP11) family (Schopfer et al, 1999; Takayama et al, 2000). The second subclass of cysteine-rich peptides are synthesized as prepropeptide with an N-terminal secretory signal peptide, which is cleaved to form a propeptide that undergoes further proteolytic processing into a mature peptide also with intramolecular disulfide bonds between an even number of cysteine residues. This subclass includes among others the RAPID ALKALINIZATION FACTOR (RALF) family (Pearce et al, 2001; Murphy & De Smet, 2014), the EPIDERMAL PATTERNING FACTOR (EPF) and EPF-LIKE family (including EPFL9/STOMAGEN) (Hara et al, 2007) (Hara et al, 2009; Sugano et al, 2010) and the ARACIN family (Neukermans et al, 2015).

### 2.1.3 Non-Cys rich/non-PTM peptides

Signaling peptides from the third class are synthesized as propeptides that are further proteolytically processed into a mature peptide without disulfide bridges or post-translation modifications. This subclass includes among others: SYSTEMIN (SYS) (Pearce et al, 1991), PLANT ELLICITOR PEPTIDES (PEPs) (Pearce et al, 2008) and GRIM REAPER PEPTIDE (GRIp) (Wrzaczek et al, 2015).

## 2.2 Peptide processing

At the moment, there are few enzymes that have been linked to propeptide-processing into mature peptides for the above-mentioned peptide families. There are over 700 putative protease-encoding genes encoded in the *Arabidopsis* genome (Tsiatsiani et al, 2012). From these, the subtilisin-like serine proteases (subtilases/AtSBTs) are suggested as signal peptide proteases. Only a few of the 56 subtilases encoded in the *Arabidopsis* genome have been linked to a peptide family (Rautengarten et al, 2005). The PSK4 propeptide is cleaved by AtSBT1.1 (Srivastava et al, 2008), the RGF/GLV/CLEL

peptides are processed by AtSBT6.1 and AtSBT6.2 (Ghorbani et al., in press), the RALF23 propeptide is likely cleaved by AtSBT6.1 subtilase (Srivastava et al, 2009), and overexpression of AtSBT5.4 was shown to reproduce a *clavata*-like mutant phenotype with enhanced SAM formation, although cleavage of CLV3 could not be proven (Liu et al, 2009). Another two subtilisin-like serine proteases are STOMATA DENSITY AND DISTRIBUTION 1 (SDD1) and ABNORMAL LEAF SHAPE 1 (ALE1) and are likely involved in processing the EPF peptides, which bind the ERECTA family of RLKs (Berger & Altmann, 2000). However, not only proteases of the subtilase family are signal peptide processing enzymes, as the propeptide of CLE19 might be cleaved by the $Zn^{2+}$ carboxypeptidase SUPRESSOR OF LIGAND-LIKE PROTEIN 1 (SOL1) (Casamitjana-Martinez et al, 2003), and the GRIp peptide is processed by a member of the metacaspase family, METACASPASE-9 (Wrzaczek et al, 2015).

# 3. Features of Receptor-Like Kinases

Over 600 RLKs proteins are encoded in the *Arabidopsis* genome (Shiu & Bleecker, 2001). The largest group by far is the Leucine-Rich Repeat (LRR)-RLK group, with over 200 members in *Arabidopsis*. These receptors are known to bind a wide range of ligands such as phytohormones, pathogen-associated molecular pattern (PAMP)-derived peptides, microbe-associated molecular pattern (MAMP)-derived peptides, damage-associated molecular pattern (DAMP)-derived peptides and secreted signaling peptides. Most currently characterized secreted signaling peptides bind to LRR-RLKs. LRR-RLKs contain an N-terminal secretion signal peptide sequence that targets them to the plasma membrane via the secretion pathway, followed by an extracellular receptor LRR domain, a single helical transmembrane region and a C-terminal cytoplasmic kinase domain that is involved in downstream signaling. A closely related group of proteins is formed by the receptor-like proteins (RLPs), which similarly contain an extracellular (LRR) receptor domain and a transmembrane region, but lack a cytoplasmic kinase domain **(Figure 3)**.

## 3.1 The extracellular receptor domain

The LRR domain of LRR-RLKs counts 4 to 28 LRR repeating units, which are known to be involved in protein-ligand and protein-protein interactions (Kobe & Kajava, 2001). The LRR domains evolved to display a large variety of surface amino acids combinations on a relatively invariant scaffold to allow interaction with a wide array of proteins (Kobe & Kajava, 2001; Bella et al, 2008). These LRR repeating units are usually 23-25 residues long and can be divided into a highly conserved segment (HCS) followed by a variable segment (VS). The HCS consists of an 11 residue motif LxxLxLxxNxL or a 12 residue motif LxxLxLxxCxxL (with typically L = Leu, Ile, Val or Phe; N = Asn, Thr, Ser or Cys; C = Cys, Ser or Asn; and x = any amino acid), while the VS consists of a 13 residue motif SGxIPxxLxxLxx (with typically S = Ser or Thr; G = Gly or Ser; I = Ile or Leu; L = Leu, Ile, Val, Phe or Met; and x = any amino acid). Each LRR repeating unit is thought to form a β-strand – turn – α-helix structure, and all LRR units together fold into a right-handed superhelix that adopts an arc shape that contains an exterior array of alpha helices and an interior beta sheet that forms the binding pocket for its ligand (Bella et al, 2008) **(Figure 3)**.

Some LRR-RLKs contain an 'island domain' (ID), a non-LRR loop, which is inserted between LRR units and is involved in ligand binding. For example, well-known LRR-RLKs with an island domain include: BRI1, PSKR, PSYR1 and RPK2. Well-known LRR-RLPs with an island domain include: CLV2 and RLP2. Notably, in most cases the island domain tends to be located between the $4^{th}$ and $5^{th}$ LRR unit counting from the transmembrane region (Matsushima & Miyashita, 2012).

Smaller ligands (*e.g.* brassinosteroid hormones or small 5-aa PSK signaling peptides) tend to require these island domains for specific ligand binding, while larger ligands (*e.g.* flg22 peptide or CLE signaling peptides) do not need an island domain, but bind along a stretch of LRR units at the inner side of the LRR receptor backbone. The sequence of these interacting LRR units generally slightly deviates from the consensus LRR sequence (Shinohara et al, 2012; Sun et al, 2013a). This might allow mapping the LRR units involved in ligand binding based on sequence alignment analysis of LRR receptor domains.

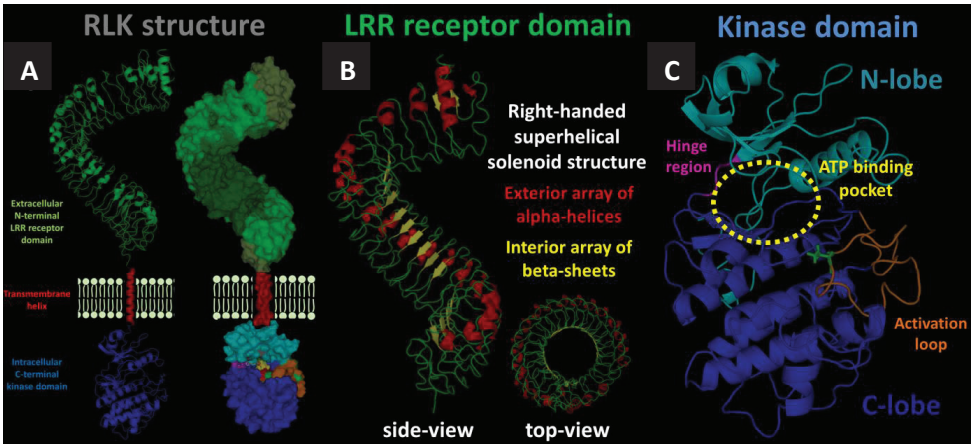


**Figure 3. Structure of LRR-RLK. (A)** Overall structure of a LRR-RLK, with an extracellular N-terminal LRR receptor domain, a single transmembrane helix and an intracellular C-terminal kinase domain. **(B)** The LRR receptor domain adopts a right-handed superhelical solenoid structure with an exterior array of alpha-helices and an interior array of beta-sheets acting as the peptide ligand binding site. **(C)** The kinase domain is composed of two lobes, the N-lobe and C-lobe, connected by a flexible hinge region, with the catalytic cleft and ATP binding pocket sandwiched in between them. The C-lobe contains the activation loop, which contains phosphorylation sites and is crucial for switching between active/inactive states of the kinase. (Figures from structure of XIP1/CEPR1, generated *in silico* with i-Tasser software)

The LRR-domain is usually flanked by N-terminal (NT) and C-terminal (CT) caps containing two or four cysteine residues that form disulfide bridges, and are referred to as the LRRNT and outer juxtamembrane LRRCT domain respectively. These structures are thought to shield the hydrophobic core of the first and last LRR unit (Bella et al, 2008; Botos et al, 2011). While most LRR-RLKs contain an LRRNT, not all contain an LRRCT (Matsushima & Miyashita, 2012).

Based on several observations, the LRR receptor domain is believed to undergo glycosylation modifications required for functionality. Mutations that affect N-linked glycosylation in EFR were shown to abolish its functionality (Li et al, 2009). The LRR-domain from FLS2 is predicted to have 21 NxS/T glycosylation sites. Based on the difference between the measured electrophoretic mobility of 175 kDa versus the calculated molecular size of 126 kDa, and the shift to 130 kDa upon chemical deglycosylation, glycosylation at these sites seems likely (Chinchilla et al, 2006; Haweker et al, 2010). Glycosylation is unlikely to be involved in ligand binding, since it occurs at the convex surface of the receptor domain, while introducing an N-glycosylation site at the concave surface abolishes functionality of the receptor (van der Hoorn et al, 2005). The glycosylation modifications occur in the endoplasmic reticulum and are implicated in correct folding and stability of the receptor (Liebrand et al, 2012).

## 3.2 The intracellular kinase domain

The intracellular kinase domain of LRR-RLKs is involved in ligand-induced downstream signaling by initiating a phosphorylation cascade that involves other kinase proteins. Kinase domains catalyze the transfer of the γ-phosphate group from adenosine triphosphate (ATP) to a substrate protein. Most currently described typical RLKs are members of the Ser/Thr kinase domain family. The Ser/Thr kinase domain is structurally divided in two lobes, an N-terminal lobe formed mainly from beta strands, and a C-terminal lobe formed almost entirely from alpha helices. Sandwiched between the two lobes, which are connected by a flexible hinge region, lies the catalytic cleft with the ATP nucleotide binding site. The flexible hinge between the two lobes allows major conformational changes that accompany activation/inactivaton of the kinase domain. Highly conserved residues from both lobes shape the ATP nucleotide binding site. The N-lobe typically contains a conserved glycine loop (GxGxxG) that is involved in creating a cleft for ATP binding. The N-lobe also contains a conserved Lys residue that interacts with the α- and β-phosphate groups of ATP and forms a salt bridge with a conserved Glu residue, which stabilizes the activated form of the kinase. A conserved Glu and Met residue from the hinge region make H-bonds with the adenine base group of ATP. The C-lobe contains a conserved Asn residue that interacts with the α- and β-phosphate group of ATP, and a conserved Asp residue that coordinates a $Mn^{2+}$ ion, which interacts with the β- and γ-phosphate groups of ATP. Another conserved Asp residue in the C-lobe (situated next to a conserved Arg residue, together forming the RD-motif), together with a nearby conserved Lys residue, interacts with the γ-phosphate group of ATP and acts as the catalytic base in the phospho-transfer reaction to the acceptor Thr residue in the activation-loop (A-loop). The A-loop is located in the C-lobe between strand β8 and helix αEF, starting and finishing at the conserved triplets Asp-Phe-Gly (DFG) and Ala-Pro-Glu (APE). The A-loop plays a central role in regulating catalytic activity. In an activated state of the kinase domain, a phosphorylation site in the A-loop is phosphorylated, which induces a specific conformational change that brings the phospho-acceptor Thr residue in close proximity to the catalytic base of the conserved Asp residue from the RD-motif in the ATP binding pocket. In an inactivated state, the A-loop is completely disordered and sterically blocks the ATP binding pocket and perturbs the positioning of the catalytic residues. The C-lobe also contains a variable region that is involved in substrate binding and determines kinase specificity (Bojar et al, 2014) **(Figure 4)**.

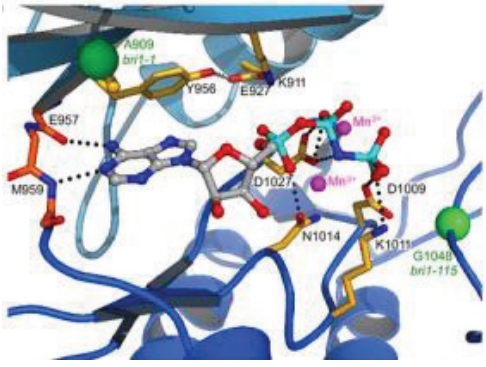


**Figure 4. Conserved residues in the ATP-binding pocket of the BRI1 Ser/Thr kinase domain.** . Gatekeeper Y956 H-bonds to E927, which salt-bridges to K911 to keep the kinase domain in its active conformation. E957 and M959 from the hinge region H-bond with the adenine base group of ATP. N1014 interacts with the α- and β-phosphate group of ATP, and D1027 coordinates a $Mn^{2+}$ ion, which interacts with the β- and γ-phosphate groups of ATP. D1009, together with K1011, interacts with the γ-phosphate group of ATP and acts as the catalytic base in the phospho-transfer reaction to the acceptor Thr residue in the activation-loop (A-loop). (Bojar et al, 2014)

**Table 1. Overview of interaction pairs between some members of ligand families and some members of receptor families**

| Ligand type | Name ligand family | Abbr. | # | Name receptor(s) | Abbr. | # | LRR | ID | KD | References |
|---|---|---|---|---|---|---|---|---|---|---|
| **Steroid hormone** | brassinolide | BL | 1 | BRASSINOSTEROID-INSENSITIVE 1 / BRI1-LIKE 1/2/3 | BRI1 / BRL1/2/3 | 4 | yes | yes | Ser/Thr | Wang et al., 2001 |
| **PAMP-derived protein sequence** | flagellin-derived flg22 peptide | flg22 | 1 | FLAGELLIN SENSING 2 | FLS2 | 1 | yes | no | Ser/Thr | Chinchilla et al., 2006 |
| | EF-Tu-derived elf18 peptide | elf18 | 1 | EF-Tu RECEPTOR | EFR | 1 | yes | no | Ser/Thr | Zipfel et al., 2006 |
| **Small PTM signaling peptide** | PHYTOSULFOKINE | PSK | 6 | PSK-RECEPTOR 1/2 | PSKR1 / PSKR2 | 2 | yes | yes | Ser/Thr | Matsubayashi et al., 2006 |
| | PLANT PEPTIDE CONTAINING SULFATED TYROSINE 1 | PSY1 | 1 | PSY1-RECEPTOR 1 | PSYR1 | 1 | yes | yes | Ser/Thr | Amano et al., 2007 |
| | CLAVATA3/ENDOSPERM SURROUNDING REGION RELATED PROTEIN | CLV3/CLE | 32 | CLAVATA 1 / BARELY ANY MERISTEM 1/2/3 | CLV1 / BAM1/2/3 | 4 | yes | no | Ser/Thr | Ogawa et al., 2008 |
| | | CLV3/CLE | 32 | RECEPTOR-LIKE PROTEIN KINASE 2 | RPK2 | 1 | yes | yes | Ser/Thr | Kinoshita et al., 2010 |
| | TRACHEARY DIFFERENTIATION INHIBITORY FACTOR | TDIF = CLE41/42/44 | 2 | TDIF-RECEPTOR/ PHLOEM INTERCALATED XYLEM / PXY-LIKE 1/2/3 | TDR/PXY / PXL1/2/3 | 3 | yes | no | Ser/Thr | Hirakawa et al., 2008 |
| | INFLORESCENCE DEFICIENT IN ABSCISSION / IDA-LIKE | IDA/IDL | 9 | HAESA / HAESA-LIKE 1/2 | HAE / HSL1/2 | 3 | yes | no | Ser/Thr | Stenvik et al., 2008 |
| | PAMP-INDUCED SECRETED PEPTIDE / PIP-LIKE | PIP/PIPL | 11 | RECEPTOR-LIKE KINASE 7 | RLK7 | 1 | yes | no | Ser/Thr | Hou et al., 2014 |
| | C-TERMINALLY ENCODED PEPTIDE | CEP | 15 | XYLEM INTERMIXED WITH PHLOEM1/CEP RECEPTOR 1/2 | XIP1/CEPR1/2 | 2 | yes | no | Ser/Thr | Tabata et al., 2014 |
| | ROOT GROWTH FACTORS / GOLVEN / CLE-LIKE | RGF/GLV/CLEL | 12 | RGF RECEPTOR 1/2/3 | RGFR1/2/3 | 3 | yes | no | Ser/Thr | Shinohara et al., 2016 |
| **Cys-rich signaling peptide** | EPIDERMAL PATTERNING FACTOR / EPF-LIKE | EPF/EPFL | 10 | ERACTA / ERECTA-LIKE 1/2 | ER / ERL1/2 | 3 | yes | no | Ser/Thr | Lee et al., 2012 |
| | RAPID ALKALINIZATION FACTOR / RALF-LIKE | RALF/RALFL | 34 | FERONIA | FER | 1 | no | no | Ser/Thr | Haruta et aL;, 2014 |
| **Non-Cys/non-PTM peptide** | PROPEP | AtPep | 8 | PEP RECEPTOR 1/2 | PEPR1 / PEPR2 | 2 | yes | no | Ser/Thr | Yamaguchi et al., 2006 |

**Abbr.** = abbreviation; **#** = number of family members; **LRR** = presence of LRR-domain; **ID** = presence of island domain; **KD** = type of kinase domain

# 4. Ligand – Receptor binding and downstream signaling

An overview of well-known signaling peptide – LRR-RLK pairs in *Arabidopsis*, along with some other types of ligand – LRR-RLK pairs is provided in **Table 1**. It should be noted that in most cases only some members of the ligand families have been shown to bind to some members from the receptor families. For some of these ligand – receptor pairs, a large part of the signaling pathway has been unraveled; from ligand binding to the receptor domain, followed by a downstream phosphorylation cascade of multiple kinase proteins, and finally (in)activation of target transcription factors. Based on these studies, co-receptors were revealed as important components, both for ligand binding and initiating the phosphorylation cascade. Several well-characterized cases will be described below, and can be used as a foundation for other ligand – receptor signaling pathways, since many components are conserved.

## 4.1 Brassinosteroid hormone signaling

### 4.1.1 Brassinosteroid receptors

Brassinosteroids are a type of phytohormones that play an important role in plant development (Clouse & Sasse, 1998). The best known brassinosteroid is brassinolide (BL), which is perceived by its receptor BRASSINOSTEROID INSENSITIVE 1 (BRI1) (Li & Chory, 1997) **(Figure 5)**. BRI1 is a member of a LRR-RLK subfamily containing three other members: BRI1-LIKE1 (BRL1), BRI1-LIKE2 (BRL2)/VASCULAR HIGHWAY1 (VH1) and BRI1-LIKE3 (BRL3). Each member contains 25 LRRs and a 70 amino acid island domain between LRR21 and LRR22. BRL1 and BRL3 are most closely related to BRI1 and have also been shown to bind brassinosteroid ligands, while BRL2 does not (Cano-Delgado et al, 2004; Zhou et al, 2004). All members are expressed in the vasculature and mutants show defects in vascular development (Clay & Nelson, 2002; Cano-Delgado et al, 2004).

### 4.1.2 SERK co-receptors

BRI1-ASSOCIATED RECEPTOR KINASE 1 (BAK1) was identified as a co-receptor for BRI1, and was found to be necessary for functional signal transduction (Li et al, 2002) **(Figure 5)**. BAK1 belongs to the subfamily II of LRR-RLKs and is a member of the SOMATIC EMBRYOGENESIS RECEPTOR-LIKE KINASE (SERK) family, containing 5 LRR units. This family counts five members: SERK1, SERK2, BAK1/SERK3, BAK1-LIKE1 (BKK1)/SERK4 and SERK5. SERKs are highly conserved in sequence, and functional analysis revealed that they are rather redundant in many unrelated biological processes (*e.g.* brassinosteroid signaling, innate immunity, male sporogenesis, stomata development and abscission). Some reports suggest that they are not completely interchangeable and that there are differences in affinity and specificity (Aan den Toorn et al, 2015; Meng et al, 2015). Nonetheless, besides BAK1/SERK3, BRI1 has also been suggested to heterodimerize with SERK1, SERK2 and BKK1/SERK4 (Gou et al, 2012; Santiago et al, 2013; Sun et al, 2013a). Noteworthy, SERK5 seems to be non-functional in the Col-0 accession due to a natural mutation in the highly conserved RD motif in the kinase domain that interacts with the γ-phosphate group of ATP and catalyzes substrate phosphorylation. However, in other accessions, such as Landsberg *erecta* (L*er*), SERK5 acts as a functional co-receptor (Wu et al, 2015).

### 4.1.3 BL-BRI1-SERK complex formation and activation

Structural analysis, through X-Ray crystallography, of the BL-BRI1-SERK1 complex allowed determining how BRI1 and SERK proteins interact with each other. In the absence of BL the BRI1 receptor forms homodimers and its cytoplasmic kinase domain interacts with the membrane-anchored BRI1 KINASE INHIBITOR 1 (BKI1), blocking its interaction with the kinase domain of BAK1. The hydrophobic BL ligand binds to a small island-domain inserted between LRR21 and LRR22. This insertion of a 70 amino acid non-LRR loop is probably an adaptation to the challenge of sensing the small steroid ligand. The island domain forms an anti-parallel β-sheet sandwiched between the LRR core and a $3_{10}$ helix, and contains a disulfide bridge for stabilization (Hothorn et al, 2011). Binding of BL to BRI1 triggers a conformational change of the island domain, and forms a docking platform for the shape-complementary co-receptor protein SERK1. Next to the island domain, the LRR capping domains also take part in the BRI1-SERK1 interaction interface. The LRRNT of SERK1 folds on top of the BRI1 binding pocket, where it interacts with the BRI1 island domain, with LRR25 from BRI1 and with the ligand itself. The LRRCT of BRI1 also contributes to complex formation by interacting with LRRs 1 to 4 from SERK1. The SERK1 interface residues that interact directly with BRI1 are highly conserved in all SERK-family members. The strong loss-of-function allele *bri1-102* has a point mutation in the center of the BRI1-SERK1 interface, which explains the strong phenotype. Taken together, the brassinosteroid hormone ligand acts as a molecular glue between the BRI1 receptor domain and the SERK1 receptor domain, bringing together the cytoplasmic kinase domains. This triggers transphosphorylation events between BRI1 and the SERK co-receptor, followed by further downstream signaling (Santiago et al, 2013).

### 4.1.4 Intracellular components in the brassinosteroid signaling pathway

Upon activation of the BRI1 – SERK co-receptor complex, an intracellular signaling cascade is activated, which is mainly mediated by phosphorylation and de-phosphorylation events by several different families of kinases and phosphatases **(Figure 5)**. BAK1-INTERACTING RECEPTOR-LIKE KINASE 2 (BIR2) is a LRR-RLK containing an extracellular domain of 5 LRRs and a cytoplasmic pseudo-kinase domain, in which the ATP binding pocket is occluded, making it kinase-dead. BIR2 binds to BAK1/SERK3, thereby preventing BAK1/SERK3 from binding to BRI1 and in this manner negatively regulates brassinosteroid signaling. Upon ligand binding, BAK1 has been shown to phosphorylate BIR2, thereby ending their interaction (Blaum et al, 2014; Halter et al, 2014). The cytoplasmic kinase domain of BRI1 is inhibited by interaction with the cytoplasmic BRI1 KINASE INHIBITOR 1 (BKI1). BL ligand binding to the extracellular BRI1 – BAK1/SERK3 co-receptor complex leads to the dissociation of BKI1 from BRI1, after which the cytoplasmic kinase domain from BAK1/SERK3 interacts with BRI1 (Wang et al, 2014). Another cytoplasmic inhibitor protein interacting with the cytoplasmic domain of BRI1 is BOTRYTIS-INDUCED KINASE 1 (BIK1), which dissociates after phosphorylation by BAK1/SERK3 in a ligand-induced manner (Lin et al, 2014). Close homologs of BIK1 are avrPphB SUSCEPTIBLE 1 (PBS1), PBS1-LIKE 1 (PBL1) and PBS1-LIKE 2 (PBL2), all containing a Ser/Thr kinase domain. The ligand-activated BRI1 can then directly phosphorylate BR-SIGNALING KINASES (BSKs), which constitute a membrane-associated receptor-like cytoplasmic Ser/Thr kinase sub-family (RLCK-XII class) with 12 members (Tang et al, 2008; Sreeramulu et al, 2013). And ligand-activated BRI1 also phosphorylates and activates CONSTITUTIVE DIFFERENTIAL GROWTH 1 (CDG1) and its homolog CDG1-LIKE 1 (CDL1), which are also membrane-associated receptor-like cytoplasmic Ser/Thr kinase. CDG1 and CDL1 act together with BSKs to phosphorylate and activate the cytoplasmic phosphatase *bri1* SUPPRESSOR1 (BSU1), or its homologs BSU1-LIKE 1 (BSL1), BSL2 and BSL3. These phosphatases dephosphorylate the

GLYCOGEN SYNTHASE KINASE 3 (GSK3)-LIKE KINASES (GSKs)/ARABIDOPIS SHAGGY-RELATED PROTEIN KINASES (AtSKs) at a conserved tyrosine residue, which leads to their inactivation (Kim et al, 2011). The GSK/AtSK protein family counts 10 members in *Arabidopsis*, which can be categorized into four subgroups: clade I consists of AtSK11, AtSK12 and AtSK13; clade II consists of AtSK21/BIN2, AtSK22/BIL2 and AtSK23/BIL1; clade III consists of AtSK31 and AtSK32; and clade IV consists of AtSK41 and AtSK42 (according to new nomenclature) (Jonak & Hirt, 2002; Youn & Kim, 2015). It has been suggested that in total seven AtSKs are involved in brassinosteroid signaling, including the well-known AtSK21/BRASSINOSTEROID INSENSITIVE 2 (BIN2), which in the absence of brassinosteroids induce the phosphorylation of transcription factors BRASSINAZOLE RESISTANT 1 (BZR1) and BZR2/*bri1* EMS SUPPRESSOR 1 (BES1) (He et al, 2002; Kim et al, 2009; Rozhon et al, 2010; Youn et al, 2013). This promotes interaction of these phosphorylated transcription factors with 14-3-3 proteins and leads to their nuclear export, thereby preventing BZR1 and BZR2/BES1 transcriptional activity (Ryu et al, 2010). Thus, brassinosteroid signaling leads to AtSK21/BIN2 inactivation through BSU1-mediated de-phosphorylation, and allows BZR1 and BZR2/BES1 to transcriptionally induce the expression of brassinosteroid primary response genes. Furthermore, AtSKs are believed to negatively control MITOGEN ACTIVATED PROTEIN (MAP) kinase cascades, involving MAP KINASE KINASE KINASE (MAPKKK) proteins (*e.g.* MAPKKK4/YODA), MAP KINASE KINASE (MAPKK) proteins (*e.g.* MAPKK4 and MAPKK5) and MAP KINASE (MAPK) proteins (*e.g.* MAPK3 and MAPK6), which leads to the phosphorylation of downstream transcription factors at other sites than AtSK phosphorylation sites (Casson & Hetherington, 2012; Khan et al, 2013; Youn et al, 2013; Kang et al, 2015). PROTEIN PHOSPHATASE 2A (PP2A) phosphatases are believed to play a dual role, as PP2As are believed to dephosphorylate the ligand-activated BRI1 kinase domain in the cytoplasm and thereby deactivating it, but are also presumed to dephosphorylate the downstream transcription factor BZR1 in the nucleus (Wang et al, 2016).

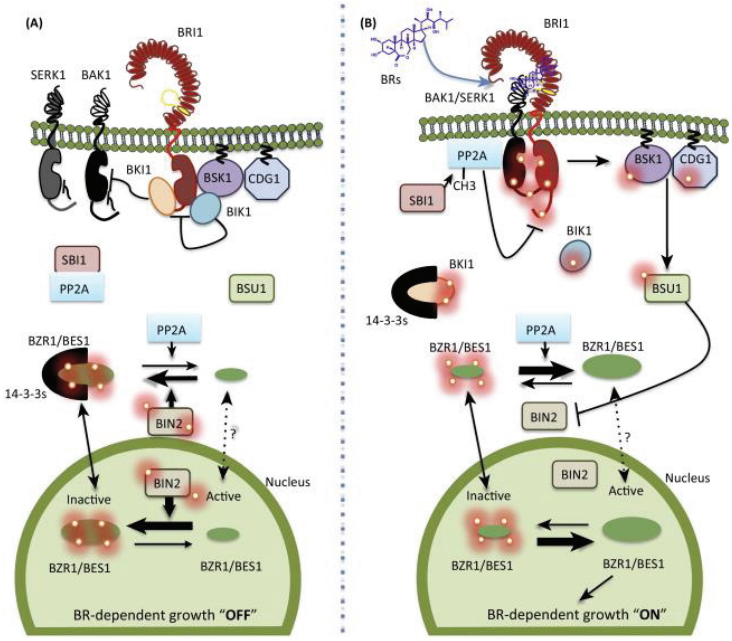


**Figure 5. BRI1 signaling pathway in inactive and activated status (see text for details).** (Figure from Belkhadir et al, 2014)

## 4.2 PAMP-induced FLS2 and EFR signaling

Receptors from the pattern recognition receptor (PRR) group perceive the so-called pathogen-associated molecular pattern (PAMP) ligands during plant immunity responses against potential pathogens (Monaghan & Zipfel, 2012). The two best known examples are the FLAGELLIN SENSING2 (FLS2) receptor that binds the flg22 peptide ligand derived from the N-terminus of bacterial flagellin, and the EF-Tu receptor (EFR) that recognizes the elf18 peptide derived from the N-terminus of bacterial EF-Tu (Chinchilla et al, 2006; Zipfel et al, 2006). FLS2 belongs to the subfamily XII of LRR-RLKs and contains an intracellular Ser/Thr kinase domain with an ATP-binding pocket and an activation loop. However, there are some differences with other Ser/Thr kinase domains. The typical GxGxxG motif at the ATP-binding pocket and the conserved RD motif in the activation loop are absent. This RD motif is typically associated with the activity of kinases to autophosphorylate, which in turn allows interaction and transphosphorylation of substrates. Many other plant PRRs also belong to the group of non-RD kinases (Dardick et al, 2012). Unlike BRI1, FLS2 and EFR do not seem to contain an interruption in the regular LRR backbone by a non-LRR island domain, and the peptide ligand binding is thought to occur along a stretch of multiple LRRs at the concave surface. FLS2 and EFR also require the SERK co-receptors (*e.g.* BAK1/SERK3) for ligand binding (Roux et al, 2011). Mutating residues in the flg22 ligand binding site of FLS2, or in FLS2 at the direct FLS2 – BAK1/SERK3 binding interface, or in the BAK1/SERK3 LRR domain that interacts with the flg22-FLS2 complex disrupt the interaction between the receptor and co-receptor (Sun et al, 2013a; Koller & Bent, 2014). Apparently, a kinase-dead BAK1 still interacts with FLS2, but is impaired in downstream signaling. This illustrates that ligand binding is the first step that triggers the interaction between the receptor and co-receptor, and not the interactions between the cytoplasmic kinase domains (Schulze et al, 2010; Schwessinger et al, 2011). A MAPK signaling cascade has been shown to act downstream of flg22 – FLS and elf18 - EFR, involving MAPK3 and MAPK6 (Rodriguez et al, 2010; Meng & Zhang, 2013). The KAPP phosphatase was found to interact with the FLS2 kinase domain and is possibly involved in its de-phosphorylation (Gomez-Gomez et al, 2001).

## 4.3 Signaling pathways of post-translationally modified peptides

### 4.3.1 CLAVATA3/CLE peptide signaling

The textbook example of secreted peptide signaling in plant development is the CLAVATA3 peptide – CLAVATA1 LRR-RLK pair that controls the stem cell pool in the shoot apical meristem (SAM) (Fletcher et al, 1999). The CLV3 peptide is expressed in the outer layers of the central zone in the SAM and is secreted towards the underlying tissue layer where it binds the CLV1 receptor. This inactivates the membrane-associated POLTERGEIST (POL) and POL-LIKE1 (PLL1) phosphatases, which contain an N-terminal lipid tail for insertion in the plasma membrane. POL and PLL1 promote the expression of the homeodomain transcription factor WUSCHEL (WUS) in the organizing center (OZ), which is required to keep the stem cells in the SAM in an undifferentiated state. As a feedback loop, WUS controls expression of *CLV3* in the overlaying tissue. The MAPKK4 – MAPK6 module has been shown to play a role in the CLV3 – CLV1 downstream signaling pathway (Betsuyaku et al, 2011) **(Figure 6A)**.

A similar signaling pathway is also active in the root apical meristem (RAM), with the CLE40 peptide binding to CLV1 and thereby inhibiting the expression of WUSCHEL-RELATED HOMEOBOX5 (WOX5) in the quiescent center (QC) to maintain stem cell identity in the neighboring stem cell niche (Stahl et al, 2009; Stahl et al, 2013) **(Figure 6B)**. Recently, it was found that WOX5 locally inhibits the expression of CYCD3;3 and CYCD1;1 in the QC to keep them from dividing (Forzani et al, 2014).

Yet another similar signaling cascade was discovered in the vascular meristem region, with the TRACHEARY ELEMENT DIFFERENTIATION INHIBITORY FACTOR (TDIF)/CLE41/44 peptide – TDIF RECEPTOR (TDR)/PHLOEM INTERCALATED WITH XYLEM (PXY) receptor pair regulating WOX4 expression in the (pro)cambium cells for stem cell maintenance (Hirakawa et al, 2010). AtSKs, such as BIN2/AtSK21, were shown to be involved in TDIF – TDR signaling, leading to the phosphorylation of transcription factors, such as ARF7 and ARF19 (Cho et al, 2014; Kondo et al, 2014) **(Figure 6C)**.

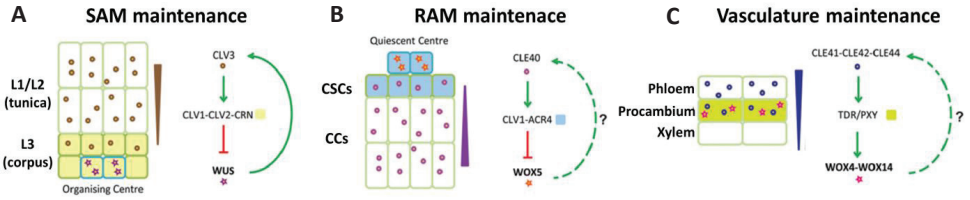


**Figure 6. CLE signaling during development. (A)** Shoot apical meristem maintenance by CLV3 – CLV1 signaling controlling WUS expression in the organizing center. **(B)** Root apical meristem maintenance by CLE40 – CLV1 signaling controlling WOX5 expression in the quiescent center. **(C)** Vascular meristem maintenance by TDIF (CLE41/42/44) – TDR/PXY signaling controlling WOX4/14 expression in the procambium (Figure adapted from Czyzewicz et al.; 2013)

BARELY ANY MERISTEM 1 (BAM1), BAM2 and BAM3 are the closest homologs to CLV1 and were also suggested to act as receptor for the CLV3/CLE peptide family (DeYoung et al, 2006; Deyoung & Clark, 2008; Guo et al, 2010; Shinohara et al, 2012; Shimizu et al, 2015). Over the years, several studies showed that the CLV3 peptide also binds to RECEPTOR-LIKE KINASE2 (RPK2)/TOADSTOOL2 (TOAD2) or the CLAVATA2 (CLV2) – CORYNE (CRN)/SUPPRESSOR OF LLP1 2 (SOL2) complex (Miwa et al, 2008; Muller et al, 2008; Bleckmann et al, 2010; Guo et al, 2010; Kinoshita et al, 2010). However, a recent study suggested that the CLV3 peptide only directly binds to the LRR-RLKs CLV1 and BAM1, and not to RPK2 or the CLV2-CRN complex (Shinohara & Matsubayashi, 2015).

Interestingly, there appears to be a correlation between CLV3/CLE peptide sequence and their specificity to activate a certain developmental pathway. Three main groups have been reported with different overexpression phenotypes. Overexpression or synthetic peptide treatments of TRACHEARY ELEMENT DIFFERENTIATION INHIBITORY FACTOR (TDIF)/CLE41/CLE44 and CLE42 leads to reduced tracheary elements (TE) differentiation, while they have no effect on primary root (PR) growth or lateral root (LR) outgrowth under nitrogen (N)-deficient conditions. This group of peptides differs from the other CLE peptide groups by having a histidine (H) residue at position 1 instead of the typical arginine (R) residue, and a serine (S) residue at position 11 instead of the typical histidine (H) residue and signal through TDR/PXY receptors. Another group is formed from the CLE1/CLE3/CLE4, CLE2, CLE5/CLE6 and CLE7 peptides, for which overexpression or synthetic peptide treatment leads to reduced LR outgrowth under N-deficient conditions and a moderate reduction in PR growth, but no effect on TE differentiation can be observed. This group differs from the other CLE peptides by having a hydrophilic serine (S) residue at position 3 instead of a typical hydrophobic valine (V) or isoleucine (I) residue, also by having a hydrophobic glycine (G) residue at position 5 instead of a hydrophilic residue, and finally by having a hydrophilic arginine (R) or glutamine (Q) at position 10 instead of a typical hydrophobic isoleucine (I) or leucine (L) residue. The third and largest group contains the other CLE peptides, for which overexpression or synthetic peptide treatment leads to severely reduced primary root growth by a gradual consumption of the root apical meristem, while having no effect on TE differentiation or N-dependent LR outgrowth (Ito et al, 2006; Hirakawa et al, 2008; Whitford et al, 2008; Araya et al, 2014a; Araya et al, 2014b) **(Figure 7)**.

| | | | | | | | | | | | | | | Reduced TE diff | Reduced PR growth | Reduced LR growth |
|---|---|---|---|---|---|---|---|---|---|---|---|---|---|---|---|---|
| CLE41/44 | H | E | V | P | S | G | P | N | P | I | S | N | | ++ | - | - |
| CLE42 | H | G | V | P | S | G | P | N | P | I | S | N | | ++ | - | - |
| CLE1/3/4 | R | L | S | P | G | G | P | D | P | R | H | H | | - | + | ++ |
| CLE2 | R | L | S | P | G | G | P | D | P | Q | H | H | | - | + | ++ |
| CLE5/6 | R | V | S | P | G | G | P | D | P | Q | H | H | | - | + | ++ |
| CLE7 | R | F | S | P | G | G | P | D | P | Q | H | H | | - | + | ++ |
| CLV3 | R | T | V | P | S | G | P | D | P | L | H | H | | - | ++ | - |
| CLE25 | R | K | V | P | N | G | P | D | P | I | H | N | | - | ++ | - |
| CLE26 | R | K | V | P | R | G | P | D | P | I | H | N | | - | ++ | - |
| CLE40 | R | Q | V | P | T | G | S | D | P | L | H | H | | - | ++ | - |
| CLE18 | R | Q | I | P | T | G | P | D | P | L | H | N | | - | ++ | - |
| CLE19 | R | V | I | P | T | G | P | N | P | L | H | N | | - | ++ | - |
| CLE21 | R | S | I | P | T | G | P | N | P | L | H | N | | - | ++ | - |
| CLE27 | R | I | V | P | S | C | P | D | P | L | H | N | | - | ++ | - |
| CLE45 | R | R | V | R | R | G | S | D | P | I | H | N | | - | ++ | - |
| CLE8 | R | R | V | P | T | G | P | N | P | L | H | H | | - | ++ | - |
| CLE9/10 | R | L | V | P | S | G | P | N | P | L | H | N | | - | ++ | - |
| CLE11 | R | V | V | P | S | G | P | N | P | L | H | H | | - | ++ | - |
| CLE12 | R | R | V | P | S | G | P | N | P | L | H | H | | - | ++ | - |
| CLE13 | R | L | V | P | S | G | P | N | P | L | H | H | | - | ++ | - |
| CLE14 | R | L | V | P | K | G | P | N | P | L | H | N | | - | ++ | - |
| CLE16 | R | L | V | H | T | G | P | N | P | L | H | N | | - | ++ | - |
| CLE17 | R | V | V | H | T | G | P | N | P | L | H | N | | - | ++ | - |
| CLE20 | R | K | V | K | T | G | S | N | P | L | H | N | | - | ++ | - |
| CLE22 | R | R | V | F | T | G | P | N | P | L | H | N | | - | ++ | - |

**Figure 7. Functional subgroups in the CLV3/CLE peptide family.** Overview of CLE peptides, grouped according to their phenotypes when they are overexpressed or when plants are grown in the presence of applied synthetic mature CLE peptide. They are scored for three phenotypes: reduced tracheary element (TE) differentiation, reduced primary root (PR) growth, and reduced lateral root (LR) outgrowth under N-limiting conditions. The amino acid residues that are crucial for their functionality are highlighted in red.

Differences in residues in the mature CLE peptides could potentially also be coupled to differences in specificity for their receptors. The CLE41/CLE44 and CLE42 peptides bind to the LRR-RLK PHLOEM INTERCALATED WITH XYLEM (PXY)/TDIF RECEPTOR (TDR) receptor. While some CLE peptides from the other groups were shown to bind to the LRR-RLK CLAVATA1 (CLV1) or the closely related BARELY ANY MERISTEM1 (BAM1), BAM2 or BAM3 receptors. For example, the CLV3 peptide binds to CLV1 and BAM1 (Shinohara & Matsubayashi, 2015), the CLE3 peptide is believed to bind CLV1 (Araya et al, 2014a), the CLE9 peptide binds to BAM1 (Shinohara et al, 2012), and the CLE45 peptide is believed to bind to BAM3 (Depuydt et al, 2013).

### 4.3.2 IDA/IDL peptide signaling

Cell separation processes, such as floral organ abscission and lateral root emergence, are regulated by the INFLORESCENCE DEFICIENT IN ABSCISSION (IDA)/IDA-LIKE (IDL) peptide family, which consists of 9 members (Butenko et al, 2003; Kumpf et al, 2013; Vie et al, 2015). These post-translationally modified small signaling peptides, derived from the 12 amino acid PIP motif, act through binding to LRR-RLKs HAESA (HAE) and HAESA-LIKE 2 (HSL2), which contain an extracellular receptor domain with 22 LRR-repeats and an intracellular Ser/Thr kinase domain (Jinn et al, 2000; Cho et al, 2008; Stenvik et al, 2008; Santiago et al, 2016). The IDA peptide was shown to bind to the LRR2-14 region of HAE (Meng et al, 2016; Santiago et al, 2016). Noteworthy, closely-related HAESE-LIKE 1 (HSL1) has not been implicated in IDA/IDL signaling (yet). Members of the SERK LRR-RLK proteins were suggested to function as co-receptors with HAE/HSL2 for binding IDA/IDL peptides and activating downstream signaling (Lewis et al, 2010; Meng et al, 2016; Santiago et al, 2016). The LRR-RLK EVERSHED (EVR)/SUPPRESSOR OF BIR1-1 (SOBIR1), containing 5 LRRs and an intracellular dual-specificity

Ser/Thr-Tyr kinase domain, was shown to negatively regulate IDA/IDL – HAE/HSL2 – SERK signaling (Leslie et al, 2010; Gubert & Liljegren, 2014). NEVERSHED (NEV) is an ADP-ribosylation factor GTPase-activating protein that is localized in the trans-Golgi network (TGN)/early endosome (EE) and believed to act as a membrane trafficking regulator recycling RLKs to the plasma membrane (Liljegren et al, 2009; Liu et al, 2013). The receptor-like cytoplasmic kinase CAST AWAY (CST), containing an N-terminal myristoylated tail anchoring it in the plasma membrane, is suggested to interact with HAE and EVR and sequester them at the plasma membrane (Burr et al, 2011). The MAPKK proteins MAPKK4 and MAPKK5, and MAPK proteins MAPK3 and MAPK6, were proposed to act downstream in IDA/IDL – HAE/HSL2 – SERK signaling (Cho et al, 2008). IDA/IDL signaling leads to phosphorylation and inactivation of HOMEOBOX transcription factor KNOTTED-LIKE FROM ARABIDOPSIS THALIANA 1 (KNAT1)/BREVIPEDICELLUS (BP) (Shi et al, 2011). This promotes expression of KNAT2 and KNAT6, which induce cell wall remodeling enzymes that degrade the middle lamella at the site of abscission (Butenko et al, 2012) **(Figure 8)**.

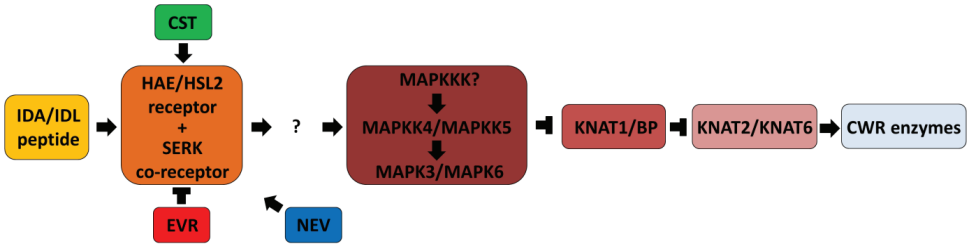


**Figure 8. IDA/IDL peptide signaling.** IDA/IDL peptides binds and activate the HAE/HSL2 receptor – SERK co-receptor complex, which through a currently unknown manner triggers a downstream MAPK cascade that leads to the phosphorylation and inactivation of KNAT1/BP transcription factor. This leads to the activation of KNAT2 and KNAT6, which induce the expression of cell wall remodeling enzymes that promote cell separation/abscission. LRR-RLK EVR negatively regulates IDA/IDL signaling, CST sequesters the LRR-RLK at the plasma membrane, while NEV regulates recycling of the RLK to the plasma membrane (based on model from Liu et al., 2013).

### 4.3.3 CEP peptide signaling

The CEP peptide family is represented by 15 *CEP* genes in *Arabidopsis*, coding for CEP prepropeptides varying in length from 76 to 243 amino acid residues, which all contain an N-terminal secretory signal peptide with a predicted conserved arginine residue as cleavage site, and one to five C-terminally conserved sequence regions of 15 amino acid residues, termed CEP domains (Ohyama et al, 2008; Delay et al, 2013; Roberts et al, 2013). Mass spectrometry analysis revealed that the functional mature CEP peptides are 15 amino acids in length and are derived from each of these CEP domains through proteolytic processing. The mature CEP peptides contain conserved proline residues that can undergo post-translational modifications to form hydroxyproline residues, which can be further modified by triarabinosylations (Ohyama et al., 2008; Tabata et al., 2014; Mohd-Radzman et al., 2015). Through NMR structure analysis, it was proposed that CEP peptides contain a β-turn-like-conformation, and that the hydroxylation modifications alter the surface area and conformational plasticity of the peptide, which affects the conformational space the peptide can sample in order to bind its receptor (Bobay et al, 2013). Two receptor proteins for CEP peptides have been identified: CEP RECEPTOR 1/XYLEM INTERMIXED WITH PHLOEM 1 (CEPR1/XIP1) (At5g49660) and CEP RECEPTOR2 (CEPR2) (At1g72180) (Tabata et al, 2014). These are LRR-RLKs from the subfamily XI and contain a short secretory signal peptide (SP) sequence, an N-terminal extracellular LRR receptor domain, a single helical transmembrane region and a C-terminal cytoplasmic serine/threonine kinase domain.

The first *CEP* gene functionally characterized in *Arabidopsis* was *CEP1*. Both constitutive overexpression of *CEP1* and treatment with chemically synthetized CEP1 peptide led to reduced primary and lateral root growth. This was correlated with a reduced number of cells in the RAM zone, and a reduced cell size in the mature region. However, *CEP1* is not expressed in the RAM, suggesting that the ectopic overabundance of CEP1 might possibly take over the role of another CEP peptide that is expressed in the RAM, or that this phenotype is caused by an indirect secondary effect (Ohyama et al, 2008). Later studies showed that constitutive overexpression and application of chemically synthesized peptides from several other CEP peptides, such as CEP3 and CEP5, also displayed similar reduced primary and lateral root growth. It was also observed that the aboveground shoot was drastically affected in these overexpression lines, with differences in height of the inflorescence, leaf size, leaf number, rosette diameter and affected leaf epinasty (Delay et al, 2013; Roberts et al, 2013). At the physiological level, CEP-CEPR signaling is suggested to play an important role in the nitrogen starvation response. It has been proposed that *CEP* genes are transcriptionally upregulated in roots in regions with low nitrogen levels, after which the produced CEP peptides act as systemic root-derived ascending signals that are perceived by CEPRs in the shoot and trigger the production of a currently unknown shoot-derived descending signal that upregulates *NRTs* in the other parts of the root system to stimulate nitrogen uptake (Tabata et al., 2014).

In *Medicago truncatula*, the *MtCEP1* gene was shown to modulate the number of lateral roots and nodules. It is expressed in the root cap, root apical meristem, in developing vascular tissue in the elongation zone, in the pericycle, in developing lateral root primordia, in developing nodules and in the procambium of a mature root, but not in the phloem, or cortical or epidermal cells. Low nitrogen together with high $CO_2$ concentrations increased *MtCEP1* expression levels. Overexpression did not have an effect on primary root growth, but resulted in reduced emerged lateral roots and an increase in nodule numbers, even at high nitrate conditions, which normally suppress nodule formation. On the other hand, an RNAi knock-down line contained an increased number of lateral roots, while nodule number was unaffected. Furthermore, overexpression or application of synthetic peptide also led to regions with circumferential cell proliferation (CCP) root swellings, which arose from extra cortical and pericycle divisions, and from which lateral roots could emerge after increased auxin levels, hinting toward the possibility that these swellings might contain arrested lateral root primordia. The *MtCEP1* gene codes for a prepropeptide with two CEP domains each giving rise to a separate mature CEP peptide: Domain 1 (D1) *Mt*CEP1 and Domain 2 (D2) *Mt*CEP1. Different variants for these peptides were found with differences in prolinehydroxylation and triarabinosylation state, in which the hydroxylated variants constituted 93.5% of the total amount, while the triarabinosylated variants only counted for 6.5% of the total. These different peptide variants displayed different effects on lateral root formation, suggesting that different modification states can lead to distinct functional effects (Imin et al, 2013; Mohd-Radzman et al, 2015).

## 4.4 Cysteine-rich EPF peptide – ERECTA signaling

Most plants contain stomata, which are valves formed by two specialized epidermal guard cells that regulate oxygen, carbon dioxide and water vapor flow in and out of the leaf. Guard cells are formed through a complex differentiation process of leaf epidermal cells. Protodermal cells in the leaf can either develop into pavement cells, which make up most part of the underside of the leaf surface, or they can become a meristemoid mother cell (MMC). MMCs undergo an asymmetrical division into another meristemoid daughter cell and a stomatal-lineage ground cell (SLGG) daughter cell.

The latter can either differentiate into a normal pavement cell or gives rise to another MMC that forms a second satellite meristemoid cell. The meristemoid cell undergoes asymmetric divisions, and finally becomes a guard mother cell (GMC) that divides into a pair of guard cells (Pillitteri & Dong, 2013).

The secreted cysteine-rich peptides EPIDERMAL PATTERNING FACTOR 1 (EPF1) and EPF2 are known (negative) regulators of stomata development (Hara et al, 2007; Hara et al, 2009). EPF2 is expressed during the early stages of stomata development: it is secreted from differentiated meristemoids and perceived by neighboring protodermal cells to suppress their differentiation into meristemoids. EPF1 is expressed during later stages and is involved in orienting stomatal spacing and prevents guard cell differentiation. EFP peptides are perceived by the LRR-RLKs ERECTA (ER), ERECTA-LIKE 1 (ERL1) and ERECTA-LIKE 2 (ERL2) (Shpak et al, 2005). EPF2 binds to ER, while EPF1 binds to ERL1 (Lee et al, 2012). TOO MANY MOUTHS (TMM) was identified as an LRR-RLK that negatively regulates the ER – ERL1/2 receptors (Nadeau & Sack, 2002; Shpak et al, 2005). Ligand binding triggers a MAPK cascade, and is composed of YODA (YDA, MAPKKK4), MAPKK4/MAPKK5 and MAPK3/MAPK6 (Wang et al, 2007). It was shown that EPF2 – ER signaling triggers MAPK3/MAPK6-induced phosphorylation of the basic helix-loop-helix transcription factor SPEECHLESS (SPCH) on several Ser/Thr residues in the so-called MAPK-target domain and thereby inactivates SPCH (Lampard et al, 2008). The EPF1 – ERL1 cascade triggers in a similar manner the phosphorylation of MUTE, a transcription factor closely related to SPCH. FAMA is a third related transcription factor that is involved in the final division into the two guard cells (Pillitteri et al, 2007) **(Figure 9)**.

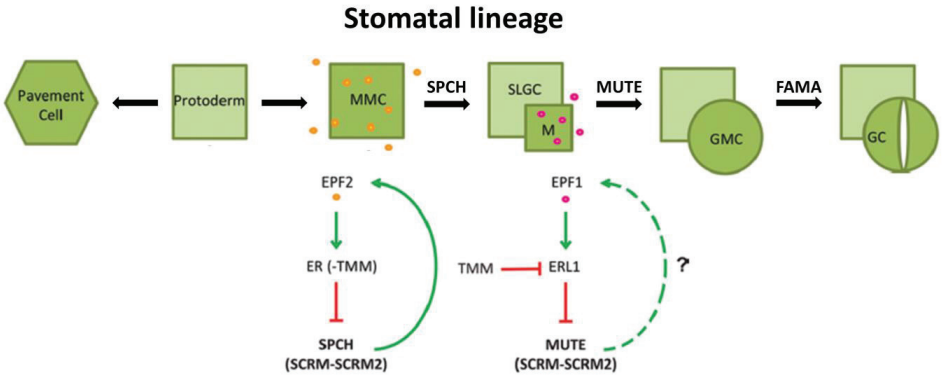


**Figure 9. Stomata development.** The stomata lineage is controlled by sequential EPF2 – ER signaling controlling SPCH expression, followed by EPF1 – ERL1 signaling controlling MUTE expression, and the final step by FAMA (Figure adapted from Czyzewicz et al.; 2013)

Recently, an interesting observation was made in this signaling pathway, namely competitive binding of antagonistic peptides for the same receptor. The signaling peptide STOMAGEN/EPF-LIKE9 was previously identified as a positive regulator of stomata development, in contrast to EPF2 and EPF1 (Sugano et al, 2010). It was discovered that STOMAGEN actively competes with EPF2 for binding to the ER receptor. However, STOMAGEN – ER binding does not activate the MAPK signaling cascade that leads to the phosphorylation of SPCH (Jewaria et al, 2013; Lee et al, 2015). This illustrates a competitive inhibition mechanism between close related signaling peptides with opposing activating or inhibitory functions during patterning of stomata. A similar antagonistic mechanism was also discovered in CLE signaling (Song et al, 2013).

## 4.5 A common mechanism for ligand – LRR-RLK signaling

### 4.5.1 LRR-RLK receptor - SERK co-receptor hetero-dimerization

Based on the examples above, it seems that ligand-induced LRR-RLK receptor – SERK co-receptor hetero-dimerization acts as a common mechanism in RLK signaling. The SERK co-receptors have been shown to interact with many different LRR-RLKs **(Table 1)**. In each case, the LRR domain of the SERK protein is thought to directly interact both with the LRR domain of the main receptor and with the bound ligand. It is intriguing how these promiscuous SERK co-receptors can interact with such a wide array of different LRR-RLKs and ligands. Some reports described that different receptors use different residues for interacting with their SERK co-receptors. The BRI1-SERK1 interaction is thought to occur near the transmembrane region close to the C-terminal region of the LRR domain, in contrast to the FLS2-BAK1 interaction that occurs a lot further from the transmembrane domain with the FLS2 ectodomain bending down toward the co-receptor (Santiago et al, 2013; Sun et al, 2013a; Sun et al, 2013b). A recent study hypothesized that the relatively small LRR domain of the co-receptor would interact close to the C-terminal end of the large LRR domain of the receptor at a conserved region. The authors found that several different LRR-RLKs indeed contained a conserved region at this location, but this region does not serve as a universal SERK protein interaction site, but is rather involved in correct processing and glycosylation of the receptor domain (Koller & Bent, 2014). SERK reporter lines might allow determining which SERK co-receptors can pair up with which LRR-RLK receptor, by overlap in expression patterns (Meng et al, 2016).

**Table 1: SERK co-receptors interact with many different LRR-RLKs**

| Receptor | Co-Receptor(s) | References |
|---|---|---|
| BRI1 | SERK1, SERK3/BAK1 and SERK4/BKK1 | Gou et al., 2012; Santiago et al., 2013; Sun et al., 2013 |
| FLS2 | SERK3/BAK1 and SERK4/BKK1 | Chinchilla et al., 2007; Roux et al., 2011 |
| EFR | SERK3/BAK1 | Schulze et al., 2010 |
| HAE/HSL2 | SERK1, SERK2, SERK3/BAK1 and SERK4/BKK1 | Lewis et al., 2010; Meng et al., 2016 |
| ER | SERK1, SERK2, SERK3/BAK1 and SERK4/BKK1 | Meng et al., 2015 |
| PEPR1/PEPR2 | SERK3/BAK1 | Schulze et al., 2010; Tang et al., 2015 |
| PSKR1 | SERK3/BAK1 | Ladwig et al., 2015; Wang et al., 2015 |

### 4.5.2 MAPK signaling

A common mechanism in ligand – RLK downstream signaling is MAP kinase signaling, in which sequentially a MAP KINASE KINASE KINASE (MAPKKK) phosphorylates a MAP KINASE KINASE (MAPKK), which in turn phosphorylates a MAP KINASE (MAPK) that finally phosphorylates another substrate, such as a transcription factor. During plant evolution, there has been a large increase in the number of RLKs, but this was not accompanied by a proportional increase in MAPK components (Doczi et al, 2012). In *Arabidopsis*, there are 20 MAPKs/MPKs, 10 MAPKKs/MKKs/MEKs and 12 MAPKKKs/MKKKs/MEKK (Group, 2002; Hamel et al, 2006) **(Figure 10)**. The *Arabidopsis* genome encodes for a single MAPK phosphatase 1 (MKP1) that is thought to dephosphorylate MAPKs (Anderson et al, 2011).

MAPKKKs, MAPKKs and MAPKs do not mix-and-match to form all 2,400 possible combinations (12x10x20), but rather have specific combinations in which one component cannot simply be replaced by any other (*e.g.* MAPKK4 only interacts with MAPK3 and MAPK6 during many different developmental pathways). A Yeast-2-Hybrid screen using all 10 MAPKKs as bait and all 20 MAPKs as prey was used to identify specific MAPKK-MAPK interaction pairs (Lee et al, 2008) **(Table 2)**.

This reveals that MAPKKs tend to interact with MAPKs that are closely related to each other. For example: MAPKK1 interacts with the closely related MAPK4 and MAPK11, while MAPKK3 interacts with the close related MAPK1, MAPK2, MAPK7 and MAPK14 **(Table 2 & Figure 10)**. Structural knowledge of critical phosphorylation sites in the activation loop of the kinase domain of MAPK proteins can help in elucidating the downstream signaling pathway. For example, inducible expression of a constitutively active MAPKK5 variant, in which two serines in the activation loop of the kinase domain were substituted by phosphomimicing aspartic acid residues, allowed identifying many downstream phosphorylation targets through mass spectrometry phosphoproteomics (Lee et al, 2004; Lassowskat et al, 2014).

It seems difficult to understand how different ligand-receptor pairs can signal through such a narrow selection of MAPK components to trigger different developmental programs. This is probably mainly achieved by spatiotemporal expression of their upstream ligands and LRR-RLKs, as well as downstream MAPK substrates, and crosstalk with other signaling pathways.

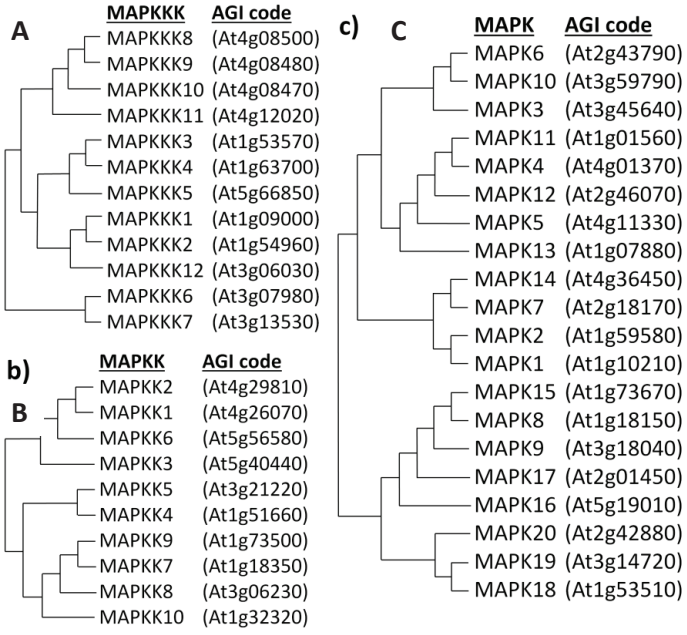


**Figure 10. Phylogenetic relationships of (A) MAPKKKs, (B) MAPKKs and (C) MAPKs in *Arabidopsis*.**

**Table 2. MAPKK – MAPK interactions based on Y2H interaction study from Lee et al., 2008**

| MAPKK (bait) | MAPK (prey) |
|---|---|
| MAPKK1 | MAPK4 and MAPK11 |
| MAPKK2 | MAPK4, MAPK6, MAPK10, MAPK11, MAPK13 |
| MAPKK3 | MAPK1, MAPK2, MAPK7 and MAPK14 |
| MAPKK4 | MAPK3 and MAPK6 |
| MAPKK5 | MAPK6 |
| MAPKK6 | MAPK4, MAPK6, MAPK11 and MAPK13 |
| MAPKK7 | MAPK2 and MAPK15 |
| MAPKK8 | none |
| MAPKK9 | MAPK10, MAPK17, MAPK20 |
| MAPKK10 | MAPK17 |

### 4.5.3 A consensus signaling mechanism

Along with LRR-RLK – SERK dimerization and MAPK signaling, phosphatases, AtSK kinases, and transcription factor phosphorylation also seem to be conserved in ligand – LRR-RLK signaling. Combining findings from the aforementioned cases, a schematic overview of a common conserved ligand – RLK signaling pathway can be created **(Figure 11)**. Future studies will shed light on how specificity is achieved for each signaling pathway.

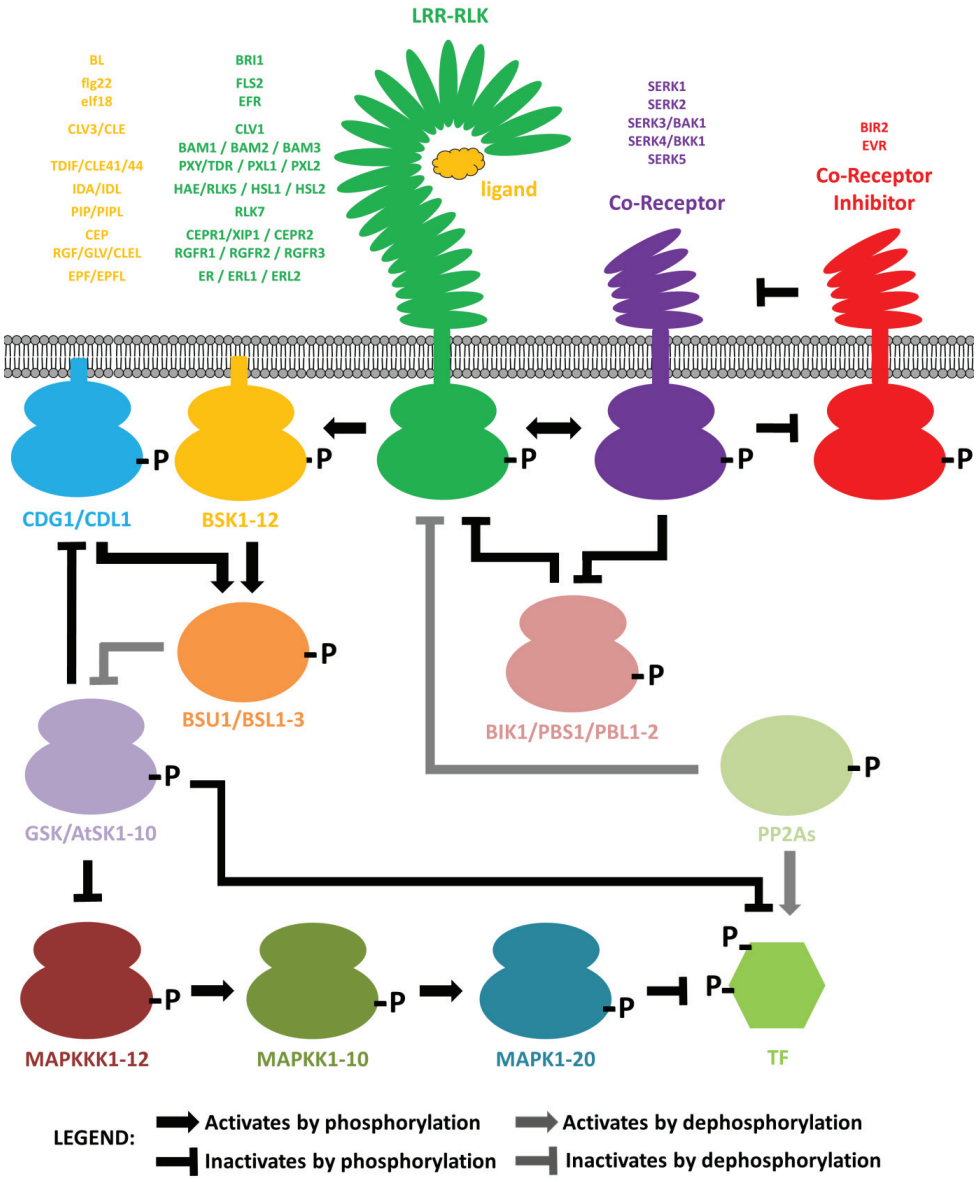


**Figure 11. Ligand-activated LRR-RLK signaling acts through a conserved mechanism largely mediated by phosphorylation and de-phosphorylation events.**

# 5. Receptor Turnover

It is reasonable to assume that once the peptide ligand binds to the receptor – co-receptor complex, it is irreversible. This renders the receptor useless for future ligand binding and therefore would require degradation and internalization of the ligand – receptor complex. Emerging evidence suggests that endocytosis and degradation of receptors serve as a common mechanism to modulate signaling outputs in both plants and animals (Robatzek et al, 2006; Sorkin & von Zastrow, 2009).

A well-studied example is the clathrin-mediated endocytosis of the BRI1 receptor upon perceiving its brassinosteroid ligand, which is regulated by the TPLATE-complex, followed by adaptor protein complex-2 (AP-2), clathrin, and dynamin-related protein recruitment (Di Rubbo et al, 2013; Gadeyne et al, 2014). Another regulator of BRI1 endocytosis is ADP ribosylation factor – GDP/GTP exchange factor (ARF-GEF) GNOM (GN), which enhances brassinosteroid signaling by retaining activated BRI1-SERK complexes at the plasma membrane (Irani et al, 2012). Internalization of BRI1 is believed to be triggered by its phosphorylation (probably) by the ligand-mediated interacting SERK co-receptor (Russinova et al, 2004).

Receptor endocytosis and lysosomal targeting can also be triggered by another type of post-translational modification: the ubiquitination of the intracellular domain of the receptors (Marino et al, 2012; Li et al, 2014). Ubiquitination is a post-translational modification that involves covalent attachment of ubiquitin moieties to substrates. This involves a sequential stepwise process including an ubiquitin-activating enzyme (E1), an ubiquitin-conjugating enzyme (E2) and an ubiquitin-protein ligase (E3). The E1 enzyme first activates the ubiquitin protein by forming a covalent bond between a Cys residue of the E1 enzyme and the C-terminal Gly residue of ubiquitin. This activated ubiquitin is then transferred to a Cys residue of the E2 enzyme. The E3 enzyme recognizes its substrate and catalyzes the ubiquitin transfer from the E2 conjugating enzyme to its substrate by a covalent bond between the C-terminal Gly of ubiquitin and the ε–amino group of a Lys in the substrate protein. Afterwards, the conjugated ubiquitin can be removed from its target by de-ubiquitination enzymes (DUBs) or the ubiquitinated protein can be targeted for 26S proteasomal degradation, releasing the ubiquitin moieties (Kerscher et al, 2006) **(Figure 12)**.

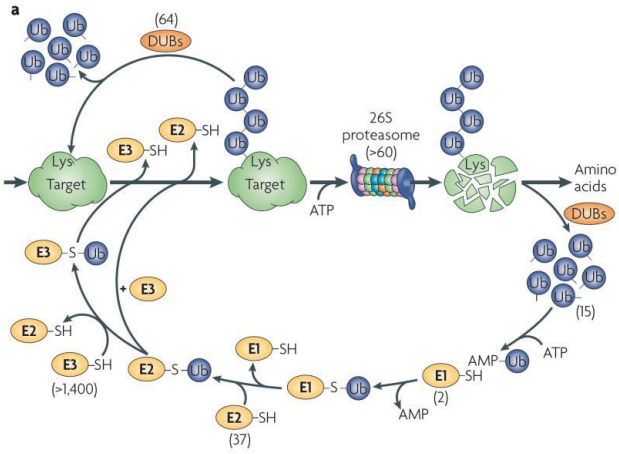


**Figure 12. The ubiquitination pathway (Kerscher et al, 2006).**

The FLS2 kinase domain contains a PEST sequence, which is a known signature for the conjugation of ubiquitin moieties and associated with endocytosis (Haglund et al, 2003). Binding of the ligand flg22 to the heterodimer FLS2-BAK1 receptor complex induces recruitment of two closely related U-box E3 ubiquitin ligases PUB12 and PUB13. BAK1 phosphorylates PUB12/13 and then triggers FLS2-PUB12/13 association after which PUB12/13 polyubiquitinate FLS2 and promote flagellin-induced FLS2 endocytosis followed by degradation (Lu et al, 2011).

# 6. References


Aan den Toorn M, Albrecht C, de Vries S (2015) On the Origin of SERKs: Bioinformatics Analysis of the Somatic Embryogenesis Receptor Kinases. *Molecular plant* **8:** 762-782

Amano Y, Tsubouchi H, Shinohara H, Ogawa M, Matsubayashi Y (2007) Tyrosine-sulfated glycopeptide involved in cellular proliferation and expansion in Arabidopsis. *Proceedings of the National Academy of Sciences of the United States of America* **104:** 18333-18338

Anderson JC, Bartels S, Gonzalez Besteiro MA, Shahollari B, Ulm R, Peck SC (2011) Arabidopsis MAP Kinase Phosphatase 1 (AtMKP1) negatively regulates MPK6-mediated PAMP responses and resistance against bacteria. *The Plant journal : for cell and molecular biology* **67:** 258-268

Araya T, Miyamoto M, Wibowo J, Suzuki A, Kojima S, Tsuchiya YN, Sawa S, Fukuda H, von Wiren N, Takahashi H (2014a) CLE-CLAVATA1 peptide-receptor signaling module regulates the expansion of plant root systems in a nitrogen-dependent manner. *Proc Natl Acad Sci U S A* **111:** 2029-2034

Araya T, von Wiren N, Takahashi H (2014b) CLE peptides regulate lateral root development in response to nitrogen nutritional status of plants. *Plant signaling & behavior* **9:** e29302

Belkhadir Y, Yang L, Hetzel J, Dangl JL, Chory J (2014) The growth-defense pivot: crisis management in plants mediated by LRR-RK surface receptors. *Trends in biochemical sciences* **39:** 447-456

Bella J, Hindle KL, McEwan PA, Lovell SC (2008) The leucine-rich repeat structure. *Cellular and molecular life sciences : CMLS* **65:** 2307-2333

Berger D, Altmann T (2000) A subtilisin-like serine protease involved in the regulation of stomatal density and distribution in Arabidopsis thaliana. *Genes & development* **14:** 1119-1131

Betsuyaku S, Takahashi F, Kinoshita A, Miwa H, Shinozaki K, Fukuda H, Sawa S (2011) Mitogen-activated protein kinase regulated by the CLAVATA receptors contributes to shoot apical meristem homeostasis. *Plant Cell Physiol* **52:** 14-29

Blaum BS, Mazzotta S, Noldeke ER, Halter T, Madlung J, Kemmerling B, Stehle T (2014) Structure of the pseudokinase domain of BIR2, a regulator of BAK1-mediated immune signaling in Arabidopsis. *Journal of structural biology* **186:** 112-121

Bleckmann A, Weidtkamp-Peters S, Seidel CA, Simon R (2010) Stem cell signaling in Arabidopsis requires CRN to localize CLV2 to the plasma membrane. *Plant Physiol* **152:** 166-176

Bobay BG, DiGennaro P, Scholl E, Imin N, Djordjevic MA, McK Bird D (2013) Solution NMR studies of the plant peptide hormone CEP inform function. *FEBS Lett* **587:** 3979-3985

Bojar D, Martinez J, Santiago J, Rybin V, Bayliss R, Hothorn M (2014) Crystal structures of the phosphorylated BRI1 kinase domain and implications for brassinosteroid signal initiation. *The Plant journal : for cell and molecular biology* **78:** 31-43

Botos I, Segal DM, Davies DR (2011) The structural biology of Toll-like receptors. *Structure* **19:** 447-459

Burr CA, Leslie ME, Orlowski SK, Chen I, Wright CE, Daniels MJ, Liljegren SJ (2011) CAST AWAY, a membrane-associated receptor-like kinase, inhibits organ abscission in Arabidopsis. *Plant Physiol* **156:** 1837-1850

Butenko MA, Patterson SE, Grini PE, Stenvik GE, Amundsen SS, Mandal A, Aalen RB (2003) Inflorescence deficient in abscission controls floral organ abscission in Arabidopsis and identifies a novel family of putative ligands in plants. *Plant Cell* **15:** 2296-2307

Butenko MA, Shi CL, Aalen RB (2012) KNAT1, KNAT2 and KNAT6 act downstream in the IDA-HAE/HSL2 signaling pathway to regulate floral organ abscission. *Plant signaling & behavior* **7:** 135-138

Butenko MA, Vie AK, Brembu T, Aalen RB, Bones AM (2009) Plant peptides in signalling: looking for new partners. *Trends Plant Sci* **14:** 255-263

Cano-Delgado A, Yin Y, Yu C, Vafeados D, Mora-Garcia S, Cheng JC, Nam KH, Li J, Chory J (2004) BRL1 and BRL3 are novel brassinosteroid receptors that function in vascular differentiation in Arabidopsis. *Development* **131:** 5341-5351

Casamitjana-Martinez E, Hofhuis HF, Xu J, Liu CM, Heidstra R, Scheres B (2003) Root-specific CLE19 overexpression and the sol1/2 suppressors implicate a CLV-like pathway in the control of Arabidopsis root meristem maintenance. *Current biology : CB* **13:** 1435-1441

Casson SA, Hetherington AM (2012) GSK3-like kinases integrate brassinosteroid signaling and stomatal development. *Sci Signal* **5:** pe30

Chinchilla D, Bauer Z, Regenass M, Boller T, Felix G (2006) The Arabidopsis receptor kinase FLS2 binds flg22 and determines the specificity of flagellin perception. *Plant Cell* **18:** 465-476

Cho H, Ryu H, Rho S, Hill K, Smith S, Audenaert D, Park J, Han S, Beeckman T, Bennett MJ, Hwang D, De Smet I, Hwang I (2014) A secreted peptide acts on BIN2-mediated phosphorylation of ARFs to potentiate auxin response during lateral root development. *Nature cell biology* **16:** 66-76

Cho SK, Larue CT, Chevalier D, Wang H, Jinn TL, Zhang S, Walker JC (2008) Regulation of floral organ abscission in Arabidopsis thaliana. *Proc Natl Acad Sci U S A* **105:** 15629-15634

Clark SE, Jacobsen SE, Levin JZ, Meyerowitz EM (1996) The CLAVATA and SHOOT MERISTEMLESS loci competitively regulate meristem activity in Arabidopsis. *Development* **122:** 1567-1575

Clay NK, Nelson T (2002) VH1, a provascular cell-specific receptor kinase that influences leaf cell patterns in Arabidopsis. *Plant Cell* **14:** 2707-2722

Clouse SD, Sasse JM (1998) BRASSINOSTEROIDS: Essential Regulators of Plant Growth and Development. *Annual review of plant physiology and plant molecular biology* **49:** 427-451

Cock JM, McCormick S (2001) A large family of genes that share homology with CLAVATA3. *Plant physiology* **126:** 939-942

Cock JM, Vanoosthuyse V, Gaude T (2002) Receptor kinase signalling in plants and animals: distinct molecular systems with mechanistic similarities. *Curr Opin Cell Biol* **14:** 230-236

Czyzewicz N, Yue K, Beeckman T, De Smet I (2013) Message in a bottle: small signalling peptide outputs during growth and development. *J Exp Bot* **64:** 5281-5296

Dardick C, Schwessinger B, Ronald P (2012) Non-arginine-aspartate (non-RD) kinases are associated with innate immune receptors that recognize conserved microbial signatures. *Curr Opin Plant Biol* **15:** 358-366

Delay C, Imin N, Djordjevic MA (2013) CEP genes regulate root and shoot development in response to environmental cues and are specific to seed plants. *J Exp Bot* **64:** 5383-5394

Depuydt S, Rodriguez-Villalon A, Santuari L, Wyser-Rmili C, Ragni L, Hardtke CS (2013) Suppression of Arabidopsis protophloem differentiation and root meristem growth by CLE45 requires the receptor-like kinase BAM3. *Proc Natl Acad Sci U S A* **110:** 7074-7079

DeYoung BJ, Bickle KL, Schrage KJ, Muskett P, Patel K, Clark SE (2006) The CLAVATA1-related BAM1, BAM2 and BAM3 receptor kinase-like proteins are required for meristem function in Arabidopsis. *The Plant journal : for cell and molecular biology* **45:** 1-16

Deyoung BJ, Clark SE (2008) BAM receptors regulate stem cell specification and organ development through complex interactions with CLAVATA signaling. *Genetics* **180:** 895-904

Di Rubbo S, Irani NG, Kim SY, Xu ZY, Gadeyne A, Dejonghe W, Vanhoutte I, Persiau G, Eeckhout D, Simon S, Song K, Kleine-Vehn J, Friml J, De Jaeger G, Van Damme D, Hwang I, Russinova E (2013) The clathrin adaptor complex AP-2 mediates endocytosis of brassinosteroid insensitive1 in Arabidopsis. *Plant Cell* **25:** 2986-2997

Doczi R, Okresz L, Romero AE, Paccanaro A, Bogre L (2012) Exploring the evolutionary path of plant MAPK networks. *Trends Plant Sci* **17:** 518-525

Fernandez A, Drozdzecki A, Hoogewijs K, Nguyen A, Beeckman T, Madder A, Hilson P (2013a) Transcriptional and functional classification of the GOLVEN/ROOT GROWTH FACTOR/CLE-like signaling peptides reveals their role in lateral root and hair formation. *Plant physiology* **161:** 954-970

Fernandez A, Hilson P, Beeckman T (2013b) GOLVEN peptides as important regulatory signalling molecules of plant development. *Journal of experimental botany* **64:** 5263-5268

Fletcher JC, Brand U, Running MP, Simon R, Meyerowitz EM (1999) Signaling of cell fate decisions by CLAVATA3 in Arabidopsis shoot meristems. *Science* **283:** 1911-1914

Forzani C, Aichinger E, Sornay E, Willemsen V, Laux T, Dewitte W, Murray JA (2014) WOX5 suppresses CYCLIN D activity to establish quiescence at the center of the root stem cell niche. *Current biology : CB* **24:** 1939-1944

Gadeyne A, Sanchez-Rodriguez C, Vanneste S, Di Rubbo S, Zauber H, Vanneste K, Van Leene J, De Winne N, Eeckhout D, Persiau G, Van De Slijke E, Cannoot B, Vercruysse L, Mayers JR, Adamowski M, Kania U, Ehrlich M, Schweighofer A, Ketelaar T, Maere S, Bednarek SY, Friml J, Gevaert K, Witters E, Russinova E, Persson S, De Jaeger G, Van Damme D (2014) The TPLATE adaptor complex drives clathrin-mediated endocytosis in plants. *Cell* **156:** 691-704

Ghorbani S, Lin YC, Parizot B, Fernandez A, Njo MF, Van de Peer Y, Beeckman T, Hilson P (2015) Expanding the repertoire of secretory peptides controlling root development with comparative genome analysis and functional assays. *Journal of experimental botany*

Gomez-Gomez L, Bauer Z, Boller T (2001) Both the extracellular leucine-rich repeat domain and the kinase activity of FSL2 are required for flagellin binding and signaling in Arabidopsis. *Plant Cell* **13:** 1155-1163

Gou X, Yin H, He K, Du J, Yi J, Xu S, Lin H, Clouse SD, Li J (2012) Genetic evidence for an indispensable role of somatic embryogenesis receptor kinases in brassinosteroid signaling. *PLoS genetics* **8:** e1002452

Group M (2002) Mitogen-activated protein kinase cascades in plants: a new nomenclature. *Trends Plant Sci* **7:** 301-308

Gubert CM, Liljegren SJ (2014) HAESA and HAESA-LIKE2 activate organ abscission downstream of NEVERSHED and EVERSHED in Arabidopsis flowers. *Plant signaling & behavior* **9:** e29115

Guo Y, Han L, Hymes M, Denver R, Clark SE (2010) CLAVATA2 forms a distinct CLE-binding receptor complex regulating Arabidopsis stem cell specification. *The Plant journal : for cell and molecular biology* **63:** 889-900

Haglund K, Di Fiore PP, Dikic I (2003) Distinct monoubiquitin signals in receptor endocytosis. *Trends in biochemical sciences* **28:** 598-603

Halter T, Imkampe J, Mazzotta S, Wierzba M, Postel S, Bucherl C, Kiefer C, Stahl M, Chinchilla D, Wang X, Nurnberger T, Zipfel C, Clouse S, Borst JW, Boeren S, de Vries SC, Tax F, Kemmerling B (2014) The leucine-rich repeat receptor kinase BIR2 is a negative regulator of BAK1 in plant immunity. *Current biology : CB* **24:** 134-143

Hamel LP, Nicole MC, Sritubtim S, Morency MJ, Ellis M, Ehlting J, Beaudoin N, Barbazuk B, Klessig D, Lee J, Martin G, Mundy J, Ohashi Y, Scheel D, Sheen J, Xing T, Zhang S, Seguin A, Ellis BE (2006) Ancient signals: comparative genomics of plant MAPK and MAPKK gene families. *Trends Plant Sci* **11:** 192-198

Hara K, Kajita R, Torii KU, Bergmann DC, Kakimoto T (2007) The secretory peptide gene EPF1 enforces the stomatal one-cell-spacing rule. *Genes & development* **21:** 1720-1725

Hara K, Yokoo T, Kajita R, Onishi T, Yahata S, Peterson KM, Torii KU, Kakimoto T (2009) Epidermal cell density is autoregulated via a secretory peptide, EPIDERMAL PATTERNING FACTOR 2 in Arabidopsis leaves. *Plant Cell Physiol* **50:** 1019-1031

Haruta M, Sabat G, Stecker K, Minkoff BB, Sussman MR (2014) A peptide hormone and its receptor protein kinase regulate plant cell expansion. *Science* **343:** 408-411

Haweker H, Rips S, Koiwa H, Salomon S, Saijo Y, Chinchilla D, Robatzek S, von Schaewen A (2010) Pattern recognition receptors require N-glycosylation to mediate plant immunity. *The Journal of biological chemistry* **285:** 4629-4636

He JX, Gendron JM, Yang Y, Li J, Wang ZY (2002) The GSK3-like kinase BIN2 phosphorylates and destabilizes BZR1, a positive regulator of the brassinosteroid signaling pathway in Arabidopsis. *Proc Natl Acad Sci U S A* **99:** 10185-10190

Hirakawa Y, Kondo Y, Fukuda H (2010) TDIF peptide signaling regulates vascular stem cell proliferation via the WOX4 homeobox gene in Arabidopsis. *Plant Cell* **22:** 2618-2629

Hirakawa Y, Shinohara H, Kondo Y, Inoue A, Nakanomyo I, Ogawa M, Sawa S, Ohashi-Ito K, Matsubayashi Y, Fukuda H (2008) Non-cell-autonomous control of vascular stem cell fate by a CLE peptide/receptor system. *Proc Natl Acad Sci U S A* **105:** 15208-15213

Hothorn M, Belkhadir Y, Dreux M, Dabi T, Noel JP, Wilson IA, Chory J (2011) Structural basis of steroid hormone perception by the receptor kinase BRI1. *Nature* **474:** 467-471

Hou S, Wang X, Chen D, Yang X, Wang M, Turra D, Di Pietro A, Zhang W (2014) The secreted peptide PIP1 amplifies immunity through receptor-like kinase 7. *PLoS pathogens* **10:** e1004331

Imin N, Mohd-Radzman NA, Ogilvie HA, Djordjevic MA (2013) The peptide-encoding CEP1 gene modulates lateral root and nodule numbers in Medicago truncatula. *J Exp Bot* **64:** 5395-5409

Irani NG, Di Rubbo S, Mylle E, Van den Begin J, Schneider-Pizon J, Hnilikova J, Sisa M, Buyst D, Vilarrasa-Blasi J, Szatmari AM, Van Damme D, Mishev K, Codreanu MC, Kohout L, Strnad M, Cano-Delgado AI, Friml J, Madder A, Russinova E (2012) Fluorescent castasterone reveals BRI1 signaling from the plasma membrane. *Nature chemical biology* **8:** 583-589

Ito Y, Nakanomyo I, Motose H, Iwamoto K, Sawa S, Dohmae N, Fukuda H (2006) Dodeca-CLE peptides as suppressors of plant stem cell differentiation. *Science* **313:** 842-845

Jewaria PK, Hara T, Tanaka H, Kondo T, Betsuyaku S, Sawa S, Sakagami Y, Aimoto S, Kakimoto T (2013) Differential effects of the peptides Stomagen, EPF1 and EPF2 on activation of MAP kinase MPK6 and the SPCH protein level. *Plant Cell Physiol* **54:** 1253-1262

Jinn TL, Stone JM, Walker JC (2000) HAESA, an Arabidopsis leucine-rich repeat receptor kinase, controls floral organ abscission. *Genes & development* **14:** 108-117

Jonak C, Hirt H (2002) Glycogen synthase kinase 3/SHAGGY-like kinases in plants: an emerging family with novel functions. *Trends Plant Sci* **7:** 457-461

Kang S, Yang F, Li L, Chen H, Chen S, Zhang J (2015) The Arabidopsis transcription factor BRASSINOSTEROID INSENSITIVE1-ETHYL METHANESULFONATE-SUPPRESSOR1 is a direct substrate of MITOGEN-ACTIVATED PROTEIN KINASE6 and regulates immunity. *Plant Physiol* **167:** 1076-1086

Kerscher O, Felberbaum R, Hochstrasser M (2006) Modification of proteins by ubiquitin and ubiquitin-like proteins. *Annual review of cell and developmental biology* **22:** 159-180

Khan M, Rozhon W, Bigeard J, Pflieger D, Husar S, Pitzschke A, Teige M, Jonak C, Hirt H, Poppenberger B (2013) Brassinosteroid-regulated GSK3/Shaggy-like kinases phosphorylate mitogen-activated protein (MAP) kinase kinases, which control stomata development in Arabidopsis thaliana. *The Journal of biological chemistry* **288:** 7519-7527

Kim TW, Guan S, Burlingame AL, Wang ZY (2011) The CDG1 kinase mediates brassinosteroid signal transduction from BRI1 receptor kinase to BSU1 phosphatase and GSK3-like kinase BIN2. *Molecular cell* **43:** 561-571

Kim TW, Guan S, Sun Y, Deng Z, Tang W, Shang JX, Sun Y, Burlingame AL, Wang ZY (2009) Brassinosteroid signal transduction from cell-surface receptor kinases to nuclear transcription factors. *Nature cell biology* **11:** 1254-1260

Kinoshita A, Betsuyaku S, Osakabe Y, Mizuno S, Nagawa S, Stahl Y, Simon R, Yamaguchi-Shinozaki K, Fukuda H, Sawa S (2010) RPK2 is an essential receptor-like kinase that transmits the CLV3 signal in Arabidopsis. *Development* **137:** 3911-3920

Kobe B, Kajava AV (2001) The leucine-rich repeat as a protein recognition motif. *Current opinion in structural biology* **11:** 725-732

Koller T, Bent AF (2014) FLS2-BAK1 extracellular domain interaction sites required for defense signaling activation. *PloS one* **9:** e111185

Komori R, Amano Y, Ogawa-Ohnishi M, Matsubayashi Y (2009) Identification of tyrosylprotein sulfotransferase in Arabidopsis. *Proceedings of the National Academy of Sciences of the United States of America* **106:** 15067-15072

Kondo T, Sawa S, Kinoshita A, Mizuno S, Kakimoto T, Fukuda H, Sakagami Y (2006) A plant peptide encoded by CLV3 identified by in situ MALDI-TOF MS analysis. *Science* **313:** 845-848

Kondo Y, Ito T, Nakagami H, Hirakawa Y, Saito M, Tamaki T, Shirasu K, Fukuda H (2014) Plant GSK3 proteins regulate xylem cell differentiation downstream of TDIF-TDR signalling. *Nature communications* **5:** 3504

Kumpf RP, Shi CL, Larrieu A, Sto IM, Butenko MA, Peret B, Riiser ES, Bennett MJ, Aalen RB (2013) Floral organ abscission peptide IDA and its HAE/HSL2 receptors control cell separation during lateral root emergence. *Proc Natl Acad Sci U S A* **110:** 5235-5240

Lampard GR, Macalister CA, Bergmann DC (2008) Arabidopsis stomatal initiation is controlled by MAPK-mediated regulation of the bHLH SPEECHLESS. *Science* **322:** 1113-1116

Lassowskat I, Bottcher C, Eschen-Lippold L, Scheel D, Lee J (2014) Sustained mitogen-activated protein kinase activation reprograms defense metabolism and phosphoprotein profile in Arabidopsis thaliana. *Frontiers in plant science* **5:** 554

Lease KA, Walker JC (2006) The Arabidopsis unannotated secreted peptide database, a resource for plant peptidomics. *Plant physiology* **142:** 831-838

Lee J, Rudd JJ, Macioszek VK, Scheel D (2004) Dynamic changes in the localization of MAPK cascade components controlling pathogenesis-related (PR) gene expression during innate immunity in parsley. *The Journal of biological chemistry* **279:** 22440-22448

Lee JS, Hnilova M, Maes M, Lin YC, Putarjunan A, Han SK, Avila J, Torii KU (2015) Competitive binding of antagonistic peptides fine-tunes stomatal patterning. *Nature* **522:** 439-443

Lee JS, Huh KW, Bhargava A, Ellis BE (2008) Comprehensive analysis of protein-protein interactions between Arabidopsis MAPKs and MAPK kinases helps define potential MAPK signalling modules. *Plant signaling & behavior* **3:** 1037-1041

Lee JS, Kuroha T, Hnilova M, Khatayevich D, Kanaoka MM, McAbee JM, Sarikaya M, Tamerler C, Torii KU (2012) Direct interaction of ligand-receptor pairs specifying stomatal patterning. *Genes & development* **26:** 126-136

Leslie ME, Lewis MW, Youn JY, Daniels MJ, Liljegren SJ (2010) The EVERSHED receptor-like kinase modulates floral organ shedding in Arabidopsis. *Development* **137:** 467-476

Lewis MW, Leslie ME, Fulcher EH, Darnielle L, Healy PN, Youn JY, Liljegren SJ (2010) The SERK1 receptor-like kinase regulates organ separation in Arabidopsis flowers. *The Plant journal : for cell and molecular biology* **62:** 817-828

Li B, Lu D, Shan L (2014) Ubiquitination of pattern recognition receptors in plant innate immunity. *Molecular plant pathology* **15:** 737-746

Li J, Chory J (1997) A putative leucine-rich repeat receptor kinase involved in brassinosteroid signal transduction. *Cell* **90:** 929-938

Li J, Wen J, Lease KA, Doke JT, Tax FE, Walker JC (2002) BAK1, an Arabidopsis LRR receptor-like protein kinase, interacts with BRI1 and modulates brassinosteroid signaling. *Cell* **110:** 213-222

Li J, Zhao-Hui C, Batoux M, Nekrasov V, Roux M, Chinchilla D, Zipfel C, Jones JD (2009) Specific ER quality control components required for biogenesis of the plant innate immune receptor EFR. *Proc Natl Acad Sci U S A* **106:** 15973-15978

Liebrand TW, Smit P, Abd-El-Haliem A, de Jonge R, Cordewener JH, America AH, Sklenar J, Jones AM, Robatzek S, Thomma BP, Tameling WI, Joosten MH (2012) Endoplasmic reticulum-quality control chaperones facilitate the biogenesis of Cf receptor-like proteins involved in pathogen resistance of tomato. *Plant Physiol* **159:** 1819-1833

Liljegren SJ, Leslie ME, Darnielle L, Lewis MW, Taylor SM, Luo R, Geldner N, Chory J, Randazzo PA, Yanofsky MF, Ecker JR (2009) Regulation of membrane trafficking and organ separation by the NEVERSHED ARF-GAP protein. *Development* **136:** 1909-1918

Lin W, Li B, Lu D, Chen S, Zhu N, He P, Shan L (2014) Tyrosine phosphorylation of protein kinase complex BAK1/BIK1 mediates Arabidopsis innate immunity. *Proc Natl Acad Sci U S A* **111:** 3632-3637

Liu B, Butenko MA, Shi CL, Bolivar JL, Winge P, Stenvik GE, Vie AK, Leslie ME, Brembu T, Kristiansen W, Bones AM, Patterson SE, Liljegren SJ, Aalen RB (2013) NEVERSHED and INFLORESCENCE DEFICIENT IN ABSCISSION are differentially required for cell expansion and cell separation during floral organ abscission in Arabidopsis thaliana. *J Exp Bot* **64:** 5345-5357

Liu JX, Srivastava R, Howell S (2009) Overexpression of an Arabidopsis gene encoding a subtilase (AtSBT5.4) produces a clavata-like phenotype. *Planta* **230:** 687-697

Lu D, Lin W, Gao X, Wu S, Cheng C, Avila J, Heese A, Devarenne TP, He P, Shan L (2011) Direct ubiquitination of pattern recognition receptor FLS2 attenuates plant innate immunity. *Science* **332:** 1439-1442

Marino D, Peeters N, Rivas S (2012) Ubiquitination during plant immune signaling. *Plant Physiol* **160:** 15-27

Marshall E, Costa LM, Gutierrez-Marcos J (2011) Cysteine-rich peptides (CRPs) mediate diverse aspects of cell-cell communication in plant reproduction and development. *J Exp Bot* **62:** 1677-1686

Matsubayashi Y (2014) Posttranslationally modified small-peptide signals in plants. *Annual review of plant biology* **65:** 385-413

Matsubayashi Y, Shinohara H, Ogawa M (2006) Identification and functional characterization of phytosulfokine receptor using a ligand-based approach. *Chem Res* **6:** 356-364

Matsubayashi Y, Sakagami Y (1996) Phytosulfokine, sulfated peptides that induce the proliferation of single mesophyll cells of Asparagus officinalis L. *Proc Natl Acad Sci U S A* **93:** 7623-7627

Matsushima N, Miyashita H (2012) Leucine-Rich Repeat (LRR) Domains Containing Intervening Motifs in Plants. *Biomolecules* **2:** 288-311

Matsuzaki Y, Ogawa-Ohnishi M, Mori A, Matsubayashi Y (2010) Secreted peptide signals required for maintenance of root stem cell niche in Arabidopsis. *Science* **329:** 1065-1067

Meng X, Chen X, Mang H, Liu C, Yu X, Gao X, Torii KU, He P, Shan L (2015) Differential Function of Arabidopsis SERK Family Receptor-like Kinases in Stomatal Patterning. *Current biology : CB* **25:** 2361-2372

Meng X, Zhang S (2013) MAPK cascades in plant disease resistance signaling. *Annual review of phytopathology* **51:** 245-266

Meng X, Zhou J, Tang J, Li B, de Oliveira MV, Chai J, He P, Shan L (2016) Ligand-Induced Receptor-like Kinase Complex Regulates Floral Organ Abscission in Arabidopsis. *Cell reports* **14:** 1330-1338

Miwa H, Betsuyaku S, Iwamoto K, Kinoshita A, Fukuda H, Sawa S (2008) The receptor-like kinase SOL2 mediates CLE signaling in Arabidopsis. *Plant Cell Physiol* **49:** 1752-1757

Mohd-Radzman NA, Binos S, Truong TT, Imin N, Mariani M, Djordjevic MA (2015) Novel MtCEP1 peptides produced in vivo differentially regulate root development in Medicago truncatula. *J Exp Bot* **66:** 5289-5300

Monaghan J, Zipfel C (2012) Plant pattern recognition receptor complexes at the plasma membrane. *Curr Opin Plant Biol* **15:** 349-357

Muller R, Bleckmann A, Simon R (2008) The receptor kinase CORYNE of Arabidopsis transmits the stem cell-limiting signal CLAVATA3 independently of CLAVATA1. *Plant Cell* **20:** 934-946

Murphy E, De Smet I (2014) Understanding the RALF family: a tale of many species. *Trends in plant science* **19:** 664-671

Murphy E, Smith S, De Smet I (2012) Small signaling peptides in Arabidopsis development: how cells communicate over a short distance. *Plant Cell* **24:** 3198-3217

Nadeau JA, Sack FD (2002) Control of stomatal distribution on the Arabidopsis leaf surface. *Science* **296:** 1697-1700

Neukermans J, Inze A, Mathys J, De Coninck B, van de Cotte B, Cammue BP, Van Breusegem F (2015) ARACINs, Brassicaceae-specific peptides exhibiting antifungal activities against necrotrophic pathogens in Arabidopsis. *Plant Physiol* **167:** 1017-1029

Ogawa-Ohnishi M, Matsushita W, Matsubayashi Y (2013) Identification of three hydroxyproline O-arabinosyltransferases in Arabidopsis thaliana. *Nature chemical biology* **9:** 726-730

Ogawa M, Shinohara H, Sakagami Y, Matsubayashi Y (2008) Arabidopsis CLV3 peptide directly binds CLV1 ectodomain. *Science* **319:** 294

Ohyama K, Ogawa M, Matsubayashi Y (2008) Identification of a biologically active, small, secreted peptide in Arabidopsis by in silico gene screening, followed by LC-MS-based structure analysis. *The Plant journal : for cell and molecular biology* **55:** 152-160

Ohyama K, Shinohara H, Ogawa-Ohnishi M, Matsubayashi Y (2009) A glycopeptide regulating stem cell fate in Arabidopsis thaliana. *Nature chemical biology* **5:** 578-580

Okamoto S, Shinohara H, Mori T, Matsubayashi Y, Kawaguchi M (2013) Root-derived CLE glycopeptides control nodulation by direct binding to HAR1 receptor kinase. *Nature communications* **4:** 2191

Okuda S, Tsutsui H, Shiina K, Sprunck S, Takeuchi H, Yui R, Kasahara RD, Hamamura Y, Mizukami A, Susaki D, Kawano N, Sakakibara T, Namiki S, Itoh K, Otsuka K, Matsuzaki M, Nozaki H, Kuroiwa T, Nakano A, Kanaoka MM, Dresselhaus T, Sasaki N, Higashiyama T (2009) Defensin-like polypeptide LUREs are pollen tube attractants secreted from synergid cells. *Nature* **458:** 357-361

Pearce G, Moura DS, Stratmann J, Ryan CA, Jr. (2001) RALF, a 5-kDa ubiquitous polypeptide in plants, arrests root growth and development. *Proc Natl Acad Sci U S A* **98:** 12843-12847

Pearce G, Strydom D, Johnson S, Ryan CA (1991) A polypeptide from tomato leaves induces wound-inducible proteinase inhibitor proteins. *Science* **253:** 895-897

Pearce G, Yamaguchi Y, Munske G, Ryan CA (2008) Structure-activity studies of AtPep1, a plant peptide signal involved in the innate immune response. *Peptides* **29:** 2083-2089

Pillitteri LJ, Dong J (2013) Stomatal development in Arabidopsis. *The Arabidopsis book / American Society of Plant Biologists* **11:** e0162

Pillitteri LJ, Sloan DB, Bogenschutz NL, Torii KU (2007) Termination of asymmetric cell division and differentiation of stomata. *Nature* **445:** 501-505

Rautengarten C, Steinhauser D, Bussis D, Stintzi A, Schaller A, Kopka J, Altmann T (2005) Inferring hypotheses on functional relationships of genes: Analysis of the Arabidopsis thaliana subtilase gene family. *PLoS computational biology* **1:** e40

Robatzek S, Chinchilla D, Boller T (2006) Ligand-induced endocytosis of the pattern recognition receptor FLS2 in Arabidopsis. *Genes & development* **20:** 537-542

Roberts I, Smith S, De Rybel B, Van Den Broeke J, Smet W, De Cokere S, Mispelaere M, De Smet I, Beeckman T (2013) The CEP family in land plants: evolutionary analyses, expression studies, and role in Arabidopsis shoot development. *J Exp Bot* **64:** 5371-5381

Rodriguez MC, Petersen M, Mundy J (2010) Mitogen-activated protein kinase signaling in plants. *Annu Rev Plant Biol* **61:** 621-649

Roux M, Schwessinger B, Albrecht C, Chinchilla D, Jones A, Holton N, Malinovsky FG, Tor M, de Vries S, Zipfel C (2011) The Arabidopsis leucine-rich repeat receptor-like kinases BAK1/SERK3 and BKK1/SERK4 are required for innate immunity to hemibiotrophic and biotrophic pathogens. *Plant Cell* **23:** 2440-2455

Rozhon W, Mayerhofer J, Petutschnig E, Fujioka S, Jonak C (2010) ASKtheta, a group-III Arabidopsis GSK3, functions in the brassinosteroid signalling pathway. *The Plant journal : for cell and molecular biology* **62:** 215-223

Russinova E, Borst JW, Kwaaitaal M, Cano-Delgado A, Yin Y, Chory J, de Vries SC (2004) Heterodimerization and endocytosis of Arabidopsis brassinosteroid receptors BRI1 and AtSERK3 (BAK1). *Plant Cell* **16:** 3216-3229

Ryu H, Cho H, Kim K, Hwang I (2010) Phosphorylation dependent nucleocytoplasmic shuttling of BES1 is a key regulatory event in brassinosteroid signaling. *Molecules and cells* **29:** 283-290

Santiago J, Brandt B, Wildhagen M, Hohmann U, Hothorn LA, Butenko MA, Hothorn M (2016) Mechanistic insight into a peptide hormone signaling complex mediating floral organ abscission. *Elife* **5**

Santiago J, Henzler C, Hothorn M (2013) Molecular mechanism for plant steroid receptor activation by somatic embryogenesis co-receptor kinases. *Science* **341:** 889-892

Schopfer CR, Nasrallah ME, Nasrallah JB (1999) The male determinant of self-incompatibility in Brassica. *Science* **286:** 1697-1700

Schulze B, Mentzel T, Jehle AK, Mueller K, Beeler S, Boller T, Felix G, Chinchilla D (2010) Rapid heteromerization and phosphorylation of ligand-activated plant transmembrane receptors and their associated kinase BAK1. *The Journal of biological chemistry* **285:** 9444-9451

Schwessinger B, Roux M, Kadota Y, Ntoukakis V, Sklenar J, Jones A, Zipfel C (2011) Phosphorylation-dependent differential regulation of plant growth, cell death, and innate immunity by the regulatory receptor-like kinase BAK1. *PLoS genetics* **7:** e1002046

Shi CL, Stenvik GE, Vie AK, Bones AM, Pautot V, Proveniers M, Aalen RB, Butenko MA (2011) Arabidopsis class I KNOTTED-like homeobox proteins act downstream in the IDA-HAE/HSL2 floral abscission signaling pathway. *Plant Cell* **23:** 2553-2567

Shimizu N, Ishida T, Yamada M, Shigenobu S, Tabata R, Kinoshita A, Yamaguchi K, Hasebe M, Mitsumasu K, Sawa S (2015) BAM 1 and RECEPTOR-LIKE PROTEIN KINASE 2 constitute a signaling pathway and modulate CLE peptide-triggered growth inhibition in Arabidopsis root. *The New phytologist* **208:** 1104-1113

Shinohara H, Matsubayashi Y (2013) Chemical synthesis of Arabidopsis CLV3 glycopeptide reveals the impact of hydroxyproline arabinosylation on peptide conformation and activity. *Plant & cell physiology* **54:** 369-374

Shinohara H, Matsubayashi Y (2015) Reevaluation of the CLV3-receptor interaction in the shoot apical meristem: dissection of the CLV3 signaling pathway from a direct ligand-binding point of view. *The Plant journal : for cell and molecular biology* **82:** 328-336

Shinohara H, Moriyama Y, Ohyama K, Matsubayashi Y (2012) Biochemical mapping of a ligand-binding domain within Arabidopsis BAM1 reveals diversified ligand recognition mechanisms of plant LRR-RKs. *The Plant journal : for cell and molecular biology* **70:** 845-854

Shinohara H, Mori A, Yasue N, Sumida K, Matsubayashi Y (2016) Identification of three LRR-RKs involved in perception of root meristem growth factor in Arabidopsis. *Proc Natl Acad Sci U S A* **113:** 3897-3902

Shiu SH, Bleecker AB (2001) Receptor-like kinases from Arabidopsis form a monophyletic gene family related to animal receptor kinases. *Proc Natl Acad Sci U S A* **98:** 10763-10768

Shpak ED, McAbee JM, Pillitteri LJ, Torii KU (2005) Stomatal patterning and differentiation by synergistic interactions of receptor kinases. *Science* **309:** 290-293

Song XF, Guo P, Ren SC, Xu TT, Liu CM (2013) Antagonistic peptide technology for functional dissection of CLV3/ESR genes in Arabidopsis. *Plant Physiol* **161:** 1076-1085

Sorkin A, von Zastrow M (2009) Endocytosis and signalling: intertwining molecular networks. *Nature reviews Molecular cell biology* **10:** 609-622

Sreeramulu S, Mostizky Y, Sunitha S, Shani E, Nahum H, Salomon D, Hayun LB, Gruetter C, Rauh D, Ori N, Sessa G (2013) BSKs are partially redundant positive regulators of brassinosteroid signaling in Arabidopsis. *The Plant journal : for cell and molecular biology* **74:** 905-919

Srivastava R, Liu JX, Guo H, Yin Y, Howell SH (2009) Regulation and processing of a plant peptide hormone, AtRALF23, in Arabidopsis. *The Plant journal : for cell and molecular biology* **59:** 930-939

Srivastava R, Liu JX, Howell SH (2008) Proteolytic processing of a precursor protein for a growth-promoting peptide by a subtilisin serine protease in Arabidopsis. *The Plant journal : for cell and molecular biology* **56:** 219-227

Stahl Y, Grabowski S, Bleckmann A, Kuhnemuth R, Weidtkamp-Peters S, Pinto KG, Kirschner GK, Schmid JB, Wink RH, Hulsewede A, Felekyan S, Seidel CA, Simon R (2013) Moderation of Arabidopsis root stemness by CLAVATA1 and ARABIDOPSIS CRINKLY4 receptor kinase complexes. *Current biology : CB* **23:** 362-371

Stahl Y, Wink RH, Ingram GC, Simon R (2009) A signaling module controlling the stem cell niche in Arabidopsis root meristems. *Current biology : CB* **19:** 909-914

Stenvik GE, Tandstad NM, Guo Y, Shi CL, Kristiansen W, Holmgren A, Clark SE, Aalen RB, Butenko MA (2008) The EPIP peptide of INFLORESCENCE DEFICIENT IN ABSCISSION is sufficient to induce abscission in arabidopsis through the receptor-like kinases HAESA and HAESA-LIKE2. *Plant Cell* **20:** 1805-1817

Sugano SS, Shimada T, Imai Y, Okawa K, Tamai A, Mori M, Hara-Nishimura I (2010) Stomagen positively regulates stomatal density in Arabidopsis. *Nature* **463:** 241-244

Sun Y, Han Z, Tang J, Hu Z, Chai C, Zhou B, Chai J (2013a) Structure reveals that BAK1 as a co-receptor recognizes the BRI1-bound brassinolide. *Cell research* **23:** 1326-1329

Sun Y, Li L, Macho AP, Han Z, Hu Z, Zipfel C, Zhou JM, Chai J (2013b) Structural basis for flg22-induced activation of the Arabidopsis FLS2-BAK1 immune complex. *Science* **342:** 624-628

Takayama S, Shiba H, Iwano M, Shimosato H, Che FS, Kai N, Watanabe M, Suzuki G, Hinata K, Isogai A (2000) The pollen determinant of self-incompatibility in Brassica campestris. *Proceedings of the National Academy of Sciences of the United States of America* **97:** 1920-1925

Tang W, Kim TW, Oses-Prieto JA, Sun Y, Deng Z, Zhu S, Wang R, Burlingame AL, Wang ZY (2008) BSKs mediate signal transduction from the receptor kinase BRI1 in Arabidopsis. *Science* **321:** 557-560

Tavormina P, De Coninck B, Nikonorova N, De Smet I, Cammue BP (2015) The Plant Peptidome: An Expanding Repertoire of Structural Features and Biological Functions. *Plant Cell* **27:** 2095-2118

Thomma BP, Cammue BP, Thevissen K (2002) Plant defensins. *Planta* **216:** 193-202

Tsiatsiani L, Gevaert K, Van Breusegem F (2012) Natural substrates of plant proteases: how can protease degradomics extend our knowledge? *Physiologia plantarum* **145:** 28-40

van der Hoorn RA, Wulff BB, Rivas S, Durrant MC, van der Ploeg A, de Wit PJ, Jones JD (2005) Structure-function analysis of cf-9, a receptor-like protein with extracytoplasmic leucine-rich repeats. *Plant Cell* **17:** 1000-1015

Vie AK, Najafi J, Liu B, Winge P, Butenko MA, Hornslien KS, Kumpf R, Aalen RB, Bones AM, Brembu T (2015) The IDA/IDA-LIKE and PIP/PIP-LIKE gene families in Arabidopsis: phylogenetic relationship, expression patterns, and transcriptional effect of the PIPL3 peptide. *J Exp Bot* **66:** 5351-5365

Wang H, Ngwenyama N, Liu Y, Walker JC, Zhang S (2007) Stomatal development and patterning are regulated by environmentally responsive mitogen-activated protein kinases in Arabidopsis. *Plant Cell* **19:** 63-73

Wang J, Jiang J, Wang J, Chen L, Fan SL, Wu JW, Wang X, Wang ZX (2014) Structural insights into the negative regulation of BRI1 signaling by BRI1-interacting protein BKI1. *Cell research* **24:** 1328-1341

Wang R, Liu M, Yuan M, Oses-Prieto JA, Cai X, Sun Y, Burlingame AL, Wang ZY, Tang W (2016) The Brassinosteroid-Activated BRI1 Receptor Kinase Is Switched off by Dephosphorylation Mediated by Cytoplasm-Localized PP2A B' Subunits. *Molecular plant* **9:** 148-157

Wang ZY, Seto H, Fujioka S, Yoshida S, Chory J (2001) BRI1 is a critical component of a plasma-membrane receptor for plant steroids. *Nature* **410:** 380-383

Whitford R, Fernandez A, De Groodt R, Ortega E, Hilson P (2008) Plant CLE peptides from two distinct functional classes synergistically induce division of vascular cells. *Proc Natl Acad Sci U S A* **105:** 18625-18630

Whitford R, Fernandez A, Tejos R, Perez AC, Kleine-Vehn J, Vanneste S, Drozdzecki A, Leitner J, Abas L, Aerts M, Hoogewijs K, Baster P, De Groodt R, Lin YC, Storme V, Van de Peer Y, Beeckman T, Madder A, Devreese B, Luschnig C, Friml J, Hilson P (2012) GOLVEN secretory peptides regulate auxin carrier turnover during plant gravitropic responses. *Dev Cell* **22:** 678-685

Wrzaczek M, Vainonen JP, Stael S, Tsiatsiani L, Help-Rinta-Rahko H, Gauthier A, Kaufholdt D, Bollhoner B, Lamminmaki A, Staes A, Gevaert K, Tuominen H, Van Breusegem F, Helariutta Y, Kangasjarvi J (2015) GRIM REAPER peptide binds to receptor kinase PRK5 to trigger cell death in Arabidopsis. *The EMBO journal* **34:** 55-66

Wu W, Wu Y, Gao Y, Li M, Yin H, Lv M, Zhao J, Li J, He K (2015) Somatic embryogenesis receptor-like kinase 5 in the ecotype Landsberg erecta of Arabidopsis is a functional RD LRR-RLK in regulating brassinosteroid signaling and cell death control. *Frontiers in plant science* **6:** 852

Yamaguchi Y, Pearce G, Ryan CA (2006) The cell surface leucine-rich repeat receptor for AtPep1, an endogenous peptide elicitor in Arabidopsis, is functional in transgenic tobacco cells. *Proc Natl Acad Sci U S A* **103:** 10104-10109

Yang H, Matsubayashi Y, Hanai H, Sakagami Y (2000) Phytosulfokine-alpha, a peptide growth factor found in higher plants: its structure, functions, precursor and receptors. *Plant & cell physiology* **41:** 825-830

Yang H, Matsubayashi Y, Nakamura K, Sakagami Y (1999) Oryza sativa PSK gene encodes a precursor of phytosulfokine-alpha, a sulfated peptide growth factor found in plants. *Proceedings of the National Academy of Sciences of the United States of America* **96:** 13560-13565

Yang H, Matsubayashi Y, Nakamura K, Sakagami Y (2001) Diversity of Arabidopsis genes encoding precursors for phytosulfokine, a peptide growth factor. *Plant physiology* **127:** 842-851

Youn JH, Kim TW (2015) Functional insights of plant GSK3-like kinases: multi-taskers in diverse cellular signal transduction pathways. *Molecular plant* **8:** 552-565

Youn JH, Kim TW, Kim EJ, Bu S, Kim SK, Wang ZY, Kim TW (2013) Structural and functional characterization of Arabidopsis GSK3-like kinase AtSK12. *Molecules and cells* **36:** 564-570

Yuasa K, Toyooka K, Fukuda H, Matsuoka K (2005) Membrane-anchored prolyl hydroxylase with an export signal from the endoplasmic reticulum. *The Plant journal : for cell and molecular biology* **41:** 81-94

Zhou A, Wang H, Walker JC, Li J (2004) BRL1, a leucine-rich repeat receptor-like protein kinase, is functionally redundant with BRI1 in regulating Arabidopsis brassinosteroid signaling. *The Plant journal : for cell and molecular biology* **40:** 399-409

Zipfel C, Kunze G, Chinchilla D, Caniard A, Jones JD, Boller T, Felix G (2006) Perception of the bacterial PAMP EF-Tu by the receptor EFR restricts Agrobacterium-mediated transformation. *Cell* **125:** 749-760

## Scope and outline of the thesis

With the increasing world population, the shrinking available land for agriculture and global climate changes, a Second Green Revolution will be required to increase yield in crops, in order to cope with these challenges. The root system is an important target for engineering, considering its vital function, the uptake of water and growth-limiting nutrients from the soil. The efficiency of the root system is determined by the three-dimensional distribution of the root network, which is termed the root system architecture. The main contributor to root system architecture is the lateral root network, making it the primary target for engineering.

The 'Root Development Group' from Prof. Dr. Tom Beeckman (Plant Systems Biology Department, Ghent University/VIB) mainly focuses on studying the lateral root development process in the model plant *Arabidopsis thaliana*, with the goal to translate findings to crop species. Several genome-wide transcriptional studies using lateral root inducible systems have been performed over the last decade, which have led to the identification of important regulators of lateral root development (Himanen et al, 2004; Vanneste et al, 2005; De Smet et al, 2008; De Rybel et al, 2012; Xuan et al, 2015). From these analyses, the gene At5g66815 was picked up as a top-candidate regulator of the earliest event in lateral root development: the priming event in the basal meristem. This gene codes for the secreted signalling peptide C-TERMINALLY ENCODED PEPTIDE 5 (CEP5). At that time, the group from Prof. Dr. Yoshikatsu Matsubayashi (Nagoya University, Japan) had only recently identified the *CEP* peptide family, counting five members, and reported that *CEP1* has an effect on root development (Ohyama et al, 2008). Considering cell-to-cell signalling mediated by secreted signalling peptides and membrane-localized receptors is known to be an important mechanism to regulate developmental processes, the CEP peptides might be important regulators for (lateral) root development. Therefore, we decided to functionally characterize the CEP peptide family, with the emphasis on their putative role in root development.

The scientific questions we aimed to answer in this project were:

- A phylogenetic analysis of the CEP peptide family?
- Does the CEP5 peptide play a role during (lateral) root development?
- Do all CEP peptides have an impact on root development?
- Identity of the CEP receptor protein(s)?
- What is the mode-of-action of CEP signalling and how does this translate to an effect on development?

During my research, these questions were addressed, and answers to most of them are documented in this thesis:

In **Part I** of this thesis, background knowledge on root development *(Chapter 1)* and peptide signalling *(Chapter 2)* is provided. In **Part II**, the results of the study on the *CEP* family are described. Through *in silico* analysis, we discovered an additional ten members of the *CEP* family in *Arabidopsis*, increasing the total count from five to fifteen *CEP* genes, and an evolutionary phylogenetic analysis revealed the presence of *CEP* genes from the seed plant lineage onwards (Roberts et al, 2013) *(Chapter 3)*. All fifteen members, together with the recently identified receptor proteins CEP RECEPTOR 1 (CEPR1)/XYLEM INTERMIXED WITH PHLOEM 1 (XIP1) and CEP RECEPTOR 2 (CEPR2) (Tabata et al, 2014), were characterized by means of gene expression studies, gain-of-function approaches and loss-of-function analysis *(Chapter 4)*. The role of CEP5, together with its proposed receptor CEPR1/XIP1, during lateral root initiation was investigated in more detail *(Chapter 5)*. The mechanism by which CEP5 might regulate root development was discovered to potentially occur through stabilizing Aux/IAA proteins, thereby fine-tuning the auxin response *(Chapter 6)*. During the first steps of the project, based on preliminary results, we anticipated that the membrane-associated receptor kinase ARABIDOPSIS CRINKLY 4 (ACR4), which was previously identified in our group as an important regulator of lateral root initiation (De Smet et al, 2008), could be the potential receptor for CEP5. Therefore, an EMS-mutagenesis screen on the *acr4-2* mutant was performed to identify regulators within the assumed CEP5 – ACR4 signalling pathway. However, further analysis revealed that CEP5 doesn't signal through ACR4, but is thought to occur through the proposed receptors CEPR1/XIP1 and CEPR2. We did not identify regulators of the ACR4 signalling pathway, but we did identify molecular components that have a drastic impact on root systems architecture in an ACR4-independent manner. Furthermore, for the first time, root system architecture on the standard *in vitro* ½ MS growth medium Petri plates was shown to be retained in more natural growth conditions in soil, using min-rhizotrons *(Chapter 7)*. The latter approach of studying root system architecture will likely play an important role in future studies on root development. In **part III**, general conclusions are presented, with an emphasis on the scientific aims mentioned in the scope, along with perspectives for future experiments.

## REFERENCES

De Rybel B, Audenaert D, Xuan W, Overvoorde P, Strader LC, Kepinski S, Hoye R, Brisbois R, Parizot B, Vanneste S, Liu X, Gilday A, Graham IA, Nguyen L, Jansen L, Njo MF, Inze D, Bartel B, Beeckman T (2012) A role for the root cap in root branching revealed by the non-auxin probe naxillin. *Nature chemical biology* **8:** 798-805

De Smet I, Vassileva V, De Rybel B, Levesque MP, Grunewald W, Van Damme D, Van Noorden G, Naudts M, Van Isterdael G, De Clercq R, Wang JY, Meuli N, Vanneste S, Friml J, Hilson P, Jurgens G, Ingram GC, Inze D, Benfey PN, Beeckman T (2008) Receptor-like kinase ACR4 restricts formative cell divisions in the Arabidopsis root. *Science* **322:** 594-597

Himanen K, Vuylsteke M, Vanneste S, Vercruysse S, Boucheron E, Alard P, Chriqui D, Van Montagu M, Inzé D, Beeckman T (2004) Transcript profiling of early lateral root initiation. *Proc Natl Acad Sci U S A* **101:** 5146-5151

Ohyama K, Ogawa M, Matsubayashi Y (2008) Identification of a biologically active, small, secreted peptide in Arabidopsis by in silico gene screening, followed by LC-MS-based structure analysis. *The Plant journal : for cell and molecular biology* **55:** 152-160

Roberts I, Smith S, De Rybel B, Van Den Broeke J, Smet W, De Cokere S, Mispelaere M, De Smet I, Beeckman T (2013) The CEP family in land plants: evolutionary analyses, expression studies, and role in Arabidopsis shoot development. *J Exp Bot* **64:** 5371-5381

Tabata R, Sumida K, Yoshii T, Ohyama K, Shinohara H, Matsubayashi Y (2014) Perception of root-derived peptides by shoot LRR-RKs mediates systemic N-demand signalling. *Science* **346:** 343-346

Vanneste S, De Rybel B, Beemster GT, Ljung K, De Smet I, Van Isterdael G, Naudts M, Iida R, Gruissem W, Tasaka M, Inze D, Fukaki H, Beeckman T (2005) Cell cycle progression in the pericycle is not sufficient for SOLITARY ROOT/IAA14-mediated lateral root initiation in Arabidopsis thaliana. *Plant Cell* **17:** 3035-3050

Xuan W, Audenaert D, Parizot B, Moller BK, Njo MF, De Rybel B, De Rop G, Van Isterdael G, Mahonen AP, Vanneste S, Beeckman T (2015) Root Cap-Derived Auxin Pre-patterns the Longitudinal Axis of the Arabidopsis Root. *Current biology : CB* **25:** 1381-1388

# PART II:
# Results

# Chapter 3:

## The CEP family in land plants: evolutionary analyses, expression studies, and a role in *Arabidopsis* shoot development

**Contributions**

I.R. and S.S. contributed equally to this work. I.R. conducted the experimental work that led to the identification of the 10 novel *CEP* genes (represented in fig1-2, and figS1), and performed the expression analysis of the previously identified 5 *CEP* genes (represented in fig4-8, and figS2-3). S.S. conducted the experimental work of the *in silico* transcriptional analysis of the *CEP* genes (represented in Table 2, and supplemental tables 1 and 2), and performed the shoot phenotypical analysis of *CEP5* transgenic lines (represented in fig9). The data was analyzed by I.R., S.S., B.D.R., I.D.S. and T.B.. I.D.S. and T.B. supervised the research. The manuscript was written by I.D.S., with contributions from I.R., S.S. and T.B..

This chapter is published in Journal of Experimental Botany (2013) 64: 5371-5381

# The CEP family in land plants: evolutionary analyses, expression studies, and a role in *Arabidopsis* shoot development

Ianto Roberts[1,2,†], Stephanie Smith[3,†], Bert De Rybel[1,2,*], Jana Van Den Broeke[1,2], Wouter Smet[1,2], Sarah De Cokere[1,2], Marieke Mispelaere[1,2], Ive De Smet[1,2,3,4,‡,$] and Tom Beeckman[1,2,‡]

[1]Department of Plant Systems Biology, VIB, Technologiepark 927, B-9052 Ghent, Belgium
[2]Department of Plant Biotechnology and Genetics, Ghent University, Technologiepark 927, B-9052 Ghent, Belgium
[3]Division of Plant and Crop Sciences, School of Biosciences, University of Nottingham, Sutton Bonington Campus, Loughborough, Leicestershire LE12 5RD, UK
[4]Centre for Plant Integrative Biology, University of Nottingham, Nottingham LE12 5RD, UK
[*]Present address: Laboratory of Biochemistry, Wageningen University, Dreijenlaan 3, 6703 HA Wageningen, The Netherlands.
[†]These authors contributed equally to this manuscript.
[‡]These authors contributed equally to this manuscript.
[$]To whom correspondence should be addressed. E-mail: ive.desmet@psb.vib-ugent.be

## ABSTRACT

In *Arabidopsis*, more than 1000 putative small signalling peptides have been predicted, but very few have been functionally characterized. One class of small post-translationally modified signalling peptides is the C-TERMINALLY ENCODED PEPTIDE (CEP) family, of which one member has been shown to be involved in regulating root architecture. This work applied a bioinformatics approach to identify more members of the CEP family. It identified 10 additional members and revealed that this family only emerged in flowering plants and was absent from extant members of more primitive plants. The data suggest that the CEP proteins form two subgroups according to the CEP domain. This study further provides an overview of specific *CEP* expression patterns that offers a comprehensive framework to study the role of the CEP signalling peptides in plant development. For example, expression patterns point to a role in aboveground tissues which was corroborated by the analysis of transgenic lines with perturbed *CEP* levels. These results form the basis for further exploration of the mechanisms underlying this family of peptides and suggest their putative roles in distinct developmental events of higher plants.

**Key words:** *Arabidopsis*, small signalling peptides, phylogeny, evolutionary analyses, *CEP* expression, shoot development.

## INTRODUCTION

In the last 20 years, the importance of small signalling peptides in plant cell-to-cell communication has become increasingly clear, with several families of small signalling peptides known at present to play vital roles in plant growth and development (Butenko et al., 2009; Matsubayashi, 2011; Murphy et al., 2012; Czyzewicz et al., 2013). The majority of small signalling peptides falls into one of two broad groups: the cysteine-rich peptides, which are characterized by a typical mature peptide length of <160 amino acids with a cysteine-rich C-terminal domain; and the small post-translationally modified peptides, which are expressed as longer precursor proteins before undergoing post-translational modifications and subsequent cleavage to form an active, mature peptide <20 amino acids in length (Matsubayashi, 2011; Murphy et al., 2012). Three types of post-translational modification - tyrosine sulfation, proline hydroxylation, and hydroxyproline-arabinosylation - are known to occur in small post-translationally modified peptides, and these modifications appear to be crucial for optimal peptide bioactivity (Matsubayashi, 2011; Shinohara and Matsubayashi, 2013).

Identification of small signalling peptides in plants can be challenging due to the small size of their encoding genes (Murphy et al., 2012). An *in silico* approach, specifically designed to identify genes encoding the hallmarks of small peptide signals, led to the discovery of the C-TERMINALLY ENCODED PEPTIDE (CEP) family of putative small posttranslationally modified peptides (Ohyama et al., 2008). In this initial study, five small genes encoding peptides of 82–126 amino acids in length were identified. The five different members of the CEP family display considerable sequence diversity in the majority of the expressed protein, with the exception of a conserved domain at the C-terminus, which represents the mature, active peptide following proteolytic cleavage from the expressed precursor. This was confirmed using mass spectrometry on *CEP1* (At1g47485) overexpression lines, further revealing that the mature product of 15 amino acids contains two hydroxyprolinated residues (Ohyama et al., 2008). Initial analyses showed that overexpression of *CEP1* arrests root growth through repression of meristematic cell division and expansion, while no effects were observed in the quiescent centre and adjacent stem cells (Ohyama et al., 2008).

Apart from these observations restricted to one member of the CEP family, hardly anything is known about the other members and their potential importance for plant growth and development. Therefore, this study further explored this family of small signalling peptides. First, the phylogenetic results showed that the CEP family contains more than five members and is conserved throughout higher land plants. Second, analysis of the expression of CEP family members revealed distinct patterns throughout plant development. Third, altering the expression levels of CEP family members resulted in dramatic growth and developmental phenotypes in aboveground plant parts.

## RESULTS AND DISCUSSION

**Extended CEP family in *A. thaliana***

Originally, the CEP family was described as containing five members in *A. thaliana* (Ohyama et al., 2008). In addition to these five, the current work and Delay et al. (2013) identified 10 additional members. We used blast searches and filtered for proteins with an N-terminal signal peptide sequence, a C-terminal 'CEP-like' sequence, and a total length of 75–250 amino acids **(Table 1)**. The genes are located on different chromosomes, but not chromosome 4, and *CEP3* and *CEP11*, and *CEP5*, *CEP6*, *CEP7*, and *CEP8* are organized in tandem repeats **(Supplementary Figure S1)**. The phylogenetic relationships between the CEP family proteins are shown in **Figure 1A**.

In agreement with the five original CEP family members, this study predicted the presence and location of putative signal peptide cleavage sites in all CEP pre-propeptides using SignalP4.1 **(Figure 1B and Supplementary Dataset S1)**. Although SignalP4.1 does not always predict this, it is likely that the cleavage occurs at a conserved arginine at the N-terminus **(Supplementary Dataset S1)**.

Previously, a C-terminal conserved domain was identified in the original five members of the CEP family (Ohyama et al., 2008). To identify the presence and distribution of this domain in all CEP family members, pattern analyses were performed on the full-length *A. thaliana* CEP proteins using MEME (with optimized settings following iterative analyses) (Bailey and Elkan, 1994). Indeed, a motif that is similar to the active CEP1 peptide sequence (Ohyama et al., 2008) is present across all CEP protein sequences **(Figure 1B and Supplementary Dataset S1)**, and therefore this was called the CEP domain. Interestingly, in several instances the CEP domain occurs multiple times within one pre-propeptide and not exclusively at the C-terminus **(Figure 1B and Supplementary Dataset S2)**.

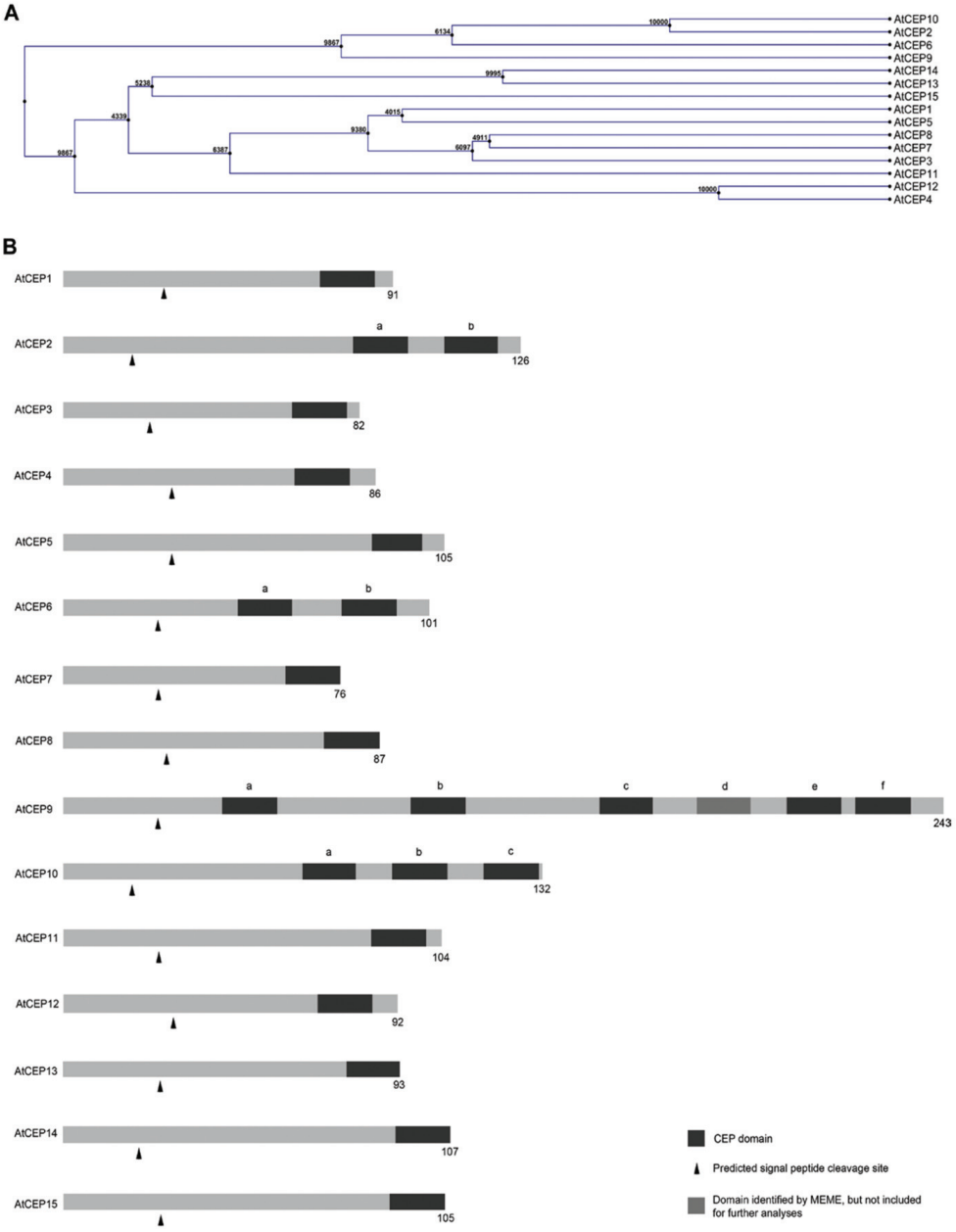


**Figure 1. The CEP family in *Arabidopsis*. (A)** Phylogenetic tree of *Arabidopsis* CEP family members (based on full length protein sequences). Bootstrap values based on 10 000 replications are shown at branch nodes. **(B)** Schematic representation of *Arabidopsis* CEP family members. Numbers are number of amino acids). Dark grey, CEP domain; light grey, predicted CEP domain by MEME but with deviating sequence and not included for further analyses; arrowhead, predicted signal peptide cleavage site.

**Table 1. The 15 members of the CEP family**

| Gene | Locus | Publication |
|---|---|---|
| *CEP1* | At1g47485 | Ohyama *et al.* (2008) |
| *CEP2* | At1g59835 | Ohyama *et al.* (2008) |
| *CEP3* | At2g23440 | Ohyama *et al.* (2008) |
| *CEP4* | At2g35612 | Ohyama *et al.* (2008) |
| *CEP5* | At5g66815 | Ohyama *et al.* (2008) |
| *CEP6* | At5g66816 | This study and Delay *et al.* (2013) |
| *CEP7* | Between At5g66817–At5g66820[a] | This study and Delay *et al.* (2013) |
| *CEP8* | Between At5g66817–At5g66820[a] | This study and Delay *et al.* (2013) |
| *CEP9* | At3g50610 | This study and Delay *et al.* (2013) |
| *CEP10* | Between At1g36040–At1g36050[a] | This study and Delay *et al.* (2013) |
| *CEP11* | Between At2g23440–At2g23450[a] | This study and Delay *et al.* (2013) |
| *CEP12* | At1g31670[b] | This study and Delay *et al.* (2013) |
| *CEP13* | At1g16950 | This study and Delay *et al.* (2013) |
| *CEP14* | At1g29290 | This study and Delay *et al.* (2013) |
| *CEP15* | At2g40530 | This study and Delay *et al.* (2013) |

[a], not listed on TAIR; [b], likely incorrectly annotated on TAIR.

This work then used all the CEP domains to build a phylogenetic tree, which revealed two main branches within the CEP family **(Figure 2A)**. Based on these phylogenetic relationships, the CEP family was divided into two groups: group I, CEP1–CEP12; and group II, CEP13–CEP15 **(Figure 2A)**. The amino acid sequences for the CEP domains for groups I and II were separately aligned, which resulted in a consensus sequence for these two groups **(Figure 2B)**. For both groups, the C-terminal part of the CEP domain (SPGV/IGH) showed high amino acid similarity **(Figure 2B)**. The CEP domain in group I contains three prolines, while in group II it contains two prolines. This is important as LC-MS/MS analysis of CEP1 revealed hydroxylation of some of the prolines within the CEP domain (Ohyama et al., 2008). This hydroxyprolination likely affects bioactivity and hydrophilic nature of the CEP peptides. In future, it will be important to assess to what extent these *in silico* results are supported by biological validation.

**The CEP family is evolutionarily conserved in monocot and eudicot plants**

Notwithstanding the fact that CEP pre-proproteins are short and the CEP domain is only 15 amino acids (AAs) long **(Figures 1 and 2)**, BLAST analysis with *A. thaliana* full-length CEP proteins and 15-amino-acid CEP domain sequences and phylogenetic analyses were used to identify CEP family genes within the supergroup *Plantae* (data not shown). This revealed that CEP peptides are present in eudicots and monocots, but absent in lower land plants (*Selaginella moellendorffii* and *Physcomitrella patens*) and in the green algae for which a genome sequence was available **(Figure 3)**.

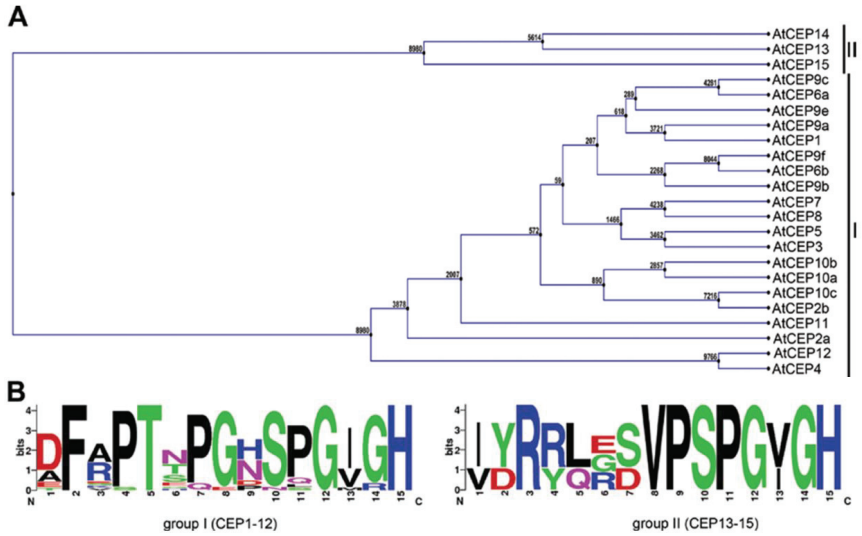


**Figure 2. The CEP family groups into two groups based on CEP domain. (A)** Phylogenetic tree based on CEP domain sequences (see Figure 1B, dark grey). Groups I and II are indicated. Bootstrap values are indicated on the tree. **(B)** Weblogo representation of group I and group II CEP domains.

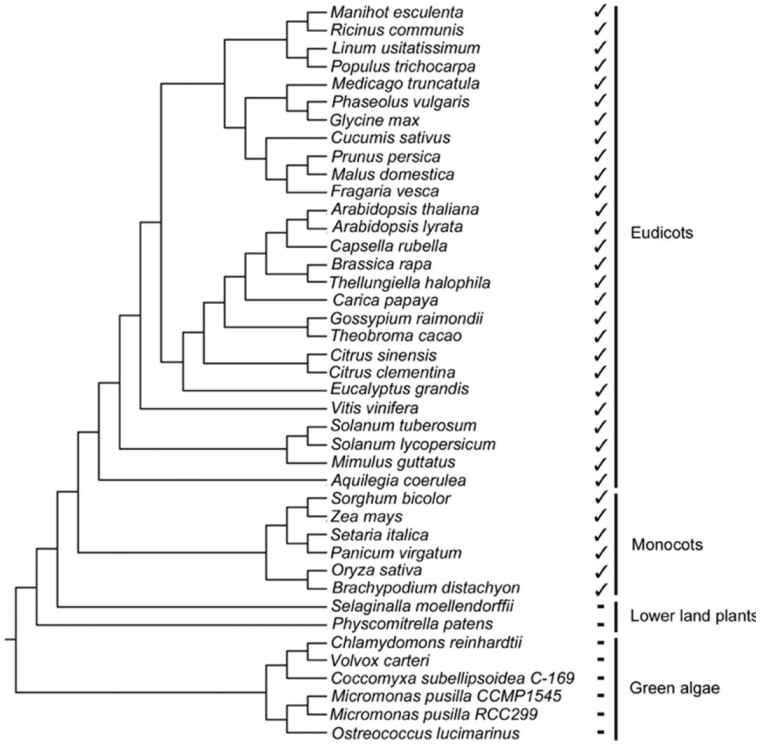


**Figure 3. Evolutionary analysis of the CEP family.** Phylogenetic tree indicating the presence (v) or absence (–) of CEP family members in the indicated species.

**CEP family members display limited transcriptional control by hormones and nutrients in *Arabidopsis***

Whilst small signalling peptides are often not well represented on available micro-arrays (Murphy et al., 2012), *in silico* expression data for 7 out of 15 *CEPs* were available (*CEP2*, *CEP4*, *CEP6*, *CEP7*, *CEP8*, *CEP10*, *CEP11* and *CEP14* are not represented on the Affymetrix GeneChip ATH1). To examine, *CEP* family gene expression changes under several hormonal and nutritional stimuli, this study used the transcriptome meta-analysis tool Genevestigator (Hruz et al., 2008) **(Table 2)**. Both *CEP5* and *CEP15* were downregulated by salicylic acid treatment, gibberellic acid induced expression of *CEP5* and *CEP13*, abscisic acid decreased expression of *CEP15*, whilst jasmonic acid increased expression of *CEP12*. Contrastingly, auxin (IAA) had opposite effects on the expression of some CEP family genes, namely an increase in expression of *CEP1* and *CEP3* but a decrease in *CEP5* and *CEP9* expression. Similarly, brassinolide reduced expression of *CEP5* and induced *CEP15* expression. Other hormones, such as ethylene, strigolactone, and cytokinin, did not have a significant effect on *CEP* expression. With respect to nutrients, a high nitrogen level downregulated *CEP3*, *CEP5*, and *CEP13*, and upregulated *CEP1* and *CEP9*. Phosphorus upregulated expression of *CEP5*. In addition, potassium downregulated *CEP3* expression and upregulated *CEP9* expression.

**Table 2. The effect of hormones and nutrients on CEP expression**

All data used were generated on the Affymetrix GeneChip ATH1 22K platform. +, Increased expression following stimulus; –, reduced expression; =, no significant effect on expression (defined as $p<0.05$ and/or a <1.5 fold change in expression levels compared with control); ND, *CEP* genes and/or stimuli for which no expression data are currently available in Genevestigator. ABA, abscisic acid; BR, brassinosteroids; GA, gibberellic acid; JA, jasmonic acid; SA, salicylic acid; Strigo, strigolactone; Cyto, cytokinin. (*Note: CEP2*, *CEP4*, *CEP6*, *CEP7*, *CEP8*, *CEP10*, *CEP11*, and *CEP14* are ND, as these genes are not represented on the Affymetrix GeneChip ATH1 22k platform).

| Gene | Hormones | | | | | | | | | Nutrients | | |
|---|---|---|---|---|---|---|---|---|---|---|---|---|
| | ABA | Ethylene[a] | BR[b] | GA | Auxin[c] | JA | SA | Strigo | Cyto[d] | N | P | K |
| *CEP1* | = | ND | ND | ND | + | ND | = | ND | ND | + | = | = |
| *CEP3* | = | = | = | = | + | = | = | ND | = | – | ND | – |
| *CEP5* | = | = | – | + | – | ND | – | ND | = | – | + | = |
| *CEP9* | = | = | = | = | – | = | = | = | = | + | = | + |
| *CEP12* | ND | ND | ND | ND | ND | + | ND | ND | ND | ND | ND | ND |
| *CEP13* | = | = | = | + | = | ND | = | ND | = | – | = | = |
| *CEP15* | – | = | + | = | = | = | – | = | = | = | = | = |

[a–d]Measurements were taken using: [a]ACC (1-aminocyclopropane-1-carboxylic acid); [b]brassinolide; [c]indole-3-acetic acid, 1-naphthaleneacetic acid, and 2,4-dichlorophenoxyacetic acid; [d]zeatin.

**CEP family members display distinct expression patterns during *Arabidopsis* development**

To gain further insight in the expression patterns of the *CEP* family during development, the *CEP* expression data were first compiled and visualized from online repositories, namely eFP browser (Winter et al., 2007) and Genevestigator v3 (Hruz et al., 2008). These *in silico* expression patterns suggested that CEP peptides are expressed throughout the plant **(Figure 4, Supplementary Tables S1 and S2)**. *CEP1*, *CEP3*, and *CEP9* were expressed in the shoot apical meristem of the vegetative shoot, and *CEP3* was also expressed in the shoot apical meristem of the inflorescence stem. Only *CEP1* and *CEP15* were expressed in the primary root apical meristem, making these likely candidates for controlling root apical meristem maintenance. *CEP3*, *CEP9*, *CEP13*, and *CEP15* were expressed in cotyledons and/or leaves. During flower development, *CEP1*, *CEP3*, *CEP9*, and *CEP13* were expressed. During lateral root development, *CEP1*, *CEP3*, *CEP5*, *CEP9*, *CEP13*, and *CEP15* were expressed.

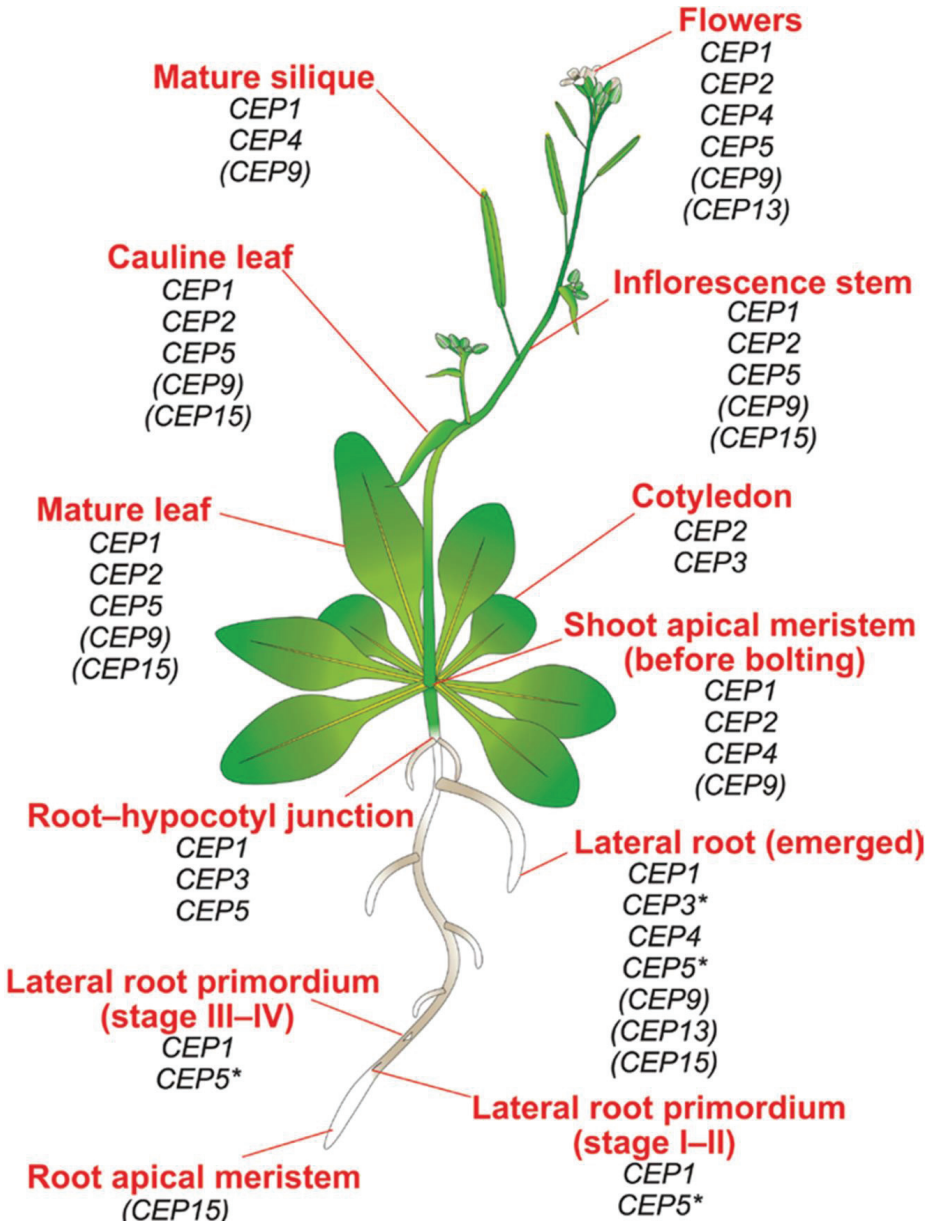


**Figure 4. Expression of *CEP* genes throughout the *Arabidopsis* plant**, based on data from *in planta* (GUS expression; see Figs. 5–8) and predicted by *in silico* (eFP Browser; mentioned in parentheses) studies. *In silico* patterns were not included in the figure if there was a discrepancy with the GUS expression data. *, Associated with vasculature and phloem pole pericycle cells of the primary root at these stages. (*Note: CEP2*, *CEP4*, *CEP6*, *CEP7*, *CEP8*, *CEP10*, *CEP11*, and *CEP14* are not represented on the Affymetrix GeneChip ATH1 22k platform, and therefore no expression pattern could be predicted based on *in silico* analysis)

To further explore *CEP* expression patterns *in planta*, this study selected the five CEPs from group I that were also identified by Ohyama et al. (2008), generated *promoter::GUS* reporter lines, and characterized the reported lines throughout plant development **(Figures 4–8)**.

In the shoot apical meristem of the vegetative shoot of a 5-d-old seedling, only *CEP1* and *CEP2* were expressed **(Figure 5A and E)**, while in a 2-week-old plant, *CEP4* was also expressed **(Figure 5C, G, and O)**. In cotyledons and leaves, the expression domains of the CEP peptides were remarkably distinct and restricted to specific regions. In the cotyledon of 5-d-old seedlings, *CEP2* was expressed in the leaf veins and *CEP3* was expressed only in the tip of the cotyledons **(Figure 5F and J)**. In the leaves of 2-week-old plants, *CEP1* was expressed in the small dentations at the leaf margin and *CEP2* was expressed in the leaf veins **(Figure 5D and H)**. Both *CEP2* and *CEP5* are expressed in the leaf petioles **(Figure 5Q and S)**.

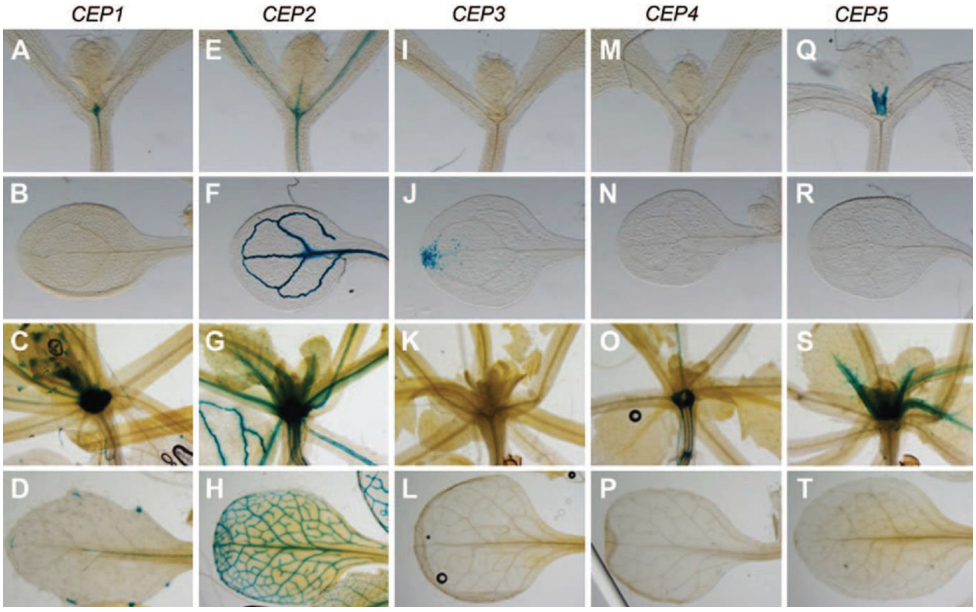


**Figure 5. *CEP* expression in the vegetative shoot. (A–D)** *pCEP1::GUS* reporter line, **(E–H)** *pCEP2::GUS* reporter line, **(I–L)** *pCEP3::GUS* reporter line, **(M–P)** *pCEP4::GUS* reporter line, **(Q–T)** *pCEP5::GUS* reporter line. **(A, E, I, M, Q)** Shoot apical meristem region of 5-d-old seedling. **(B, F, J, N, R)** Cotyledon of 5-d-old seedling. **(C, G, K, O, S)** Shoot apical meristem region of 2-week-old seedling. **(D, H, L, P, T)** Leaf of 2-week-old seedling.

In the cauline leaves of the inflorescence, a similar expression pattern for *CEP1*, *CEP2*, and *CEP5* as in the mature vegetative leaves was observed **(Figure 6C, F, and O)**. In the shoot apical meristem of the inflorescence shoot, *CEP1*, *CEP2*, and *CEP5* were expressed **(Figure 6A, D, and M)**. During flower development, *CEP1* and *CEP2* were expressed in the gynoecium **(Figure 6B)**. In the androecium, both *CEP2* and *CEP4* were expressed in the filaments **(Figure 6E and K)** and *CEP5* was expressed in the anthers **(Figure 6N)**.

In maturing siliques, *CEP1* and *CEP4* were expressed (Figure 7A, B, C, and L), and both were expressed in the abscission zone (Figure 7C and L). None of the five investigated CEP peptides showed a signal in the root apical meristem of the primary root **(Supplementary Figure S2)**. During adventitious root development at the root–hypocotyl junction, expression of *CEP1*, *CEP3*, *CEP4*, and *CEP5* was observed **(Supplementary Figure S3)**.

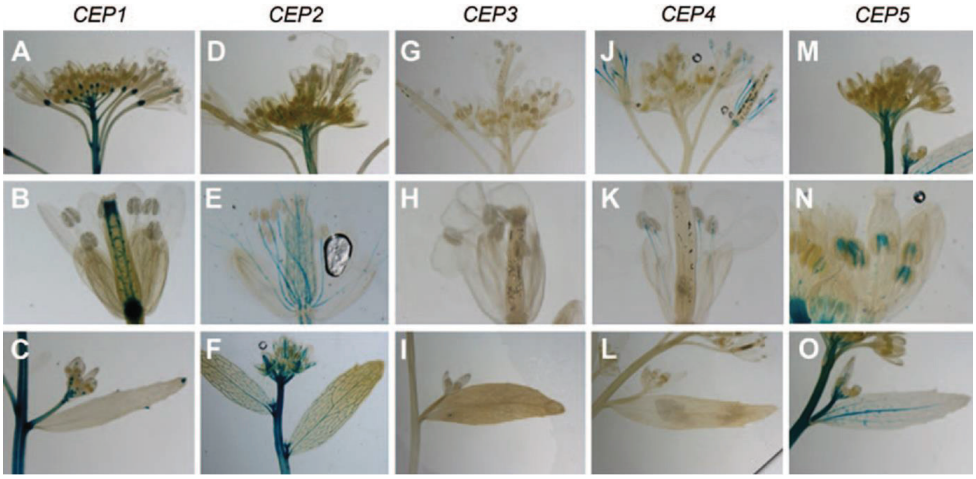


**Figure 6. *CEP* expression in the inflorescence. (A–C)** *pCEP1::GUS* reporter line, **(D–F)** *pCEP2::GUS* reporter line, **(G–I)** *pCEP3::GUS* reporter line, **(J–L)** *pCEP4::GUS* reporter line, **(M–O)** *pCEP5::GUS* reporter line. **(A, D, G, J, M)** *CEP* expression in the apical part of inflorescence. **(B, E, H, K, N)** *CEP* expression during flower development. **(C, F, I, L, O)** *CEP* expression in a cauline leaf.

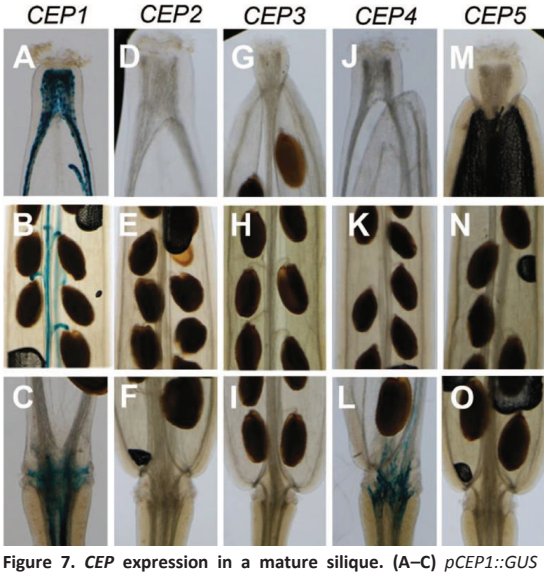


**Figure 7. *CEP* expression in a mature silique. (A–C)** *pCEP1::GUS* reporter line, **(D–F)** *pCEP2::GUS* reporter line, **(G–I)** *pCEP3::GUS* reporter line, **(J–L)** *pCEP4::GUS* reporter line, **(M–O)** *pCEP5::GUS* reporter line. **(A, D, G, J, M)** *CEP* expression in the tip of a mature silique. **(B, E, H, K, N)** *CEP* expression in middle part of mature silique. **(C, F, I, L, O)** *CEP* expression at the base of a mature silique.

During lateral root development *CEP1*, *CEP3*, and *CEP5* were expressed at various stages **(Figure 8)**. For example, *CEP1* was expressed in the inner layer of the stage II primordium **(Figure 8B)**, and later in the central core of the developing lateral root primordium, coinciding with the (future) vasculature (**Figure 8E–H)**. Both *CEP3* and *CEP5* were expressed at the base of the lateral roots, where *CEP5* is expressed from an earlier time point in development compared to *CEP3* **(Figure 8W, X, and AH–AO)**. *CEP4* was also expressed at the base and in the vasculature of the emerged lateral root **(Figure 8AG)**.

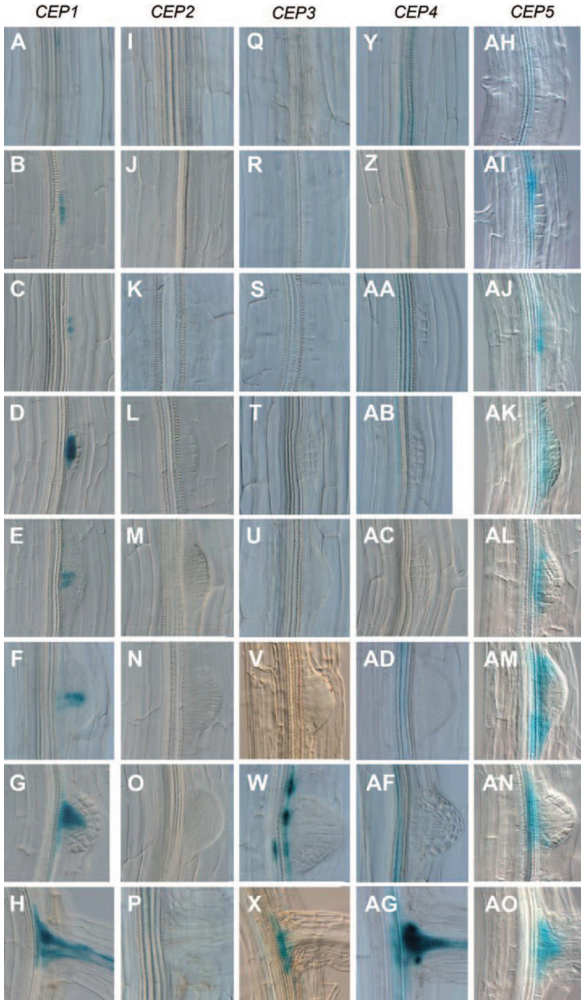


**Figure 8. *CEP* expression during lateral root development. (A–H)** *pCEP1::GUS* reporter line, **(I–P)** *pCEP2::GUS* reporter line, **(Q–X)** *pCEP3::GUS* reporter line, **(Y–AG)** *pCEP4::GUS* reporter line, **(AH–AO)** *pCEP5::GUS* reporter line. Stages of lateral root development, from initiation **(A, I, Q, Y, AH)** to an emerged lateral root **(H, P, X, AG, AO)**, are shown.

The combination of *in planta* and *in silico* expression patterns showed that *CEP* genes are expressed throughout plant development **(Figure 4)**. This study observed some variation between *in planta* and *in silico* data **(Supplementary Table S1)**, which could be due to experimental conditions (*e.g.* responsiveness of *CEPs* to external and/or environmental stimuli). It is also interesting to note that the *CEP* expression patterns were often associated with the vasculature during a specific developmental process. At present, there is no functional evidence for any evolutionary reason behind these vasculature-associated expression patterns. However, CEPs are absent in the more primitive groups of the green lineage, such as green algae, the non-vascular land plant *P. patens*, and *S. moellendorffii*, which is a representative of the earliest vascular plants that has a simple protostele (phloem surrounding the xylem). Therefore, one explanation could be that the appearance of CEPs coincides with the formation of more complex vascular tissues, such as actinosteles and eusteles in which the vascular tissue becomes more fragmented in separate bundles.

**CEP5 is involved in aboveground growth**

Since a role for CEP1 in root growth and development had been described previously (Ohyama et al., 2008), this work focused on the effects of perturbing *CEP* levels on aboveground parts to determine if CEPs play a role in shoot development. Overexpression and knockdown lines were generated and analysed for *CEP5*, which is expressed in the shoot **(Figure 4)**. Multiple lines with a range of *CEP5* expression levels and displaying similar phenotypes were generated (data not shown), but this work selected representative knockdown and overexpression lines. The obtained phenotypes for knockdown or overexpression lines **(Figure 9)** were correlated with reduced or increased *CEP5* expression levels, respectively **(Supplementary Figure S4)**.

RNAi knockdown plants for *CEP5* after 3 weeks of growth post-bolting demonstrated a slight increase in plant height compared to Col-0 **(Figure 9A and D)**. In contrast, a strong overexpression line for *CEP5* was extremely stunted and displayed a loss of shoot gravitropic response **(Figure 9A–D)**. A weaker *CEP5* overexpression line did not display the same dramatic phenotype but appeared mildly defected in stem gravitropism **(Figure 9A)**. The rosette diameter was significantly reduced in the strong *CEP5* overexpression line, compared to the control **(Figure 9E)**. In addition, strong *CEP5* overexpression resulted in smaller, often curled, leaves **(Figure 9F)**. However, given the *CEP5* expression pattern, the leaf size phenotype might be due to non-specific effects and might reflect a role for another, highly similar, CEP peptide.

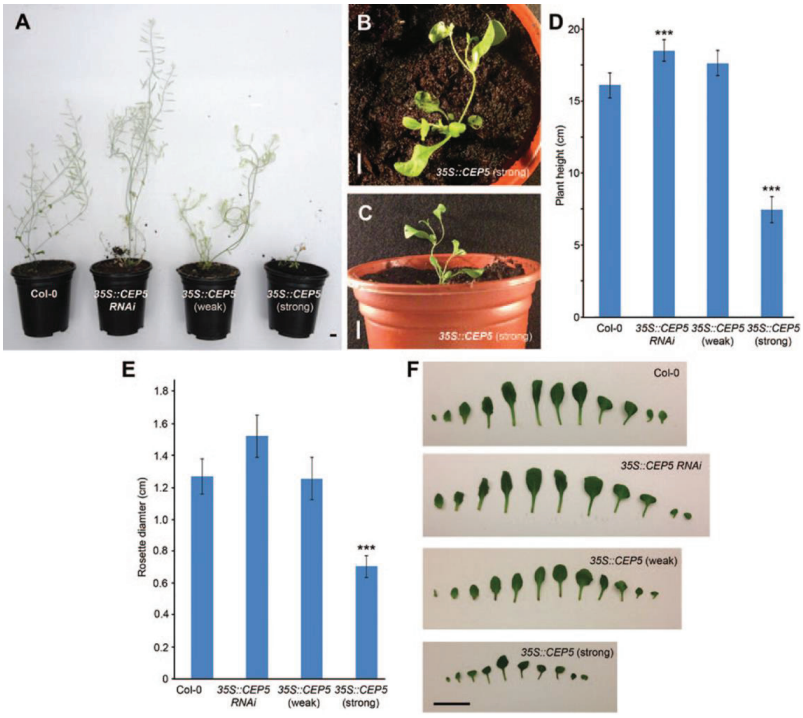


**Figure 9. Characterization of aboveground growth in lines with perturbed CEP5 expression levels. (A)** Representative shoot of Col-0 (background line), *p35S::CEP5 RNAi* knockdown line, and two overexpression lines [*p35S::CEP5* (weak) and *p35S::CEP5* (strong)] after 3 weeks of growth post-bolting. **(B and C)** Severely stunted growth of *p35S::CEP5* (strong) plants after 3 weeks of growth post-bolting. **(D)** Quantification of the plant height. **(E)** Rosette area 18 d after germination. **(F)** Representative leaf series of Col-0 (background line), *p35S::CEP5 RNAi*, *p35S::CEP5* (weak), and *p35S::CEP5* (strong). Data in D and E are means ± standard errors of at least 20 plants. ***, Student's *t*-test with a *p*-value <0.05. Bars, 1 cm.

## CONCLUSION

In conclusion, in *A. thaliana*, more than 1000 small signaling peptides have been predicted, but very few have been functionally characterized (Lease and Walker, 2006; Butenko et al., 2009; Matsubayashi, 2011; Murphy et al., 2012; Czyzewicz et al., 2013). One class of small post translationally modified signalling peptides is the CEP family (Ohyama et al., 2008). One member of this family has already been shown to be involved in regulating root architecture (Ohyama et al., 2008). Here, a bioinformatics approach was applied to identify more members of this family and to reveal that this family only emerged from higher land plants onward. The data further suggest that the CEP proteins form two subgroups according to their CEP domain. The specific *CEP* expression patterns offer a comprehensive framework to study the role of the CEP signalling peptides in plant development and hint to a possible role in cell communication mechanisms in the more complex vasculature of flowering plants. Expression patterns and perturbing levels of CEP family peptides pointed to a role in aboveground tissues, such as leaf and flower development. These results form the basis for further exploration of the mechanisms underlying this family of peptides and suggest that this family of small signalling peptides has a distinct role associated with developmental events associated with higher plants.

**ACKNOWLEDGEMENTS**

The authors thank Michael Djordjevic and co-workers for useful discussions and Maria Njo for help with the figures. This work was supported by a BBSRC David Phillips Fellowship (BB_BB/H022457/1) and a Marie Curie European Reintegration Grant (PERG06-GA-2009–256354) to I.D.S. S.S. received a Biotechnology and Biological Science Research Council doctoral training grant studentship. I.R. was supported by the Agency for Innovation by Science and Technology (IWT). B.D.R. was funded by the Special Research Fund of Ghent University, a long-term Federation of European Biochemical Societies fellowship, and a Marie Curie long-term FP7 Intra-European Fellowship (IEF-2009–252503). This work was in part financed by grants of the Interuniversity Attraction Poles Programme (IAP VI/33 and IUAP P7/29 'MARS') from the Belgian Federal Science Policy Office.

## MATERIALS AND METHODS

**Plant growth**

For analyses of aboveground parts, plants were grown on Levington M3 compost (Everris, Ipswich UK) in a glasshouse at 20–22 °C under long-day conditions (16/8 light/dark). Measurements were taken after 3 weeks of growth, immediately post-bolt. For rosette area quantification and leaf series analysis, plants were grown horizontally on square Petri plates (12 cm × 12 cm, Greiner Labortechnik) containing 50 ml solid half-strength MS growth medium (per liter: 2.15 g MS salts, 0.1 g myo-inositol, 0.5 g MES, 10 g plant tissue culture agar; pH adjusted to 5.7 with KOH) in a growth room at 22 °C under continuous light. Measurements were taken at 18 d after germination. For GUS expression analyses, seedlings were grown at 22 °C under continuous light (110 µE $m^{-2}$ $s^{-1}$ photosynthetically active radiation, supplied by cool-white fluorescent tungsten tubes, Osram) on square Petri plates containing 50 ml solid half-strength MS growth medium supplemented with 1% sucrose (per liter: 2.15 g MS salts, 0.1 g myo-inositol, 0.5 g MES, 10 g sucrose, 8 g plant tissue culture agar; pH adjusted to 5.7 with KOH), and flowering plants were grown in a greenhouse at 21 °C under long-day conditions.

**Sequence identification and conserved motif analysis of CEP proteins**

New members of the CEP family in *Arabidopsis thaliana* were identified using the 15-amino-acid mature region from known CEP peptides as input sequences for a TBLASTN search in all six open reading frames of the complete A. *thaliana* genome nucleotide sequence (http://blast.ncbi.nlm.nih.gov/Blast.cgi), and CEP assignment and naming was aligned with the results from Delay et al. (2013). The position on the genome of each hit was determined (using the SeqViewer browser from TAIR, http://tairvm09.tacc.utexas.edu/servlets/sv) and was screened in all six possible open reading frames (using the translate tool from ExPASy; http://web.expasy.org/translate/) for a peptide of approximately 75–250 amino acids (Supplementary Dataset S1, available at JXB online). If these proteins contained an N-terminal signal peptide (SignalP4.1; http://www.cbs.dtu.dk/services/SignalP; with standard settings, except for a D-cutoff of 0.45) and a 'CEP-like' sequence in the C-terminal region of the peptide, they were classified as CEP peptides.

To identify potential members of the CEP gene family in the plant lineage, *A. thaliana* CEP family members were used as a query in blast searches against Phytozome version 9.0 (http://www.phytozome.net/search.php), which contains the most up-to-date list of genomes (13 December 2012). The blast analyses using full-length protein sequences were performed using standard settings (except for an E threshold of 10). The program MEME (Bailey et al., 2009) (http://meme.nbcr.net/meme/cgi-bin/meme.cgi) was used to identify motifs in the candidate CEP protein sequences. MEME was run with the following parameters: number of repetitions = any, maximum number of motifs = 5, and with optimum motif widths constrained to between 6 and 50 residues. Weblogo (http://weblogo.berkeley.edu/logo.cgi) was used with standard settings to represent the consensus CEP domains.

**Data mining analyses**

For environmental and hormonal effects on *CEP* genes, the transcriptome meta-analysis tool Genevestigator (Hruz et al., 2008) was used, with a significance level of <0.05. For cell, tissue, and organ *CEP* expression data, the eFP browser (http://bar.utoronto.ca/efp/cgi-bin/efpWeb.cgi) was used with standard settings.

**Alignment and phylogenetic analysis**

Phylogenetic analyses of the CEP proteins and CEP domains based on amino acid sequences were carried out using UPGMA methods in the CLC Main Workbench version 6.8.1 (www.clcbio.com). Support for each node was tested with 10 000 bootstrap replicates.

**CEP constructs**

Gateway cloning was used for every construct. Entry clones containing the CEP promoter sequences (*CEP1*, 1997 bp; *CEP2*, 1400 bp; *CEP3*, 1560 bp; *CEP4*, 2000 bp; *CEP5*, 900 bp) were created by cloning PCR-fragments into the pDONRP4P1R vector. The *pCEPx::GUS* constructs were created by cloning the promoter fragment into the pEX-K7SNFm14GW destination vector. An entry clone containing the genomic coding sequence of *CEP5* (318 bp) was created by cloning the PCR-fragment into the pDONR221 vector. The *p35S::CEP5* construct was created by cloning this genomic coding sequence in the pK7GW2 destination vector. The *p35S::CEP5 RNAi* (CATMA5a62210) construct was created using the pAGRIKOLA constructs (Hilson et al., 2004). Constructs were transformed in Col-0 using floral dip (Clough and Bent, 1998).

**GUS expression**

For the GUS assays, plants were put overnight in 90% acetone, then transferred to a GUS-solution [1 mM X-Glc, 0.5% (v/v) dimethylformamide (DMF), 0.5% (v/v) Triton X-100, 1 mM EDTA (pH 8), 0.5 mM potassium ferricyanide ($K_3Fe(CN)_6$), 0.5% potassium ferrocyanide ($K_4Fe(CN)_6$), 500 mM phosphate buffer (pH 7)] and incubated at 37 °C for GUS staining, and finally washed in 500 mM phosphate buffer (pH 7). For microscopic analysis, samples were cleared with 90% lactic acid or as described in Malamy and Benfey (1997). Samples were analysed by differential interference contrast microscopy (Olympus BX53) and a stereomicroscope (Leica MZ16).

**RNA extraction, cDNA synthesis, and qRT-PCR analysis**

*Arabidopsis* RNA was isolated from 20 pooled seedlings at 7 d after germination using a Plant RNeasy Kit (Qiagen, Germany) according to the manufacturer's instructions. cDNA was subsequently prepared from a minimum of 250 ng RNA (determined by UV spectrophotometry) using a SuperScript II reverse transcriptase kit and Oligo(dT)12–18 primers (Invitrogen, USA), according to the manufacturer's instructions. Quantitative real-time PCR (qRT-PCR) was performed in a 384-well white dish format using a LightCycler 480 (Roche Applied Science, USA) with 40 PCR amplification cycles using SYBR Green I fluorescent dye (Quanta Biosciences, USA) and primers for CEP5 (5′-CCATGGACGAACCCTAAAAG-3′ and 5′-TGCCATCATCGTCTTGCTAT-3′) and ACTIN (5′-CTGGAGGTTTTGAGGCTGGTAT-3′ and 5′-CCAAGGGTGAAAGCAAGAAGA-3′). Expression was determined from a minimum of three biological replicates, each with three technical repeats, and normalized against ACTIN.

## REFERENCES


Bailey TL, Boden M, Buske FA, Frith M, Grant CE, Clementi L, Ren JY, Li WW, Noble WS (2009) MEME SUITE: tools for motif discovery and searching. *Nucleic Acids Research* **37:** 202–208.

Bailey TL, Elkan C (1994) Fitting a mixture model by expectation maximization to discover motifs in biopolymers. *Proceedings: International Conference on Intelligent Systems for Molecular Biology* **2:** 28–36.

Butenko MA, Vie AK, Brembu T, Aalen RB, Bones AM (2009) Plant peptides in signalling: looking for new partners. *Trends Plant Sci* **14:** 255–263.

Clough SJ, Bent AF (1998) Floral dip: a simplified method for Agrobacterium-mediated transformation of *Arabidopsis thaliana*. *The Plant Journal* **16:** 735–743.

Czyzewicz N, Yue K, Beeckman T, De Smet I (2013) Message in a bottle: small signalling peptide outputs during growth and development *J Exp Bot* **64:** 5281-5296

Delay C, Imin N, Djordjevic MA (2013) CEP genes regulate root and shoot development in response to environmental cues and are specific to seed plants. *J Exp Bot* **64:** 5383-5394

Hilson P, Allemeersch J, Altmann T, Aubourg S, Avon A, Beynon J, Bhalerao RP, Bitton F, Caboche M, Cannoot B, Chardakov V, Cognet-Holliger C, Colot V, Crowe M, Darimont C, Durinck S, Eickhoff H, de Longevialle AF, Farmer EE, Grant M, Kuiper MT, Lehrach H, Léon C, Leyva A, Lundeberg J, Lurin C, Moreau Y, Nietfeld W, Paz-Ares J, Reymond P, Rouzé P, Sandberg G, Segura MD, Serizet C, Tabrett A, Taconnat L, Thareau V, Van Hummelen P, Vercruysse S, Vuylsteke M, Weingartner M, Weisbeek PJ, Wirta V, Wittink FR, Zabeau M, Small I (2004) Versatile genespecific sequence tags for *Arabidopsis* functional genomics: transcript profiling and reverse genetics applications. *Genome Res* **14:** 2176–2189.

Hruz T, Laule O, Szabo G, Wessendorp F, Bleuler S, Oertle L, Widmayer P, Gruissem W, Zimmermann P (2008) Genevestigator v3: a reference expression database for the meta-analysis of transcriptomes. *Advances in Bioinformatics* **2008:** 420747.

Lease KA, Walker JC (2006) The *Arabidopsis* unannotated secreted peptide database, a resource for plant peptidomics. *Plant Physiol* **142:** 831–838.

Malamy JE, Benfey PN (1997) Organization and cell differentiation in lateral roots of Arabidopsis thaliana. *Development* **124:** 33–44.

Matsubayashi Y (2011) Small post-translationally modified Peptide signals in Arabidopsis. *The Arabidopsis Book* **9:** e0150.

Murphy E, Smith S, De Smet I (2012) Small signaling peptides in *Arabidopsis* development: how cells communicate over a short distance. *Plant Cell* **24:** 3198–3217.

Ohyama K, Ogawa M, Matsubayashi Y (2008) Identification of a biologically active, small, secreted peptide in *Arabidopsis* by *in silico* gene screening, followed by LC-MS-based structure analysis. *Plant Journal* **55:** 152–160.

Shinohara H, Matsubayashi Y (2013) Chemical synthesis of *Arabidopsis* CLV3 glycopeptide reveals the impact of hydroxyproline arabinosylation on peptide conformation and activity. *Plant Cell Physiol* **54:** 369–374.

Winter D, Vinegar B, Nahal H, Ammar R, Wilson GV, Provart NJ (2007) An 'Electronic Fluorescent Pictograph' browser for exploring and analyzing large-scale biological data sets. *PLoS One* **2:** e718.

## SUPPLEMENTAL DATA

### Supplemental Dataset 1 - *Arabidopsis* CEP proteins

*Yellow, Signal P 4.1 predicted cleavage position*
*Boxed, conserved arginine (R)*
*Grey, CEP domain (based on MEME prediction; light grey indicates a motif we excluded from further analyses)*

**>At_CEP1_At1g47485**
MGMSNRSVSTSIFFLALVVLHGIQDTEERHLKTTSLEIEGIYKKTEAEHPSIVVTYTRRGVLQKEVIAHPTDFRPTNPGNSPGVGHSNGRH

**>At_CEP2_At1g59835**
MKLFIITVVTILTISRVFDKTPATTEARRKSKKMVGHEHFNEYLDPTFAGHTFGVVKEDFLEVKKLKKIGDENNLKNRFINEFAPTNPEDSLGIGHPR
VLNNKFTNDFAPTNPGDSPGIRHPGVVNV

**>At_CEP3_At2g23440**
MATINVYVFAFIFLLTISVGSIEGRKLTKFTVTTSEEIRAGGSVLSSSPPTEPLESPPSHGVDTFRPTEPGHSPGIGHSVHN

**>At_CEP4_At2g35612**
MVSRGCSITVLFRFLIVLLVIQVHFENTKAARHAPVVSWSPPEPPKDDFVWYHKINRFKNIEQDAFRPTHQGPSQGIGHKNPPGAP

**>At_CEP5_At5g66815**
MESFMGQKKTLYACYFLMLVFFLGFNCVHGRTLKVDDKINGGHYDSKTMMALAKHNDMMVDDKAMQFSPPPPPPPPSQSGGKDAEDFR
PTTPGHSPGIGHSLSHN

**>At_CEP6_At5g66816**
MKLSVYIILSILFISTVFYEIQFTEARRQLRKTDDQDHDDHHFTVGYTDDFGPTSPGNSPGIGHKMKENEENAGGYKDDFEPTTPGHSPGVGHAV
KNNEPNA

**>At_CEP7 (between At5g66817 - At5g66820)**
MAKCTLTSLILLLIVLVLIQESHIVEGRRPLKSSRISNVSKKFAAGNSNLSSKLTTEDHSLDAFRPTNPGNSPGIGH

**>At_CEP8 (between At5g66817 - At5g66820)**

MAKALFFNFCISLLIIAILVSHEIIPTEARRHLRTHRKSIKNSTLTVHEGAGGLRTGGGSVKTDISKEEHGVDEFRPTTPGNSPGIGH

**>At_CEP9_At3g50610**
MKLLSITLTSIVISMVFYQTPITTEARRSLRKTNDQDHFKAGFTDDFVPTSPGNSPGVGHKKGNVNVEGFQDDFKPTEGRKLLKTNVQDHFKTGS
TDDFAPTSPGHSPGVGHKKGNVNVESSEDDFKHKEGRKLQQTNGQNHFKTGSTDDFAPTSPGNSPGIGHKKGHANVKGFKDDFAPTEEIRL
QKMNGQDHFKTGSTDDFAPTTPGNSPGMGHKKGDDFKPTTPGHSPGVGHAVKNDEPKA

**>AtCEP10 (between At1g36040 - At1g36050)**
MKLFIIIVVTSLTISKVFDKTLVTIEARRNLRKMDRHEHFNANEDFVEAKMLKKIDNKNNLNNRCINDFAPTNPGHNSGIGHPKVINNKFTKDFAP
TNPGHSPGIGHLRVVNNKFTNDFAPTNPGNSPGIRHP

**>At_CEP11 (between At2g23440 - At2g23450)**
MAKTRRVIYLFLTIVLLFCELIDEAQGSRRFRCHHSEDYSCKKRSSHHHHHHHHHQQQQHHHKDTPPEELQGSIKTRRSKDIYGLNAFRSTEPGH
SPGVGHLIKT

**>At_CEP12_At1g31670 (first exon of At1g31670, likely incorrectly annotated)**
MVNRDNSIVALSFFMLFLLVLHLHFETTTAARKPVRVFGPPSSIEWSPPSPPKDDFEWFEINIYKNIEQTAFRPTGQGPSQGIGHKDPPGAP

**>At_CEP13_At1g16950**
MARPRISISMICLLILIVGFVLQSSQARKVLVPYGTSKGLFLSALPKGNVPPSGPSDKGHTSPPDDTDQRMVPENSPEIYRRLESVPSPGVGH

**>At_CEP14_At1g29290**
MAVRLIPTIWLFIVFAVIVSALPSLVSSRKLLEVKKQENLTVREEEKSHMPHVTKTSTLSALPKGKIPNSTPSKKGHAAVFAGKLRSRHLSTVDRYL
RSVPSPGVGH

**>At_CEP15_At2g40530**
MDATKIKFDVILLSFLLIISGIPSNLGLSTSVRGTTRSEPEAFHGGKFPAMKMRKLMAPNMEVDYSSDYYDGGSSSSTTSPSPPVPDYDDIYRRQ
GDVPSPGIGH

**Supplemental Dataset 2 – CEP domains predicted by MEME**

**>At_CEP1_AT1G47485**
DFRPTNPGNSPGVGH
**>At_CEP2a_AT1G59835**
EFAPTNPEDSLGIGH
**>At_CEP2b_AT1G59835**
DFAPTNPGDSPGIRH
**>At_CEP3_AT2G23440**
TFRPTEPGHSPGIGH
**>At_CEP4_AT2G35612**
AFRPTHQGPSQGIGH
**>At_CEP5_AT5G66815**
DFRPTTPGHSPGIGH
**>At_CEP6a_AT5G66816**
DFGPTSPGNSPGIGH
**>At_CEP6b_AT5G66816**
DFEPTTPGHSPGVGH
**>At_CEP7_AT5G66818**
AFRPTNPGNSPGIGH
**>At_CEP8_AT5G66819**
EFRPTTPGNSPGIGH
**>At_CEP9a_AT3G50610**
DFVPTSPGNSPGVGH
**>At_CEP9b_AT3G50610**
DFAPTSPGHSPGVGH
**>At_CEP9c_AT3G50610**
DFAPTSPGNSPGIGH
**>At_CEP9d_AT3G50610**
DFAPTTPGNSPGMGH
**>At_CEP9e_AT3G50610**
DFKPTTPGHSPGVGH
**>AtCEP10a_AT1G36045**
DFAPTNPGHNSGIGH
**>AtCEP10b_AT1G36045**
DFAPTNPGHSPGIGH
**>AtCEP10c_AT1G36045**
DFAPTNPGNSPGIRH
**>At_CEP11_AT2G23445**
AFRSTEPGHSPGVGH
**>At_CEP12_At1g31670**
AFRPTGQGPSQGIGH
**>At_CEP13_AT1G16950**
IYRRLESVPSPGVGH
**>At_CEP14_AT1G29290**
VDRYLRSVPSPGVGH
**>At_CEP15_AT2G40530**
IYRRQGDVPSPGIGH

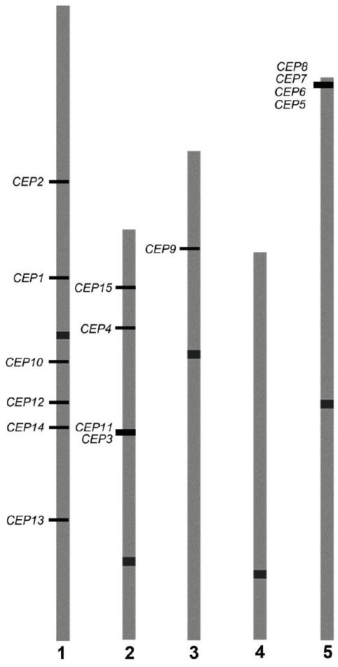


**Supplemental Figure 1. Position of *CEP* family members on the 5 *Arabidopsis* chromosomes.**

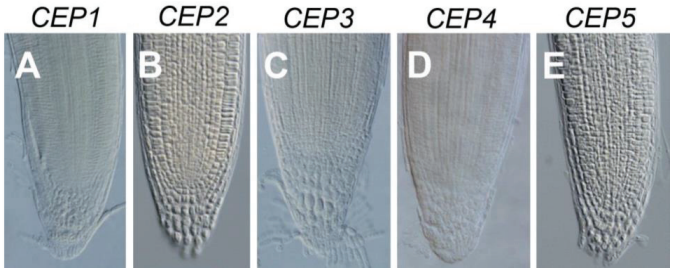


**Supplemental Figure 2. Expression patterns of *CEP1* – *CEP5* in the root apical meristem. (A)** *pCEP1::GUS* reporter line, **(B)** *pCEP2::GUS* reporter line, **(C)** *pCEP3::GUS* reporter line, **(D)** *pCEP4::GUS* reporter line, **(E)** *pCEP5::GUS* reporter line. None of the above CEP genes are expressed in the RAM in five day old or two week old seedlings.

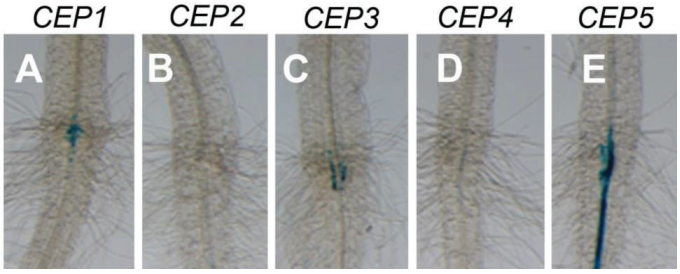


**Supplemental Figure 3. *CEP1* – *CEP5* transcription profiles in the root-hypocotyl junction. (A)** *pCEP1::GUS* reporter line, **(B)** *pCEP2::GUS* reporter line, **(C)** *pCEP3::GUS* reporter line, **(D)** *pCEP4::GUS* reporter line, **(E)** *pCEP5::GUS* reporter line. **(A, C, D, E)** *CEP1*, *CEP3*, *CEP4* and *CEP5* are expressed at the root-hypocotyl junction in five day old and two week old seedlings.

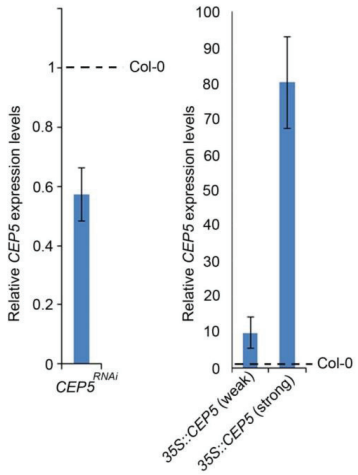


**Supplemental Figure 4. *CEP5* expression levels in *p35S::CEP5RNAi* and *p35S::CEP5* lines depicted in Figure 9.**

**Supplemental Table 1. Comparison of *in silico* (eFP browser)/*in planta* (*pCEPx::GUS*) *CEP* expression**

| | *CEP1* | *CEP2* | *CEP3* | *CEP4* | *CEP5* | *CEP6* | *CEP7* | *CEP8* | *CEP9* | *CEP10* | *CEP11* | *CEP12* | *CEP13* | *CEP14* | *CEP15* |
|---|---|---|---|---|---|---|---|---|---|---|---|---|---|---|---|
| **Shoot Apical Meristem** | +/+ | NA/+ | +/- | NA/- | -/- | NA/NA | NA/NA | NA/NA | +/NA | NA/NA | NA/NA | NA/NA | -/NA | NA/NA | -/NA |
| **Cotyledon** | -/- | NA/+ | +/+ | NA/- | -/- | NA/NA | NA/NA | NA/NA | +/NA | NA/NA | NA/NA | NA/NA | -/NA | NA/NA | +/NA |
| **Leaf** | -/+ | NA/+ | +/+ | NA/- | -/+ | NA/NA | NA/NA | NA/NA | +/NA | NA/NA | NA/NA | NA/NA | +/NA | NA/NA | +/NA |
| **Flower** | +/+ | NA/+ | +/+ | NA/+ | -/+ | NA/NA | NA/NA | NA/NA | +/NA | NA/NA | NA/NA | NA/NA | +/NA | NA/NA | -/NA |
| **Root Apical Meristem** | +/- | NA/- | -/- | NA/- | -/- | NA/NA | NA/NA | NA/NA | -/NA | NA/NA | NA/NA | NA/NA | -/NA | NA/NA | +/NA |
| **Lateral Root** | +/+ | NA/- | +/+ | NA/+ | +/+ | NA/NA | NA/NA | NA/NA | +/NA | NA/NA | NA/NA | NA/NA | +/NA | NA/NA | +/NA |

+, present; -, absent; NA, no data available

**Supplemental Table 2. Genevestigator data on *CEP* expression**

| Gene | Germinated seed | Seedling | Young rosette | Developed rosette | Bolting | Young flower | Developed flower | Flowers and siliques | Mature siliques | Senescence |
|---|---|---|---|---|---|---|---|---|---|---|
| ***CEP1*** | 184 | 191 | 157 | 168 | 430 | 194 | 236 | 352 | 188 | 296 |
| ***CEP2*** | ND | 105 | 117 | ND | ND | ND | 119 | ND | ND | ND |
| ***CEP3*** | 198 | 210 | 201 | 207 | 215 | 235 | 227 | 222 | 227 | 215 |
| ***CEP4*** | ND | 142 | 209 | ND | ND | ND | 190 | ND | ND | ND |
| ***CEP5*** | 323 | 677 | 339 | 266 | 216 | 207 | 192 | 217 | 182 | 205 |
| ***CEP6*** | ND | 112 | 175 | ND | ND | ND | 158 | ND | ND | ND |
| ***CEP7*** | ND | ND | ND | ND | ND | ND | ND | ND | ND | ND |
| ***CEP8*** | ND | ND | ND | ND | ND | ND | ND | ND | ND | ND |
| ***CEP9*** | 255 | 282 | 273 | 213 | 235 | 246 | 239 | 251 | 283 | 291 |
| ***CEP10*** | ND | ND | ND | ND | ND | ND | ND | ND | ND | ND |
| ***CEP11*** | ND | ND | ND | ND | ND | ND | ND | ND | ND | ND |
| ***CEP12*** | 417 | 449 | 552 | 418 | 445 | 408 | 526 | 483 | 1606 | 374 |
| ***CEP13*** | 247 | 245 | 216 | 234 | 250 | 329 | 317 | 619 | 289 | 252 |
| ***CEP14*** | ND | 776 | 837 | ND | ND | ND | 657 | ND | ND | ND |
| ***CEP15*** | 312 | 309 | 374 | 460 | 347 | 318 | 607 | 343 | 249 | 197 |

ND, no data available. Numbers highlighted in red are likely noise.

# Chapter 4:

## Functional characterization of the CEP peptide family and their proposed receptors in *Arabidopsis*

**Contributions:**

I.R. was the main author of this work. I.R. conducted all the experimental work, analyzed the data and wrote the manuscript. T.B. and I.D.S. contributed to the writing and supervised the research.

# Functional characterization of the CEP peptide family and their proposed receptors in *Arabidopsis*

Ianto Roberts[1,2], Ive De Smet[1,2] and Tom Beeckman[1,2]

[1]Department of Plant Systems Biology, VIB B-9052 Gent, Belgium
[2]Department of Plant Biotechnology and Bioinformatics, Ghent University, B-9052 Gent, Belgium

## ABSTRACT

Intercellular communication by signaling peptides has been shown to play a crucial role during plant development. This study aimed to gain more insight into the developmental processes potentially regulated by the C-TERMINALLY ENCODED PEPTIDE (CEP) signaling peptide family and their proposed receptors, CEP RECEPTOR 1/XYLEM INTERMIXED WITH PHLOEM 1 (CEPR1/XIP1) and CEP RECEPTOR 2 (CEPR2). Overexpression lines for all 15 *CEP* genes were created and examined for effects on root and shoot growth. Based on a correlation between similarities in amino acid residues and accompanying similarities in overexpression phenotype, the CEP peptides could be divided into four functional groups. In addition, systematic expression analysis of all 15 *CEP* genes during plant growth revealed large overlaps, mainly in vasculature-associated tissues. This observation, together with the highly conserved peptide sequences and relatively weak morphological phenotypes of single *cep* mutants, suggested a high degree of functional redundancy. Therefore, based on expression analysis and sequence similarity, higher order *cep* mutants were generated and characterized. In contrast to single mutants, higher order *cep* mutants showed an increase in the size of the root system, opposite to the phenotype observed in corresponding overexpression lines. Expression analysis of *CEPR1/XIP1* and *CEPR2* showed distinct expression patterns, such as *CEPR1/XIP1* expression at the phloem pole and *CEPR2* at the xylem pole in the root vasculature, suggesting that each receptor might control a different developmental process. A phenotypical analysis of the *cepr* mutants uncovered a different effect on root growth, with *xip1-1* mutant having drastically reduced root growth and *cepr2* mutants a slightly positive effect on root growth. Altogether, CEP peptides and their proposed receptors have an impact on the size of the root system.

## INTRODUCTION

The C-TERMINALLY ENCODED PEPTIDE (CEP) peptide family belongs to the class of small-post-translationally modified peptides, and counts 15 members in *Arabidopsis thaliana*, that were divided into two groups *(Ohyama et al, 2008; Delay et al, 2013; Roberts et al, 2013)*. The *CEP* genes encode small prepropeptides, ranging in size from 76 to 243 amino acids, with an N-terminal signal peptide (SP) sequence, a middle variable region, and one or more highly conserved CEP domain(s) at the C-terminus. From these CEP domain motifs, the active mature CEP peptides of 15 amino acids are derived after proteolytic processing and are further post-translationally modified by proline hydroxylation and arabinosylations (Ohyama et al, 2008; Tabata et al, 2014; Mohd-Radzman et al, 2015). Several of the mature CEP peptides from group I were shown to be perceived by the leucine-rich repeat – receptor-like kinase (LRR-RLK) receptors CEP RECEPTOR 1/XYLEM INTERMIXED WITH PHLOEM 1 (CEPR1/XIP1) and CEP RECEPTOR 2 (CEPR2) (Tabata et al, 2014).

At a physiological level, CEP-CEPR signaling is suggested to play an important role in the nitrogen starvation response (Delay et al, 2013; Imin et al, 2013; Tabata et al, 2014). It was proposed that *CEP* genes are transcriptionally upregulated in roots in regions with low nitrogen levels, after which the CEP peptides act as systemic root-derived ascending signals that are perceived by CEPRs in the shoot and trigger the production of a currently unknown shoot-derived descending signal that upregulates *NITRATE TRANSPORTER* (*NRT*) genes in the other parts of the root system to stimulate nitrogen uptake (Tabata et al, 2014).

At a morphological level, it was shown for some CEPs that treatment with synthetic CEP peptides or constitutive overexpression affects shoot growth or leads to reduced root growth by a gradual decrease in root apical meristem (RAM) size (Ohyama et al, 2008; Delay et al, 2013; Roberts et al, 2013). It is currently not known if all CEP peptides induce a similar phenotype or whether there are differences between the individual members.

For several members of the CEP peptide family and their proposed receptors, the expression pattern has only been superficially described. (Roberts et al, 2013; Tabata et al, 2014). Detailed expression analysis for all members of the *CEP* family (including the previously un-described *CEP12-15* genes) and detailed localization of CEPR1 and CEPR2 proteins is currently still lacking.

At the moment, most results on CEP functional analysis is derived from gain-of-function studies using *CEP* overexpression lines and/or synthetic CEP peptide treatments instead of loss-of-function *cep* mutants. The lack of *cep* mutant data originates from common problems that are encountered in studies of peptide families. One problem is functional redundancy, which is caused by the combination of highly similar mature peptide sequences and largely overlapping expression patterns. Another is the lack of loss-of-function mutants for all members of the peptide family, due to the small size of the open reading frame of signaling peptides. Higher order mutants are likely required to attain information on their impact on developmental processes.

In this work, overexpression lines for all 15 *CEP* genes were generated and phenotypically analyzed for effects on root and shoot growth, revealing four functional subgroups (Ia, Ib, Ic and II). Furthermore, an overview of the expression patterns for all 15 *CEP* genes during plant development, as well as a detailed expression analysis of *CEPR1* and *CEPR2*, is provided. And finally, a collection of T-DNA insertion lines for several members of the *CEP* family was compiled and used to generate higher order *cep* mutants based on a meta-analysis of overlapping expression patterns, sequence homology of the promoter and coding sequence, and their response to hormone treatments. Remarkably, while gain-of-function lines of *CEP* genes from subgroup Ib all led to an inhibition of root growth, higher order mutants from this subgroup all showed enhanced root growth, strongly arguing for the fact that these CEP peptides are most likely part of a root growth restraining mechanism.

## RESULTS

**Analysis of *CEP* overexpression phenotypes in the shoot and root**

Transgenic plants were generated with the coding sequence from *CEP1* to *CEP15* expressed under the control of the constitutive cauliflower mosaic virus *CaMV 35S* promoter (*p35S::CEP* lines). For each CEP gene, two representative independent overexpression lines were selected, based on overexpression levels and similar phenotype (**Supplemental Figure S1)**. Analysis of shoot and root growth in these overexpression lines allowed defining distinct phenotypical classes among CEP peptides.

The root system of *CEP2*, *CEP9* and *CEP10* overexpression lines showed a similar primary root length with a slight increase in emerged lateral root density compared to Col-0 control seedlings. In contrast, overexpression of *CEP1*, *CEP3*, *CEP4*, *CEP5*, *CEP7*, *CEP8*, *CEP11* and *CEP12* led to a strong reduction in primary root length and a strong reduction in the number of emerged lateral roots, but an increased emerged lateral root density. Only a moderate reduction of primary root growth and number of emerged lateral roots was observed in the *CEP6* overexpression line. In contrast, overexpression of the group II *CEP* members, *CEP13*, *CEP14* and *CEP15*, induced a larger root system, with a significantly longer primary root in *CEP14* and *CEP15* overexpression lines, and an increase in the number of emerged lateral roots in *CEP13*, *CEP14* and *CEP15* overexpression lines **(Figure 1-2)**.

The drastic reduction in primary root length in the *CEP5* overexpression line was due to a significant reduction in the size of the root apical meristem (RAM, measured as the distance between the quiescent center cells and the site of first cortical cell elongation). And this phenotype could be pheno-copied by growing Col-0 seedlings on growth medium supplemented with synthetic CEP5p$^{Hyp}$ peptide at increasing concentrations **(Supplementary Figure S2A)**. Furthermore, it was observed that prolonged exposure to elevated levels of (ectopic) CEP5 peptide leads to a gradual decrease in size of the RAM over time: in Col-0 control seedlings, the RAM size increased in size over time, whereas in the *CEP5*$^{OE}$ line and CEP5p$^{Hyp}$ treatment, the RAM size decreased in size over time and eventually led to vascular differentiation very close to the root tip **(Supplementary Figure S2B-C)**. A similar effect on the RAM size was observed in the overexpression lines of *CEP1*, *CEP3*, *CEP4*, *CEP7*, *CEP8*, *CEP11* and *CEP12* **(not shown)**, and in all cases led to the drastic reduction in primary root length.

Next to the root system, the shoot of the *CEP* overexpression lines were analyzed of plants in the (early and late) reproductive phase (34 and 43 days after germination, respectively), to check the effect of *CEP* gain-of-function on the above-ground part of the plant. Overexpression of *CEP2*, *CEP9* or *CEP10* led to a similar flowering time and number of vegetative leaves compared with Col-0, but with a slightly larger inflorescence size,. On the other hand, plants overexpressing *CEP1*, *CEP3*, *CEP4*, *CEP5*, *CEP7*, *CEP8*, *CEP11* or *CEP12* triggered an obvious delay in flowering time, with a smaller bushier inflorescence and a drastic increase in the number of vegetative leaves. Only a moderate delay in flowering time, with a moderate decrease in inflorescence size and a slightly increased number of vegetative leaves, was observed in the *CEP6* overexpression line. Overexpression of group II *CEP13*, *CEP14* and *CEP15* showed no drastic differences in flowering time, number of vegetative leaves or inflorescence size compared to Col-0 **(Figure 3 and 4, and Supplementary Figure S3)**.

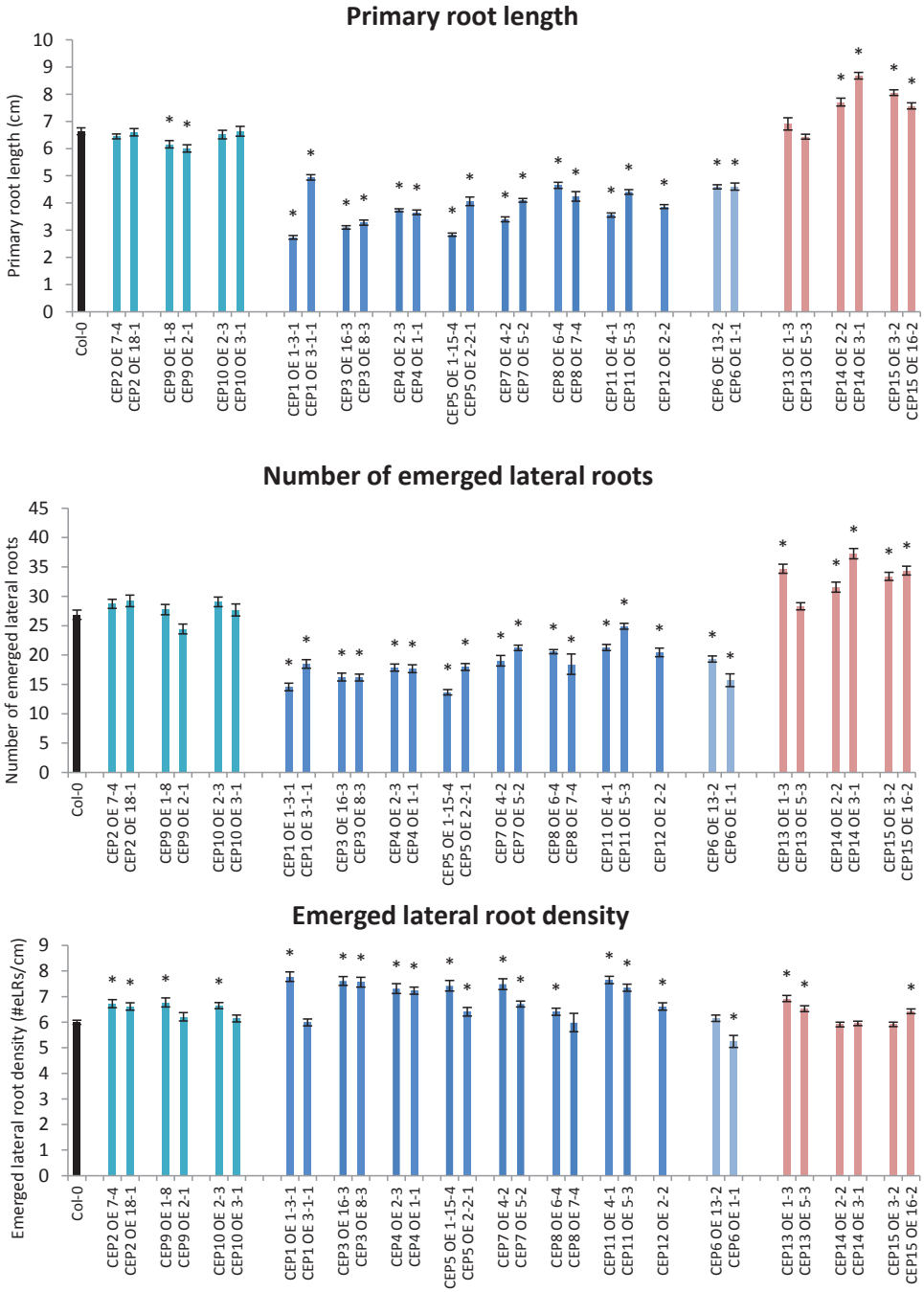


**Figure 1. Root phenotype of *CEP*$^{OE}$ lines.** Primary root length measurements, number of emerged lateral roots and the emerged lateral root density for two independent overexpression lines for each *CEP* gene in 10 day old seedlings grown on ½ MS growth medium. Group I CEP members are marked in blue (further divided in three subgroups based on phenotype) and group II CEP members are marked in pink. Graphs shown mean ± SE, n > 20, * $p < 0.05$ according to Student's *t*-test.

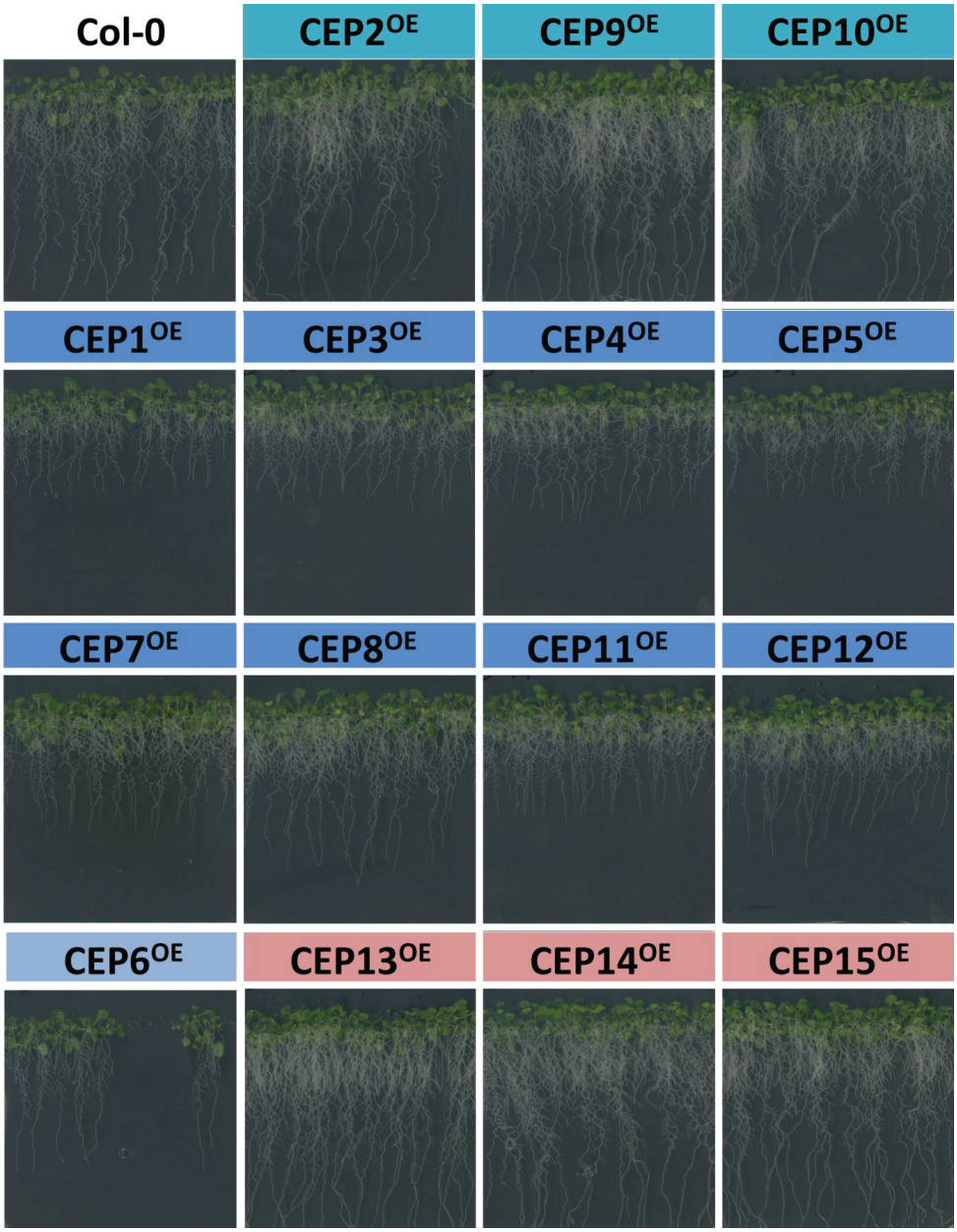


**Figure 2. Root phenotype of *CEP*$^{OE}$ lines.** Seedlings of *p35S::CEP* overexpression lines compared to Col-0 control grown for 13 days on ½ MS growth medium. Group I CEP members are marked in blue (further divided in three subgroups based on phenotype) and group II CEP members are marked in pink.

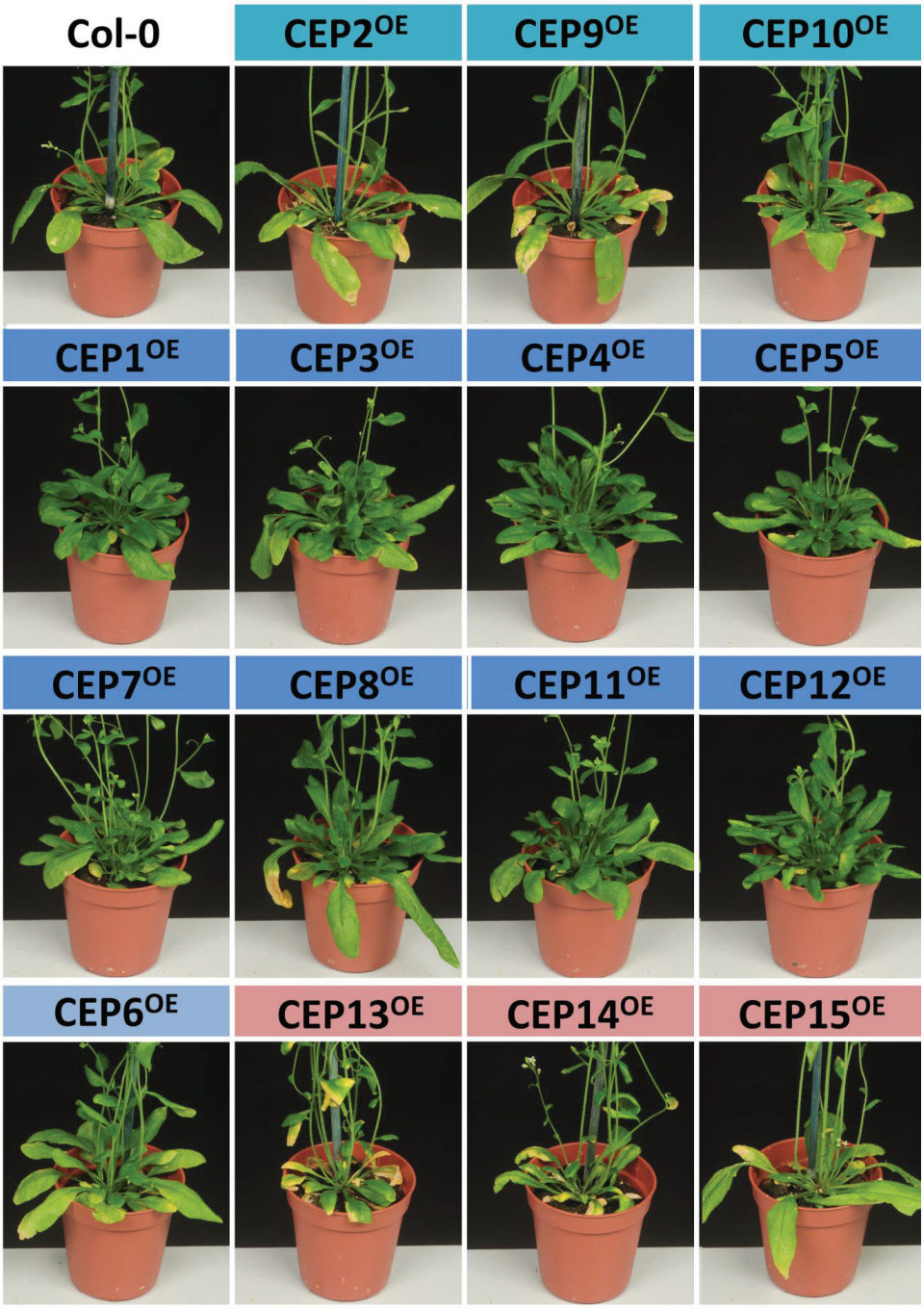


**Figure 3. Shoot phenotype of *CEP*$^{OE}$ lines.** Leaf rosettes of 43-day-old mature plants of *p35S::CEP* overexpression lines compared to Col-0 control. Group I CEP members are marked in blue (further divided in three subgroups based on phenotype) and group II CEP members are marked in pink.

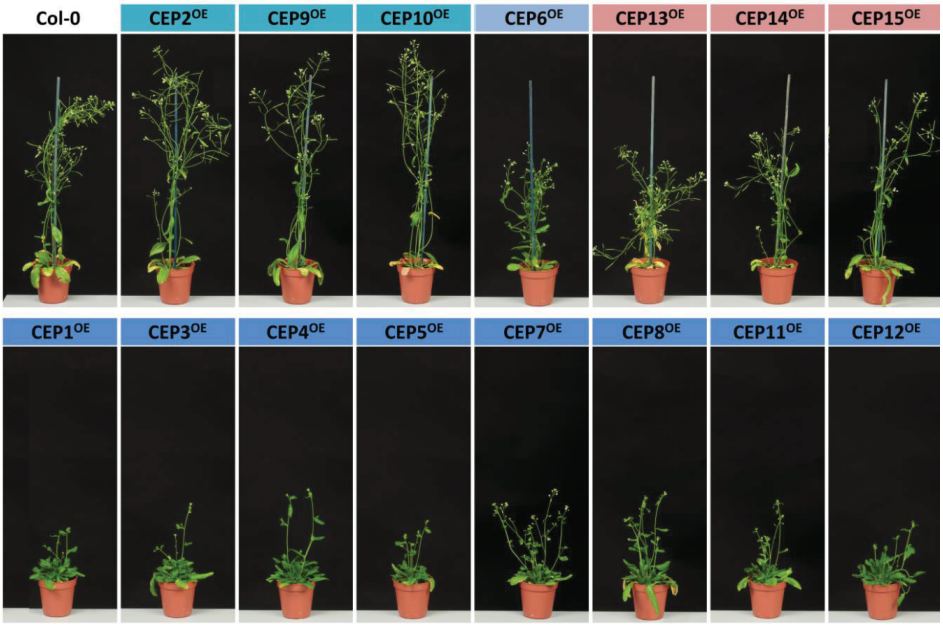


**Figure 4. Shoot phenotype of *CEP*$^{OE}$ lines.** Inflorescence of 43 day old mature plants of *p35S::CEP* overexpression lines compared to Col-0. Group I CEP members are marked in blue (further divided in three subgroups based on phenotype) and group II CEP members are marked in pink.

**CEP subgroups based on gain-of-function phenotype and mature CEP peptide sequence**

In order to check if the differences in phenotype among the *CEP* gain-of-function functional subgroups could be explained by corresponding differences in their mature peptides, the mature CEP peptides were grouped together according to their gain-of-function phenotype and their sequences were compared. The functional subgroups in group I *CEP* overexpression lines could not be correlated with corresponding differences in potential hydroxyproline/tri-arabinosylated hydroxyproline residues, since the conserved proline residue at position 4 is present in all group I CEP peptides, except in CEP11; the conserved proline residue at position 7 is present in all group I CEP peptides, except in CEP4 and CEP12; and the conserved proline residue at position 11 is present in all group I CEP peptides, except in CEP2a, CEP10a, CEP4 and CEP12 **(Figure 5)**.

On the other hand, mature CEP peptides from *CEP2*, *CEP9* and *CEP10* genes generally contain a hydrophobic alanine (A) or valine (V) residue at position 3, with the exception of CEP9e containing a hydrophilic lysine (K) **(Figure 5)**. While the mature CEP peptides from *CEP1*, *CEP3*, *CEP4*, *CEP5*, *CEP7*, *CEP8*, *CEP11* and *CEP12* all contain a positively charged hydrophilic arginine (R) residue at position 3, and CEP6 peptides contain a hydrophobic glycine (G) (CEP6a) or negatively charged hydrophilic glutamic acid (E) (CEP6b) residue at position 3 **(Figure 5)**. This suggests that the amino acid at position 3 is important for specificity and the gain-of-function phenotype. The slight reduction in primary root length in the *CEP9* overexpression line could be attributed to the the positively charged lysine (K) residue at position 3 in the CEP9e peptide, which has some similarity to the positively charged arginine (R) in subgroup Ib CEP peptides **(Figure 1 and 5)**. Thus, based on the correlation between the overexpression phenotype and the amino acid residue at position 3 in the mature peptide, the group I CEP peptides were subdivided into subgroups Ia, Ib and Ic **(Figure 5)**.

The group II CEP peptides differ in multiple residues compared to group I CEP peptides: the highly conserved phenylalanine (F) residue at position 2 is replaced by a tyrosine (Y) or aspartic acid (D); the highly conserved threonine residue at position 5 is substituted by leucine (L) or glutamine (Q); the highly conserved glycine (G) residue at position 8 is replaced by a valine (V) residue; as well as some differences in conserved proline (P) residues. Therefore, the effect on the phenotype could not be attributed to a single amino acid residue, but likely depends on the other observed differences in conserved residues **(Figure 5)**. Altogether, the CEP peptide family could be subdivided according to a correlation between the sequence of the mature CEP peptides and the effect of their gain-of-function shoot and root phenotype.

| Group | Name | Peptide sequence | Reduced Root Gr | Reduced Inflor |
|---|---|---|---|---|
| Ia | CEP2a | E F A P T N P E D S L G I G H | - | - |
| | CEP2b | D F A P T N P G D S P G I R H | - | - |
| | CEP9a | D F V P T S P G N S P G V G H | - | - |
| | CEP9b | D F A P T S P G H S P G V G H | - | - |
| | CEP9c | D F A P T S P G N S P G I G H | - | - |
| | CEP9d | D F A P T T P G N S P G M G H | - | - |
| | CEP9e | D F K P T T P G H S P G V G H | - | - |
| | CEP10a | D F A P T N P G H N S G I G H | - | - |
| | CEP10b | D F A P T N P G H S P G I G H | - | - |
| | CEP10c | D F A P T N P G N S P G I R H | - | - |
| Ib | CEP1 | D F R P T N P G N S P G V G H | ++ | ++ |
| | CEP5 | D F R P T T P G H S P G I G H | ++ | ++ |
| | CEP3 | T F R P T E P G H S P G I G H | ++ | ++ |
| | CEP8 | E F R P T T P G N S P G I G H | ++ | ++ |
| | CEP7 | A F R P T N P G N S P G I G H | ++ | ++ |
| | CEP11 | A F R S T E P G H S P G V G H | ++ | ++ |
| | CEP4 | A F R P T H Q G P S Q G I G H | ++ | ++ |
| | CEP12 | A F R P T G Q G P S Q G I G H | ++ | ++ |
| Ic | CEP6a | D F G P T S P G N S P G I G H | + | + |
| | CEP6b | D F E P T T P G H S P G V G H | + | + |
| II | CEP13 | I Y R R L E S V P S P G V G H | -- | - |
| | CEP14 | V D R Y L R S V P S P G V G H | -- | - |
| | CEP15 | I Y R R Q G D V P S P G I G H | -- | - |

**Figure 5. Link between CEP peptide sequence and overexpression phenotypes.** Overview of the mature CEP peptide sequences, grouped according to their overexpression phenotypes: reduced root growth and reduced inflorescence, and to their amino acid residue at position 3. Amino acid differences of interest are highlighted in red (position 3) and yellow (location of proline residues in consensus). (*Note:* Some CEP prepropeptides contain more than one conserved CEP domain from which mature CEP peptides are derived, and are designated as: a, b, c, d and e)

### Expression analysis of the *CEP* family

Constitutive overexpression or synthetic peptide treatments allows to have a broad idea about the overall action of a given peptide. However to gain insight in which specific developmental processes each CEP peptide is involved, knowledge on their expression patterns is crucial. Previously, we reported the expression patterns of *CEP1* to *CEP5* throughout plant development (Roberts et al, 2013). For this study, additional *pCEP::nls-GFP/GUS* reporter lines were generated for the remaining *CEP* genes to explore the expression patterns of the complete *CEP* family throughout plant development.

In the shoot apex, *CEP1*, *CEP2*, *CEP5*, *CEP6*, *CEP7*, *CEP10*, *CEP11*, *CEP13*, *CEP14* and *CEP15* are expressed in five-day-old seedlings, with *CEP9* expression appearing and *CEP10* expression disappearing in twelve-day-old seedlings. *CEP1*, *CEP7*, *CEP9*, *CEP10*, *CEP11* and *CEP14* are expressed in the shoot apical meristem (SAM) region, while *CEP2*, *CEP6* and *CEP15* are expressed in the vasculature running through the shoot apex, and *CEP2*, *CEP5*, *CEP6*, *CEP14* and *CEP15* are expressed in young developing vegetative leaves in the shoot apex. Subgroup II *CEP* members, *CEP13*, *CEP14* and *CEP15*, are also expressed in the stipules **(Figure 6 and Figure 7)**.

In the cotyledons of five day old seedlings, *CEP2*, *CEP6*, *CEP7* and *CEP15* are expressed in the vasculature, while *CEP3* and *CEP7* are expressed at the tip, presumably in the single apical developing hydathode **(Figure 8 and 10)**. In the vegetative leaves of twelve day old seedlings, *CEP2*, *CEP6*, *CEP7* and *CEP15* are expressed in the smaller veins of the leaves, while *CEP1* and *CEP5* are expressed in the mid veins. Similar to their expression in the cotyledon, *CEP3* and *CEP7* are expressed in the hydathodes at the edges of the vegetative leaf, with in addition *CEP1* becoming strongly expressed in the hydathodes at this stage. In addition, *CEP14* is expressed in the socket cells at the base of leaf trichomes **(Figure 9 and 11)**. In the cauline leaves, *CEP2*, *CEP5*, *CEP6*, *CEP7* and *CEP15* are expressed in the vasculature, *CEP12* and *CEP14* are expressed at different zones in the cauline leaf, and *CEP1* is expressed at the hydathodes at the edges of the cauline leaf. Further, *CEP1*, *CEP2*, *CEP5*, *CEP6*, *CEP7*, *CEP11*, *CEP14* and *CEP15* are expressed in the inflorescence stem, while *CEP9* and *CEP10* are expressed at the cauline leaf axils **(Figure 12)**.

During flower development, almost all *CEP* genes are expressed in various flower organs with large overlaps in expression. For example, *CEP2*, *CEP6*, *CEP7*, *CEP10*, *CEP14* and *CEP15* are expressed in the petal veins. In the pistils, *CEP1*, *CEP2*, *CEP6*, *CEP11*, *CEP12*, *CEP13*, *CEP14* and *CEP15* are expressed in different zones at different times during flower development. In the stamen, *CEP5*, *CEP8*, *CEP9*, *CEP10*, *CEP11* and *CEP13* are expressed at different parts and times during development. At the receptacle or base of the flower, *CEP1*, *CEP2*, *CEP5*, *CEP6*, *CEP7*, *CEP11*, *CEP14* and *CEP15* are expressed **(Figure 13)**.

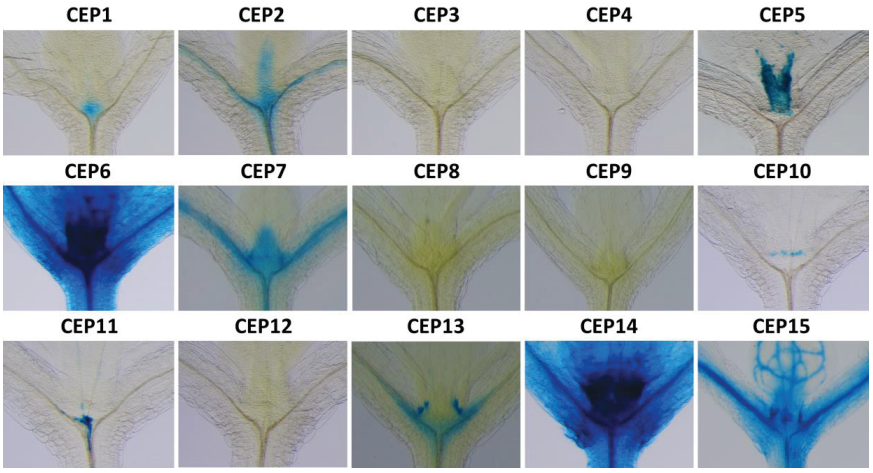


**Figure 6. *CEP* expression in the shoot apical meristem region of five day old seedlings.** *CEP* expression was monitored through *promoter::NLS:GUS:GFP* reporter lines.

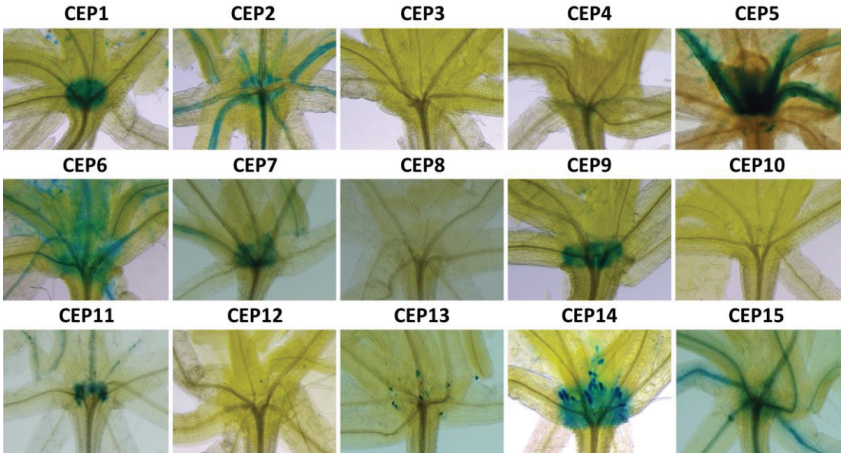


**Figure 7. *CEP* expression in the shoot apical meristem region in twelve day old seedlings.** *CEP* expression was monitored through *promoter::NLS:GUS:GFP* reporter lines.

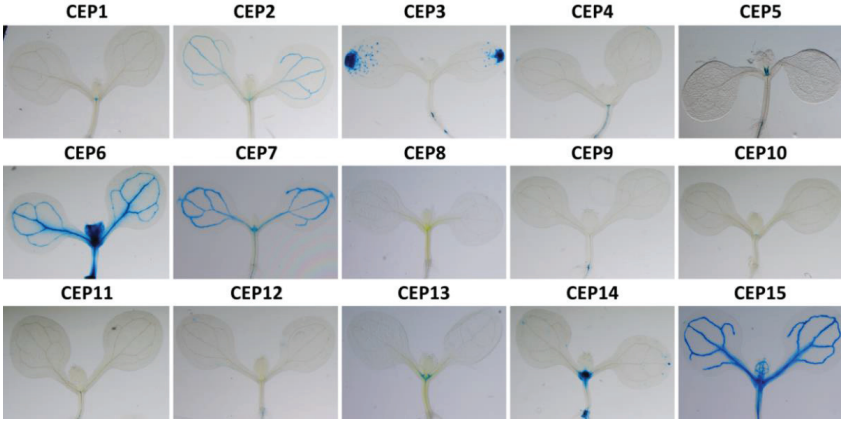


**Figure 8. Overview of *CEP* expression patterns in the shoot of five day old seedlings.** *CEP* expression was monitored through *promoter::NLS:GUS:GFP* reporter lines.

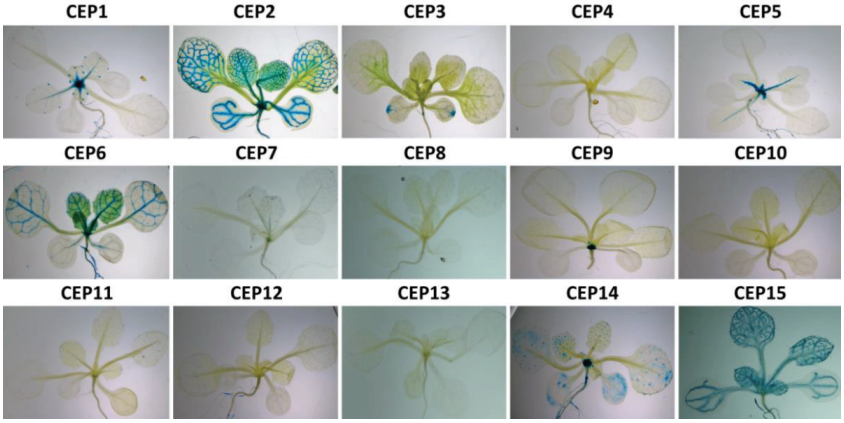


**Figure 9. Overview of *CEP* expression in the shoot of twelve day old seedlings.** *CEP* expression was monitored through *promoter::NLS:GUS:GFP* reporter lines.

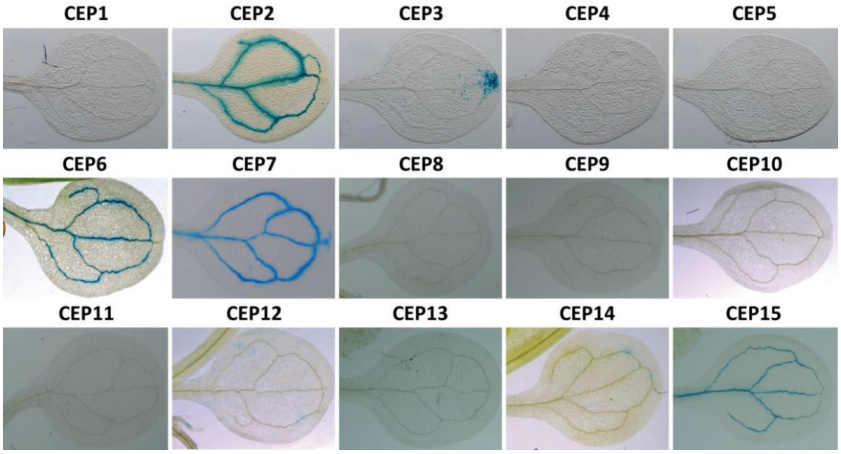


**Figure 10. *CEP* expression in the cotyledon of five day old seedlings.** *CEP* expression was monitored through *promoter::NLS:GUS:GFP* reporter lines.

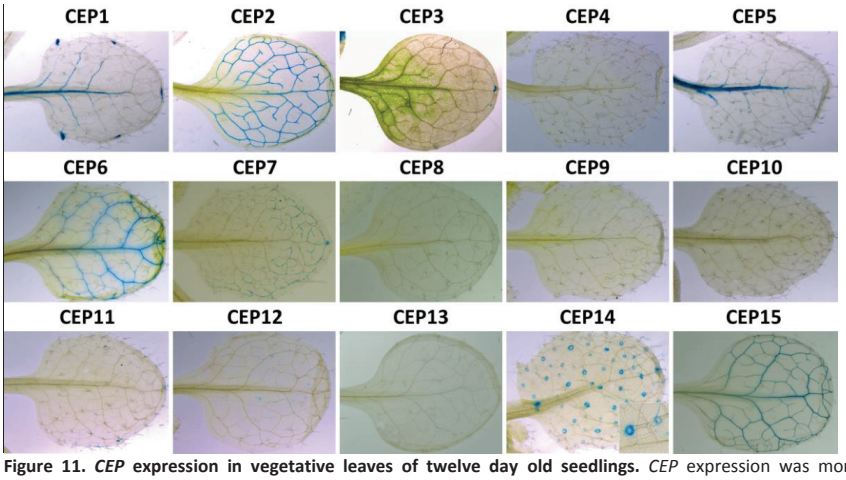


**Figure 11. *CEP* expression in vegetative leaves of twelve day old seedlings.** *CEP* expression was monitored through *promoter::NLS:GUS:GFP* reporter lines.

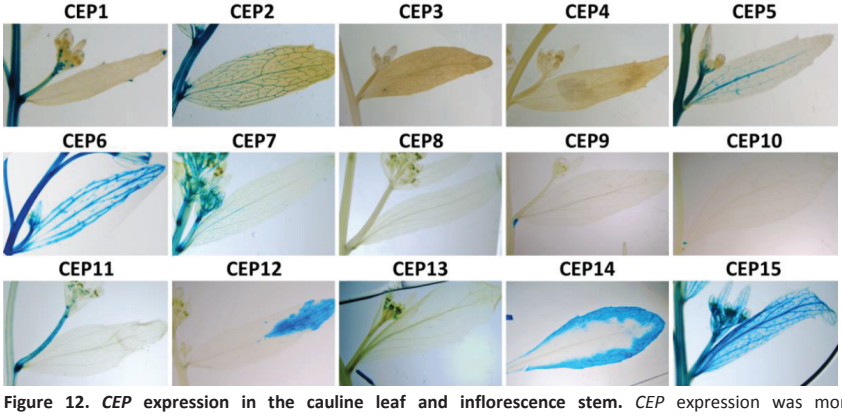


**Figure 12. *CEP* expression in the cauline leaf and inflorescence stem.** *CEP* expression was monitored through *promoter::NLS:GUS:GFP* reporter lines.

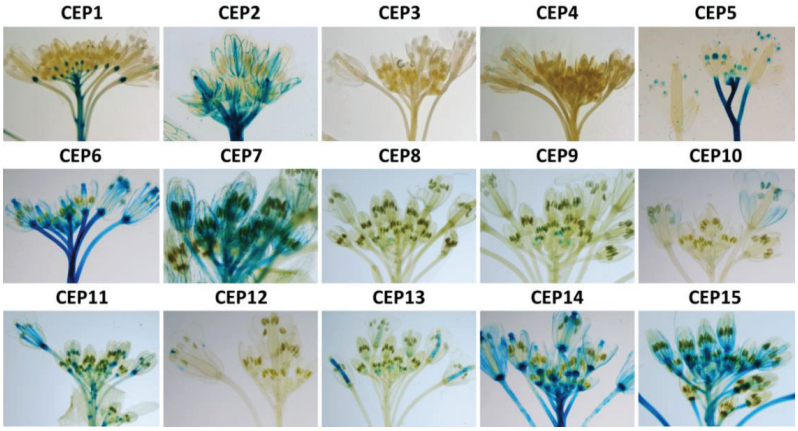


**Figure 13. *CEP* expression during flower development in the apical part of the inflorescence.** *CEP* expression was monitored through *promoter::NLS:GUS:GFP* reporter lines.

At the root-hypocotyl junction, *CEP1*, *CEP3*, *CEP4*, *CEP5*, *CEP6*, *CEP7*, *CEP9*, *CEP11*, *CEP12*, *CEP14* and *CEP15* are expressed in the vasculature and/or during adventitious root development **(Figure 14)**. In the primary root, *CEP4*, *CEP7*, *CEP11* and *CEP15* are expressed in the developing vasculature, *CEP14* is expressed in the xylem pole pericycle (XPP) cells, while *CEP6* is expressed in all tissues, with the strongest expression levels in the XPP cells **(Figure 15)**. In the primary root apical meristem (RAM) region, *CEP6*, *CEP7*, *CEP11* and *CEP15* are expressed in the developing vascular bundle, while *CEP14* is the only *CEP* member that is expressed in the entire apical root tip, with the strongest expression in the root cap **(Figure 16)**. During lateral root development, *CEP1*, *CEP11* and *CEP15* are expressed in the developing lateral root primordium. On the other hand, *CEP4, CEP6* and *CEP7* are expressed in the vasculature at the base of the developing lateral root primordium, while *CEP3*, *CEP5* and *CEP9* are expressed at the phloem pole pericycle (PPP) cells that are associated with a lateral root primordium. Interestingly, *CEP14* is expressed in the xylem pole pericycle (XPP) cells at the borders of the lateral root primordium, as well as at the tip of the emerging lateral root, and *CEP12* is expressed specifically in the epidermal cells that are overlaying an emerging lateral root **(Figure 17)**.

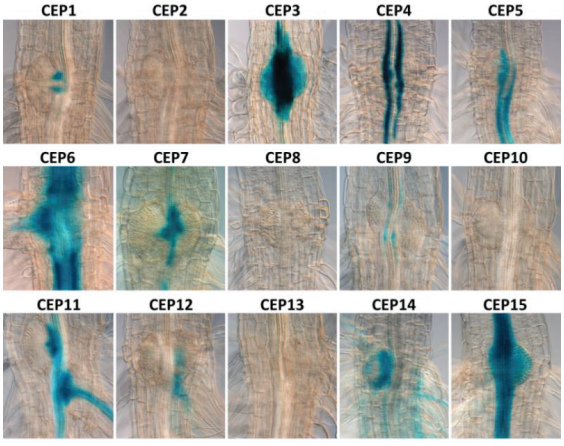


**Figure 14. *CEP* expression at the root – hypocotyl junction, containing the region of adventitious root development.** *CEP* expression was monitored through *promoter::NLS:GUS:GFP* reporter lines.

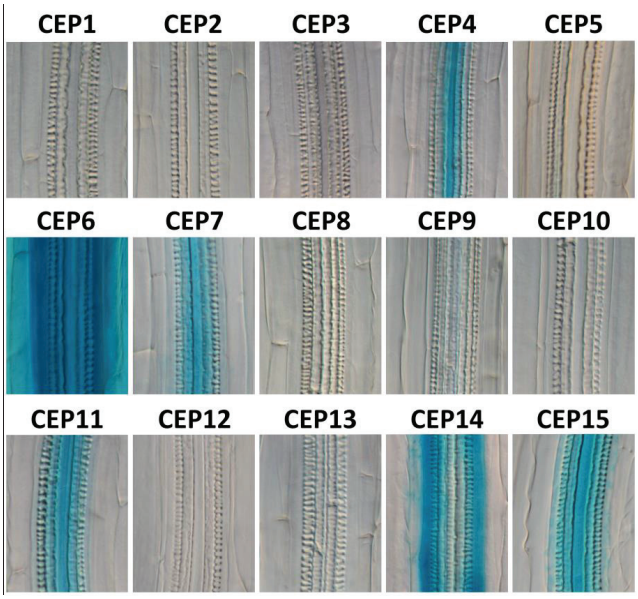


**Figure 15. *CEP* expression in the root vasculature (oriented with the xylem poles in plane).** *CEP* expression was monitored through *promoter::NLS:GUS:GFP* reporter lines.

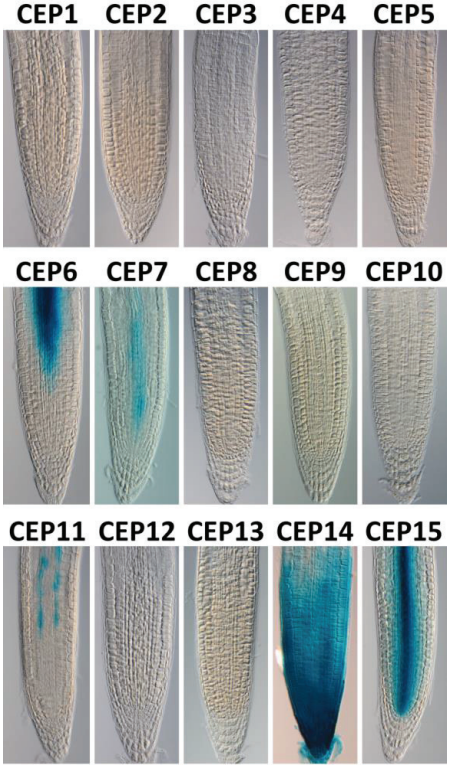


**Figure 16. *CEP* expression in the root apical meristem region.** *CEP* expression was monitored through *promoter::NLS:GUS:GFP* reporter lines.

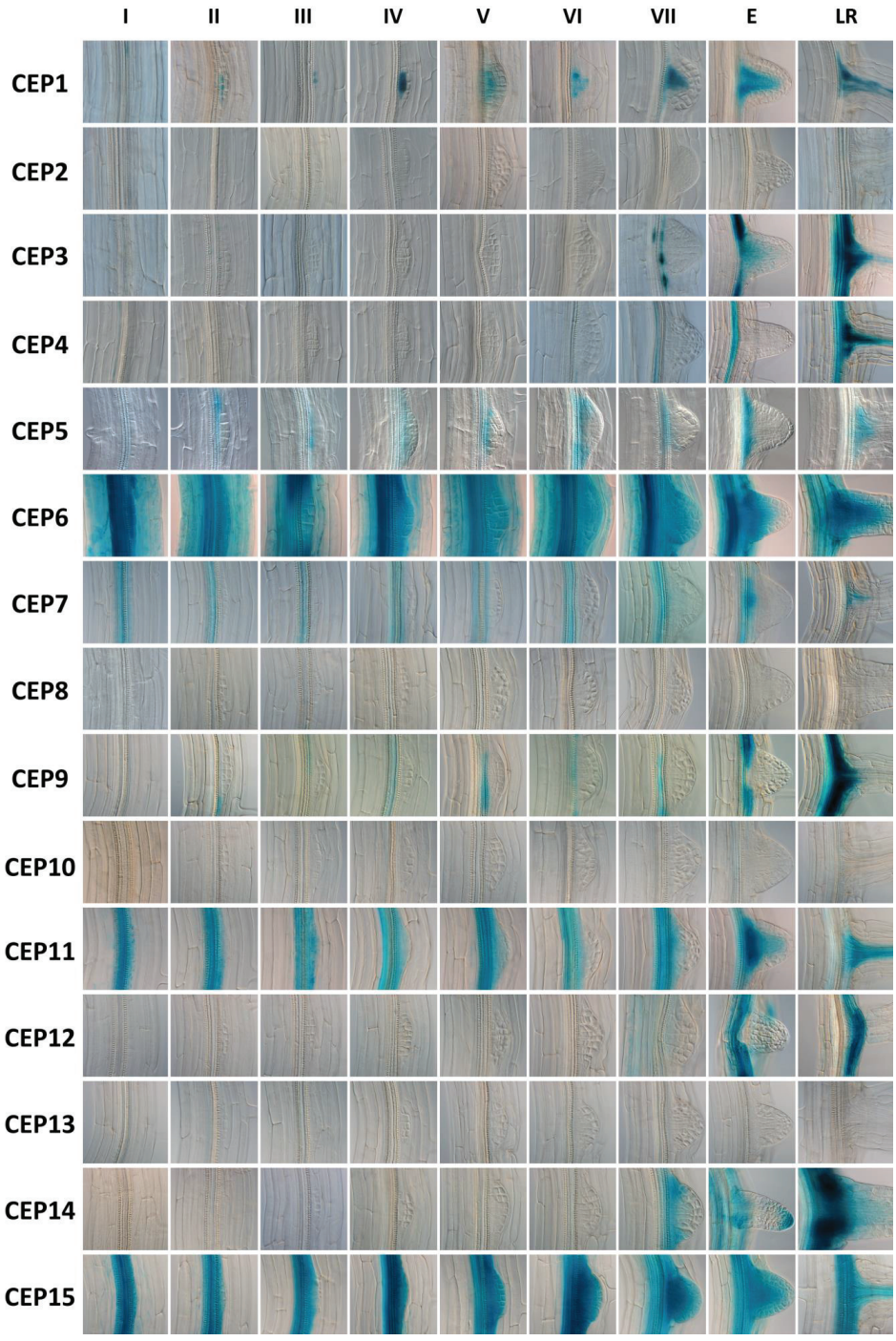


**Figure 17. *CEP* expression during the different stages of lateral root primordium development (stage I to VII), followed by lateral root primordium emergence (E), and finally at the site of an independently outgrowing lateral root (LR).** *CEP* expression was monitored through *promoter::NLS:GUS:GFP* reporter lines.

**Expression analysis of *CEPR1/XIP1* and *CEPR2***

A detailed overview on the expression patterns of *CEPR1/XIP1* and *CEPR2* might be helpful to predict possible peptide ligand – receptor pairs during different developmental processes. Although a general overview of the expression pattern of both receptors in the shoot and root of seedlings has been provided (Bryan et al, 2012; Tabata et al, 2014), it remains unknown in which tissue *CEPR2* is expressed.

To increase the resolution of the tissue-specific expression patterns, *pCEPR::nls-GFP/GUS* reporter lines were generated and characterized. In the shoot, *CEPR1/XIP1* is expressed specifically in the veins of the cotyledons, vegetative leaves and cauline leaves, whereas *CEPR2* is expressed more broadly in the leaves **(Figure 18)**. In the shoot apical meristem (SAM) region, *CEPR1/XIP1* is expressed in the vasculature running beneath the SAM, while *CEPR2* is expressed in a region closer to or containing the actual SAM **(Figure** 18 **18)**. In the flowers, *CEPR1/XIP1* is expressed at the base of the flower and in the vasculature of the petals, while *CEPR2* is expressed in the pistil and stamen **(Figure** 18 **18)**. At the root-hypocotyl junction, both *CEPR1/XIP1* and *CEPR2* are expressed in the stele **(Figure 19)**. In the primary root, both *CEPR1/XIP1* and *CEPR2* are expressed throughout the vasculature. Closer inspection revealed that *CEPR1/XIP1* appears to be specifically expressed at the phloem poles, whereas *CEPR2* is expressed at the xylem poles and also in the pericycle **(Figure 19)**. At the root tip, *CEPR2* is expressed in the root cap, while *CEPR1/XIP1* expression is absent **(Figure 19)**. During lateral root development, *CEPR1/XIP1* is in the vascular tissue near the base of the developing lateral root primordium (LRP) and later becomes expressed in the young differentiating vasculature of an emerging lateral root. On the other hand, *CEPR2* is mainly expressed in the vasculature and pericycle cells, in the developing lateral root primordia, and is finally strongly expressed at the tip of the young lateral root after emergence, similar to its expression in the primary root tip **(Figure 19)**. Altogether, *CEPR1/XIP1* and *CEPR2* are expressed in different tissues, with minimal overlap in expression domains.

To further check in which type of vascular cells the CEPR1/XIP1 and CEPR2 proteins are localized, *pCEPR::CEPR-GFP* translational fusion lines were created and characterized. This revealed that the CEPR1/XIP1-GFP protein is localized in the phloem companion cells in the mature region of the root, and in early differentiating vasculature of young lateral roots **(Figure 20)**. On the other hand, the CEPR2-GFP protein is localized at the plasma membrane in the metaxylem cells and the (xylem pole-associated) pericycle. In the primary root tip, CEPR2-GFP is present in the quiescent center cells, the surrounding initials and the columella root cap cells. In lateral root primordia just before emergence, CEPR2 accumulates at the site where the new lateral root stem cell niche is formed **(Figure 21)**.

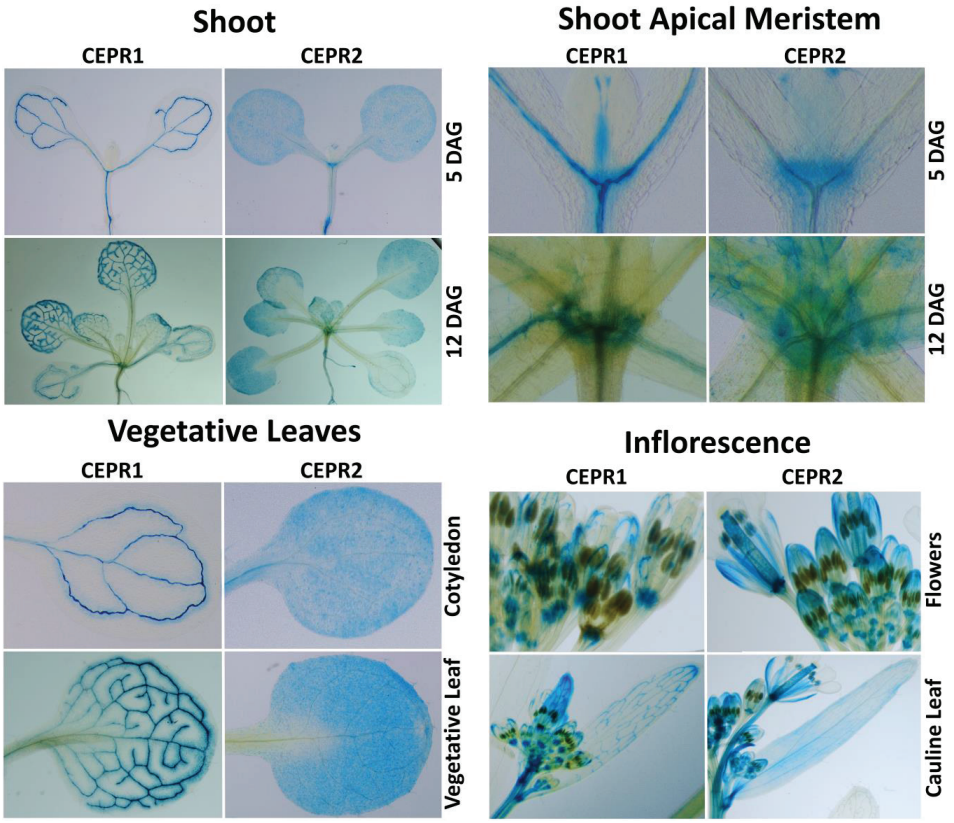


**Figure 18 Overview of *pCEPR1/XIP1::NLS:GFP:GUS* and *pCEPR2::NLS:GFP:GUS* expression during shoot development.**

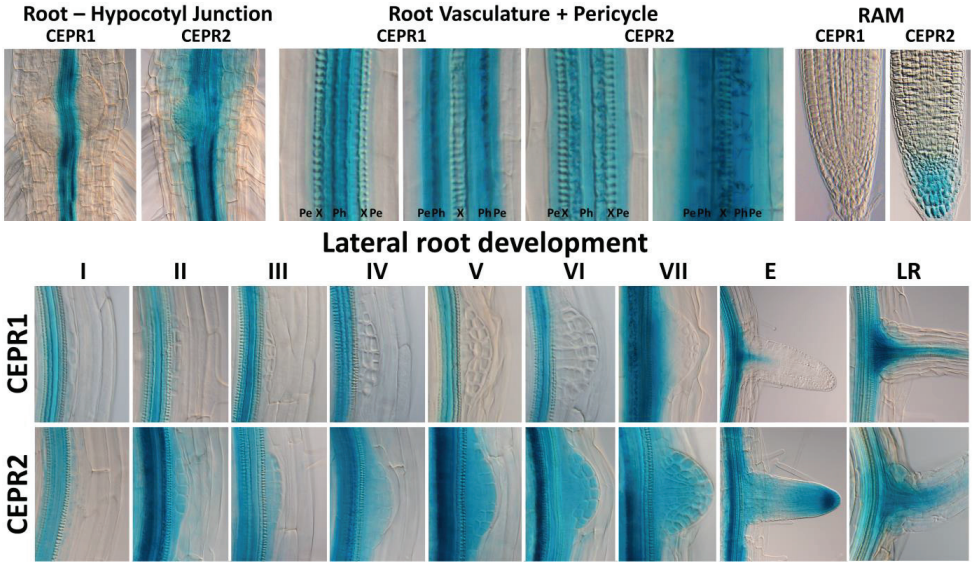


**Figure 19. Overview of *pCEPR1/XIP1::NLS:GFP:GUS* and *pCEPR2::NLS:GFP:GUS* expression during root development (RAM = root apical meristem; Pe = pericycle; X = xylem; Ph = phloem; I-VII = stages of LRP; E = emerged; LR = lateral root).**

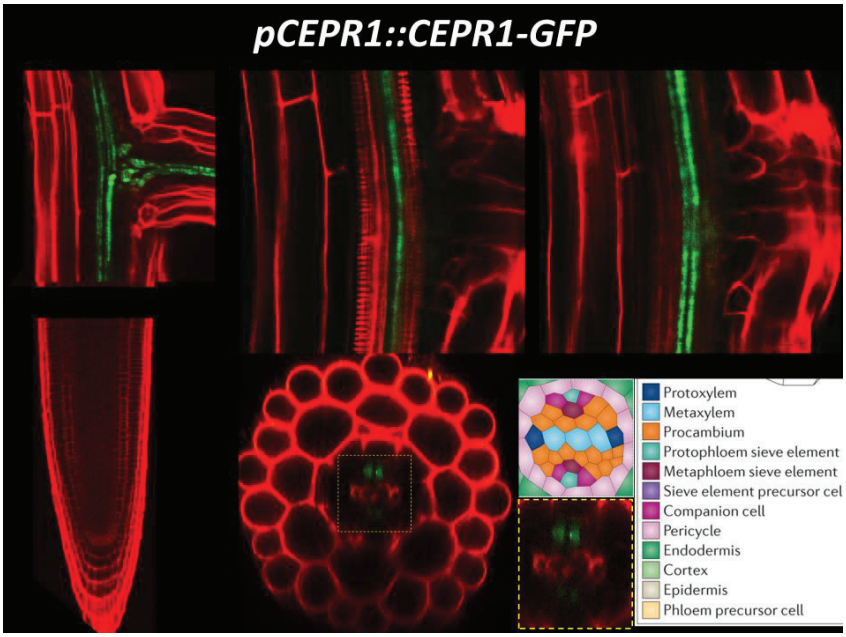


**Figure 20. CEPR1/XIP1 protein localization.** *pCEPR1::CEPR1-GFP* localizes to the phloem companion cells in the root vasculature (visualized as two narrow strands at the phloem pole in the longitudinal and cross-section). (schematic picture of stele from (De Rybel et al, 2016))

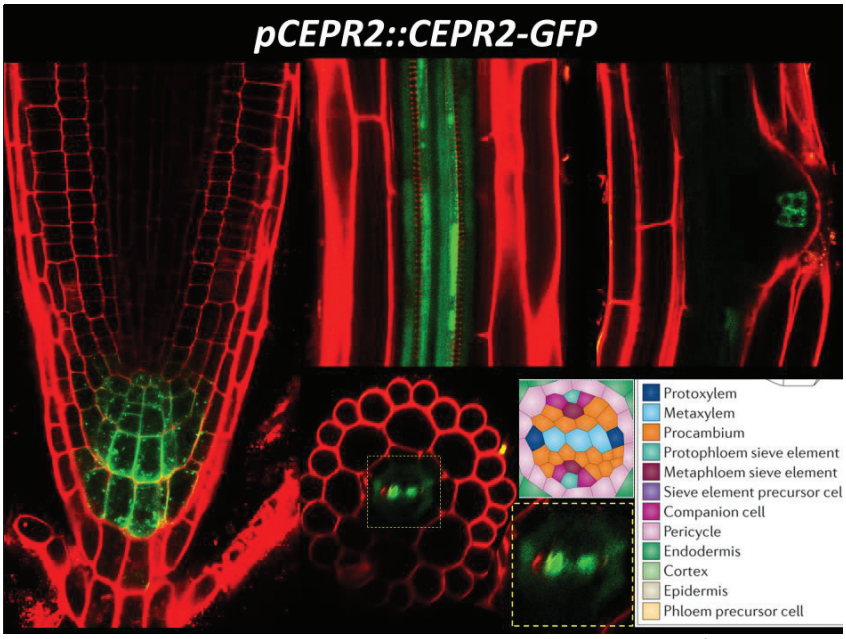


**Figure 21. CEPR2 localization.** *pCEPR2::CEPR2-GFP* localizes to the plasma membrane of the QC cells, surrounding initials and columella root cap cells at the primary root tip, and in the tip of an emerging lateral root primordium. In the vasculature, CEPR2 is present in the metaxylem cells (visualized as two big strands next to the protoxylem strands in the longitudinal and cross-section) and also in surrounding (xylem pole) pericycle cells. (schematic picture of stele from (De Rybel et al, 2016))

***CEP* expression responses to phytohormone treatments**

Considering *XIP1/CEPR1* and several *CEP* genes are expressed at the phloem pole, a site with low auxin and high cytokinin activity, while *CEPR2* and several other *CEP* genes are expressed at the xylem pole and XPP, sites with (local) high auxin and low cytokinin activity, transcriptional responses of *CEP* genes to both phytohormones in the root were investigated.

An indole-3-acetic acid (IAA) auxin treatment of 2 hours and 6 hours on Col-0 roots triggered a significant downregulation of group I *CEP* genes *CEP8*, *CEP5, CEP6*, *CEP7, CEP9, CEP1, CEP3* and *CEP4*, no significant change in expression for *CEP1* and *CEP11*, while a significant upregulation was detected for group II *CEP* genes *CEP14* and *CEP15* (*CEP2*, *CEP10* and *CEP13* are not expressed in the root) **(Figure 22)**.

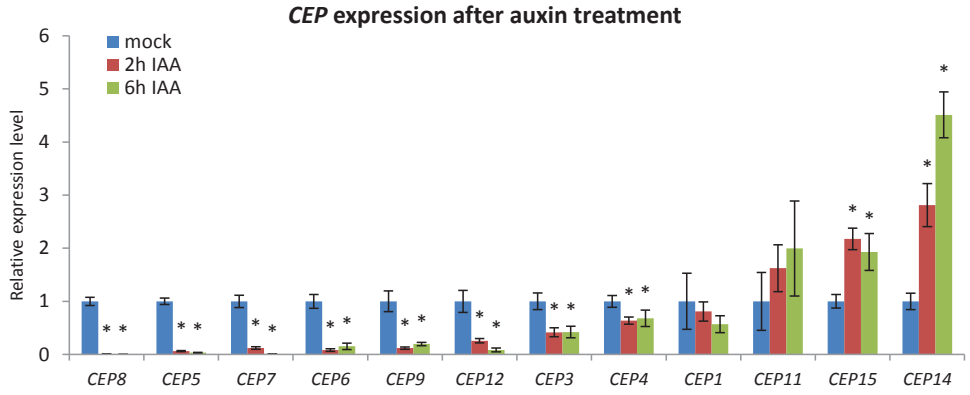


**Figure 22. Relative *CEP* expression level after 2 and 6 hours treatment with 1 µM IAA on roots of 7 days old Col-0 seedlings. (mean ± SE, 5 biological repeats, Student's *t*-test, * $p < 0.05$)**

A 6-benzylaminopurine (BAP) cytokinin treatment of 2 hours on Col-0 roots leads to an upregulation of *CEP12*, *CEP11*, *CEP9*, *CEP14*, *CEP3*, *CEP7* and *CEP6*, but no drastic changes in expression of the remaining *CEP15*, *CEP1*, *CEP4*, *CEP5* and *CEP8*. A longer cytokinin treatment of 6 hours induced a downregulation of *CEP8*, *CEP5*, *CEP6*, *CEP7* and *CEP4* compared to non-treated seedlings, and *CEP9* also reduced back to control level (*CEP2*, *CEP10* and *CEP13* are not expressed in the root) **(Figure 23)**.

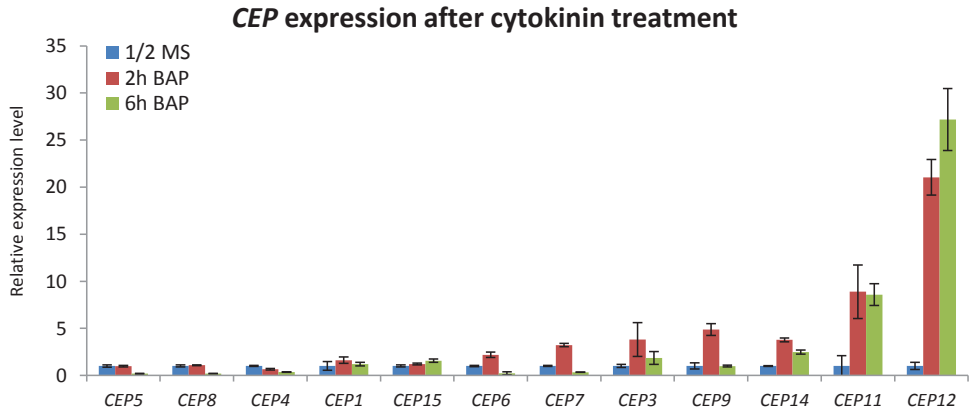


**Figure 23. Relative *CEP* expression level after 2 and 6 hours treatment with 10 µM BAP on roots of 4 days old Col-0 seedlings. (mean ± SE, 3 technical repeats)**

Taken together, the majority of the group I *CEP* genes showed a significant downregulation in expression two hours after auxin treatment, while group II *CEP* genes were instead upregulated. And the majority of *CEP* genes were upregulated two hours after cytokinin treatment. Thus, a general trend of an antagonistic response to auxin and cytokinin is observed, which has been previously been described as a common theme in the root tissues (Chandler & Werr, 2015).

**Phenotypic analysis of T-DNA insertion mutants for *CEPR* and *CEP* genes**

The study the biological role of CEP signaling during plant development, loss-of-function analysis is required next to gain-of-function analysis. Therefore, mutant lines were requested for the *CEPR1/XIP1* and *CEPR2* genes **(Figure 24 and Supplemental Table S1)**. For *CEPR1/XIP1*, the *xip1-1* loss-of-function mutant was used, which contains an EMS-induced point-mutation of serine (S) to phenylalanine (F) at residue number 677 (S677F) (remark: wrongly annotated as S677P in Bryan et al. (2012)). The *xip1-1* mutant showed a drastic decrease in primary root length and number of emerged lateral roots compared to control. For the *CEPR2* gene, T-DNA insertion lines were used, for which *cepr2-1* (GK_572B08), *cepr2-2* (GK_644G02) and *cepr2-3* (GK_695D11) did not show a significant difference in root length or number of emerged lateral roots in 9-day-old seedlings, while *cepr2-4* (SALK_014533) showed a significant increase in root length and number of lateral roots in 10-day-old seedlings. The difference in mutant phenotype, in addition to the different expression patterns, further suggests that each receptor plays a different role in plant development. To check how plant development is affected when both receptors are lost, a *xip1-1* x *cepr2-4* double mutant was generated and revealed no significant difference in root length or number of lateral roots, as if the mutants cancelled each other out **(Figure 25)**.

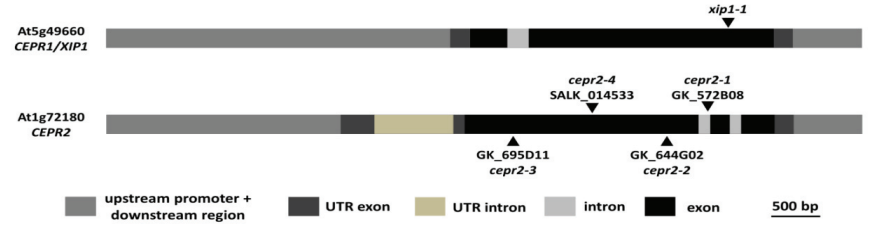


**Figure 24. Overview of the S677F mutation in the *xip1-1* mutant, and the T-DNA insertion sites in *cepr2* mutants.**

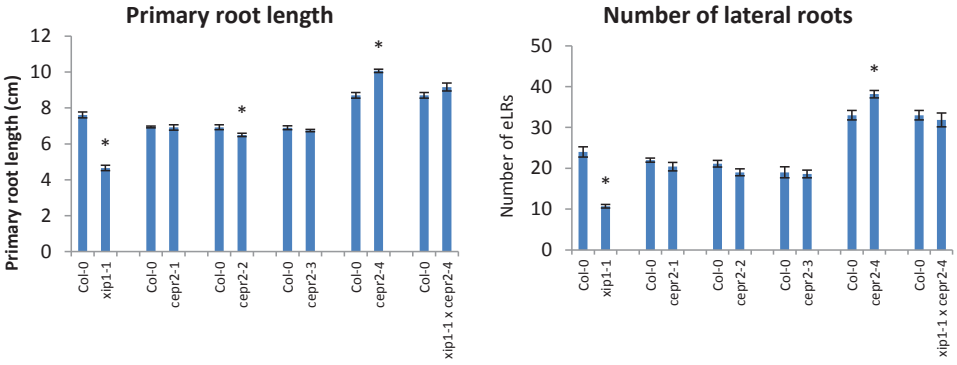


**Figure 25. Root phenotype *cepr* mutants.** Primary root length and number of emerged lateral roots in *xip1-1*, *cepr2-1*, *cepr2-2* and *cepr2-3* compared to wild type control (Col-0) after 9 days on ½ MS growth medium; and *cepr2-4* and *xip1-1* x *cepr2-4* mutants compared to Col-0 after 10 days on ½ MS growth medium. (mean ± SE, n≥6, Student's *t*-test, * $p < 0.05$)

To determine the endogenous role of individual *CEP* genes in root development, T-DNA insertion lines were requested from publically available collections (NASC and GABI KAT) for *CEP* genes that showed expression in the root. However, due to their small size, few mutants were recovered with a T-DNA insertion within (or close to) the coding sequence of the *CEP* genes **(Figure 26 and Supplemental Table S1)**. A selection of SALK and GABI-KAT mutants was screened for effects on primary root growth and lateral root formation. This revealed small differences in primary root length and lateral root formation between the mutant lines and their corresponding wild type controls in which the T-DNA locus was segregated out **(Figure 27)**. The small differences are likely due to functional redundancy between the highly similar peptides with overlapping expression patterns, and/or due to not giving rise to a knock-out of the *CEP* gene (in some GABI-KAT lines even (partial) overexpression of the *CEP* gene was observed) **(Supplementary Figure S4)**.

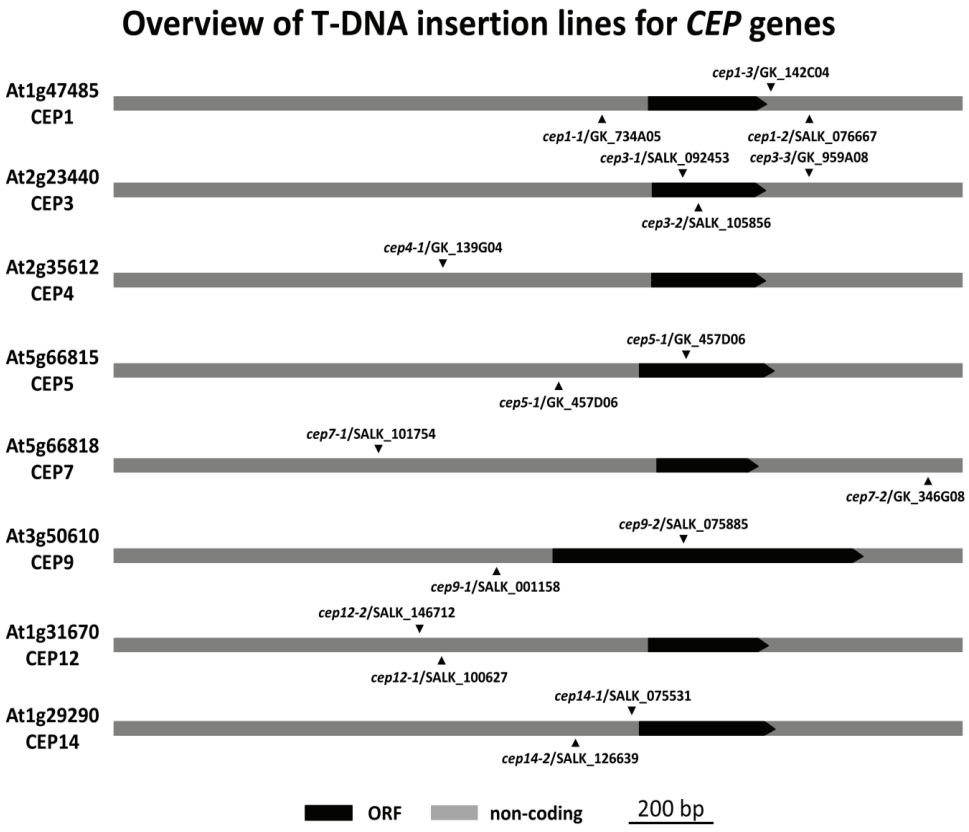


**Figure 26. Overview of T-DNA insertion sites of the *cep* mutants on the genomic sequence, based on the GBrowse tool from TAIR.**

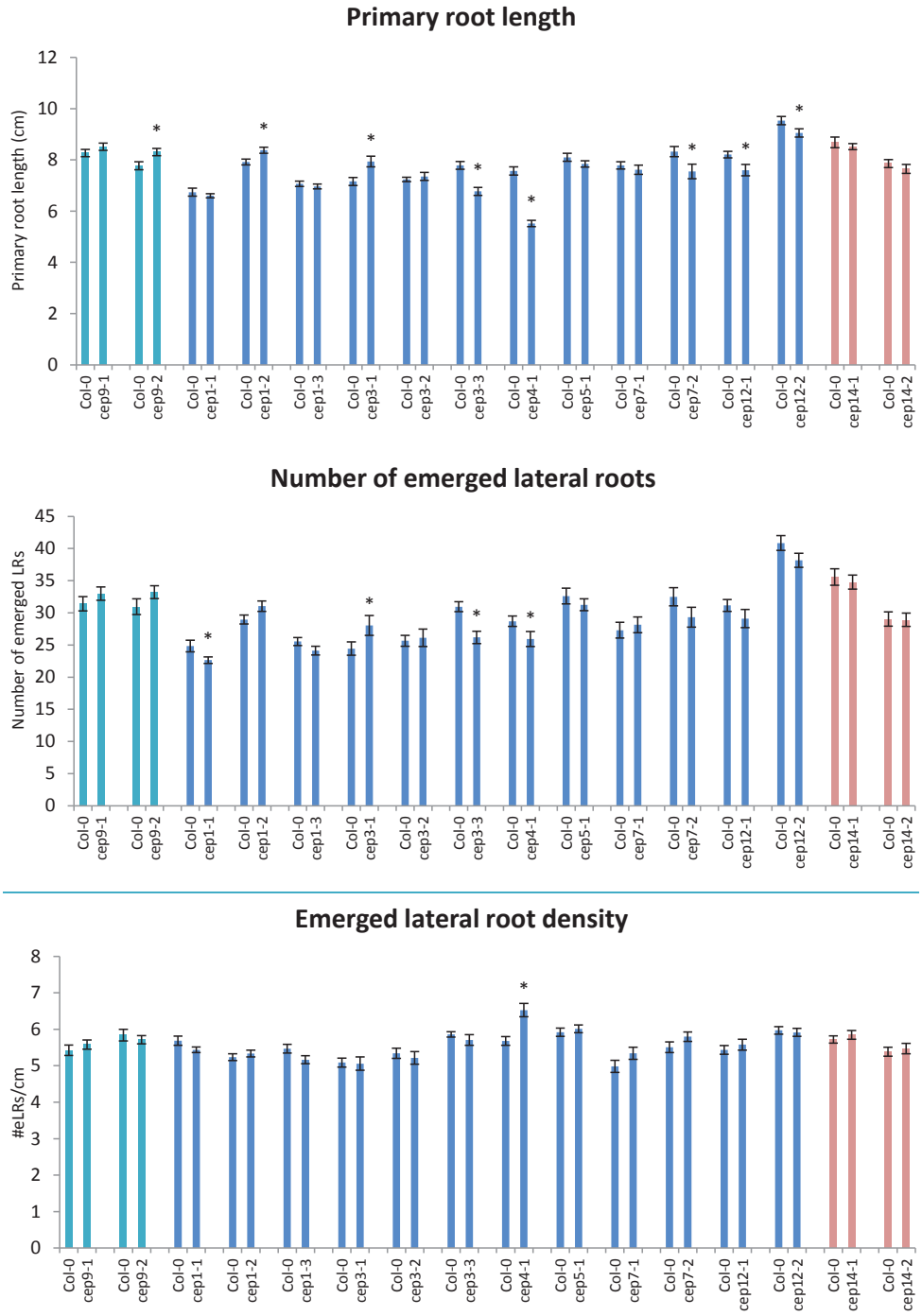


**Figure 27. Root phenotype of *cep* T-DNA insertion lines.** Primary root length measurements, number of emerged lateral roots and emerged lateral root density of *cep* mutants in comparison with wild type controls segregated out from a hemizygous parent (mean ± SE, Student's *t*-test, * $p<0.05$,$n\geq16$). (Note: colour-coded according to subgroups)

Functional redundancy between highly similar peptides with overlapping expression patterns is a recurring problem in the field of peptide signaling research. To overcome this problem, a meta-analysis was performed based on the global expression analysis described above, combined with phylogenetic relationships based on Clustal Omega analysis using the sequence of the promoter and the open reading frame region, and with the response to hormone treatments. In this manner, an overview of the degree of potential functional overlap between the different *CEP* genes was obtained **(Figure 28)**. Interestingly, the *CEP* genes grouped according to the previously described subgroups, which were based on gain-of-function phenotypes and mature CEP peptide sequence.

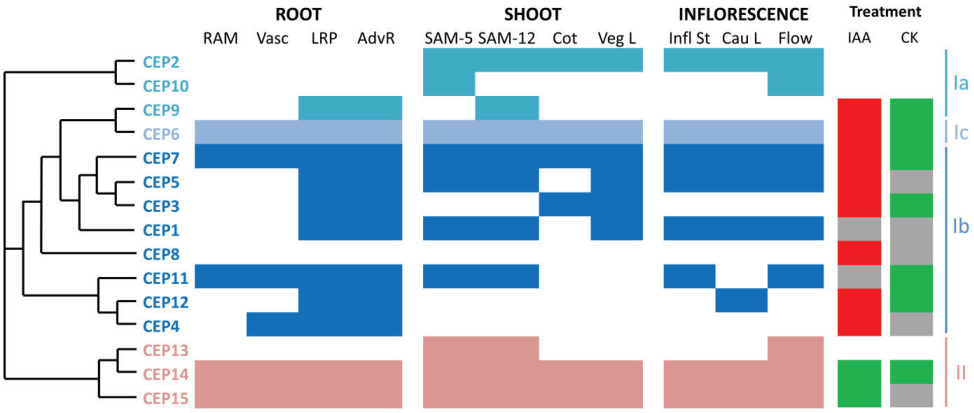


**Figure 28. Clustering meta-analysis of *CEP* genes.** Schematic overview of expression patterns of the *CEP* genes, grouped according to overlapping expression pattern and sequence homology of the promoter + coding sequence region (Clustal Omega software analysis). The early response (2 hours) to auxin (IAA) and cytokinin (CK) are indicated as followed: red = downregulation, green = upregulation, and grey = no significant difference. (RAM = root apical meristem; Vasc = root vasculature; LRP = lateral root (primordium); AdvR = adventitious root at the root–hypocotyl junction; SAM-5 = shoot apical meristem in five day old seedlings; SAM-12 = shoot apical meristem in twelve day old seedlings; Cot = cotyledon; Veg L = vegetative leaf; Infl St = inflorescence stem; Cau L = cauline leaf; Flow = flower). *CEP* genes are colour-coded according to their subgroups previously described.

Based on this meta-analysis, mutant lines for *CEP1*, *CEP3*, *CEP5* and *CEP9* were selected for their high degree of functional overlap and expression patterns associated with lateral root development, to generate higher order mutants: *CEP1* is expressed in the LRP inner core and *CEP3*, *CEP5* and *CEP9* are expressed in the LRP-associated PPP cells, while in contrast *CEP4*, *CEP7* and *CEP11* are expressed broadly in the vasculature; *CEP5*, *CEP6*, *CEP7*, *CEP8* are arranged as tandem duplications, which prevents creating crossings between mutant lines; and no T-DNA insertion lines are available for *CEP6*. Interestingly, all double and triple mutants displayed a larger root system with a significantly increased primary root length and number of emerged lateral roots, but no effect on lateral root density **(Figure 29)**. Thus, higher order loss-of-function mutants for group Ib *CEP* members showed the opposite phenotype as the corresponding gain-of-function overexpression lines. Taken together, this suggests that CEP peptides from subgroup Ib function as root growth repressing regulators.

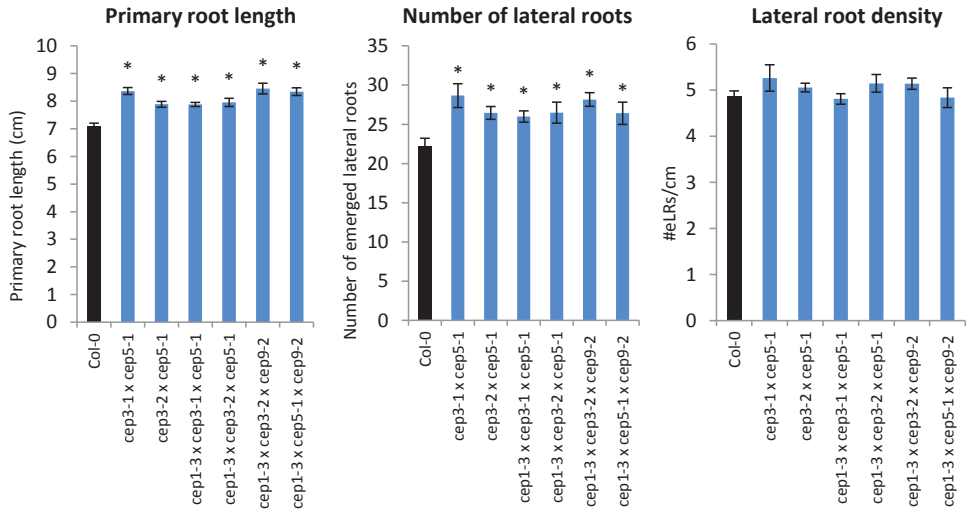


**Figure 29. RSA of higher order cep mutants.** Primary root length and number of emerged lateral roots in higher order *cep* mutants compared to Col-0 control after 9 days on ½ MS growth medium (mean ± SE, Student's *t*-test, * $p < 0.05$).

## DISCUSSION AND CONCLUSIONS

In a previous study, we identified 15 *CEP* genes in *Arabidopsis*, which we classified into two groups based on sequence homology of the mature CEP peptide (Roberts et al, 2013). We reported that a major difference between group I and group II members was the difference in conserved proline residues in the mature CEP peptides, with group I CEP peptides generally having a proline at positions 3, 7 and 11, while group II CEP peptides have a proline at positions 9 and 11. Other studies showed that for most group I CEP members, these proline residues can be post-translationally modified to hydroxyproline and/or (tri)arabinosylated hydroxyproline residues (Ohyama et al, 2008; Tabata et al, 2014; Mohd-Radzman et al, 2015). And it has been revealed that differences in modification of proline residues can affect the activity of a CEP peptide and can trigger different phenotypes (Mohd-Radzman et al, 2015).

In this study, we wanted to check if group I and group II *CEP* genes have a different impact on plant development, by analyzing overexpression lines for all *CEP* members. This revealed several clear differences between group I and group II members. And interestingly, group I CEP peptides could be further subdivided into three functional subgroups based on a correlation between gain-of-function phenotypes and the amino acid at position 3 in the mature CEP peptides **(Figure 5)**. Subgroup Ia CEP peptides, encoded by *CEP2*, *CEP9* and *CEP10*, generally contain a hydrophobic alanine residue at position 3, and their overexpression has no drastic impact on root and shoot growth. Subgroup Ib CEP peptides, encoded by *CEP1*, *CEP3*, *CEP4*, *CEP5*, *CEP7*, *CEP8*, *CEP11* and *CEP12*, all contain a positively charged hydrophilic arginine residue at position 3, and their overexpression has a drastic negative impact on root and shoot growth. Subgroup Ic only consists of the CEP6a and CEP6b peptides, which contain a hydrophobic glycine and a negatively charged hydrophilic glutamic acid residue at position 3 respectively, and their overexpression leads to intermediate reduced root and shoot growth **(Figures 1 to 5)**. This suggested that the amino acid at position 3 might possibly be the main contributor to different activity in the CEP I subgroups, instead of differences in proline-hydroxylation, since members from each subgroup were previously reported to have similar proline-

hydroxylation modifications (CEP9 peptides from subgroup Ia, CEP1, CEP3 and CEP5 peptides from subgroup Ib, and CEP6 peptides from subgroup Ic) (Ohyama et al, 2008; Tabata et al, 2014). Similarly, members of the CLV3/CLE peptide family were previously classified into three functional subgroups based on a correlation between gain-of-function phenotypes and differences in a few conserved amino acid residues (Ito et al, 2006; Hirakawa et al, 2008; Whitford et al, 2008; Araya et al, 2014a; Araya et al, 2014b) ***(see Introduction: peptide signaling, Figure 7)***. On the other hand, group II CEP peptides, encoded by *CEP13*, *CEP14* and *CEP15*, contain multiple differences in conserved amino acid residues at the N-terminal part compared to group I CEP peptides, and their overexpression leads to an increase in the size of the root system, opposite to most group I members. Another clear opposing difference between group I and group II members is their response to auxin, as most group I *CEP* genes are downregulated by auxin, while group II members are upregulated. Taken together, group II CEP peptides clearly form a separate functional class compared to group I CEP peptides, and group I CEP peptides can be subdivided into three functional subgroups based on their activity and a single amino acid residue.

At the moment, little is known about which CEP peptide binds to which CEPR receptor. Previously, the CEP1 peptide has been shown to bind both CEPR1/XIP1 and CEPR2, and CEP3 and CEP5 could actively compete with CEP1 for binding to CEPR1/XIP1 (Tabata et al, 2014). However, these interactions occurred *in vitro*, and it is not known if these interactions also occur *in planta*. One way to identify potential ligand – receptor pairs *in planta*, is to study their expression patterns. Previous studies provided a superficial overview of the expression pattern for some (but not all) *CEP* genes and their proposed receptors (Roberts et al, 2013; Tabata et al, 2014). In this work, the expression patterns of all fifteen *CEP* genes and their proposed receptors *CEPR1*/*XIP1* and *CEPR2* were investigated in detail, with the goal to reveal which developmental processes might be regulated by these regulators, to check if the members from the different subgroups are expressed in different tissues or overlap with others, and to infer possible ligand – receptor pairs. This revealed that some *CEP* genes showed very specific expression patterns, but in most cases there were large overlaps in expression of *CEP* genes from each (sub)group, and *CEPR1/XIP1* and *CEPR2* are expressed in tissues generally overlapping with *CEP* expression. Interestingly the two receptors themselves are never expressed in the same tissue throughout the plant.

Expression of *CEP* and *CEPR* genes was to a large extent associated with vascular tissues. In the shoot, *CEP2* (Ia), *CEP1*, *CEP5*, *CEP7*, *CEP11* (Ib), *CEP6* (Ic) and *CEP15* (II), together with *CEPR1*/*XIP1*, are expressed in the venation of the cotyledons, vegetative leaves and cauline leaves in an overlapping manner, potentially forming ligand – receptor pairs **(Figures 10-12 and 18)**. In contrast, *CEPR2* is expressed over the entire leaf surface, overlapping to some degree with *CEP1* (Ib) and *CEP14* (II) expression **(Figures 10-12 and 18)**. In the root, *CEP6* (Ic), *CEP4*, *CEP7*, *CEP11* (Ib) and *CEP15* (II) are expressed in the vasculature of the primary root and in the vasculature associated with a developing lateral root. Furthermore, *CEP1* (Ib) is expressed specifically within the inner core of the lateral root primordium from which the lateral root vasculature is derived. In the pericycle, *CEP6* (Ic) and *CEP14* (II) are expressed in the xylem pole-associated pericycle cells, while *CEP3*, *CEP5* (Ib) and *CEP9* (Ia) are expressed in the phloem pole-associated pericycle cells at the site of lateral root primordium development **(Figure 15-17)**. The CEPR1/XIP1 protein is present in the phloem companion cells of the primary root, and at the base of young lateral roots during the formation of a connection with the vasculature of the main root **(Figure 20)**. While in contrast, the CEPR2 protein is localized to the metaxylem cells and the (xylem pole-associated) pericycle in the mature region of the primary root,

**(Figure 21)**. It is currently unknown if the peptides that are expressed at the phloem poles are ligands for the phloem pole localized CEPR1/XIP1, and if the peptides expressed at the xylem poles are ligands for the xylem pole localized CEPR2, or if the CEP peptides migrate from one pole to another to bind their receptor.

Besides the expression patterns associated with the vasculature, *CEP2*, *CEP9*, *CEP10* (Ia), *CEP1*, *CEP7*, *CEP11* (Ib), *CEP6* (Ic), *CEP14* and *CEP15* (II) are expressed In the shoot apex, overlapping with *CEPR1/XIP1* and *CEPR2* expression. While in contrast, in the root apical meristem and in the lateral root tip, only *CEP14* (II) and *CEPR2* are expressed in the stem cell niche and the root cap, potentially forming a ligand – receptor pair **(Figure 6, 7, 20 and 21)**. And finally, in the floral organs, *CEPR1/XIP1* is expressed at the receptacle and petal veins, while *CEPR2* is expressed in the pistil and stamen, in both cases along with a tremendous overlap in expression of nearly every *CEP* gene **(Figure 13 and 18)**. Taken together, with the exception of the root apical meristem, a general trend can be observed with large overlapping expression patterns of *CEP* genes from each subgroup together with the *CEPR* genes, which themselves do not show overlapping expression patterns.

To determine which developmental processes are regulated by CEP signaling, gain-of-function and loss-of-function studies are required. Gain-of-function analysis suggested that group Ib CEP members have a negative impact on root growth, while group II CEP members have a positive impact on root growth **(Figure 1-2)**. Some small differences were observed in the degree of the effect on root growth between the two independent selected overexpression lines for each *CEP* gene. This could be explained by the corresponding small differences in the level of overexpression (*e.g.* $CEP1^{OE}$ *3-1-1* showed a lower overexpression level of *CEP1* compared to $CEP1^{OE}$ *1-3-1*, and resulted in a less drastic reduction in primary root length and number of lateral roots) **(Figure 1 and Supplementary Figure S1)**.

Although overexpression of each *CEP* gene separately can give clues on the activities and processes that are regulated by these peptides, these results should generally be taken with care, as constitutive ectopic overexpression in all tissues might not always reflect the *in planta* function of that individual *CEP* gene. Therefore, loss-of-function mutant analysis is necessary to unveil the endogenous role of each CEP peptide. However, a problem frequently encountered in studies on small signaling peptides is the overall lack of T-DNA insertions within each gene of the family, due to their small open reading frames, and the *CEP* family was no exception to this. T-DNA insertion lines for a couple of *CEP* genes were recovered and were analyzed for the effect on root growth. Considering the large overlaps in expression and sequence homology, it was no surprise that these single mutants did not show drastic phenotypes due to functional redundancy **(Figure 27)**. To overcome this problem, we performed a clustering meta-analysis to reveal the degree of functional overlap between each member **(Figure 28)**, and used this knowledge to generate higher order mutants for several *CEP* Ib members. Unfortunately, besides the T-DNA insertion lines for *CEP14*, no T-DNA insertion lines are available for *CEP13* and *CEP15*, and therefore no higher order mutants for group II *CEP* members could be generated to check their effect on root growth. For the *CEP* Ib higher order mutants, a significant increase in primary root length and the number of emerged lateral roots was observed, a phenotype opposite to the overexpression lines **(Figures 1, 2 and 29)**. The increase in number of emerged lateral roots has been suggested not to be simply a consequence of a longer primary root length, since it has been shown that the formation of lateral roots is correlated to the time of growth, with lateral roots formed at regular intervals, irrespective of the effect on the

elongation rate of the primary root (Moreno-Risueno et al., 2010). This suggests that CEP Ib peptides act as regulators that control the size of the root system by stimulating both primary root elongation and lateral root formation.

Another way to study the role of the CEP signaling during root development was to check loss-of-function mutants for the receptors. The root phenotype of the examined loss-of-function mutants for *CEPR1/XIP1* and *CEPR2* were different from one another. The *xip1-1* mutant was previously identified as a loss-of-function mutant for the *CEPR1/XIP1* gene, and contains a point-mutation S677F that potentially abolishes an important phosphorylation site in the kinase domain (Bryan et al, 2012). The *xip1-1* mutant showed reduced primary root growth and a reduced number of lateral roots, similar to *CEP* Ib overexpression lines and opposite to *CEP* II overexpression lines and *cep* Ib higher order mutants **(Figure 25)**. This might suggest that CEPR1/XIP1 has a positive effect on root growth, and is inhibited by CEP Ib peptides and potentially activated by CEP II peptides. In contrast, the *cepr2* mutant lines did not show a drastic impact on primary root length and lateral root number in seedlings nine days after germination, while a slight increase in the root system was observed in older seedlings **(Figure 25)**. The *xip1-1* x *cepr2* double mutant did not show a significant difference in root architecture **(Figure 25)**. This is in contrast to the findings from the work from Tabata et al. (2014), where they reported no obvious phenotype in the single *cepr1* or *cepr2* mutants, but a significant increase in size of the root system in the double mutant. These differences could possibly be due to differences in genetic background, with mutants from Tabata et al. (2014) from the Nössen ecotype (RIKEN transposon collection), while the mutants used in this study are in Col-0 ecotype background. On the other hand, based on our expression analysis, *CEPR1*/*XIP1* and *CEPR2* are not expressed in the same tissues, and might therefore control entirely different developmental programs instead of acting redundantly.

Currently, it is unknown how CEP signaling might affect root growth. The CEP Ib overexpression lines showed a drastic reduction in primary root length due to a gradual consumption of the root apical meristem **(Figure 1 and Supplemental Figure S2)**. It could be hypothesized that the ectopic overabundance of CEP Ib peptides in the root apical stem cell niche, a region where *CEP* Ib genes are normally not expressed, might compete with the locally present CEP14 (II) peptide for CEPR2, and this might trigger the observed phenotype. Noteworthy however, both *cep14* T-DNA insertion lines were not affected in root growth. Alternatively, our expression analysis showed a close association of *CEP* and *CEPR* genes with the vasculature, and the study from Bryan et al. (2012) reported that mutations in the *CEPR1*/*XIP1* gene affect phloem specification. It has already been described that mutants in phloem differentiation, such as the *brevis radix* (*brx*) and *octopus* (*ops*) mutants (Mouchel et al, 2004; Truernit et al, 2012), display an arrest of primary root growth and an increased lateral root density, similar to the phenotype observed for overexpression of *CEP* Ib genes **(Figure 1)**. It has been hypothesized that this is caused by the interruption in normal phloem-mediated shoot-to-root transfer of growth-limiting nutrients and developmental signals, such as auxin (Depuydt et al, 2013). In another study, we showed that the auxin response is severely reduced in the root of *CEP5* overexpression lines and after synthetic CEP5 peptide treatments (*Chapter 6*, Smith and Roberts et al., in preparation). Furthermore, we showed that prolonged exposure to high concentrations of CEP5 could induce lateral root formation events right next to each other (*Chapter 5*, Roberts et al., accepted J. Exp. Bot), a phenotype often seen when auxin signaling or transport is interrupted.

In conclusion, this systematic analysis of the CEP peptide family and their receptors revealed how this family could be subdivided into four functional groups based on their gain-of-function phenotypes and the presence of specific residues in the mature peptide sequence. Expression analysis of the *CEP* and *CEPR* genes showed that members from each subgroup are expressed in a highly overlapping manner with their proposed receptors, and are usually associated with the vasculature. Gain-of-function and loss-of-function analysis revealed that CEP peptides and their receptors have an impact on root growth. Overexpression of group Ib *CEP* members leads to a drastic reduction in the size of the root system, while higher order mutants from the same group Ib *CEP* members showed an increase in the size of the root system. This suggested that these CEP peptides might act as root growth repressing regulators. This work provides an overview and represents a reference collection of data for future studies on the CEP peptide family.

## MATERIAL AND METHODS

**Plant material**

*Arabidopsis thaliana* ecotype Col-0 was used in this study. The *p35S::CEP1* line was kindly provided by Yoshikatsu Matsubayashi from Nagoya University, Chikusa, Japan. The *xip1-1* mutant was kindly provided by Frans Tax from the University of Arizona, Tucson, USA. All T-DNA insertion mutants were requested from the Nottingham Arabidopsis Stock Centre (NASC) collection or from the GABI KAT collection (Universität Bielefeld, Germany). An overview of the T-DNA insertion lines can be found in the supplemental table S1.

**Genotyping mutants**

All T-DNA insertion mutants were grown on ½ MS growth medium supplemented with kanamycin (for SALK lines) or sulfadiazine (for GABI KAT lines), to select hemizygous plants with one T-DNA insertion based on segregation analysis. These plants were used for propagation, followed by a final selection for homozygous T-DNA insertion mutant and homozygous wild type offspring based on standard PCR-based genotyping. A list of all genotyping primers can be found in the supplemental table S1. For *xip1-1* genotyping, the PCR product generated with the genotyping primers was subsequently digested with HpaII for 1 hour at 37°C, as the *xip1-1* point-mutation disrupts an HpaII restriction site.

**CEP constructs**

Gateway cloning was used for every construct. Entry clones containing the *CEP* and *CEPR* promoter sequences (*CEP1*, 1997 bp; *CEP2*, 1400 bp; *CEP3*, 1560 bp; *CEP4*, 2000 bp; *CEP5*, 900 bp, *CEP6*, 2000 bp; *CEP7*, 1575 bp; *CEP8*, 2009 bp; *CEP9*, 2025 bp; *CEP10*, 1288 bp; *CEP11*, 2002 bp; *CEP12*, 2000 bp; *CEP13*, 2591 bp; *CEP14*, 3000 bp; *CEP15*, 1685 bp; *CEPR1*, 2000 bp; *CEPR2*, 3254 bp) were created by cloning PCR-fragments into the pDONRP4P1R vector. The *pCEP::nls-GFP/GUS* constructs were created by cloning the promoter fragment into the pEX-K7SNFm14GW destination vector. Entry clones containing the genomic coding sequence of *CEP* and *CEPR* genes (*CEP1*, 276 bp; *CEP2*, 381 bp; *CEP3*, 249 bp; *CEP4*, 261 bp; *CEP5*, 318 bp; *CEP6*, 306 bp; *CEP7*, 231 bp; *CEP8*, 264 bp; *CEP9*, 732 bp; *CEP10*, 399 bp; *CEP11*, 315 bp; *CEP12*, 279 bp; *CEP13*, 282 bp; *CEP14*, 324 bp; *CEP15*, 318 bp; *CEPR1*, 3134 bp; *CEPR2*, 3131 bp) were created by cloning the PCR-fragment into the pDONR221 vector. The *p35S::CEP* constructs were created by cloning this genomic coding sequence in the pK7GW2 destination vector. The *pCEPR::CEPR-GFP* constructs were created by cloning the promoter and coding sequence entry clones, together with a pEN-R2-F-L3 entry clone (C-terminal GFP construct), in the pB7m34GW destination vector. Constructs were transformed in Col-0 using floral dip (Clough and Bent, 1998). A list of cloning primers is provided in the supplemental tables S3-S4. An overview of the selection procedure for transgenic lines is shown in supplemental tables S5 and S6.

**Plant growth**

For phenotypic analysis of the root system in overexpression and mutant lines, as well as GUS expression analyses, seedlings were grown at 21 °C under continuous light (110 µE $m^{-2}$ $s^{-1}$ photosynthetically active radiation, supplied by cool-white fluorescent tungsten tubes, Osram) on square Petri plates containing 50 ml solid ½ MS growth medium supplemented with 1% sucrose (per liter: 2.15 g MS salts, 0.1 g myo-inositol, 0.5 g MES, 10 g sucrose, 8 g plant tissue culture agar; pH adjusted to 5.7 with KOH). For CEP5 peptide treatments, synthetic CEP5$p^{Hyp}$ (DFR{HYP}TT{HYP}GHS{HYP}GIGH) (Genscript) (dissolved in water) was supplemented to ½ MS growth medium at concentrations indicated in the figure legends. For liquid ½ MS growth medium, agar was omitted from the ½ MS growth medium composition listed above. For phenotypic analyses of aboveground parts and GUS expression analysis in the inflorescence, plants were grown using the Jiffy-7® pellets (www.jiffypot.com) in a greenhouse at 21 °C under long-day conditions (16/8 light/dark).

**RNA extraction, cDNA synthesis, and qRT-PCR analysis**

For the analysis of *CEP* expression levels in *p35S::CEPx* overexpression lines and for *CEP* expression levels in Col-0 seedlings after auxin or cytokinin treatment, RNA was extracted by first performing an RNA extraction with TRI Reagent® from Sigma-Aldrich according to the manufacturer's protocol, followed by a DNAse treatment on the isolated RNA (DNase I recombinant RNase-free from Roche Applied Science). This was followed by an extra RNA extraction procedure with the Plant RNeasy Mini kit from Qiagen according to the manufacturer's protocol to further clean up the RNA. Next, 1 µg of total RNA was used for cDNA synthesis using the iScript kit from Bio-Rad according to the manufacturer's protocol. The real-time qRT-PCR reaction was carried out on the LightCycler 480 from Roche Applied Science with the LightCycler 480 SYBR Green I Master Mix from Roche Applied Science. A list of primers can be found in the supplemental table S2.

**Root phenotyping**

Overexpression lines and mutants were grown in the conditions described above for the number of days indicated in figure legends. Emerged lateral roots were counted using a stereo-microscope (CETI, Belgium). A high resolution scan was made from the seedlings with a tabletop flatbed scanner. Primary root length measurements were performed on the scanned images using ImageJ software (http://rsbweb.nih.gov/ij/index.html). Data were analyzed using Microsoft Office Excel software.

**RAM measurements**

Roots of *CEP5*$^{OE}$ lines and CEP5p$^{Hyp}$ treated seedlings were cleared as followed: 1 hour at 60°C in 0.24 M HCl 20% methanol, 1 hour at room temperature (RT) in 7% NaOH 60% ethanol, 5 min at RT in 40% ethanol, 5 min at RT in 20% ethanol, 5 min at RT in 10% ethanol, 15 min at RT in 5% ethanol 25% glycerol and finally mounted on slides in 50% glycerol. Roots were imaged using differential interference contrast (DIC) microscopy (Olympus BX53). The size of the root apical meristem (RAM) was measured as the distance between the quiescent center (QC) cells and the first cortical cell number that starts elongating.

**Shoot phenotyping**

For three independent homozygous overexpression lines for each *CEP* gene, five plants per line were followed over time from germination until 43 days after germination, and were compared to ten Col-0 control plants. Pictures of the vegetative leaves and inflorescence were taken 34 and 43 days after germination, and representative images are shown in Figures 3-4 and S3 to compare flowering time. Pictures were taken with a Nikon D700 camera.

**Auxin and cytokinin treatment**

For the auxin treatment, Col-0 seedlings were grown for 6 days on vertical plates with solid ½ MS growth medium, after which the seedlings were transferred to liquid ½ MS growth medium and grown overnight. This was followed by 2 and 6 hours treatment with 1 µM indole-3-acetic acid (IAA) diluted in DMSO, or 2 and 6 hours mock (DMSO) treatment (control). For the cytokinin treatment, Col-0 seedlings were grown for 4 days on vertical plates with solid ½ MS growth medium, after which the seedlings were transferred to vertical plates with solid ½ MS growth medium supplemented with 10 µM 6-benzylaminopurine (BAP) (diluted in DMSO) for 2 and 6 hours, or harvested before transfer (control).

**GUS expression analysis**

For the GUS assays, plant material was put overnight in 90% acetone, then transferred to a GUS-solution [1 mM X-Glc, 0.5% (v/v) dimethylformamide (DMF), 0.5% (v/v) Triton X-100, 1 mM EDTA (pH 8), 0.5 mM potassium ferricyanide (K3Fe(CN)6), 0.5% potassium ferrocyanide (K4Fe(CN)6), 500 mM phosphate buffer (pH 7)] and incubated at 37 °C for GUS staining, and finally washed in 500 mM phosphate buffer (pH 7). For microscopic analysis, samples were cleared as followed: 1 hour at 60°C in 0.24 M HCl 20% methanol, 1 hour at room temperature (RT) in 7% NaOH 60% ethanol, 5 min at RT in 40% ethanol, 5 min at RT in 20% ethanol, 5 min at RT in 10% ethanol, 15 min at RT in 5% ethanol 25% glycerol and finally mounted on slides in 50% glycerol. Samples were analyzed by differential interference contrast microscopy (Olympus BX53) and a stereomicroscope (Leica MZ16).

**Confocal microscopy**

The *pCEPR::CEPR-GFP* lines were analyzed with a ZEISS Axiovert 100M confocal laser scanning microscope equipped with LSM510 software and with a Leica TCS WLL SP8 confocal laser scanning microscope.

## REFERENCES


Araya T, Miyamoto M, Wibowo J, Suzuki A, Kojima S, Tsuchiya YN, Sawa S, Fukuda H, von Wiren N, Takahashi H (2014a) CLE-CLAVATA1 peptide-receptor signaling module regulates the expansion of plant root systems in a nitrogen-dependent manner. *Proc Natl Acad Sci U S A* **111:** 2029-2034

Araya T, von Wiren N, Takahashi H (2014b) CLE peptides regulate lateral root development in response to nitrogen nutritional status of plants. *Plant signaling & behavior* **9:** e29302

Bryan AC, Obaidi A, Wierzba M, Tax FE (2012) XYLEM INTERMIXED WITH PHLOEM1, a leucine-rich repeat receptor-like kinase required for stem growth and vascular development in Arabidopsis thaliana. *Planta* **235:** 111-122

Chandler JW, Werr W (2015) Cytokinin-auxin crosstalk in cell type specification. *Trends Plant Sci* **20:** 291-300

De Rybel B, Mahonen AP, Helariutta Y, Weijers D (2016) Plant vascular development: from early specification to differentiation. *Nature reviews Molecular cell biology* **17:** 30-40

Delay C, Imin N, Djordjevic MA (2013) CEP genes regulate root and shoot development in response to environmental cues and are specific to seed plants. *J Exp Bot* **64:** 5383-5394

Depuydt S, Rodriguez-Villalon A, Santuari L, Wyser-Rmili C, Ragni L, Hardtke CS (2013) Suppression of Arabidopsis protophloem differentiation and root meristem growth by CLE45 requires the receptor-like kinase BAM3. *Proc Natl Acad Sci U S A* **110:** 7074-7079

Hirakawa Y, Shinohara H, Kondo Y, Inoue A, Nakanomyo I, Ogawa M, Sawa S, Ohashi-Ito K, Matsubayashi Y, Fukuda H (2008) Non-cell-autonomous control of vascular stem cell fate by a CLE peptide/receptor system. *Proc Natl Acad Sci U S A* **105:** 15208-15213

Imin N, Mohd-Radzman NA, Ogilvie HA, Djordjevic MA (2013) The peptide-encoding CEP1 gene modulates lateral root and nodule numbers in Medicago truncatula. *J Exp Bot* **64:** 5395-5409

Ito Y, Nakanomyo I, Motose H, Iwamoto K, Sawa S, Dohmae N, Fukuda H (2006) Dodeca-CLE peptides as suppressors of plant stem cell differentiation. *Science* **313:** 842-845

Mohd-Radzman NA, Binos S, Truong TT, Imin N, Mariani M, Djordjevic MA (2015) Novel MtCEP1 peptides produced in vivo differentially regulate root development in Medicago truncatula. *J Exp Bot* **66:** 5289-5300

Mouchel CF, Briggs GC, Hardtke CS (2004) Natural genetic variation in Arabidopsis identifies BREVIS RADIX, a novel regulator of cell proliferation and elongation in the root. *Genes & development* **18:** 700-714

Ohyama K, Ogawa M, Matsubayashi Y (2008) Identification of a biologically active, small, secreted peptide in Arabidopsis by in silico gene screening, followed by LC-MS-based structure analysis. *The Plant journal : for cell and molecular biology* **55:** 152-160

Roberts I, Smith S, De Rybel B, Van Den Broeke J, Smet W, De Cokere S, Mispelaere M, De Smet I, Beeckman T (2013) The CEP family in land plants: evolutionary analyses, expression studies, and role in Arabidopsis shoot development. *J Exp Bot* **64:** 5371-5381

Roberts I, Smith S, Stes E, De Rybel B, Staes A, Van De Cotte B, Njo MF, Dedeyne L, Demol H, Lavenus J, Audenaert D, Gevaert K, Beeckman T , De Smet I (2016) CEP5 and XIP1/CEPR1 regulate lateral root initiation in Arabidopsis. *J Exp Bot* **(accepted)**

Smith S, Roberts I, Stes E, De Rybel B, Xuan W, Cho H, Larrieu A, Dai Vu L, Goodall B, van de Cotte B, Marie Guseman J, Rigal A, Harborough S R, Vanneste S, Kirschner G, Lavenus J, Vandermarliere E, Martens L, Stahl Y, Audenaert D, Friml J, Felix G, Simon R, Bennett M J, Bishopp A, Ljung K, Kepinski S, Robert S, Nemhauser J, Hwang I, Gevaert K, Beeckman T, De Smet I. The small signaling peptide CEP5 attenuates the dynamic AUX/IAA equilibrium **(in preparation)**

Tabata R, Sumida K, Yoshii T, Ohyama K, Shinohara H, Matsubayashi Y (2014) Perception of root-derived peptides by shoot LRR-RKs mediates systemic N-demand signaling. *Science* **346:** 343-346

Truernit E, Bauby H, Belcram K, Barthelemy J, Palauqui JC (2012) OCTOPUS, a polarly localised membrane-associated protein, regulates phloem differentiation entry in Arabidopsis thaliana. *Development* **139:** 1306-1315

Whitford R, Fernandez A, De Groodt R, Ortega E, Hilson P (2008) Plant CLE peptides from two distinct functional classes synergistically induce division of vascular cells. *Proc Natl Acad Sci U S A* **105:** 18625-18630

Winter D, Vinegar B, Nahal H, Ammar R, Wilson GV, Provart NJ (2007) An "Electronic Fluorescent Pictograph" browser for exploring and analyzing large-scale biological data sets. *PloS one* **2:** e718

## SUPPLEMENTAL DATA

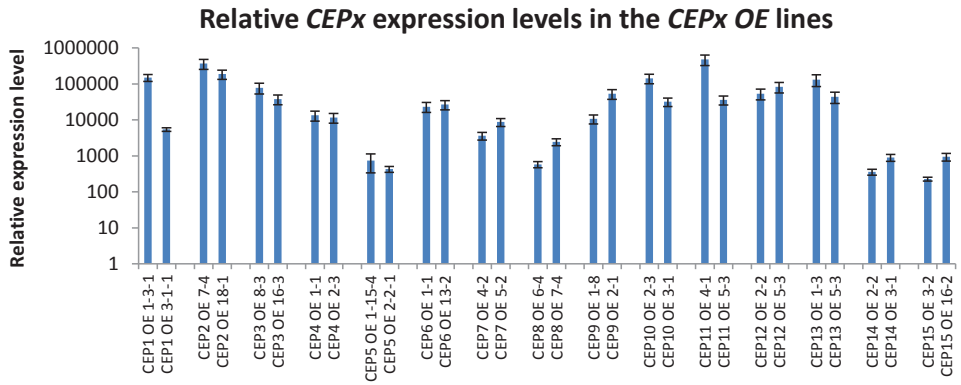


**Figure S1. Relative expression level of the *CEPx* gene in two independent *p35S::CEPx* overexpression (OE) lines compared to Col-0 control.** Root material was used. Graph shows mean ± SE; n = 3 biological repeats; * $p < 0.05$; Student's *t*-test.

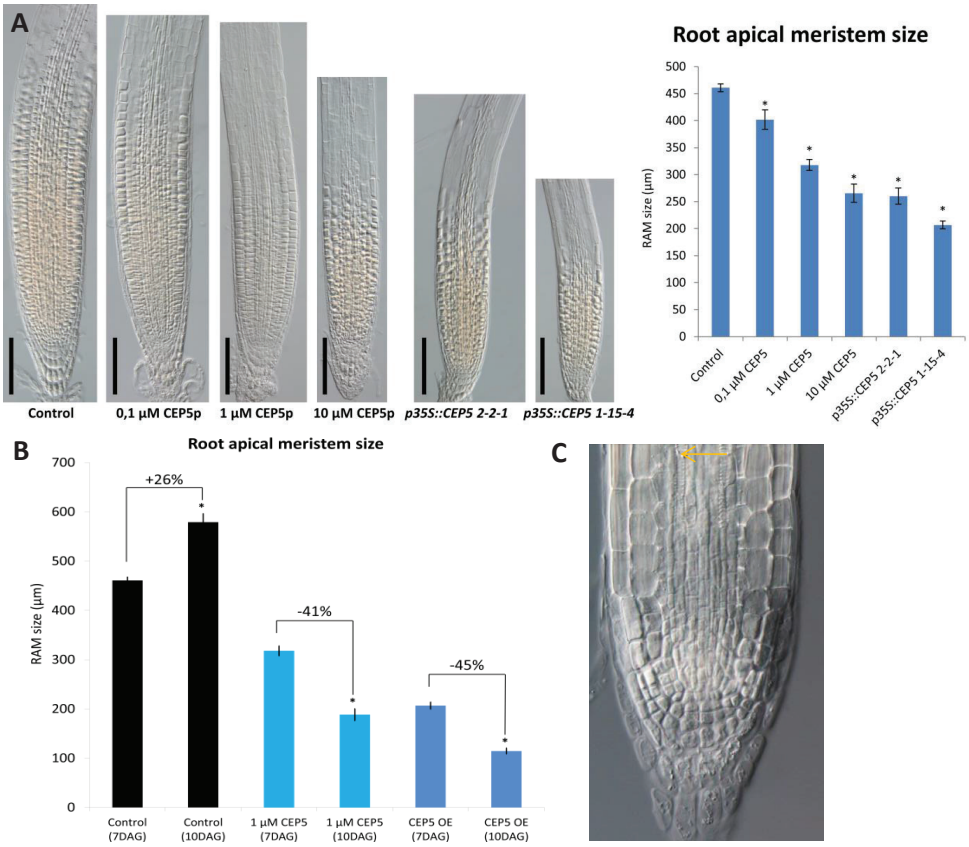


**Figure 19. Effect of CEP5 on RAM. (A)** Treatment with increasing concentrations of synthetic CEP5 peptide and overexpression of *CEP5* reduce the size of the root apical meristem (RAM) (seedlings are all 7 DAG) **(B)** The RAM increases in size in seedlings 10 DAG compared to 7 DAG in Col-0 control, while the RAM is gradually consumed over time by CEP5 peptide treatment or *CEP5* overexpression. **(C)** Drastic RAM consumption and earlier xylem differentiation (yellow arrow) are observed after 11 days of growth on 5 µM synthetic CEP5 peptide. (scale bar = 100 µm, graphs show average ± SE, * $p<0.05$ Student's *t*-test)

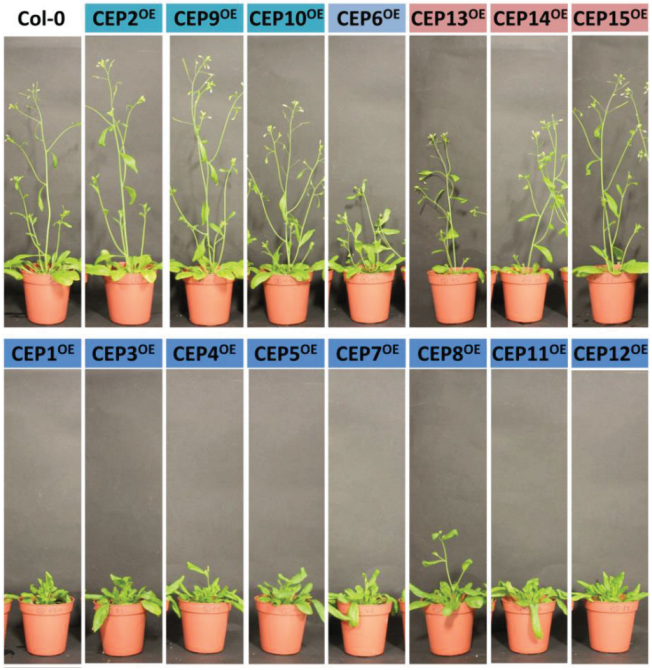


**Figure S3. Shoot phenotype of *CEP*$^{OE}$ lines.** Inflorescence of 34 day old mature plants of *p35S::CEP* overexpression lines compared to Col-0. Group I CEP members are marked in blue (further divided in three subgroups based on phenotype) and group II CEP members are marked in pink.

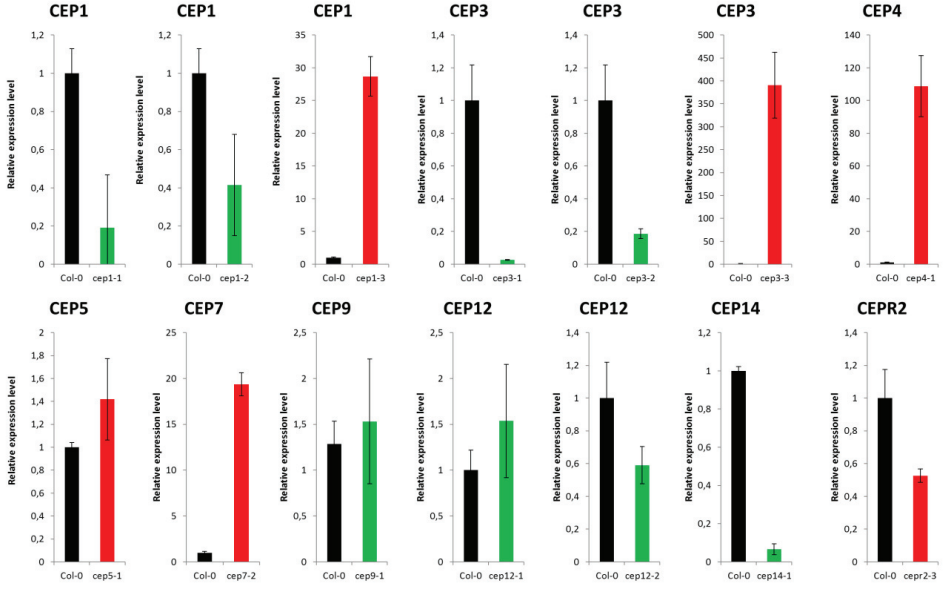


**Figure S4. Relative *CEP* expression level in T-DNA insertion lines.** Graphs show expression level of the *CEP* gene in a T-DNA insertion line compared to Col-0 control. GABI-KAT lines are indicated in red, and generally lead to overexpression of (a part of) the *CEP* gene (due to the *35S* promoter directed towards the right border of the T-DNA sequence). SALK lines are indicated in green, and generally lead to reduced expression of the *CEP* gene.

**Table S1. Overview of *cep* and *cepr* mutants with genotyping primers.**

| Gene | Mutant line | Alt. Name | NASC ID | Fw primer genotyping | Rev primer genotyping |
|---|---|---|---|---|---|
| ***CEP1*** | GK_734A05 | *cep1-1* | N470373 | TGCTCGTCTTAAATTAAAAATTCC | TGACAGTGTAACAAACCCACG |
| | SALK_076667 | *cep1-2* | N576667 | AAATGCATGGGCCATGTATAC | CGAGGGACCTAAAAGACTGAG |
| | GK_142C04 | *cep1-3* | - | TGGGAATGTCGAATAGGTCAG | GAAGAGTTTGCTCATGGCAAC |
| ***CEP3*** | SALK_092453 | *cep3-1* | N592453 | AAAAATCTTGATTGAATAACAAACG | AAACTTTTAGGTTTTTCTCCATGC |
| | SALK_105856 | *cep3-2* | N663580 | CGCTCTTGGCAATAAAGTGAG | TTCAAGCGAGTGACACATCTC |
| | GK_959A08 | *cep3-3* | - | TTATCTCCTCAAGTGTTGCGC | CCTAATATCTCCCTAATATCCCCC |
| ***CEP4*** | GK_139G04 | *cep4-1* | - | GACAAGATTCAAAATCAGCCG | AAACTGTGATTGAACAACCGC |
| ***CEP5*** | GK_457D06 | *cep5-1* | - | TATGGGCCTTAATCAAAAGCC | TGGGATAAACTATGGCCAATG |
| ***CEP7*** | SALK_101754 | *cep7-1* | N601754 | ATACTTGCCATGTGCAAAAGG | AATTTCCAAGCTTCTGGGAAG |
| | GK_346G08 | *cep7-2* | - | AACTCGAATCTGTCGAGCAAG | AGTTTTGAGCGTCGTGGATAC |
| ***CEP9*** | SALK_001158 | *cep9-1* | N680979 | GGCTCTATTTATCGTCCGTCC | TCCGGTTTTGAAATGATCTTG |
| | SALK_075885 | *cep9-2* | N575885 | TACATTCTCTTTGGGGCACTC | TCCATATCAACACTACGGACG |
| ***CEP12*** | SALK_100627 | *cep12-1* | N600627 | ATCGGCAATATCATCAACACC | TTCAAAGTCATCCTTTGGTGG |
| | SALK_146712 | *cep12-2* | N646712 | CAAAACCCAAATTTGTTTCCC | TCAACACAAGGGAGAAGGATG |
| ***CEP14*** | SALK_075531 | *cep14-1* | N575531 | TAGCCTACCGAACTCATTTGC | TAGGAACGGATCGGAGATACC |
| | SALK_126639 | *cep14-2* | N626639 | CTTGGAACTTGGAGGCCTAAC | TAGGAACGGATCGGAGATACC |
| ***CEPR1/XIP1*** | *xip1-1* | *xip1-1* | - | CTCTCTGGTCCTATCCCCGTCTCAT | ACGTCGCATTTGATCGTTGCTTTGG |
| ***CEPR2*** | GK_572B08 | *cepr2-1* | N454836 | CGTTCTCACGTAACGAGAAGC | AACCACACCGAAGCTGTACAC |
| | GK_644G02 | *cepr2-2* | N461802 | GACCGGAGAAATCCCTAACAG | AACCACACCGAAGCTGTACAC |
| | GK_695D11 | *cepr2-3* | N466671 | AATGTTGAATCGACCGTTGAG | GGTGAGTTCGTTATCGCTGAG |
| | SALK_014533 | *cepr2-4* | N514533 | AACTCGGAGTTTTGAAGGAGC | TCACAACTCTGTAACGCAACG |

**Table S2. Overview of real-time qRT-PCR primers for the *CEP* genes and two reference genes.**

| Gene | Fw primer qRT-PCR | Rev primer qRT-PCR |
|---|---|---|
| *CEP1* | TATACACGGCGTGGTGTCC | TTGTTGGCCTAAAGTCTGTGG |
| *CEP2* | TGCAGGGCATACATTTGGAGT | CACAACTCCTGGATGCCTGA |
| *CEP3* | TGAAGGCCGAAAACTCACCA | ACGGAATGTCCAATACCGGG |
| *CEP4* | TTGGTGATACAAGTACACTTTGAG | GGTGGGTTGGTCGGAATG |
| *CEP5* | CCATGGACGAACCCTAAAAG | TGCCATCATCGTCTTGCTAT |
| *CEP6* | GGGCATTGGTCATAAGATGAAG | CGTCGTAGGTTCGAAGTCATC |
| *CEP7* | TCGAAGAAATTCGCTGCGGG | CTGTTCCCAGGGTTGGTAGG |
| *CEP8* | GCAAGACACTTGAGGACCCA | TGTTGGCCGGAACTCATCAA |
| *CEP9* | CTGGGATAGGTCACAAGAAAGG | GGTGTCGTGGGTTTGAAGTC |
| *CEP10* | GGACCGTCATGAGCATTTCA | CATGGATGCCTAATACCGGG |
| *CEP11* | CGCAAGGTAGCCGTTTTAGG | ACCGGAAAGCATTGAGACCA |
| *CEP12* | GTGTTTGGTCCGCCAAGTTC | CCAGGTGGATCCTTGTGTCC |
| *CEP13* | CCAAGGGCAATGTACCACCT | CTCCGGCGAGTTTTCTGGTA |
| *CEP14* | TCTTTGCCGTCATCGTGTCA | TGACCCTTTTTGCTCGGTGT |
| *CEP15* | TCCCGGCAATGAAGATGAGG | GCTTGGGACATCACCTTGCC |
| *EEF-1α4* | CTGGAGGTTTTGAGGCTGGTAT | CCAAGGGTGAAAGCAAGAAGA |
| *At2g32170* | GGACCTCTGTTGTATCATTTTGCG | CAACCCTCTTTACATCCTCCAAAC |

**Table S3. Overview of primers used for cloning the promoter of the *CEP* and *CEPR* genes.**

| | | |
|---|---|---|
| ***pCEP1*** | Fw | GGGGACAACTTTGTATAGAAAAGTTGGATAAGCTCTTCGATTTATCACTCCG |
| | Rev | GGGGACTGCTTTTTTGTACAAACTTGTGAGCCGGGGACAAAGACAAATCG |
| ***pCEP2*** | Fw | GGGGACAACTTTGTATAGAAAAGTTGGAGAGATGGAAGATGGCCGTTAGG |
| | Rev | GGGGACTGCTTTTTTGTACAAACTTGTGTTTCTTTTCTCTAAATTAGATAAAAG |
| ***pCEP3*** | Fw | GGGGACAACTTTGTATAGAAAAGTTGGAGGTTTTGAACGGTCAGGATTGAG |
| | Rev | GGGGACTGCTTTTTTGTACAAACTTGTTACTAGAAAAACCGAGACGAGAATTAG |
| ***pCEP4*** | Fw | GGGGACAACTTTGTATAGAAAAGTTGGATTAAGACCTGTGTTAAGCATCGAAC |
| | Rev | GGGGACTGCTTTTTTGTACAAACTTGTCACTTGACAACTTTCTGTTTTTGTGAGG |
| ***pCEP5*** | Fw | GGGGACAACTTTGTATAGAAAAGTTGGATAGAGAGGAAAAAGGACGTCGATAG |
| | Rev | GGGGACTGCTTTTTTGTACAAACTTGTTATATTGGAAGAAAAATGGGAGATA |
| ***pCEP6*** | Fw | GGGGACAACTTTGTATAGAAAAGTTGGAGAGTTAAATAAAGGGTTTAAAATGG |
| | Rev | GGGGACTGCTTTTTTGTACAAACTTGTGTTAAAAATAAAAATCTGTGAGAAG |
| ***pCEP7*** | Fw | GGGGACAACTTTGTATAGAAAAGTTGGACATAGTTTAGTACTTCTTCAATGC |
| | Rev | GGGGACTGCTTTTTTGTACAAACTTGTAGCAATTATGAGAGAGTGTTAAATG |
| ***pCEP8*** | Fw | GGGGACAACTTTGTATAGAAAAGTTGGAGCGGCAGCTATATATGGATCAATTAGGG |
| | Rev | GGGGACTGCTTTTTTGTACAAACTTGTTGATGATGATTGAGTTTTTGTTAGTC |
| ***pCEP9*** | Fw | GGGGACAACTTTGTATAGAAAAGTTGGATATAGTAGTGGTTTTGTTGATGGGG |
| | Rev | GGGGACTGCTTTTTTGTACAAACTTGTGTTGTTGTTTTTTGTGGATTTAGAAGC |
| ***pCEP10*** | Fw | GGGGACAACTTTGTATAGAAAAGTTGGAGTCCTGGTCATTTTTTTTTTAGTTGGG |
| | Rev | GGGGACTGCTTTTTTGTACAAACTTGTGTTTCTTTTCTCTAAATTAGATAAAAC |
| ***pCEP11*** | Fw | GGGGACAACTTTGTATAGAAAAGTTGGACCTCCGAAAAATGAAAACCTCTTTCCC |
| | Rev | GGGGACTGCTTTTTTGTACAAACTTGTATCCAAAACTACAAATATATAAAAATAAGG |
| ***pCEP12*** | Fw | GGGGACAACTTTGTATAGAAAAGTTGGATTTATTTGTGTAAAATATACATTCC |
| | Rev | GGGGACTGCTTTTTTGTACAAACTTGTCTCAATAACTTAAAGCTTAGTG |
| ***pCEP13*** | Fw | GGGGACAACTTTGTATAGAAAAGTTGGACCTTTCTGCTGAGAGAAAGACTAATTTTGG |
| | Rev | GGGGACTGCTTTTTTGTACAAACTTGTTACCTGATTGATTTTGTTGTATAATTTTAG |
| ***pCEP14*** | Fw | GGGGACAACTTTGTATAGAAAAGTTGGAAATATTGTTCCGTCTAATTATCAATAAAG |
| | Rev | GGGGACTGCTTTTTTGTACAAACTTGTGAAGAGCTTTGATCTTTGGGTTG |
| ***pCEP15*** | Fw | GGGGACAACTTTGTATAGAAAAGTTGGAAAGAAAGATGATTTGCTCTTTATAAATTC |
| | Rev | GGGGACTGCTTTTTTGTACAAACTTGTTCAATATAAAGGTGAAAAAATATAAGAG |
| ***pCEPR1*** | Fw | GGGGACAACTTTGTATAGAAAAGTTGGAGAAGCTGGTGGATGAATGATGCC |
| | Rev | GGGGACTGCTTTTTTGTACAAACTTGTTTCAGAGAAAGATCAAAAGTAACCTAGAGG |
| ***pCEPR2*** | Fw | GGGGACAACTTTGTATAGAAAAGTTGGAAAATTACCTTTACTTGATGGAATTTTGC |
| | Rev | GGGGACTGCTTTTTTGTACAAACTTGTTTATAGTGATTCCCAAGGGCAAAACG |

**Table S4. Overview of primers used for cloning the open reading frame (ORF) of the *CEP* and *CEPR* genes.**

| | | |
|---|---|---|
| ***ORF CEP1*** | Fw | GGGGACAAGTTTGTACAAAAAAGCAGGCTTAATGGGAATGTCGAATAGGTCAG |
| | Rev | GGGGACCACTTTGTACAAGAAAGCTGGGTATCAATGTCGCCCGTTAGAGTGTCC |
| ***ORF CEP2*** | Fw | GGGGACAAGTTTGTACAAAAAAGCAGGCTTAATGAAGCTATTCATTATCACCGTGG |
| | Rev | GGGGACCACTTTGTACAAGAAAGCTGGGTATTAAACATTCACAACTCCTGGATGC |
| ***ORF CEP3*** | Fw | GGGGACAAGTTTGTACAAAAAAGCAGGCTTAATGGCGACGATTAATGTTTACG |
| | Rev | GGGGACCACTTTGTACAAGAAAGCTGGGTATTAATTATGTACGGAATGTCC |
| ***ORF CEP4*** | Fw | GGGGACAAGTTTGTACAAAAAAGCAGGCTTAATGGTGTCTCGCGGTTGTTCAATC |
| | Rev | GGGGACCACTTTGTACAAGAAAGCTGGGTATTAAGGAGCACCTGGAGGGTTTTTG |
| ***ORF CEP5*** | Fw | GGGGACAAGTTTGTACAAAAAAGCAGGCTTAATGGAATCGTTTATGGGTC |
| | Rev | GGGGACCACTTTGTACAAGAAAGCTGGGTATCAATTATGGGATAAACTATGGC |
| ***ORF CEP6*** | Fw | GGGGACAAGTTTGTACAAAAAAGCAGGCTTAATGAAACTCTCAGTTTATATCATTC |
| | Rev | GGGGACCACTTTGTACAAGAAAGCTGGGTATTAAGCATTAGGCTCATTGTTCTTG |
| ***ORF CEP7*** | Fw | GGGGACAAGTTTGTACAAAAAAGCAGGCTTAATGGCTAAATGCACTTTGACTAGC |
| | Rev | GGGGACCACTTTGTACAAGAAAGCTGGGTACTAGTGACCAATTCCTGGACTGTTCCC |
| ***ORF CEP8*** | Fw | GGGGACAAGTTTGTACAAAAAAGCAGGCTTAATGGCAAAAGCTCTGTTCTTC |
| | Rev | GGGGACCACTTTGTACAAGAAAGCTGGGTATCAATGGCCAATGCCGGGGCTG |
| ***ORF CEP9*** | Fw | GGGGACAAGTTTGTACAAAAAAGCAGGCTTAATGGTATTTTACCAAACACCAATC |
| | Rev | GGGGACCACTTTGTACAAGAAAGCTGGGTATTAAGCTTTAGGTTCATCGTTCTTG |
| ***ORF CEP10*** | Fw | GGGGACAAGTTTGTACAAAAAAGCAGGCTTAATGAAGCTATTTATTATCATTGTGG |
| | Rev | GGGGACCACTTTGTACAAGAAAGCTGGGTATCATGGATGCCTAATACCGGG |
| ***ORF CEP11*** | Fw | GGGGACAAGTTTGTACAAAAAAGCAGGCTTAATGGCAAAGACACGTCGTGTAATTTACC |
| | Rev | GGGGACCACTTTGTACAAGAAAGCTGGGTATCAGGTCTTGATCAAGTGGCCAACACC |
| ***ORF CEP12*** | Fw | GGGGACAAGTTTGTACAAAAAAGCAGGCTTAATGGTGAACCGTGATAATTCTATTGTGG |
| | Rev | GGGGACCACTTTGTACAAGAAAGCTGGGTATTATGGAGCACCAGGTGGATCCTTGTGTCC |
| ***ORF CEP13*** | Fw | GGGGACAAGTTTGTACAAAAAAGCAGGCTTAATGGCTCGTCCAAGGATCTCC |
| | Rev | GGGGACCACTTTGTACAAGAAAGCTGGGTACTAATGACCCACGCCGGGGC |
| ***ORF CEP14*** | Fw | GGGGACAAGTTTGTACAAAAAAGCAGGCTTAATGGCCGTTCGTCTAATTCCG |
| | Rev | GGGGACCACTTTGTACAAGAAAGCTGGGTATCAATGGCCAACACCGGGAC |
| ***ORF CEP15*** | Fw | GGGGACAAGTTTGTACAAAAAAGCAGGCTTAATGGATGCAACGAAGATTAAGTTTGACG |
| | Rev | GGGGACCACTTTGTACAAGAAAGCTGGGTATCAGTGGCCAATACCAGGGCTTG |
| ***ORF CEPR1*** | Fw | GGGGACAAGTTTGTACAAAAAAGCAGGCTTAATGCGTCTCAAAAATTTCCCC |
| | Rev (C) | GGGGACCACTTTGTACAAGAAAGCTGGGTACTAGAGTCTTGTTTGCGTGAG |
| | Rev (O) | GGGGACCACTTTGTACAAGAAAGCTGGGTAGAGTCTTGTTTGCGTGAGATGATC |
| ***ORF CEPR2*** | Fw | GGGGACAAGTTTGTACAAAAAAGCAGGCTTAATGTCGAGAAGACCAGACCTCC |
| | Rev (C) | GGGGACCACTTTGTACAAGAAAGCTGGGTACTATACTGTAATCTTTCCAGTTGTGTCTTG |
| | Rev (O) | GGGGACCACTTTGTACAAGAAAGCTGGGTATACTGTAATCTTTCCAGTTGTGTCTTGAG |

**Table S5. Selection of *p35S::CEP* lines.** The table shows the number of independent lines during the selection procedure: the number of primary independent T1 transformants (T1, transf.), the number of independent T2 lines selected with the T-DNA insertion at 1 locus (T2, 1 locus), the number of independent T3 lines homozygous for the T-DNA insertion (T3, ind. hom.), and the number of independent T3 homozygous lines selected for a representative phenotype and highest overexpression level (same phenotype, highest expr. qPCR). The *CEP1*$^{OE}$ and *CEP5*$^{OE}$ lines were obtained from the Matsubayashi lab and from Bert De Rybel, respectively, and no numbers are known for the selection procedure.

| | T1 transf. | T2 1 locus | T3 ind. hom. | same phenotype highest expr. qPCR |
|---|---|---|---|---|
| ***p35S::CEP 1*** | *Matsubayashi* | | 3 | 2 |
| ***p35S::CEP 2*** | 23 | 15 | 7 | 2 |
| ***p35S::CEP 3*** | 16 | 12 | 6 | 2 |
| ***p35S::CEP 4*** | 10 | 10 | 6 | 2 |
| ***p35S::CEP 5*** | *Bert De Rybel* | | 3 | 2 |
| ***p35S::CEP 6*** | 25 | 16 | 13 | 2 |
| ***p35S::CEP 7*** | 5 | 5 | 3 | 2 |
| ***p35S::CEP 8*** | 5 | 3 | 3 | 2 |
| ***p35S::CEP 9*** | 7 | 6 | 5 | 2 |
| ***p35S::CEP 10*** | 23 | 17 | 13 | 2 |
| ***p35S::CEP 11*** | 12 | 7 | 7 | 2 |
| ***p35S::CEP 12*** | 17 | 11 | 6 | 2 |
| ***p35S::CEP 13*** | 8 | 7 | 3 | 2 |
| ***p35S::CEP 14*** | 6 | 6 | 4 | 2 |
| ***p35S::CEP 15*** | 5 | 4 | 2 | 2 |

**Table S6. Selection of *promoter::nls-GFP/GUS* and *pCEPR::CEPR-GFP* reporter lines.** The table shows the number of independent lines during the selection procedure: the number of primary independent T1 transformants (T1, transf.), the number of independent T2 lines selected with the T-DNA insertion at 1 locus (T2, 1 locus), the number of independent T3 lines homozygous for the T-DNA insertion (T3, ind. hom.), and the number of independent T3 homozygous lines selected for a representative expression pattern (similar expression pattern selection). The *pCEP1-5::nls-GFP/GUS* reporter lines were obtained from Bert De Rybel, and no numbers are known for the selection procedure.

| | T1 transf. | T2 1 locus | T3 ind. hom. | similar expression pattern selection |
|---|---|---|---|---|
| ***pCEP 1 ::nls-GFP/GUS*** | | *Bert De Rybel* | | 2 |
| ***pCEP 2 ::nls-GFP/GUS*** | | *Bert De Rybel* | | 2 |
| ***pCEP 3 ::nls-GFP/GUS*** | | *Bert De Rybel* | | 2 |
| ***pCEP 4 ::nls-GFP/GUS*** | | *Bert De Rybel* | | 2 |
| ***pCEP 5 ::nls-GFP/GUS*** | | *Bert De Rybel* | | 2 |
| ***pCEP 6 ::nls-GFP/GUS*** | 22 | 9 | 7 | 2 |
| ***pCEP 7 ::nls-GFP/GUS*** | 26 | 15 | 6 | 2 |
| ***pCEP 8 ::nls-GFP/GUS*** | 5 | 5 | 5 | 2 |
| ***pCEP 9 ::nls-GFP/GUS*** | 6 | 2 | 2 | 2 |
| ***pCEP 10 ::nls-GFP/GUS*** | 12 | 7 | 2 | 2 |
| ***pCEP 11 ::nls-GFP/GUS*** | 10 | 7 | 4 | 2 |
| ***pCEP 12 ::nls-GFP/GUS*** | 15 | 4 | 2 | 2 |
| ***pCEP 13 ::nls-GFP/GUS*** | 15 | 10 | 2 | 2 |
| ***pCEP 14 ::nls-GFP/GUS*** | 11 | 7 | 2 | 2 |
| ***pCEP 15 ::nls-GFP/GUS*** | 7 | 7 | 7 | 2 |
| ***pCEPR 1 ::nls-GFP/GUS*** | 18 | 9 | 4 | 2 |
| ***pCEPR 2 ::nls-GFP/GUS*** | 17 | 9 | 4 | 2 |
| ***pCEPR 1 ::CEPR1-GFP*** | 21 | 17 | 10 | 2 |
| ***pCEPR 2 ::CEPR2-GFP*** | 29 | 22 | 10 | 2 |

# Chapter 5:

## CEP5 and XIP1/CEPR1 regulate lateral root initiation in *Arabidopsis*

**Contributions:**

I.R. performed results in fig2, fig3, fig4A-C, fig5, fig7A-D, fig8D, figS4, figS5, figS6 and figS7; S.S. performed results in fig4C-D and fig7E; E.S., A.S. and H.D. performed results in fig6; B.D.R. and J.L. performed results in fig1 and figS2; B.V.D.C. performed results in fig8A-C and figS1A; M.F.N. performed results in figS1B; and L.D. performed results in figS3. Data analysis was performed by I.R., S.S., E.S., B.D.R. and I.D.S.. The research was supervised by D.A., K.G., T.B. and I.D.S.. The manuscript was written by I.D.S. with contributions from I.R., S.S. E.S. and T.B..

This chapter is accepted for Journal of Experimental Botany (with some minor differences).

# CEP5 and XIP1/CEPR1 regulate lateral root initiation in *Arabidopsis*

Ianto Roberts[1,2,$], Stephanie Smith[3,$], Elisabeth Stes[1,2,4,5], Bert De Rybel[1,2], An Staes[4,5], Brigitte van de Cotte[1,2], Maria Fransiska Njo[1,2], Lise Dedeyne[1,2], Hans Demol[4,5], Julien Lavenus[1,2,#], Dominique Audenaert[1,2], Kris Gevaert[4,5], Tom Beeckman[1,2,†] , and Ive De Smet[1,2,3,6,†,*]

[1]Department of Plant Systems Biology, VIB, B-9052 Ghent, Belgium
[2]Department of Plant Biotechnology and Genetics, Ghent University, B-9052 Ghent, Belgium
[3]Division of Plant and Crop Sciences, School of Biosciences, University of Nottingham, Loughborough LE12 5RD, United Kingdom
[4]Medical Biotechnology Center, VIB, 9000 Ghent, Belgium
[5]Department of Biochemistry, Ghent University, B-9000 Ghent, Belgium
[6]Centre for Plant Integrative Biology, University of Nottingham, Loughborough LE12 5RD, United Kingdom
[$]Equal contribution
[#]Current address: Institute of Plant Sciences, University of Bern, Alterbergrain 21, 3013 Bern, Switzerland
[†]Equal contribution

[*]To whom the correspondence should be addressed: E-mail: ive.desmet@psb.vib-ugent.be,
Tel: 003293313930, Fax: 003293313809

## ABSTRACT

Roots explore the soil for water and nutrients through the continuous production of lateral roots. Lateral roots are formed at regular distances in a steadily elongating organ, but how future sites for lateral root formation become established is not yet understood. Here, we identified C-TERMINALLY ENCODED PEPTIDE 5 (CEP5) as a novel, auxin-repressed and phloem pole-expressed signal assisting in the formation of lateral roots. In addition, based on genetic and expression data, we found evidence for the involvement of its proposed receptor, XYLEM INTERMIXED WITH PHLOEM 1 (XIP1)/CEP RECEPTOR 1 (CEPR1), during the process of lateral root initiation. In conclusion, we report here on the existence of a peptide ligand-receptor kinase pair that impacts lateral root initiation. Our results represent an important step towards the understanding of the cellular communication implicated in the early phases of lateral root formation.

**Key words:** CEP5, XIP1, lateral root initiation, Arabidopsis, post-translationally modified peptide, receptor kinase

## INTRODUCTION

Coordinated positioning and development of lateral roots is central to shape root system architecture allowing plants to adapt their below-ground organs for optimal soil exploration (De Smet, 2012; Smith and De Smet, 2012; Kong et al., 2014; Tian et al., 2014). Lateral root primordia are formed from approximately three pairs of xylem pole pericycle (XPP) cells arranged in neighbouring cell files that undergo asymmetric cell division and subsequently form a new organ (Dubrovsky et al., 2001; Kurup et al., 2005; De Smet et al., 2006; De Smet et al., 2007; Péret et al., 2009; Lavenus et al., 2013). In the basal meristem, close to the primary root tip and before any asymmetric cell division, a periodic transcriptional mechanism specifies pre-branch sites that are competent to form lateral roots in a regular pattern (De Smet et al., 2007; Moreno-Risueno et al., 2010; Van Norman et al., 2013; Xuan et al., 2015; Xuan et al., 2016).

Several plant hormones have been shown to affect root architecture among which auxin has been granted a central role (Lau et al., 2008; Vanneste and Friml, 2009). In addition, a number of transcription factors and miRNAs have been shown to affect lateral root development (Satbhai et al., 2015). However, several recent studies are beginning to reveal the importance of different classes of small signalling peptides during the process of lateral root development (Ohyama et al., 2008; Delay et al., 2013; Fernandez et al., 2013; Kumpf et al., 2013; Araya et al., 2014; Bergonci et al., 2014; Czyzewicz et al., 2015; Fernandez et al., 2015). However, in *Arabidopsis*, very few small signalling peptides have been linked to a receptor (Murphy et al., 2012; Czyzewicz et al., 2013), and very few receptors involved in lateral root development have been identified (De Smet et al., 2008; De Smet et al., 2009; Kumpf et al., 2013; Wierzba and Tax, 2013; Araya et al., 2014; Cho et al., 2014; Tabata et al., 2014). Recently, the leucine-rich repeat (LRR) receptor kinases XYLEM INTERMIXED WITH PHLOEM 1 (XIP1)/C-TERMINALLY ENCODED PEPTIDE (CEP) RECEPTOR 1 (CEPR1, At5g49660) and CEPR2 (At1g72180) were proposed to act as receptors for CEP1 and other members of the CEP family (Tabata et al., 2014). Both XIP1/CEPR1 and CEPR2 contain a short secretory signal peptide sequence, an N-terminal extracellular LRR receptor domain with 21 LRR-repeats, a single helical transmembrane region and a C-terminal cytoplasmic serine/threonine kinase domain. It was previously shown that a loss-of-function *xip1* mutant displays anthocyanin accumulation in the leaves, xylem-like lignification of phloem in inflorescence stems, disrupted xylem vessel formation, phloem cells sometimes located adjacent to xylem cells, and shorter inflorescence stems (Bryan et al., 2012), and that the *cepr1 cepr2* double mutant displays a pleiotropic phenotype, including pale green leaves, smaller rosette leaves, shorter floral stems, anthocyanin accumulation, reduced nitrate uptake activity, decreased expression of nitrate transporters and enhanced lateral root elongation (Tabata et al., 2014). In *Medicago truncatula,* COMPACT ROOT ARCHITECTURE 2 (CRA2) was proposed as a potential orthologue of XIP1/CEPR1. However, the *cra2* mutant did not show obvious vascular defects as observed in the *xip1* mutant, but instead was clearly affected in its root system architecture, a phenotype that was not previously described for the *xip1* mutant (Bryan et al., 2012; Huault et al., 2014). Therefore, it remains to be determined which role XIP1/CEPR1 plays in shaping the root system in *Arabidopsis*.

The post-translationally modified CEP family members contain an N-terminal signal peptide sequence and a C-terminal conserved CEP domain from which the mature 15 amino acid peptide is processed (Ohyama et al., 2008; Delay et al., 2013; Roberts et al., 2013; Tabata et al., 2014). Some members of the CEP family have already been shown to regulate lateral root development (Ohyama et al., 2008; Delay et al., 2013; Mohd-Radzman et al., 2015), but in this work we functionally characterized *C-TERMINALLY ENCODED PEPTIDE5* (*CEP5,* At5g66815) in the context of lateral root initiation. Furthermore, we explored the involvement of *XIP1/CEPR1* in lateral root initiation, and could show that *CEP5* and *XIP1/CEPR1* are co-expressed during early stages of lateral root initiation, that both affect this process, and finally, that the *xip1-1* mutant is less sensitive to CEP5p for its negative effect on primary root growth and lateral root initiation, suggesting a potential peptide ligand - receptor pair.

## RESULTS AND DISCUSSION

**Focused transcript profiling data identifies *CEP5* as a putative regulator of lateral root development**

Since the plant hormone auxin is a major regulator of primary root growth and lateral root development (Overvoorde et al., 2010; Lavenus et al., 2013), several transcript profiling studies based on auxin treatments have been performed in order to identify the molecular players involved (Himanen et al., 2004; Vanneste et al., 2005; De Smet et al., 2008). However, because of the pleiotropic effects caused by exogenous auxin application, such datasets risk compromising the spatiotemporal resolution required when looking for components specific for a single developmental process. To circumvent this, we searched for putative novel early lateral root formation regulators by screening a dataset obtained through a highly focused transcript profiling analysis on seedling roots treated with the synthetic molecule naxillin. Naxillin specifically induces an auxin response in the basal meristem associated with lateral root initiation through enhancing indole-3-butyric acid (IBA) to indole-3-acetic acid (IAA) conversion in the root cap (De Rybel et al., 2012). Driven by the recurrent programmed cell death of the outermost lateral root cap cells, a periodic input of the converted auxin into the main root contributes to a fine-tuned mechanism that results in an evenly spaced lateral root distribution pattern (Xuan et al., 2016). Importantly, through its local activity, naxillin does not display the typical pleiotropic effects of exogenous application of auxin or auxin-like molecules (De Rybel et al., 2012). In order to identify novel putative early lateral root formation regulators, seedlings were grown for 72 hours on growth medium supplemented with the polar auxin transport inhibitor N-1-naphthylphthalamic acid (NPA), which prevents lateral root initiation, followed by a transfer to growth medium supplemented with naxillin to synchronously trigger the priming event in the basal meristem. In a genome wide transcript profiling analysis, we identified *CEP5* (At5g66815) as differentially up regulated between non-treated and naxillin-treated seedling roots (De Rybel et al., 2012) **(Figure 1)**. The *CEP5* gene encodes a small protein of 105 amino acids and contains a conserved 15 amino acid C-terminal CEP domain that gives rise to a small signalling peptide (Ohyama et al., 2008; Roberts et al., 2013; Tabata et al., 2014).

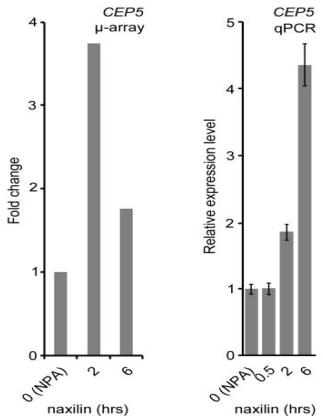


**Figure 1. *CEP5* expression levels after naxillin treatment,** determined with Affymetrix ATH1 micro-array analysis (left) and with real-time qRT-PCR analysis (right) in the roots of seedlings grown 72 hours on ½ MS growth medium supplemented with 10 µM NPA (time point 0h), followed by a transfer to ½ MS growth medium supplemented with 10 µM naxillin for 0.5, 2 and 6 hours (time points 0.5h, 2h and 6h). Graphs indicate average ± SE of 3 biological repeats.

***CEP5* expression is regulated by auxin**

Since *CEP5* is transcriptionally regulated following naxillin treatment, we subsequently checked if *CEP5* expression is also auxin-regulated. Treatment of wild-type roots with different concentrations of the synthetic auxin 1-naphthalene-acetic acid (NAA) or with indole-3-acetic acid (IAA) revealed that *CEP5* expression was down regulated by auxin **(Figure 2)**, suggesting that *CEP5* expression is (directly or indirectly) regulated by auxin.

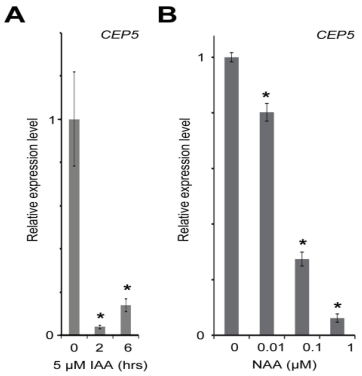


**Figure 2. Effect of auxin on *CEP5* expression. (A)** *CEP5* expression in 7 day old roots following indicated hours of auxin (1 µM IAA) treatment in liquid medium. **(B)** *CEP5* expression in 5 day old root tips of ~5 mm (including the basal meristem) following 2 hours auxin (NAA) treatment at indicated concentrations. *CEP5* levels were analyzed through real-time qRT-PCR. Graphs show average ± SE of 3 biological replicates. *, $p < 0.05$ according to Student's *t*-test compared to 0 µM NAA or IAA.

***CEP5* expression is associated with early stages of lateral root development**

Based on its naxillin-regulated expression profile, CEP5 represents a candidate peptide to be involved in the early developmental steps toward lateral root development. Using a *pCEP5::NLS:GFP:GUS* reporter line (Roberts et al., 2013), we observed regularly spaced patches of *CEP5* expression associated with lateral root primordia, confirming its potential involvement in this process (**Figure 3A-C**). We did not detect *CEP5* expression in the primary root stem cell niche, however *CEP5* was expressed in the basal meristem (**Figure 3D**). The latter is important in the context of lateral root initiation as this region is defined as part of the oscillation zone where prebranch sites are established by the input of auxin derived from the lateral root cap (De Smet et al., 2007; Moreno-Risueno et al., 2010; Xuan et al., 2016). Tissue-specific analyses showed that both in the basal meristem and during early stages of lateral root development, *CEP5* was predominantly expressed in the phloem pole associated pericycle (PPP) cells, but also in the adjacent phloem (**Figure 3E-G, Figure S1A and Supplementary Movie 1**). This *CEP5* expression pattern does not overlap with the well-documented sites of high auxin response in the root or during lateral root initiation, which in *Arabidopsis* occurs in xylem pole-associated pericycle (XPP) cells (De Smet et al., 2007). To check if the expression pattern of *CEP5* is perturbed under conditions of altered auxin response in the XPP cells, the *pCEP5::NLS:GFP:GUS* reporter line was grown on NPA. Under these conditions, we did not observe any change in the *CEP5* expression pattern (such as radial expansion) compared to control conditions **(Supplementary Figure S1B)**. Taken together, *CEP5* is negatively regulated by auxin and specifically expressed in the PPP cells that are closely associated with the lateral root development process, suggesting a negative correlation with auxin activity.

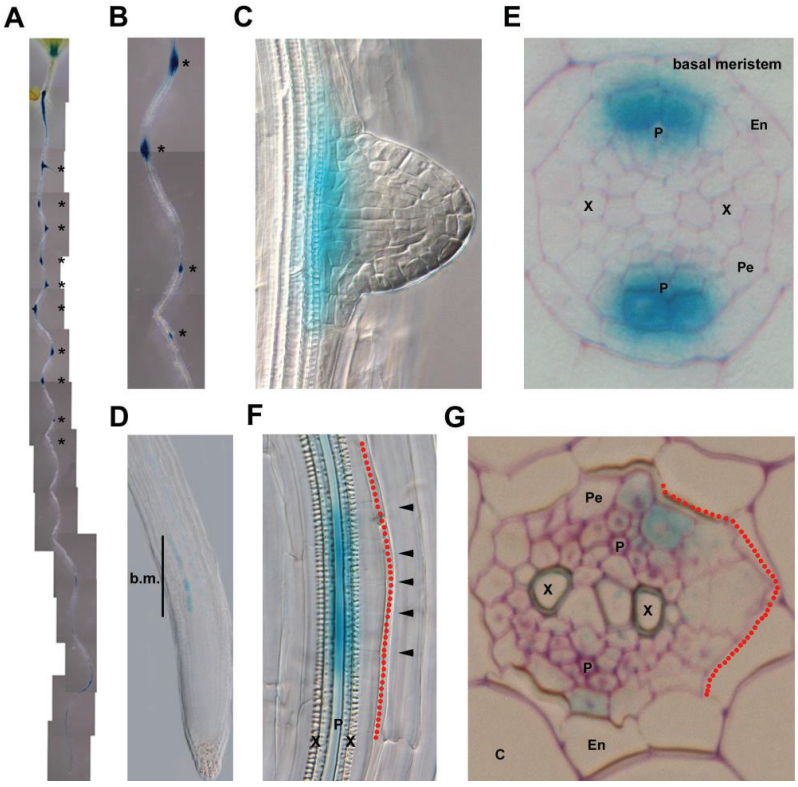


**Figure 3. *CEP5* expression in the *Arabidopsis* root. (A-G)** Representative pictures for *CEP5* expression (monitored through *GUS* expression in a *pCEP5::NLS:GFP:GUS* transgenic line) in the root: **(A)** in a complete seedling (overstained for illustrative reasons), **(B)** in a part of the root from the seedling depicted in panel A, **(C)** at the site of a lateral root primordium, **(D)** at the root apex, **(E)** in the basal meristem on a transverse section, **(F)** at a site of lateral root formation with the lateral root primordium pointing to the right (outlined with dotted red line), and **(G)** on a transverse section through a lateral root primordium (outlined with dotted red line). Seedlings are 5-6 days after germination. *, lateral root primordium; arrowheads in panel f separate individual cells; P, phloem; X, xylem; Pe, pericycle; En, endodermis; C, cortex; b.m., basal meristem.

### Altering *CEP5* expression levels affects root architecture

Given the spatial (appearing in common regions of the root, although not in the same cells) and temporal (being induced at the same time points) correlation of *CEP5* expression with lateral root initiation and development, we assessed if *CEP5* loss-of-function affected this process. A CaMV *35S* promoter-driven *CEP5* RNAi knockdown line (*CEP5*$^{RNAi}$) (Roberts et al., 2013) displayed a slightly longer primary root length compared to the control (**Figure 4A-C**). In addition, detailed analyses of lateral root initiation in this *CEP5*$^{RNAi}$ line revealed an increased number of stage I and stage II lateral root primordia compared to the control (**Figure 4D and Supplementary Figure S2**). Furthermore, in a root bending assay (Péret et al., 2012), the *CEP5*$^{RNAi}$ line progressed faster through lateral root developmental stages than wild type (**Figure 4E**). These loss-of-function data, together with the *CEP5* expression pattern, indicate that CEP5 plays a role in early lateral root initiation events.

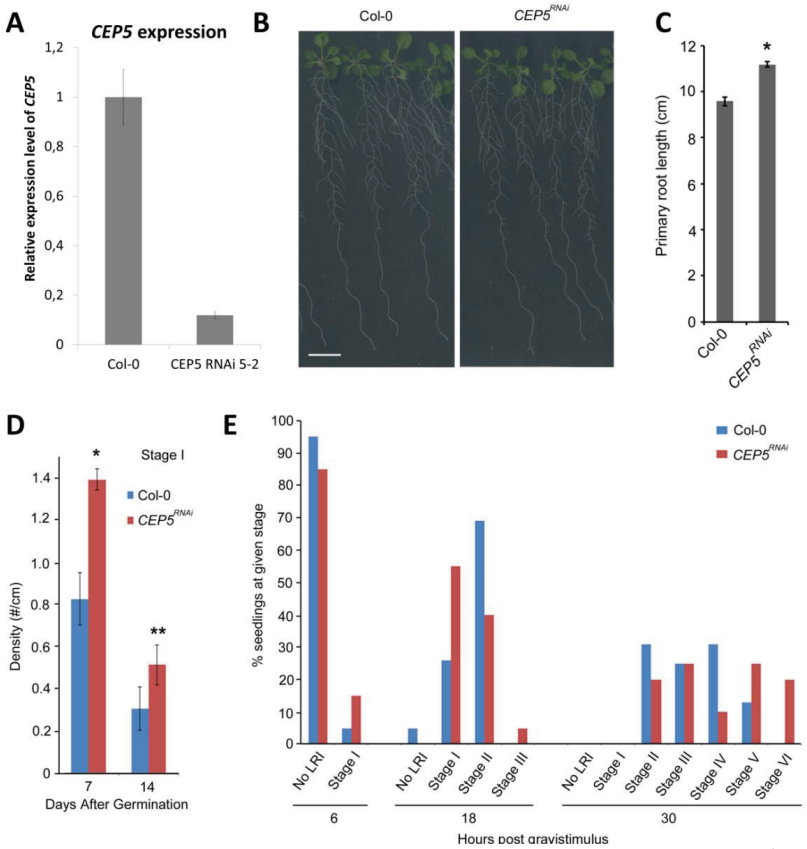


**Figure 4. Effect of reduced *CEP5* levels on root architecture. (A)** *CEP5* expression level in *CEP5*$^{RNAi}$ line compared to Col-0. **(B)** Representative picture of *CEP5*$^{RNAi}$ line and Col-0 at 12 days after germination (Scale bar, 1 cm). **(C)** Quantification of the primary root length of *CEP5*$^{RNAi}$ 12 days after germination (n ≥ 29). **(D)** Stage I lateral root primordia at indicated seedlings age (n = 10). **(E)** Progression through lateral root stages at indicated hours post gravistimulus (n ≥ 14). Graphs in B and C show average ± SE. *, $p < 0.05$ and **, $p < 0.075$ according to Student's *t*-test compared to Col-0.

Next, we analysed a line with CaMV *35S* promoter-driven constitutive overexpression of *CEP5* (*CEP5*$^{OE}$) (Roberts et al., 2013), which displayed shorter primary roots (similar to other independent *CEP5OE* lines) as compared to wild type (**Figure 5A-C, and Supplementary Figure S2**). Furthermore, the *CEP5*$^{OE}$ lines displayed a decrease in total lateral root density, with fewer non-emerged lateral roots, compared to wild type. Detailed analyses of lateral root developmental stages showed that this was mainly due to fewer initiation events (**Figure 5D, Supplementary Figure S2 and S5A**). At later stages of lateral root development, we also observed closely spaced lateral root primordia in *CEP5*$^{OE}$ lines, which we never observed as such in wild type roots (**Figure 5E**). This gain-of-function approach further suggested that CEP5 impacts root architecture, but does not exclude that this is an indirect and/or non-specific effect due to ectopic expression. In addition, overexpression of the *CEP5* coding sequence lacking the signal peptide sequence did not lead to the above mentioned gain-of-function phenotypes, indicating that the CEP5 peptide needs to go through the secretion pathway to become active **(Supplemental Figure S4)**.

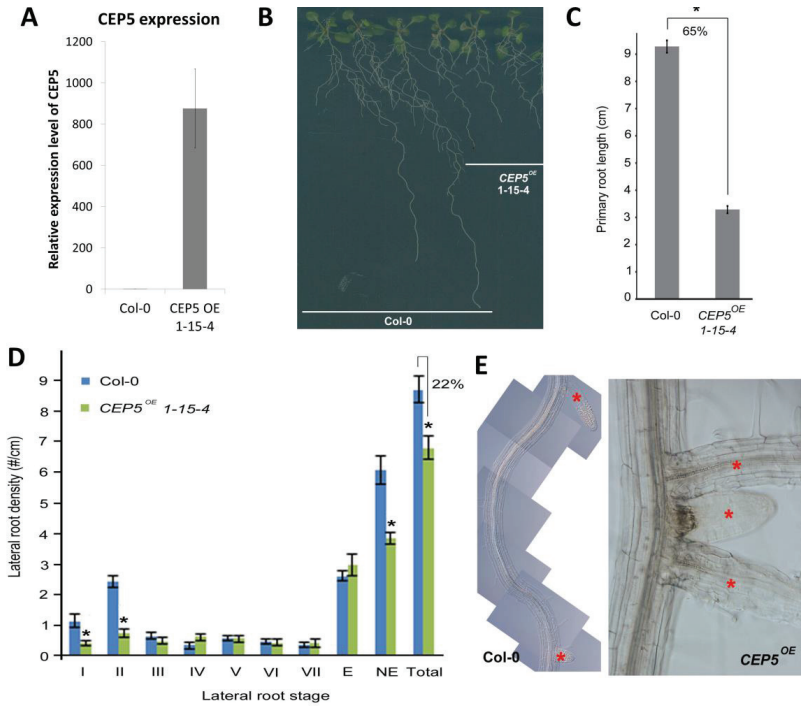


**Figure 5. Effect of increased *CEP5* levels on primary root growth and lateral root development. (A)** *CEP5* expression level in *CEP5*$^{OE}$ line compared to Col-0. **(B)** Representative picture of a *CEP5*$^{OE}$ line and Col-0 at 12 days after germination. **(C)** Quantification of primary root length at 12 days after germination. **(D)** Lateral root stages I to VII (according to Malamy and Benfey, 1997) in *CEP5*$^{OE}$ line (n ≥ 15) at 7 days after germination. The % reduction in total lateral root density is indicated. E,emerged lateral roots; NE, non-emerged lateral roots; Total, sum of E and NE. **(E)** Regular and adjacent positioning of lateral roots in wild type (Col-0) and *CEP5*$^{OE}$ seedlings, respectively, at 14 days after germination. Red * indicates lateral root. All graphs show average ± SE. *, $p < 0.05$ according to Student's *t*-test compared to Col-0.

### *CEP5* gives rise to CEP5p$^{Hyp}$

CEP5 has a conserved C-terminal CEP domain, containing three proline (Pro) residues and a predicted N-terminal signal peptide cleavage site that undergoes proteolytic processing to form a mature CEP5 peptide of 15 amino acids (CEP5p) (Roberts et al., 2013; Tabata et al., 2014) (**Figure 6A**). However, small signalling peptides are often post-translationally modified, thereby modulating – amongst others – the binding ability and specificity of peptides to their targets (Murphy et al., 2012). In this context, it was previously shown that members of the CEP family give rise to a peptide containing hydroxyproline (Hyp) residues (Tabata et al., 2014). To confirm that a 15 amino acid CEP5 peptide with three Hyp residues (CEP5p$^{Hyp}$) (**Figure 6A**) is indeed present in seedlings overexpressing *CEP5*, we performed selected reaction monitoring (SRM) on a *CEP5*$^{OE}$ line. SRM is a mass spectrometry technique that allows detection and quantification of specific (low abundant) peptides in total protein preparations (Picotti and Aebersold, 2012). Indeed, in the *CEP5*$^{OE}$ proteome spiked with a chemically synthesized version of CEP5pHyp containing an isoleucine residue with heavy, stable isotopes, transitions for both the heavy, spiked-in CEP5p$^{Hyp}$ and the light, naturally occurring CEP5$^{Hyp}$ peptide could be detected (**Figure 6B-E**). These results supported that a CEP5 peptide with three Hyp residues can be present *in planta*.

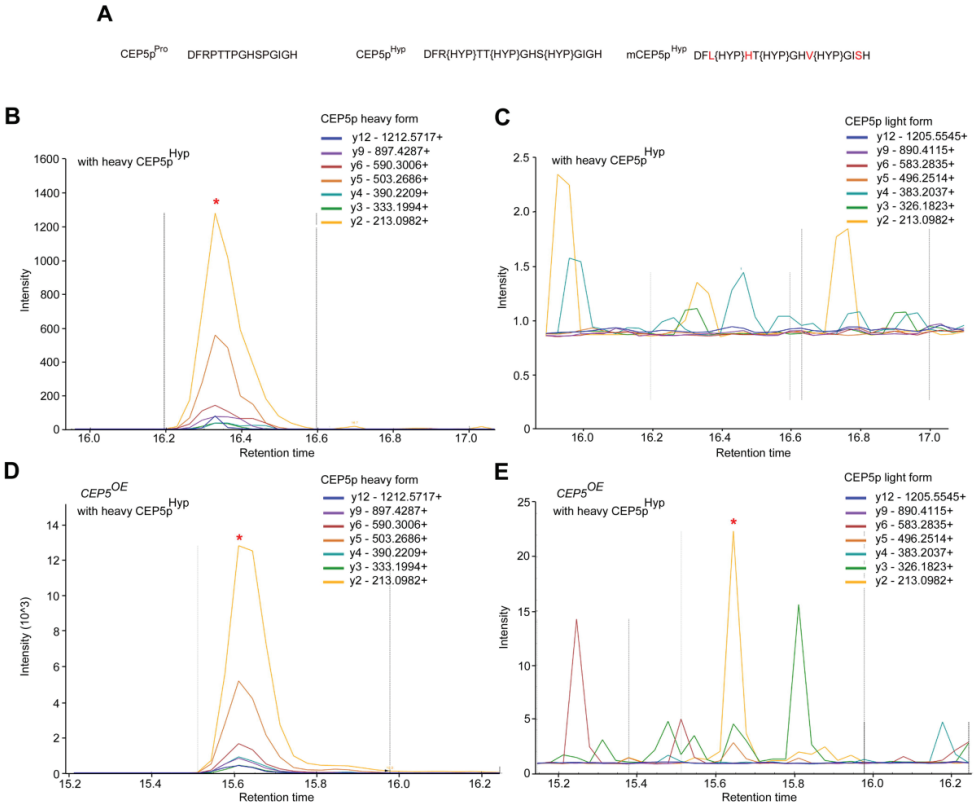


**Figure 6.** ***In planta*** **CEP5 peptide. (A)** Sequences for the synthetic variants of mature 15 amino acid CEP5: unmodified (CEP5p$^{Pro}$), with proline hydroxylation modifications on P4, P7 and P11 (CEP5p$^{Hyp}$), and hydroxyprolinated mutated CEP5 sequence with four residue substitutions (R3>L, T5>H, S10>V and G14>S; indicated in red) (mCEP5p$^{Hyp}$). **(B-E)** SRM analysis of the targeted CEP5 peptide. Characteristic y-type of fragment ions (referred to as transitions), indicated with different colors at the top of each spectrum, were monitored. As a control, the heavy CEP5p$^{Hyp}$ alone was analyzed by SRM, and the transitions of the heavy form **(B)** and the light form **(C)** were monitored. As for the latter, no transitions could be monitored, indicating the high isotopic purity of the heavy peptide. In the *CEP5*$^{OE}$ proteome spiked with heavy CEP5p$^{Hyp}$, both transitions for the heavy, spiked-in peptide **(D)** and the light, naturally occurring peptide **(E)** could be detected. Red asterisk, CEP5p$^{Hyp}$.

### Synthetic CEP5 peptide affects root architecture

Based on previous studies (Tabata et al., 2014) and the above-described results, a synthetic CEP5p$^{Hyp}$ peptide was generated for further analysis of CEP5 function (**Figure 6A**). To assess the activity of synthesized CEP5p$^{Hyp}$, we first analysed its effect on primary root growth, which has previously been shown to be a straightforward, although possibly nonspecific, assay to test the activity of small post-translationally modified CEP peptides (Delay et al., 2013). Indeed, seedlings grown in the presence of CEP5p$^{Hyp}$ displayed shorter roots compared to the mock-treated control and compared to a synthetic variant with 4 randomly positioned, but not very unlikely amino acid substitutions based on a BLOSUM62 substitution matrix within the 15 amino acid CEP5 peptide sequence, while retaining the Hyp residues at the same positions (mCEP5p$^{Hyp}$) (**Figure 6A and 7A-B and Supplementary Figure S3**).

Next, we addressed the effect of synthetic CEP5p$^{Hyp}$ on lateral root formation. Seedlings grown in the presence of different low concentrations of CEP5p$^{Hyp}$ displayed a decreased total lateral root density, which is mainly due to a significant reduction in lateral root initiation events (**Figure 7C and Supplementary Figure S5B**). Conversely, this did not occur in mCEP5p$^{Hyp}$-treated seedlings **(Supplementary Figure S6**). When lateral root initiation occurred, we occasionally observed regions of ectopic and/or aberrant pericycle cell divisions (observed in 10 out of 149 lateral root primordia evenly distributed over 8 CEP5p$^{Pro}$-treated seedlings, while this did not occur in untreated wild type) resulting in malformed lateral root primordia or closely spaced primordia in CEP5p$^{Pro/Hyp}$-treated seedlings, which differed from regularly spaced lateral roots in wild type (**Figure 7D-E**). Taken together, the similarities in primary and lateral root phenotypes between CEP5p treatment and *CEP5*$^{OE}$ indicate that the chemically synthesized CEP5p$^{Hyp}$ has the same bioactivity as the overexpressed *CEP5*. These results further support a role of CEP5p$^{Hyp}$ in lateral root initiation.

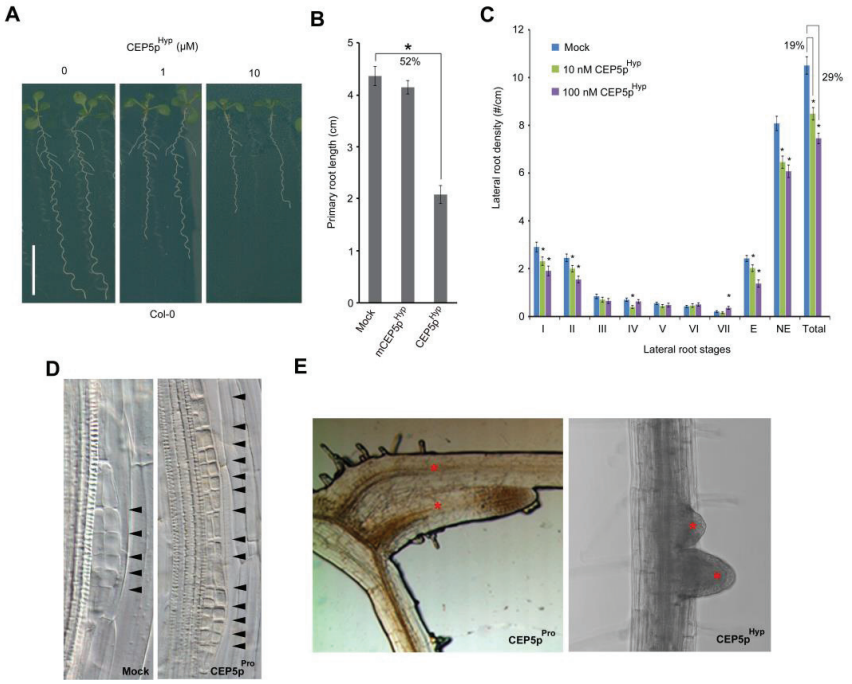


**Figure 7. Effect of synthetic CEP5p on primary root growth and lateral root development. (A)** Representative pictures of Col-0 *Arabidopsis* seedlings grown on indicated CEP5p$^{Hyp}$ concentrations for 7 days after germination. Scale bar, 1 cm. **(B)** Quantification of primary root length of Col-0 seedlings treated with 5 µM CEP5p$^{Hyp}$ compared with mock treatment and 5 µM mCEP5p$^{Hyp}$ at 7 days after germination (n ≥ 15 per condition). The % reduction in primary root length is indicated. **(C)** Lateral root stages I to VII (according to Malamy and Benfey, 1997) upon mock or CEP5p$^{Hyp}$ treatment at different concentrations at 9 days after germination (data from newly grown root part of 5 day old seedlings transferred to CEP5p$^{Hyp}$ for 4 days, n ≥ 32). E, emerged lateral roots; NE, non-emerged lateral roots; Total, total lateral roots. The % reduction in total lateral root density is indicated. **(D-E)** Adjacent positioning of lateral roots in mock (left) and 1 µM CEP5pP$^{ro}$-treated Col-0 seedlings (right) (11 days after germination) (Stage II primordia are shown). Observed in 10 out of 149 lateral root primordia (n = 8 seedlings), while this did not occur in untreated wildtype (D), in 10 µM CEP5p$^{Pro}$-treated seedlings 14 days after germination (E, left), and in 5 µM CEP5p$^{Hyp}$-treated seedlings 12 days after germination (E, right). Scale bars, 1 cm. All graphs show average ± SE of indicated sample numbers. *, $p < 0.05$ according to Student's *t*-test compared to mock. In all cases, mock refers to medium with water as used to dissolve CEP5p.

**The proposed CEP family receptor XIP1/CEPR1 regulates lateral root initiation**

Recently XIP1/CEPR1 and CEPR2 were proposed to be the receptors for CEP peptides, including CEP5 (Tabata et al., 2014). However, a role in lateral root initiation for XIP1/CEPR1 and/or CEPR2 was not yet explored. Therefore, we performed detailed analyses of a previously described *pXIP1::GUS* line (Bryan et al., 2012) and we showed that *XIP1/CEPR1* is expressed in the root from the basal meristem onwards (**Figure 8A**), a pattern that overlaps with *CEP5* expression (**Figure 3D**). Furthermore, tissue-specific analyses showed that *XIP1/CEPR1* is expressed in the phloem pole pericycle and in the adjacent phloem in the basal meristem (**Figure 8B**), overlapping with *CEP5* expression (**Figure 3E**), and is excluded from early stages of lateral root development (**Figure 8C**), similar to *CEP5* (**Figure 3C**). This closely-associated expression pattern combined with the results from Tabata et al. (2014) suggested that XIP1/CEPR1 could potentially be a receptor for CEP5 in the root and therefore might take part in lateral root initiation.

To further explore this, we assessed lateral root stages and density of the previously described *xip1-1* mutant (Bryan et al., 2012). This revealed a reduced total lateral root density in *xip1-1* in comparison with the control, which was mainly due to a reduction in stage I and II lateral root primordia and to fewer emerged lateral roots (**Figure 8D and Supplementary Figure S7**). Furthermore, the *xip1-1* mutant showed a significant reduction in primary root length **(Figure 8E)**. This suggests that XIP1/CEPR1 is a positive regulator of lateral root initiation and primary root growth.

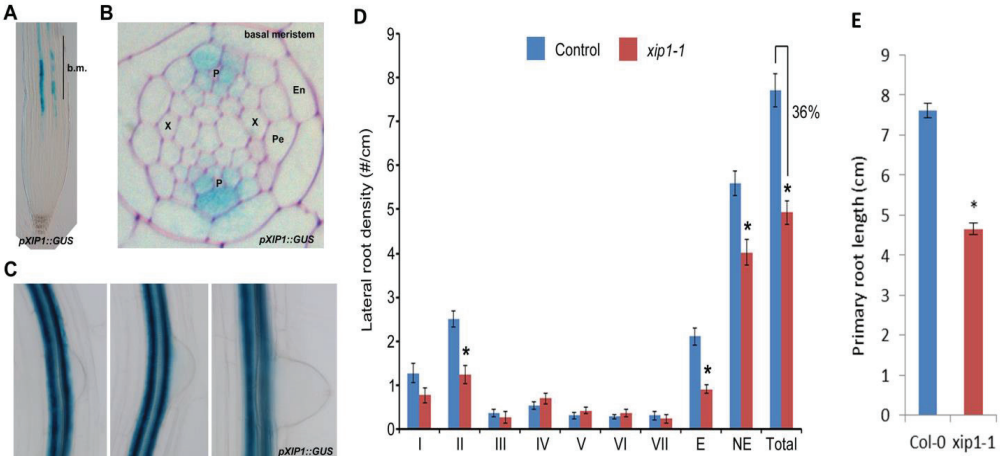


**Figure 8**. **XIP1/CEPR1 acts on lateral root initiation. (A)** Representative picture of *XIP1/CEPR1* expression in the root apex. **(B)** Transverse section through the basal meristem in a *pXIP1::GUS* transgenic reporter line. P, phloem; X, xylem; Pe, pericycle; En, endodermis; b.m., basal meristem**. (C)** Representative pictures for *XIP1* expression (monitored through *GUS* expression in a *pXIP1::GUS* transgenic line) in different stages of lateral root development in 7 day-old seedlings. **(D)** Lateral root phenotype in the *xip1-1* mutant. Lateral root stages I to VII (according to Malamy and Benfey, 1997) in Col-0 and *xip1-1* at 5 days after germination (n ≥ 14). E, emerged lateral roots; NE, non-emerged lateral roots; Total, total lateral roots. Graph shows average ± SE. *, $p < 0.05$ according to Student's *t*-test compared to Col-0.

To further evaluate an interaction between CEP5 and XIP1/CEPR1, we explored to what extent *xip1-1* is (in)sensitive to CEP5p$^{Hyp}$ treatment. This revealed that, compared to the control, *xip1-1* is less or not sensitive to CEP5p$^{Hyp}$ with respect to primary root growth and number of emerged lateral roots, respectively **(Figure 9)**.

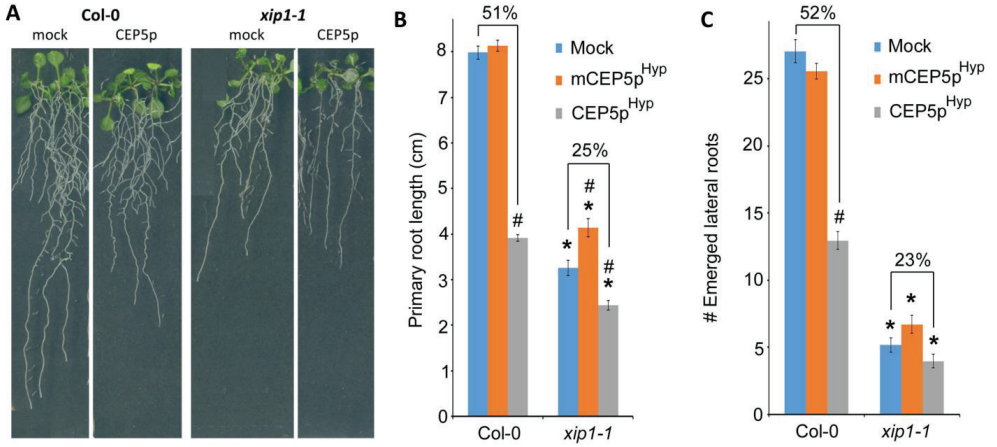


**Figure 9. Genetic evidence for a potential CEP5 - XIP1/CEPR1 ligand - receptor pair. (A)** Representative images of Col-0 and *xip1-1* seedlings grown for 10 days after germination on ½ MS supplemented with 1 µM CEP5p$^{Hyp}$ compared to mock treatment. **(B)** Quantification of primary root length and **(C)** emerged lateral root number of Col-0 and *xip1-1* seedlings treated with 1 µM CEP5p$^{Hyp}$ or mCEP5p$^{Hyp}$ compared with mock treatment at 10 days after germination (n ≥ 22 per condition). The % reduction in primary root length and lateral root number is indicated. In all cases, mock refers to medium with water as used to dissolve CEP5p. Lateral root stages I to VII (according to Malamy and Benfey, 1997); E = emerged lateral roots; NE = non-emerged lateral roots; Total = E + NE. Graphs shows average ± SE. * or #, $p < 0.05$ according to Student's *t*-test compared to Col-0 or mock treatment, respectively.

## CONCLUSIONS

Previously, a role for CEPs in regulating aspects of root architecture, namely nitrate dependent lateral root elongation, was proposed. Specifically, CEPs might act as root-derived ascending N-demand signals to the shoot, where their perception by CEPRs leads to the production of a putative shoot-derived descending signal that up-regulates nitrate transporter genes in the roots and stimulates lateral root eleongation (Tabata et al., 2014). Here, we provide evidence that CEP5 may also act during lateral root initiation. A stimulatory effect on lateral root initiation was observed in the *CEP5*$^{RNAi}$ knock-down line, while gain-of-function conditions using *CEP5*$^{OE}$ lines or synthetic CEP5p$^{Hyp}$ peptide treatments resulted in fewer lateral root initiation events, suggesting that CEP5 is part of a lateral root inhibitory mechanism. The observed clustering of lateral roots in later developmental stages in the gain-of-function condition might be a secondary effect. Slowing down lateral root development can interfere with the timely development of auxin sources and therefore retard the draining of auxin from the main root. On its turn, this might lead to higher auxin levels in the neighbourhood of existing primordia and induce ectopic and/or irregularly patterned primordia.

Based on the loss-of-function phenotypes observed in the *xip1-1* mutant, we determined that XIP1/CEPR1 acts as a positive regulator of lateral root initiation and primary root growth. Interestingly, the *cra2* mutant in *Medicago truncatula* (*CRA2* suggested as potential orthologue of *XIP1*/*CEPR1*) also showed a drastic reduction in primary root growth, but in contrast showed an increase in lateral root formation (Huault et al., 2014). This might suggest some distinct roles for this receptor in shaping root system architecture across different plant families (*Arabidopsis*: *Brassicaceae* versus *Medicago*: *Fabaceae*). However, further evidence is required to confirm that *CRA2* really serves as the functional orthologue of *XIP1*/*CEPR1*.

Furthermore, genetic evidence from this study – together with the biochemical evidence from Tabata et al. (2014) - suggests that CEP5 and XIP1/CEPR1 might potentially form a peptide ligand-receptor kinase pair acting together in the context of lateral and primary root development. However, in general, the loss-of-function mutant phenotypes of the genes encoding the peptide ligand and its receptor are very similar (Butenko et al., 2009; Czyzewicz et al., 2013; Kumpf et al., 2013; Murphy et al., 2012). But, in this case, the *xip1-1* root architecture phenotype is similar to $CEP5^{OE}$ or $CEP5p^{Hyp}$-treated seedlings and opposite to $CEP5^{RNAi}$ lines **(Figures 4, 5, 7 and 8)**, possibly suggesting that CEP5 negatively regulates XIP1/CEPR1 activity (*e.g.* by acting as an antagonist) in the context of lateral root initiation. In this context, the fact that $CEP5p^{Hyp}$ had no strong impact on *xip1-1* can also be interpreted as no further CEP5-mediated inhibitory effect if XIP1/CEPR1 is already non-functional (and hence can not be inhibited further). How this works at the molecular level remains to be investigated.

Alternatively, CEP5 might not (exclusively) act via the XIP1/CEPR1 receptor in regulating root architecture. The observed lateral root phenotypes could potentially be obtained through other mechanisms, such as XIP1/CEPR1 regulating vascular development in the root and thereby indirectly affecting root system architecture, while CEP5 might play a more direct role in shaping root system architecture, potentially acting through another receptor. Further analyses will be required to fully unravel the developmental and biochemical mechanisms underlying CEP5 and XIP1/CEPR1 activity, and to verify whether they form a functional peptide ligand-receptor kinase pair *in planta*.

Nonetheless, it is intriguing that a phloem-derived signal downstream of CEP5 and XIP1/CEPR1 has such an impact on lateral root initiation and development at the xylem pole (**Figure 10**). So far, no mutants have been reported to show lateral root initiation at the phloem poles in *Arabidopsis* (and so far we have also not observed this in loss- or gain-of-function *CEP5* or *XIP1*/*CEPR1* lines) arguing for a strong and complex lateral root inhibition mechanism in this part of the root pericycle. Earlier, a cell cycle inhibitory mechanism, based on the pericycle-specific expression of *KIP-RELATED PROTEIN2* (*KRP2*), a cyclin dependent kinase inhibitor, has been proposed as essential to spatially and temporally allow for lateral root initiation by repressing cell division activity in the entire pericycle except for sites of lateral root initiation (Himanen et al., 2002). In the future, it will be interesting to reveal if there is any direct interaction of CEP5-dependent signalling with the control on cell cycle regulation with respect to lateral root initiation. Additionally, it will be exciting to explore alternative mechanisms on how the phloem-expressed *CEP5* affects lateral root initiation in the xylem pole pericycle cells. At the moment, however, it is not yet possible to reliably visualize CEP5 peptide *in planta* in order to evaluate possible movement to other cells and/or tissues.

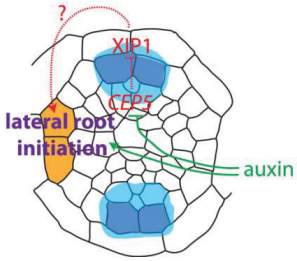


**Figure 10. Model:** The data we have – so far – suggest that *CEP5* and *XIP1/CEPR1* are expressed in the phloem pole pericycle (PPP) cells (blue cells, with the highest expression in dark blue, and domain with weaker, variable expression in light blue) associated with sites of lateral root formation and regulate lateral root initiation in the xylem pole pericycle cells (XPP) (orange cells) by a currently unknown mechanism (indicated by ?). Overall, the CEP5 peptide appears to negatively regulate XIP1/CEPR1 (activity). An auxin maximum in the XPP cells promotes lateral root initiation and possibly down regulates *CEP5* expression in these cells. As such, the auxin minimum in the neighbouring PPP cells likely allows *CEP5* expression.


### ACKNOWLEDGEMENTS

We thank Sarah De Cokere, Marieke Mispelaere and Darren Wells, for practical assistance, and Frans Tax for sharing materials. This work was supported by a BBSRC David Phillips Fellowship (BB_BB/H022457/1) and a Marie Curie European Reintegration Grant (PERG06-GA-2009–256354) (I.D.S), E.S. is a Postdoctoral Research Fellows of the Fund for Scientific Research (FWO)-Flanders (Belgium). This work was in part financed by grants of the Interuniversity Attraction Poles Programme (IAP VI/33 and IUAP P7/29 'MARS') from the Belgian Federal Science Policy Office and the Research Foundation Flanders (FWO). S.S. received a Biotechnology and Biological Science Research Council doctoral training grant studentship. I.R. was supported by the Agency for Innovation by Science and Technology (IWT). B.D.R. was funded by the Special Research Fund of Ghent University.


## MATERIALS AND METHODS

**Plant materials**

The following transgenic lines and mutants were described previously: *pCEP5::NLS:GFP:GUS, CEP5*$^{OE}$ and *CEP5*$^{RNAi}$ (Roberts et al., 2013), *xip1-1* and *pXIP1::GUS* (Bryan et al., 2012).

**Plant growth and treatment conditions**

Unless mentioned otherwise, seedlings were grown at 21 °C under continuous light (110 µE $m^{-2}$ $s^{-1}$ photosynthetically active radiation, supplied by cool-white fluorescent tungsten tubes, Osram) on square Petri plates (12 x 12 cm) containing 50 ml solid half-strength MS growth medium supplemented with sucrose (per liter: 2.15 g MS salts, 0.1 g *myo*-inositol, 0.5 g MES, 10 g sucrose, 8 g plant tissue culture agar; pH adjusted to 5.7 with KOH). For peptide treatments, media was supplemented with CEP5p$^{Pro}$ (DFRPTTPGHSPGIGH), CEP5p$^{Hyp}$ (DFR{HYP}TT{HYP}GHS{HYP}GIGH), or mCEP5p$^{Hyp}$ (DFL{HYP}HT{HYP}GHV{HYP}GISH) peptide to a concentration as indicated in the text and/or figure legends. Synthetic peptides (CEP5pPro, CEP5pHyp and mCEP5pHyp) were obtained from GenScript (www.genscript.com), and were supplemented to growth medium with concentrations as indicated in the text and/or figure legends. For auxin treatments, media was supplemented with indole-3-acetic acid (IAA) or 1- naphthaleneacetic acid (NAA) to a concentration as indicated in the text and/or figure legends.

**Primary and lateral root phenotyping**

At the indicated time, images of plates with seedlings were taken and roots were measured using ImageJ (http://rsbweb.nih.gov/ij/index.html) or FIJI software (Schindelin et al., 2012). For detailed staging of lateral roots, samples were cleared as described previously (Malamy and Benfey, 1997) and analysed by differential interference contrast microscopy (Olympus BX53).

**Transcriptome profiling data**

The naxillin-treatment transcriptome data from (De Rybel et al., 2012) can be searched in the Lateral Root Initiation eFP Browser (Winter et al., 2007).

**Histochemical GUS assays**

For GUS assays, plants were put overnight in 90% acetone, then transferred to a solution [1 mM X-Glc, 0.5% (v/v) dimethylformamide (DMF), 0.5% (v/v) Triton X-100, 1 mM EDTA (pH 8), 0.5 mM potassium ferricyanide (K3Fe(CN)6), 0.5% potassium ferrocyanide (K4Fe(CN)6), 500 mM phosphate buffer (pH 7)] and incubated at 37 °C for GUS staining, and finally washed in 500 mM phosphate buffer (pH 7). For microscopic analysis, samples were cleared with 90% lactic acid or as described previously (Malamy and Benfey, 1997). Samples were analyzed by differential interference contrast microscopy (Olympus BX53) and a stereomicroscope (Leica MZ16). For anatomical analysis (microtome transversal sectioning) of GUS-stained roots, stained samples were processed as described previously (De Smet et al., 2004).

**Real-time qRT-PCR analyses**

For the analysis of *CEP5* expression, RNA was extracted by first performing an RNA extraction with TRI Reagent® from Sigma-Aldrich according to the manufacturer's protocol, followed by an extra RNA extraction procedure with the Plant RNeasy Mini kit from Qiagen according to the manufacturer's protocol to further clean up the RNA. Next, 1 µg of total RNA was used for cDNA synthesis using the iScript cDNA synthesis kit from BIORAD according to the manufacturer's protocol. The real-time qRT-PCR reaction was carried out on the LightCycler 480 from Roche Applied Science with the LightCycler 480 SYBR Green I Master Mix from Roche Applied Science. The expression of *CEP5* (CCATGGACGAACCCTAAAAG and TGCCATCATCGTCTTGCTAT) was determined using at least three biological repeats and the reference genes *EEF-1α4* (CTGGAGGTTTTGAGGCTGGTAT and CCAAGGGTGAAAGCAAGAAGA) and *At2g32170* (GGACCTCTGTTGTATCATTTTGCG and CAACCCTCTTTACATCCTCCAAAC).

**SRM analysis of the CEP5 peptide**

For SRM experiments, the CEP5 peptide containing an isoleucine residue with heavy, stable isotopes, NH2-DFRP<hydroxy>TTP<hydroxy>GHSP<hydroxy>GI($^{13}C_6$ $^{15}N$)GH-COOH, was in-house synthesized by Fmoc (N-(9-fluorenyl)methoxycarbonyl) chemistry on a 433A peptide synthesizer (Applied Biosystems, Framingham, MA, USA). Frozen five-day-old *35S::CEP5* seedlings were ground to a fine powder in liquid N2 and proteins were extracted in 50 mM triethylammonium bicarbonate (TEAB) buffer containing 8 M urea and the suggested amounts of protease and phosphatase inhibitors according to the manufacturer's instructions (cOmplete protease inhibitor cocktail tablet and PhosStop phosphatase inhibitor cocktail tablet, Roche). After determining the protein concentration using the Bradford assay and diluting the protein extract twice with 50 mM TEAB buffer, a total of 500 µg of protein material was filtered over a 3 kDa cut-off filter (Pall Nanosep® centrifugal devices, Sigma-Aldrich) to retain only peptides with masses less than 3 kDa in the filtrate. This peptide mixture was spiked with 10 pmol of the synthetic heavy CEP5 peptide and vacuum dried. Next, the sample was re-dissolved in 2% acetonitrile (ACN) with 0.1% trifluoroacetic acid (TFA) and used for SRM analysis. SRM analysis was performed on an Ultimate 3000 RSLC nano HPLC system (Thermo Fisher scientific, Bremen, Germany) coupled to a TSQ Vantage (Thermo Fisher Scientific, Bremen, Germany). The nano-LC system was configured with a trapping column (made in-house, 100 µm internal diameter (I.D.) x 20 mm, 5 µm beads, C18 Reprosil-HD (Dr. Maisch, Ammerbuch-Entringen, Germany)) and an analytical column (made in-house, 75 µm I.D. x 150 mm, 3 µm beads, C18 Reprosil-HD (Dr. Maisch, Ammerbuch-Entringen, Germany)). The loading solvent consisted of 0.1% TFA in 2:98ACN:H2O, and the nano-LC was run with 0.1% formic acid as nano-LC solvent A and 0.1% formic acid in 80:20 ACN:H2O as nano-LC solvent B. The needle voltage in the nano-ESI source was set at 1300 V and the capillary temperature at 275°C. Of each sample, 5 µl was injected using a full loop injection. Injection was at 10 µl/min in loading solvent. After loading, the trapping column was flushed for 4 min in order to pre-concentrate the components while removing buffer components, before it was put in-line with the analytical column. Compounds were eluted at 300 nl/min with an ACN gradient of 30 min from 2% to 35% of nano-LC solvent B. The column was washed with 90% of nano-LC solvent B for 110 min and equilibrated with nano-LC solvent A for 9.5 min before analysis of the next sample. A dwell time of 120 ms for each transition was applied. Seven transitions were monitored for both the heavy and the light form of the CEP5 peptide with the doubly charged precursor as the first mass filter. Data analysis was performed through the Skyline software (MacLean et al., 2010).

## REFERENCES


Araya T, Miyamoto M, Wibowo J, Suzuki A, Kojima S, Tsuchiya YN, Sawa S, Fukuda H, von Wirén N, Takahashi H (2014) CLE-CLAVATA1 peptide-receptor signaling module regulates the expansion of plant root systems in a nitrogen-dependent manner. *Proc Natl Acad Sci U S A* **111**: 2029-2034.

Bergonci T, Ribeiro B, Ceciliato PH, Guerrero-Abad JC, Silva-Filho MC, Moura DS (2014) Arabidopsis thaliana RALF1 opposes brassinosteroid effects on root cell elongation and lateral root formation. *J Exp Bot* **65**: 2219-2230.

Bryan AC, Obaidi A, Wierzba M, Tax FE (2012) XYLEM INTERMIXED WITH PHLOEM1, a leucine-rich repeat receptor-like kinase required for stem growth and vascular development in Arabidopsis thaliana. *Planta* **235**: 111-122.

Cho H, Ryu H, Rho S, Hill K, Smith S, Audenaert D, Park J, Han S, Beeckman T, Bennett MJ, Hwang D, De Smet I, Hwang I (2014) A secreted peptide acts on BIN2-mediated phosphorylation of ARFs to potentiate auxin response during lateral root development. *Nat Cell Biol* **16**: 66-76.

Czyzewicz N, Shi C-L, Vu LD, Van De Cotte B, Hodgman C, Butenko MA, De Smet I (2015) Modulation of Arabidopsis and monocot root architecture by CLAVATA3/EMBRYO SURROUNDING REGION 26 peptide. *J Exp Bot* **66**: 5229-5243.

Czyzewicz N, Yue K, Beeckman T, De Smet I (2013) Message in a bottle: small signalling peptide outputs during growth and development. *J Exp Bot* **64**: 5281-5296.

De Rybel B, Audenaert D, Xuan W, Overvoorde P, Strader LC, Kepinski S, Hoye R, Brisbois R, Parizot B, Vanneste S, Liu X, Gilday A, Graham IA, Nguyen L, Jansen L, Njo MF, Inzé D, Bartel B, Beeckman T (2012) A role for the root cap in root branching revealed by the non-auxin probe naxillin. *Nat Chem Biol* **8**: 798-805.

De Smet I (2012) Lateral root initiation: one step at a time. *New Phytol* **193**: 867-873.

De Smet I, Chaerle P, Vanneste S, De Rycke R, Inze D, Beeckman T (2004) An easy and versatile embedding method for transverse sections. *J Microsc* **213**: 76-80.

De Smet I, Tetsumura T, De Rybel B, Frei dit Frey N, Laplaze L, Casimiro I, Swarup R, Naudts M, Vanneste S, Audenaert D, Inzé D, Bennett MJ, Beeckman T (2007) Auxin-dependent regulation of lateral root positioning in the basal meristem of Arabidopsis. *Development* **134**: 681-690.

De Smet I, Vanneste S, Inze D, Beeckman T (2006) Lateral root initiation or the birth of a new meristem. *Plant Mol Biol* **60**: 871-887.

De Smet I, Vassileva V, De Rybel B, Levesque MP, Grunewald W, Van Damme D, Van Noorden G, Naudts M, Van Isterdael G, De Clercq R, Wang JY, Meuli N, Vanneste S, Friml J, Hilson P, Jürgens G, Ingram GC, Inzé D, Benfey PN, Beeckman T (2008) Receptor-like kinase ACR4 restricts formative cell divisions in the Arabidopsis root. *Science* **322**: 594-597.

De Smet I, Voss U, Jurgens G, Beeckman T (2009) Receptor-like kinases shape the plant. *Nat Cell Biol* **11**: 1166-1173.

Delay C, Imin N, Djordjevic MA (2013) CEP genes regulate root and shoot development in response to environmental cues and are specific to seed plants. *J Exp Bot* **64**: 5383-5394.

Dubrovsky JG, Rost TL, Colon-Carmona A, Doerner P (2001) Early primordium morphogenesis during lateral root initiation in Arabidopsis thaliana. *Planta* **214**: 30-36.

Fernandez A, Drozdzecki A, Hoogewijs K, Nguyen A, Beeckman T, Madder A, Hilson P (2013) Transcriptional and functional classification of the GOLVEN/ROOT GROWTH FACTOR/CLE-like signaling peptides reveals their role in lateral root and hair formation. *Plant Physiol* **161**: 954-970.

Fernandez A, Drozdzecki A, Hoogewijs K, Vassileva V, Madder A, Beeckman T, Hilson P (2015) The GLV6/RGF8/CLEL2 peptide regulates early pericycle divisions during lateral root initiation. *J Exp Bot* **66**: 5245-5256.

Himanen K, Boucheron E, Vanneste S, de Almeida Engler J, Inze D, Beeckman T (2002) Auxin-mediated cell cycle activation during early lateral root initiation. *Plant Cell* **14**: 2339-2351.

Himanen K, Vuylsteke M, Vanneste S, Vercruysse S, Boucheron E, Alard P, Chriqui D, Van Montagu M, Inzé D, Beeckman T (2004) Transcript profiling of early lateral root initiation. *Proc Natl Acad Sci U S A* **101**: 5146-5151.

Huault E, Laffont C, Wen J, Mysore KS, Ratet P, Duc G, Frugier F (2014) Local and systemic regulation of plant root system architecture and symbiotic nodulation by a receptorlike kinase. *PLoS Genet* **10**: e1004891.

Kong X, Zhang M, De Smet I, Ding Z (2014) Designer crops: optimal root system architecture for nutrient acquisition. *Trends Biotechnol* **32:** 597-598.

Kumpf RP, Shi CL, Larrieu A, Sto IM, Butenko MA, Peret B, Riiser ES, Bennett MJ, Aalen RB (2013) Floral organ abscission peptide IDA and its HAE/HSL2 receptors control cell separation during lateral root emergence. *Proc Natl Acad Sci U S A* **110**: 5235-5240.

Kurup S, Runions J, Kohler U, Laplaze L, Hodge S, Haseloff J (2005) Marking cell lineages in living tissues. *Plant J* **42**: 444-453.

Lau S, Jurgens G, De Smet I (2008) The evolving complexity of the auxin pathway. *Plant Cell* **20**: 1738-1746.

Lavenus J, Goh T, Roberts I, Guyomarc'h S, Lucas M, De Smet I, Fukaki H, Beeckman T, Bennett M, Laplaze L (2013) Lateral root development in Arabidopsis: fifty shades of auxin. *Trends Plant Sci*. **8:** 450-45

MacLean B, Tomazela DM, Shulman N, Chambers M, Finney GL, Frewen B, Kern R, Tabb DL, Liebler DC, MacCoss MJ (2010) Skyline: an open source document editor for creating and analyzing targeted proteomics experiments. *Bioinformatics* **26**: 966-968.

Malamy JE, Benfey PN (1997) Organization and cell differentiation in lateral roots of Arabidopsis thaliana. *Development* **124**: 33-44.

Mohd-Radzman NA, Binos S, Truong TT, Imin N, Mariani M, Djordjevic MA (2015) Novel MtCEP1 peptides produced in vivo differentially regulate root development in Medicago truncatula. *J Exp Bot* **66:** 5289-5300.

Moreno-Risueno MA, Van Norman JM, Moreno A, Zhang J, Ahnert SE, Benfey PN (2010) Oscillating gene expression determines competence for periodic Arabidopsis root branching. *Science* **329**: 1306-1311.

Murphy E, Smith S, De Smet I (2012) Small signaling peptides in Arabidopsis development: how cells communicate over a short distance. *Plant Cell* **24**: 3198-3217.

Ohyama K, Ogawa M, Matsubayashi Y (2008) Identification of a biologically active, small, secreted peptide in Arabidopsis by in silico gene screening, followed by LC-MS-based structure analysis. *Plant J* **55**: 152-160.

Overvoorde P, Fukaki H, Beeckman T (2010) Auxin control of root development. *Cold Spring Harb Perspect Biol* **2**: a001537.

Péret B, De Rybel B, Casimiro I, Benková E, Swarup R, Laplaze L, Beeckman T, Bennett MJ (2009) Arabidopsis lateral root development: an emerging story. *Trends Plant Sci* **14**: 399-408.

Péret B, Li G, Zhao J, Band LR, Voß U, Postaire O, Luu DT, Da Ines O, Casimiro I, Lucas M, Wells DM, Lazzerini L, Nacry P, King JR, Jensen OE, Schäffner AR, Maurel C, Bennett MJ (2012) Auxin regulates aquaporin function to facilitate lateral root emergence. *Nat Cell Biol* **14**: 991-998.

Picotti P, Aebersold R (2012) Selected reaction monitoring-based proteomics: workflows, potential, pitfalls and future directions. *Nat Methods* **9**: 555-566.

Roberts I, Smith S, De Rybel B, Van Den Broeke J, Smet W, De Cokere S, Mispelaere M, De Smet I, Beeckman T (2013) The CEP Family in Land Plants: Evolutionary Analyses, Expression studies and Role in Arabidopsis Shoot Development *J Exp Bot*. **64**: 5371-5381

Satbhai SB, Ristova D, Busch W (2015) Underground tuning: quantitative regulation of root growth. *J Exp Bot* **66**: 1099-1112.

Schindelin J, Arganda-Carreras I, Frise E, Kaynig V, Longair M, Pietzsch T, Preibisch S, Rueden C, Saalfeld S, Schmid B, Tinevez JY, White DJ, Hartenstein V, Eliceiri K, Tomancak P, Cardona A (2012) Fiji: an open-source platform for biological-image analysis. *Nat Methods* **9**: 676-682.

Smith S, De Smet I (2012) Root system architecture: insights from Arabidopsis and cereal crops. *Philos Trans R Soc Lond B Biol Sci* **367**: 1441-1452.

Tabata R, Sumida K, Yoshii T, Ohyama K, Shinohara H, Matsubayashi Y (2014) Perception of root-derived peptides by shoot LRR-RKs mediates systemic N-demand signaling. *Science* **346**: 343-346.

Tian H, De Smet I, Ding Z (2014) Shaping a root system: regulating lateral versus primary root growth. *Trends Plant Sci* **19**: 426-431.

Van Norman JM, Xuan W, Beeckman T, Benfey PN (2013) To branch or not to branch: the role of pre-patterning in lateral root formation. *Development* **140**: 4301-4310.

Vanneste S, De Rybel B, Beemster GT, Ljung K, De Smet I, Van Isterdael G, Naudts M, Iida R, Gruissem W, Tasaka M, Inzé D, Fukaki H, Beeckman T (2005) Cell cycle progression in the pericycle is not sufficient for SOLITARY ROOT/IAA14-mediated lateral root initiation in Arabidopsis thaliana. *Plant Cell* **17**: 3035-3050.

Vanneste S, Friml J (2009) Auxin: a trigger for change in plant development. *Cell* **136**: 1005-1016.

Wierzba MP, Tax FE (2013.) Notes from the underground: receptor-like kinases in Arabidopsis root development. *J Integr Plant Biol* **55**: 1224-1237.

Winter D, Vinegar B, Nahal H, Ammar R, Wilson GV, Provart NJ (2007) An "Electronic Fluorescent Pictograph" browser for exploring and analyzing large-scale biological data sets. *PLoS One* **2**: e718.

Xuan W, Audenaert D, Parizot B, Möller BK, Njo MF, De Rybel B, De Rop G, Van Isterdael G, Mähönen AP, Vanneste S, Beeckman T (2015) Root Cap-Derived Auxin Pre-patterns the Longitudinal Axis of the Arabidopsis Root. *Current Biology* **25**: 1381-1388.

Xuan W, Band LR, Kumpf RP, Van Damme D, Parizot B, De Rop G, Opdenacker D, Möller BK, Skorzinski N, Njo MF, De Rybel B, Audenaert D, Nowack MK, Vanneste S, Beeckman T (2016) Cyclic programmed cell death stimulates hormone signaling and root development in Arabidopsis. *Science* **351**: 384-387.

## SUPPLEMENTAL FIGURES

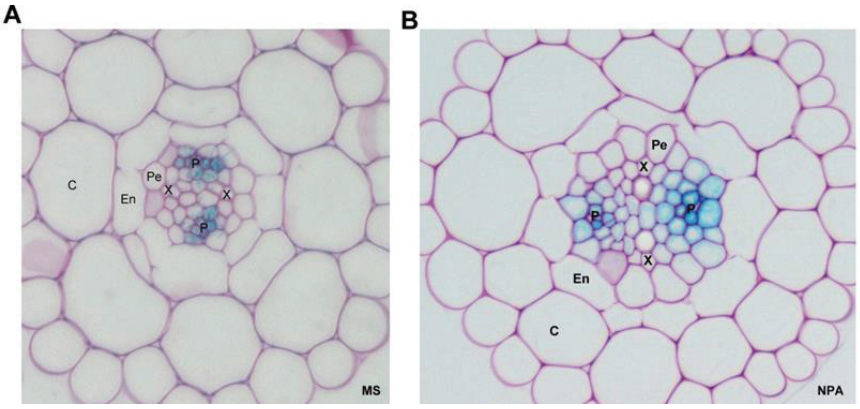


**Figure S1. *CEP5* expression on transverse sections in the root.** Representative image of *CEP5* expression (monitored through *GUS* expression in a *pCEP5::NLS:GFP:GUS* transgenic line) on a transverse section through **(A)** a mature part of a 5-7 day-old seedling root grown on ½ MS growth medium, and **(B)** a 5 day old seedling grown on ½ MS growth medium supplemented with 10 µM NPA. (P, phloem; X, xylem; Pe, pericycle; En, endodermis; C, cortex).

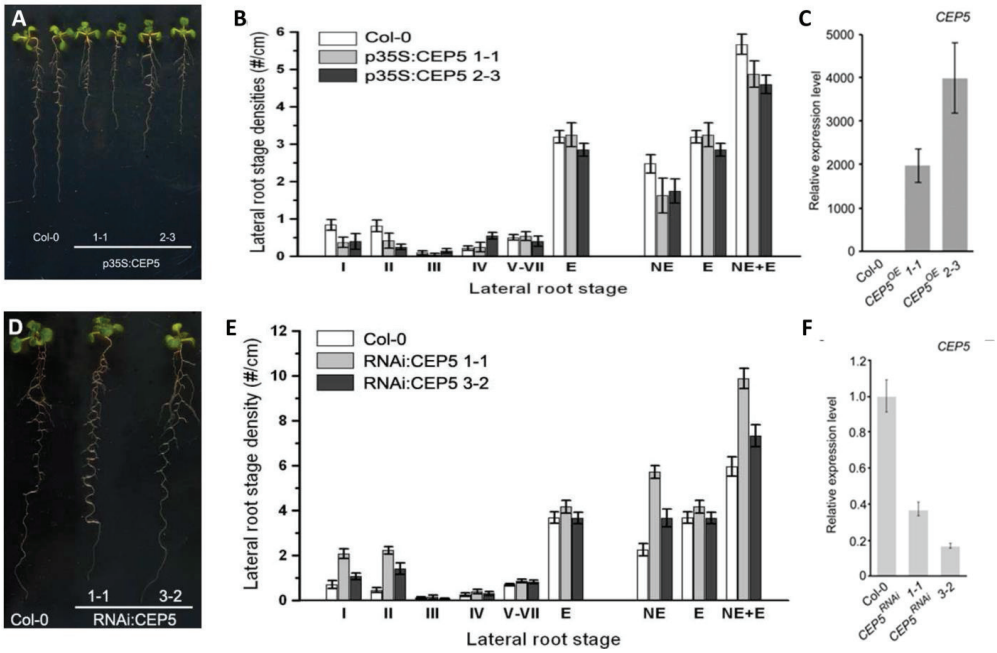


**Figure S2. Analyses of additional *CEP5*$^{OE}$ (A-C) and *CEP5*$^{RNAi}$ (D-F) lines.** Representative seedlings illustrating the reduced primary root length phenotype **(A)** and reduced lateral root initiation phenotype, (n = 6-8) at 7 days after germination **(B)** in independent *CEP5*$^{OE}$ lines with relative *CEP5* expression levels, as determined by real-time qRT-PCR compared to Col-0 control, shown in **(C).** Representative seedlings illustrating the mild impact on primary root length **(D)** and increased lateral root initiation phenotype, (n = 6-8) at 7 days after germination **(E)** in independent *CEP5*$^{RNAi}$ lines with relative *CEP5* expression levels, as determined by real-time qRT-PCR compared to Col-0 control, shown in **(F).** Graphs indicate average ± SE.

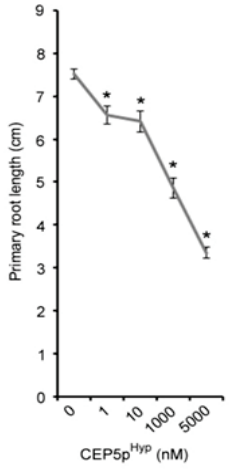


**Figure S3. Bioactivity of CEP5p$^{Hyp}$ at different concentrations (ranging from 1 nM to 5 µM) in the primary root length assay on Col-0 seedlings**, 12 days after germination (n ≥ 16 per condition). *, $p < 0.05$ according to Student's *t*-test compared to mock (medium with water as used to dissolve CEP5p).

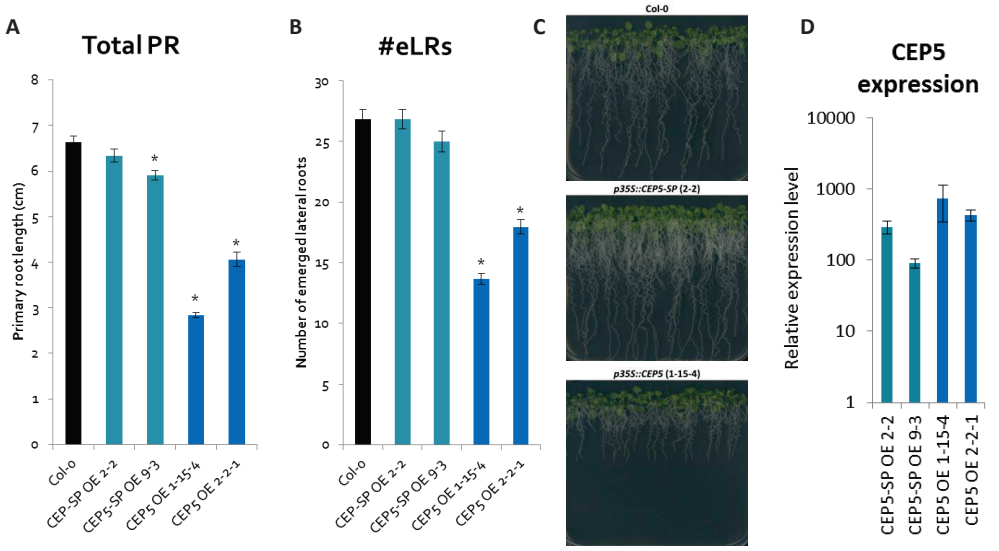


**Figure S4. The CEP5 peptide needs to go through the secretion pathway to become activated. (A)** Total primary root (PR) length and **(B)** number of emerged lateral roots (#eLRs) of two *CEP5* overexpression lines (*CEP5*$^{OE}$ 1-15-4 and 2-2-1) and two overexpression lines of the *CEP5* coding sequence without the N-terminal signal peptide (SP) (*CEP5-SP*$^{OE}$ 2-2 and 9-3) compared to Col-0 control, 10 days after germination. **(C)** Representative image of the same seedlings 13 days after germination. **(D)** Relative expression level of CEP5 in the overexpression lines compared to Col-0 control. Graphs show average ± SE; * $p < 0.05$ according to Student's *t*-test.

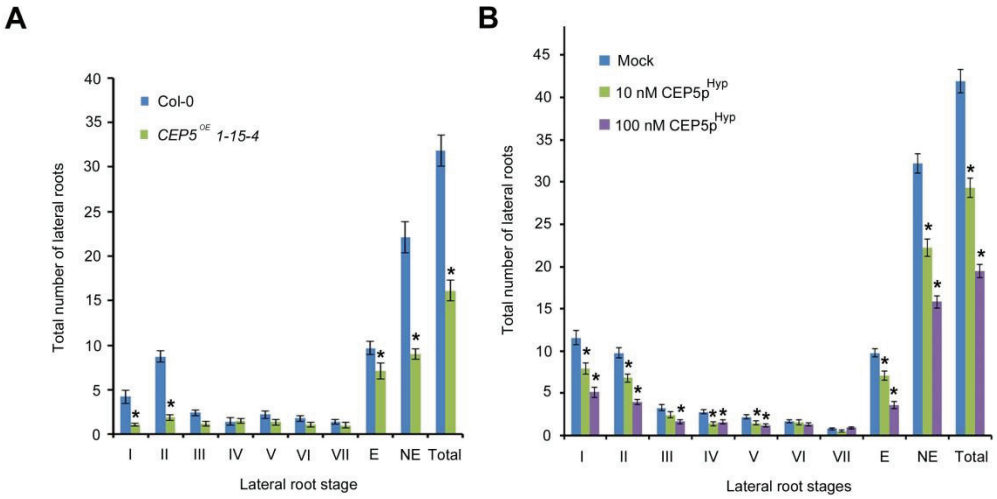


**Figure S5. Total number of lateral root primordia and emerged lateral roots** in **(A)** the CEP5$^{OE}$ line compared to Col-0 (n ≥ 15) at 7 days after germination, and **(B)** CEP5p$^{Hyp}$ treatment compared to mock treatment with indicated concentrations at 9 days after germination (data from newly grown root part of 5 day old seedlings transferred to CEP5pHyp for 4 days, n≥ 32). Mock refers to medium with water as used to dissolve CEP5p. Lateral root stages I to VII according to (Malamy and Benfey, 1997); E = emerged lateral roots; NE = non-emerged lateral roots; Total = E + NE. Graphs show average ± standard error. *, $p < 0.05$ according to Student's *t*-test compared to Col-0 or mock.

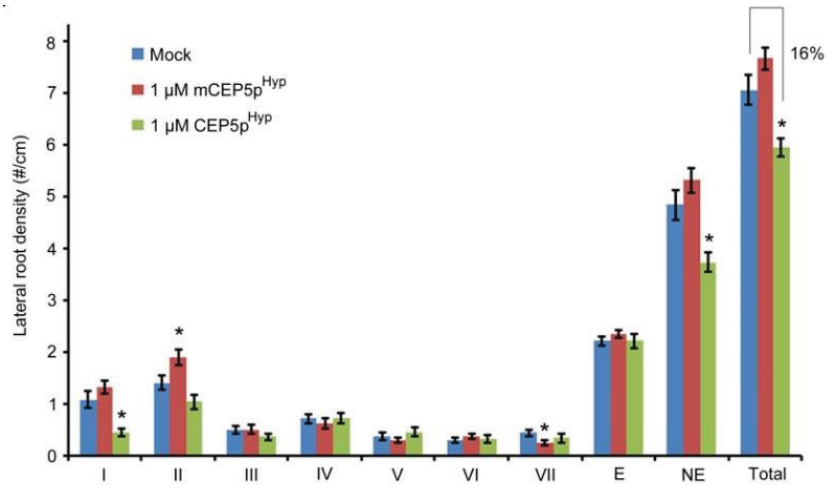


**Figure S6. Lateral root density of Col-0 seedlings treated with 1 µM CEP5p$^{Hyp}$ or mCEP5p$^{Hyp}$ compared to mock,** at 9 days after germination (data from newly grown root part of 5 day old seedlings transferred to (m)CEP5p$^{Hyp}$ for 4 days, n ≥ 23). The % reduction in total lateral root density is indicated. Mock refers to medium with water as used to dissolve CEP5p. Lateral root stages I to VII according to (Malamy and Benfey, 1997); E = emerged lateral roots; NE = non-emerged lateral roots; Total = E + NE. Graph shows average ± standard error. *, $p < 0.05$ according to Student's *t*-test compared to mock.

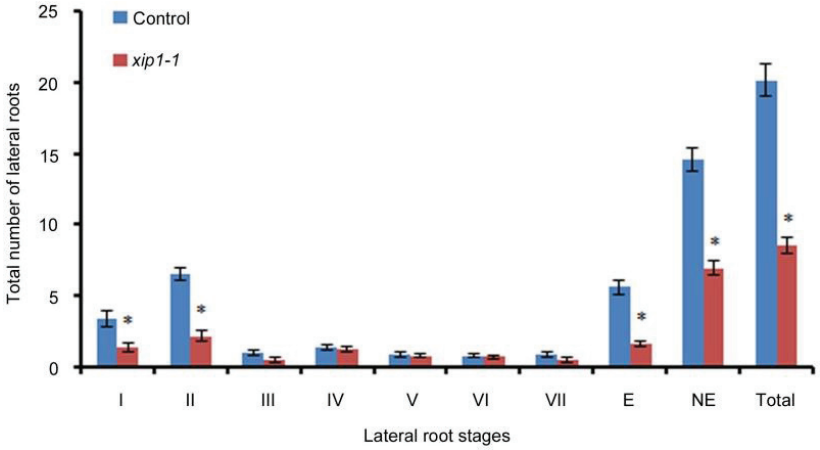


**Figure S7. Number of lateral root primordia and emerged lateral roots in *xip1-1* compared to Col-0,** at 5 days after germination (n ≥ 14)**.** Lateral root stages I to VII according to (Malamy and Benfey, 1997); E = emerged lateral roots; NE = non-emerged lateral roots; Total = E + NE. Graph shows average ± SE. *, $p < 0.05$ according to Student's *t*-test compared to Col-0.

# Chapter 6:

## The small signaling peptide CEP5 attenuates the dynamic AUX/IAA equilibrium

**Contributions:**

S.S. and I.R. conducted most of the experimental work: S.S. performed results in fig2, fig4 and figS1, I.R. performed results in fig1C-D, fig3E and fig5C., B.D.R. initiated experimental work, W.X. performed results in fig1E-F, B.V.D.C. performed results in fig1B, fig3D and fig5D-E, and E.S., H.C., A.L., L.D.V., B.G., J.M.G., A.R., S.R.H., G.K.K., J.L., E.V. performed remaining results fig1A, fig3A-C and fig5A,B,F,G. Experimental design and data analysis was mainly performed by S.S., I.R., T.B. and I.D.S., with additional contributions of S.V., L.M., Y.S., D.A., J.F., G.F., R.S., M.J.B., A.B., K.L., S.K., S.R., J.N., I.H., K.G. The research was mainly supervised by T.B. and I.D.S.. The manuscript was written by I.D.S., with contributions from I.R., S.S. E.S. and T.B..

This chapter is in preparation for submitting to The Plant Cell.

# The small signalling peptide CEP5 attenuates the dynamic AUX/IAA equilibrium

Stephanie Smith[c,1], Ianto Roberts[a,b,1], Bert De Rybel[a,b], Wei Xuan[a,b], Elisabeth Stes[a,b,d,e], Hyunwoo Cho[f], Antoine Larrieu[g,2], Lam Dai Vu[a,b,d,e], Benjamin Goodall[g], Brigitte Van De Cotte[a,b], Jessica Marie Guseman[h], Adeline Rigal[i], Sigurd R. Harborough[j], Steffen Vanneste[a,b], Gwendolyn K. Kirschner[k], Julien Lavenus[a,b,3], Elien Vandermarliere[d,e], Lennart Martens[d,e], Yvonne Stahl[k], Dominique Audenaert[a,b], Jiří Friml[a,b,l,m], Georg Felix[n], Rüdiger Simon[k], Malcolm J. Bennett[c,g], Anthony Bishopp[g], Karin Ljung[i], Stefan Kepinski[j], Stéphanie Robert[i], Jennifer Nemhauser[h], Ildoo Hwang[f], Kris Gevaert[d,e], Tom Beeckman[a,b], and Ive De Smet[a,b,c,g]

[a]Department of Plant Systems Biology, VIB, B-9052 Ghent, Belgium
[b]Department of Plant Biotechnology and Genetics, Ghent University, B-9052 Ghent, Belgium
[c]Division of Plant and Crop Sciences, School of Biosciences, University of Nottingham, Loughborough LE12 5RD, United Kingdom
[d]Department of Medical Protein Research, VIB, B-9000 Ghent, Belgium
[e]Department of Biochemistry, Ghent University, B-9000 Ghent, Belgium
[f]Department of Life Sciences, POSTECH Biotech Center, Pohang University of Science and Technology, Pohang 790-784, Korea
[g]Centre for Plant Integrative Biology, University of Nottingham, Loughborough LE12 5RD, United Kingdom
[h]Department of Biology, University of Washington, Seattle, WA 98195-1800, USA
[i]Umeå Plant Science Centre, Department of Forest Genetics and Plant Physiology, Swedish University of Agricultural Sciences, SE-901 83 Umeå, Sweden
[j]Centre for Plant Sciences, Faculty of Biological Sciences, University of Leeds, Leeds LS2 9JT, UK
[k]Institute for Developmental Genetics, Heinrich-Heine University, D-40225 Düsseldorf, Germany
[l]Mendel Centre for Plant Genomics and Proteomics, Central European Institute of Technology (CEITEC), Masaryk University (MU), Brno, CZ-625 00 Czech Republic
[m]Institute of Science and Technology Austria (IST Austria), 3400 Klosterneuburg, Austria
[n]Zentrum für Molekularbiologie der Pflanzen, Plant Biochemistry, University Tübingen, 72076 Tübingen, Germany

[1]Equal contribution
[2]Current address: Laboratoire de Reproduction et Développement des Plantes, CNRS, INRA, ENS Lyon, UCBL, Université de Lyon, 69364 Lyon, France
[3]Current address: Institute of Plant Sciences, University of Bern, Alterbergrain 21, 3013 Bern, Switzerland

## ABSTRACT

C-TERMINALLY ENCODED PEPTIDE (CEP) family peptides were shown to regulate various aspects of root architecture, including nitrate-dependent lateral root elongation. Specifically, CEPs impact on the expression of nitrate transporters and appear to signal via XIP1/CEPR1 and CEPR2. However, the (immediate) downstream mechanism remained largely elusive and other potential mechanisms have not been explored. Here, our genetic, biochemical and pharmacological results show that C-TERMINALLY ENCODED PEPTIDE 5 (CEP5) counteracts auxin signalling by stabilizing AUXIN/INDOLE ACETIC ACID INDUCIBLE (AUX/IAA) transcriptional repressors, suggesting the existence of an additional control mechanism through which plants can attenuate auxin signalling in a developmental context.

**Key words:** CEP5, Arabidopsis, root, auxin, AUX/IAA, post-translationally modified peptide

## INTRODUCTION

The phytohormone auxin regulates many plant growth and developmental processes and is prominently involved in lateral root development (Lau *et al.*, 2008; Vanneste and Friml, 2009; Lavenus *et al.*, 2013). To generate different auxin-mediated developmental outputs, a complex signalling mechanism involving spatio-temporal expression of *ARFs* and *AUX/IAAs*, variation in auxin sensitivity of AUX/IAA−TIR1/AFB co-receptor complexes, and phospho-regulation of ARF-AUX/IAA interactions is required (Delker *et al.*, 2010; Del Bianco and Kepinski, 2011; Calderon Villalobos *et al.*, 2012a; Cho *et al.*, 2014). However, fine-tuning temporal and spatial developmental responses at the protein level most likely requires additional mechanisms to the ones described above. For example, small signalling peptides are important in cell-cell communication to coordinate and integrate cellular functions (Murphy *et al.*, 2012) and the TRACHEARY ELEMENT DIFFERENTIATION INHIBITORY FACTOR (TDIF) − TDIF RECEPTOR (TDR) − BRASSINOSTEROID-INSENSITIVE2 (BIN2) signalling cascade can interfere with ARF − AUX/IAA interactions (Cho *et al.*, 2014).

We recently demonstrated that *C-TERMINALLY ENCODED PEPTIDE 5* (*CEP5,* At5g66815) plays a key role in the auxin-mediated process of lateral root initiation (Roberts *et al.*, 2016). Notwithstanding CEP peptides were shown to impact the expression of nitrate transporters and to signal via XIP1/CEPR1 and CEPR2 (Tabata *et al.*, 2014), the (immediate) downstream effects of CEP5 have not been explored extensively. Interestingly, CEP5 gain-of-function phenotypes with respect to lateral root positioning and patterning (Roberts *et al.*, 2016) are similar to what was observed with altered MONOPTEROS (MP)/ARF5 or BODENLOS (BDL)/IAA12 activity (De Smet *et al.*, 2010), and suggest that auxin-dependent lateral root patterning was disturbed. Here, we demonstrated that CEP5-dependent signalling leads to stabilization of AUX/IAA transcriptional repressors, arguing for the existence of a novel peptide-dependent mechanism contributing to fine-tuning of auxin signalling.

## RESULTS

Given the connection with auxin biology through the effect of CEP5 on primary root growth and lateral root development [both representing auxin-mediated processes (Lavenus *et al.*, 2013; Overvoorde *et al.*, 2010) and *CEP5* expression analyses (Roberts *et al.*, 2016), we assessed if the CEP5 peptide affected auxin response more directly. To facilitate these mode-of-action studies, we predominantly used available gain-of-function tools, namely a $CEP5^{OE}$ line and the synthetic $CEP5p^{Hyp}$ (Roberts *et al.*, 2016), in combination with well-established read-outs for auxin response. It should be noted that while the below analyses are experimental read-outs for (perturbed) auxin response, the gain-of-function data do not necessarily indicate a specific role for CEP5 in these processes.

### CEP5 affects auxin-responsive growth and development

To assess to what extent CEP5 interferes with auxin-responsive growth and development, we followed $CEP5p^{Hyp}$-treated seedlings after a root-gravistimulus and observed a slower auxin-dependent gravitropism-induced bending response of primary root tips relative to the untreated control (**Figure 1A**). Since, in our hands, $CEP5p^{Hyp}$ usually only has a primary root growth effect upon prolonged exposure, we reasoned that the impact on gravitropic response is not due to general primary root growth inhibition. In addition, we observed that longer exposure to 250 nM auxin results in yellowing of wild type seedlings, while $CEP5^{OE}$ seedlings remain healthy and green (**Figure 1B**). Thus, CEP5 appears to interfere with auxin-mediated growth and development.

**CEP5 affects transcriptional auxin response**

To evaluate to what extent CEP5 affects transcriptional auxin response, we made use of available *DR5*-based markers (Moreno-Risueno *et al.*, 2010; Ulmasov *et al.*, 1997). We observed reduced activity of the auxin response marker *pDR5::GUS* in the root tip and in the basal meristem following CEP5p$^{Hyp}$ treatment and in the *CEP5*$^{OE}$ line (**Figure 1C-F**). In this context, the earliest known event associated with lateral root initiation occurs in the basal meristem, where also *CEP5* is expressed (Roberts *et al.*, 2016), and can be monitored *in vivo* through the oscillating expression of *pDR5::LUC* (De Smet *et al.*, 2007; Moreno-Risueno *et al.*, 2010). Under our control conditions, transcriptional auxin-response oscillations visualised through *pDR5::LUC* occur with an average period of 3.67 ± 0.78 hours (Xuan *et al.*, 2015), but CEP5p$^{Hyp}$-treated seedlings displayed an increased average period (4.51 ± 1.74 hours) and a disturbed peak distribution (**Figure 1E and Supplementary Movies 2 and 3**). In addition, the overall average intensity of the LUCIFERASE signal was severely reduced in the root (**Figure 1F and Supplementary Movies 2 and 3**), supporting our observations with *pDR5::GUS*. In conclusion, CEP5 affects auxin-responsive gene expression in the root.

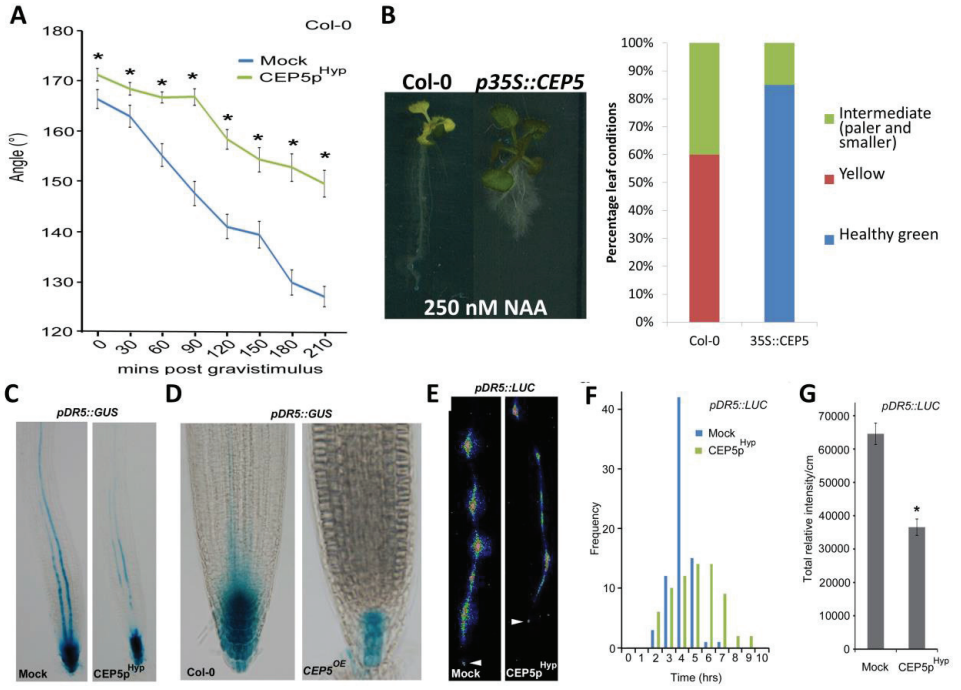


**Figure 1. Effect of CEP5 on auxin response processes. (A)** Angle of gravistimulated mock (n = 24) or 5 µM CEP5p$^{Hyp}$-treated Col-0 roots (n = 28) at indicated minutes post gravistimulus. Graphs show average ± standard error. **(B)** Col-0 versus *CEP5*$^{OE}$ compared for the effect on leaf conditions (healthy green, intermediate or yellow leaves) after growth on 250 nM NAA **(C)** *pDR5::GUS* activity in the primary root tip of 5-day old seedlings transferred to mock (left) or 1 µM CEP5p$^{Hyp}$ (right) for 4 days **(D)** or in the root tip of *CEP5*$^{OE}$ compared to Col-0 at 7 days after germination. **(E)** *pDR5::LUC* in the root of 3-day old seedlings treated with mock (left) or CEP5p$^{Hyp}$ (right). Arrowhead indicates root tip. **(F)** *pDR5::LUC* peak distribution in the oscillation zone following mock (blue) or 1 µM CEP5p$^{Hyp}$ treatment (green) (n ≥ 14). **(G)** Total relative LUC activity/cm in *pDR5::LUC* following 1 µM CEP5p$^{Hyp}$ treatment (e). The % reduction is indicated in (a). *, $p < 0.05$ according to Student's *t*-test compared to 0 nM NAA (a), or mock (b and g). In all cases, mock refers to medium with water as used to dissolve CEP5p.

**CEP5 leads to increased DII:VENUS levels**

Transcriptional responses to auxin depend principally on the auxin-activated SKP1–CUL1/CDC53–F-BOX (SCF)$^{TIR1/AFB}$-dependent degradation of AUX/IAAs (Lau *et al.*, 2008). Activity level of the SCF$^{TIR1/AFB}$ complex and/or auxin concentration can be inferred from the decrease in DII:VENUS fluorescence levels (Band *et al.*, 2012; Brunoud *et al.*, 2012). In the presence of CEP5p$^{Hyp}$ and in a *CEP5*$^{OE}$ line, DII:VENUS fluorescence was significantly increased compared to the control, and this was not caused by an equally strong transcriptional up-regulation of *DII:VENUS* expression (**Figure 2A-B and Supplemental Figure 1**). In comparison, the related CEP1p$^{Hyp}$ only had a minor, not significant impact on DII:VENUS fluorescence (**Supplemental Figure 1**). In contrast, the *CEP5*$^{RNAi}$ line displayed significantly lower DII:VENUS levels than the control (**Figure 2C**), which was not caused by an equally strong transcriptional down-regulation of *DII:VENUS* expression (**Supplemental Figure 1**). Moreover, for CEP5p$^{Hyp}$, a stabilization of DII:VENUS was already observed within 60 minutes, while for mock or mCEP5p$^{Hyp}$-treated seedlings a gradual decrease in DII:VENUS signal was observed (**Figure 2D**). The above results suggested that CEP5 (quickly) affects DII:VENUS levels, either directly through interfering with signalling components or indirectly through affecting (free) auxin levels and/or auxin distribution patterns.

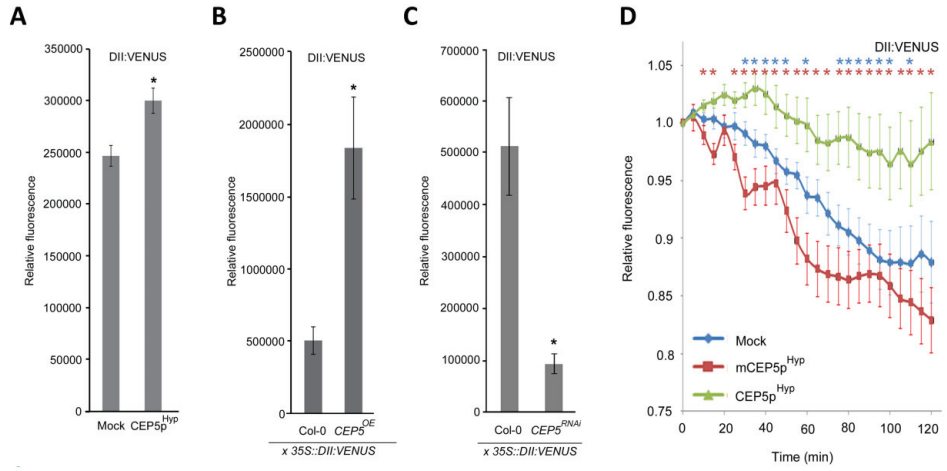


**Figure 2. Effect of CEP5 on AUX/IAA stability. (A)** Relative DII:VENUS protein fluorescence in *35S::DII:VENUS* reporter line following 18 hrs incubation with 5 µM CEP5p$^{Hyp}$ compared with mock treatment at 5-6 days after germination (n ≥ 83), and **(B-C)** in Col-0, a *CEP5*$^{OE}$ line and a *CEP5*$^{RNAi}$ line at 5-6 days after germination (n ≥ 15). **(D)** DII:VENUS levels upon treatment with CEP5p$^{Hyp}$, mCEP5p$^{Hyp}$ or mock for 120 minutes. *, $p < 0.05$ according to Student's *t*-test compared to mock (blue) or mCEP5p$^{Hyp}$ (red). All graphs show average ± standard error. With respect to mock versus mCEP5p$^{Hyp}$ (in D) there was – apart from 15, 30 and 55 min ($p < 0.05$) – no global significant different. *Note*: no auxin was used in this experiment (D).

**CEP5 does not affect auxin levels or auxin transport**

Since auxin response and DII:VENUS levels are intimately correlated with auxin levels, it is possible that increased or decreased CEP5 levels lead to lower or higher auxin levels, respectively, which in turn would result in decreased or increased auxin response. To investigate this, we compared auxin levels in wild-type, *CEP5*$^{OE}$ and *CEP5*$^{RNAi}$, but this revealed no striking differences in free auxin (IAA, indole-3-acetic acid) content (**Figure 3A**). We can however not exclude that our analysis missed local and/or more subtle changes in auxin levels.

Next, we wanted to exclude that CEP5 affects auxin uptake and/or transport and consequently (local) auxin accumulation. We therefore tested sensitivity to CEP5 of the *pin-formed 2* (*pin2*) auxin efflux and *auxin 1* (*aux1*) influx carrier mutants. Both *aux1* and *pin2* displayed similar sensitivity to CEP5p$^{Hyp}$ application compared to the wild type in the primary root growth assay (**Figure 3B-C)**. Furthermore, since CEP1 was shown to affect *NITRATE TRANSPORTER* (*NRT*) expression levels (Tabata *et al.*, 2014) and since NRT1.1/CHLORINA1 (CHL1) not only transports nitrate but also facilitates uptake of auxin (Krouk *et al.*, 2010), we evaluated this in the context of CEP5. While *NRT* expression levels are indeed up-regulated in *CEP5*$^{OE}$ (**Figure 3D**), we did not observe any obvious insensitivity of *chl1-5* (a knockout mutant for *NRT1.1*) (Tsay *et al.*, 1993) to CEP5p$^{Hyp}$ in our primary root growth assay (**Figure 3E)**. Taken together, these observations suggest that CEP5 is likely not directly affecting auxin transport and that NRT1.1 is not directly involved in the CEP5-dependent regulation of auxin response.

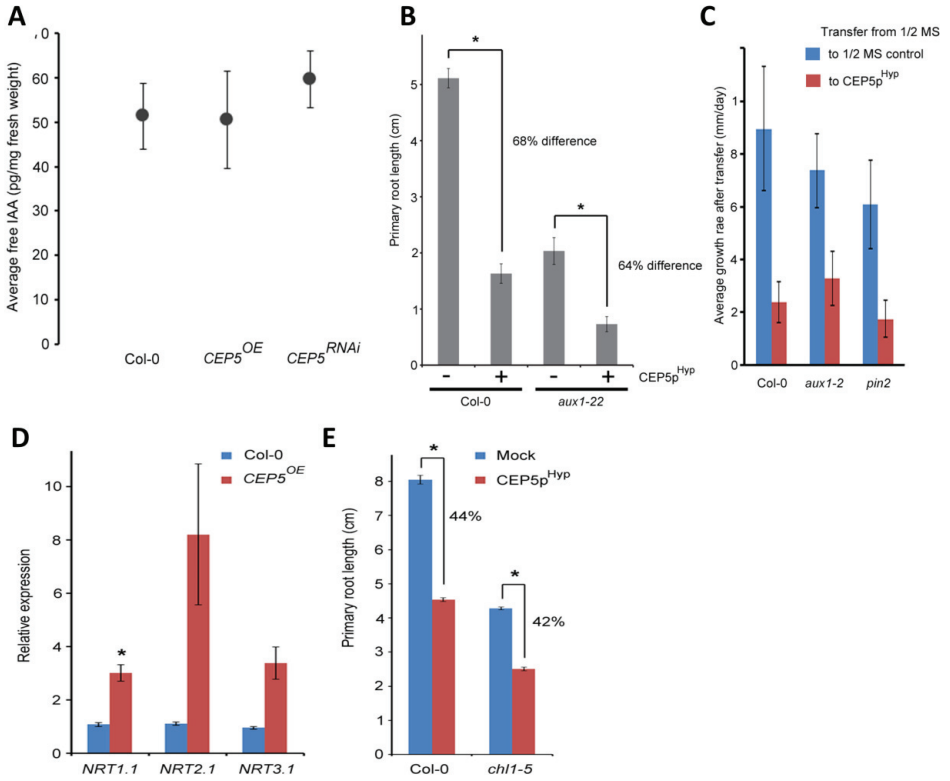


**Figure 3. (a)** Free IAA levels in Col-0, *CEP5*$^{OE}$ and *CEP5*$^{RNAi}$ seedlings at 10 days after germination. No significant differences were observed according to Student's *t*-test ($p > 0.4$). n = 4-5 (complete seedlings used). **(b)** Primary root length in *aux1-22* mutant compared to Col-0 grown in the presence or absence of 1 µM CEP5p$^{Hyp}$ (7 days after germination). The relative reduction in primary root length on ½ MS medium supplemented with 1 µM CEP5p$^{Hyp}$ compared to ½ MS control medium is indicated. **(c)** Average growth rate of the primary root after transfer from ½ MS control medium to ½ MS medium compared to ½ MS medium supplemented with 1 µM CEP5p$^{Hyp}$. **(d)** *NRT* expression as determined by qPCR in Col-0 and *CEP5*$^{OE}$ seedling roots at 5 days after germination. *, $p < 0.05$ according to Student's *t*-test compared to Col-0. **(e)** Primary root length of Col-0 and *chl1-5* (an *NRT1* mutant allele) grown on medium containing mock (with water as used to dissolve CEP5p$^{Hyp}$) or 1 µM CEP5p$^{Hyp}$ at 10 days after germination (n ≥ 9). *, $p < 0.05$ according to Student's *t*-test compared to mock. The % reduction in total lateral root density is indicated. All graphs show average ± standard error.

**CEP5 affects auxin-mediated degradation of DII:VENUS**

To assess if CEP5 can also interfere with auxin-mediated degradation of DII:VENUS, we co-incubated auxin (IAA or NAA) with CEP5p$^{Hyp}$. This resulted in a significant delay of DII:VENUS degradation compared to auxin alone, while mCEP5p$^{Hyp}$ did not affect DII:VENUS degradation (**Figure 4**). These results suggest that CEP5 counteracts auxin activity. Given the similar effect of CEP5 on IAA and NAA-induced DII-VENUS degradation (two auxins with different transport properties), this further supports that CEP5 probably has no direct effect on auxin uptake and/or transport (see above).

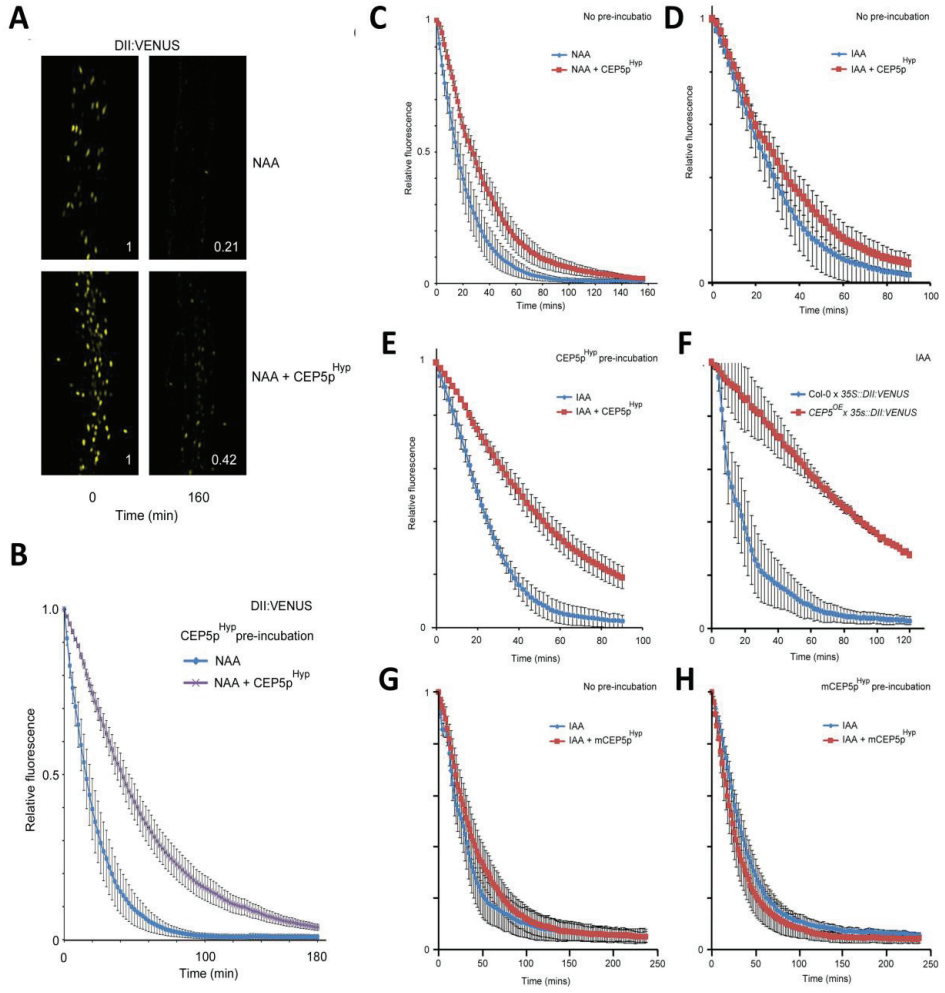


**Figure 4. (A)** Confocal image of DII:VENUS labelled nuclei from the *35S::DII:VENUS* reporter line in a section of the root that was used for measuring the DII:VENUS protein fluorescence in seedlings treated for 160 minutes (with 1 µM NAA (top) and co-treated with 5 µM CEP5p$^{Hyp}$ (bottom) (n ≥ 4). **(B)** DII:VENUS fluorescence level over time (0-180 min) after transfer to 1 µM NAA, with or without pre-incubation and co-incubation with 5 µM CEP5p$^{Hyp}$. Normalized ratio of average top 500 pixel intensity, compared to 0 min, is indicated. Graph shows average ± standard error. **(C-H)** DII:VENUS fluorescence for indicated treatments (5 µM CEP5p$^{Hyp}$, 5 µM mCEP5$^{pHyp}$, 1 µM IAA or 1 µM NAA) and in Col-0 (C, D, E, G, H) or *CEP5$^{OE}$* background (F). Pre-incubation was for 18 hrs. All graphs show average ± standard error of 10 biological replicates.

**CEP5 directly leads to stabilization of AUX/IAAs**

To validate that CEP5 also affects full length AUX/IAAs, we analysed plants expressing *IAA19:HA* (Cho *et al.*, 2014) and *pBODENLOS(BDL)::BDL:GUS* (Weijers *et al.*, 2006). Indeed, CEP5p$^{Hyp}$-treatment of these seedlings resulted in a quick stabilization or accumulation of IAA19:HA or BDL:GUS compared to mock or mCEP5p$^{Hyp}$ treatment as revealed by western blot analysis or GUS staining, respectively **(Figure 5A-C)**. Interestingly, accumulation of more stable BDL in gain-of-function *bdl* plants results in similar lateral root phenotypes as observed for increased CEP5p levels (De Smet *et al.*, 2010; Roberts *et al.*, 2016), further supporting that CEP5p affects AUX/IAA levels and disturbs auxin-dependent growth and development.

To rule out that CEP5 leads to increased AUX/IAA levels by transcriptional up-regulation and/or down-regulation of *AUX/IAAs* and/or *TIR1/AFBs,* respectively, we checked their expression levels in a *CEP5$^{OE}$* line or in CEP5p-treated seedlings. This revealed no obvious effect on *IAA12* and *IAA18* expression in CEP5p$^{Hyp}$-treated seedlings compared to the control, and actually revealed a small increase in *TIR1* and *AFB2* to *AFB5* expression levels in *CEP5$^{OE}$* roots **(Figure 5D-E)**.

To subsequently assess if CEP5 affects the degradation of AUX/IAAs via interference with the activity of the SCF$^{TIR1/AFB}$ complex *in planta*, we analysed the effect of CEP5 on the *auxin resistant 1* (*axr1*) and *tir1/afb* loss-of-function mutants. AXR1 encodes a subunit of a heterodimeric RUB-activating enzyme essential for the activation of the TIR1/AFB F-BOX proteins that function as an auxin receptor (Calderon Villalobos *et al.*, 2012b; Dharmasiri *et al.*, 2005; Tan *et al.*, 2007). Both *axr1-30* and *tir1-1 afb1-5 afb2-5* are less sensitive to CEP5p$^{Hyp}$ treatment in a primary root growth assay, suggesting that a functional SCF$^{TIR1/AFB}$ complex is – at least partially – involved in mediating CEP5 activity **(Figures 5F)**.

To further confirm this observation and to explore how CEP5 affects AUX/IAA stability, we used a yeast system engineered to monitor auxin-induced degradation of plant AUX/IAA proteins through fluorescence of YELLOW FLUORESCENT PROTEIN (YFP)-AUX/IAA fusion proteins (Havens *et al.*, 2012). For this, we integrated the wild type (*CEP5$^{Pro}$*) and mutant CEP5 15 amino acid mature peptide sequence (*mCEP5$^{Pro}$*) (**Figure 5G**) into the yeast genome under a β-estradiol-inducible promoter. It should be noted that CEP5p$^{Pro}$ and CEP5p$^{Hyp}$ give very similar results, but differ in their bio-activity (data not shown). We could show that induction of CEP5p$^{Pro}$ was sufficient to negatively affect the auxin-mediated degradation of YFP:IAA7 and YFP:IAA28 in the presence of a functional TIR1 within 100 minutes, while this was unaffected by mCEP5$^{Pro}$ (**Figure 5G**). These results indicate that CEP5 (seemingly directly) interferes with TIR1/AFB-mediated degradation of AUX/IAAs. However, it remains to be explored what the precise mechanism is and how this fits with the recent identification of CEP receptors (Tabata *et al.*, 2014).

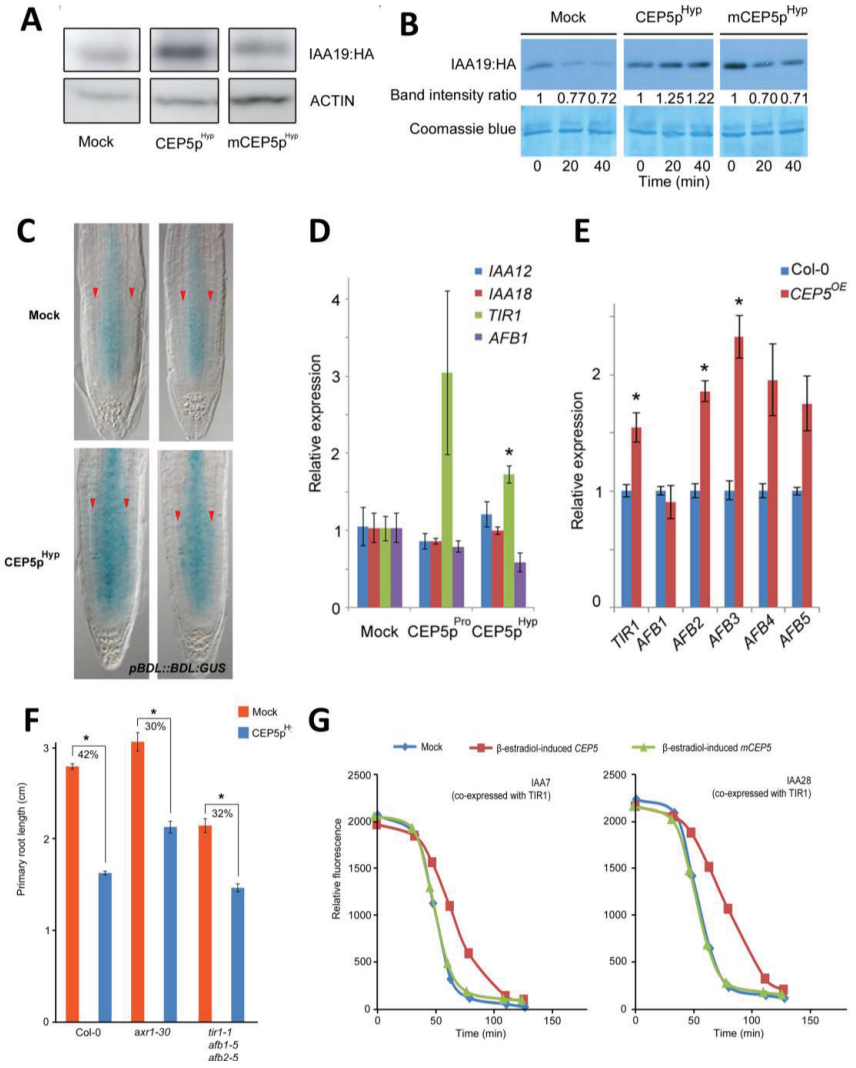


**Figure 5. (A)** Representative Western blot of IAA19:HA levels (anti-HA) in 10 day old seedlings grown in the presence of 5 µM CEP5p$^{Hyp}$ or 5 µM mCEP5p$^{Hyp}$. **(B)** Representative Western blot of IAA19:HA levels in 10 day old seedlings grown in the presence of 5 µM CEP5p$^{Hyp}$ or 5 µM mCEP5p$^{Hyp}$ for indicated (short) times. The band intensity ratio, normalized to the loading control and relative to 0 min is indicated. **(C)** BDL:GUS protein in six day old *pBDL::BDL:GUS* seedlings after transfer of 4 day old seedlings to mock or 1 µM CEP5p$^{Hyp}$ for 2 days. Two representative root tips show (i) increased GUS activity comparing mock and CEP5p$^{Hyp}$ treatment and cortex cells where BDL:GUS is not present (mock) and present following CEP5p$^{Hyp}$ treatment (as indicated by red arrowhead). In all cases, mock refers to medium with water as used to dissolve CEP5p. **(D)** Expression levels of *TIR1/AFBs* and/or *AUX/IAAs* in CEP5p$^{Pro}$ or CEP5p$^{Hyp}$-treated 5 day old wild type seedlings **(E)** and in roots of *CEP5$^{OE}$* compared to Col-0 in 5 day old seedlings. **(F)** Primary root length in Col-0, axr1-30 and *tir1-1/afb1-5/afb2-5* grown on ½ MS medium supplemented with mock or 1 µM mCEP5p$^{Hyp}$. The relative reduction in primary root length is indicated. **(G)** Yeast system engineered to monitor auxin-induced degradation of plant AUX/IAA proteins through fluorescence of YFP-IAA7 and YFP-IAA28 fusion proteins (Havens et al., 2012). Wild type (CEP5Pro) and mutant CEP5 15 amino acid mature peptide sequence (mCEP5Pro) are placed into the yeast genome under a β-estradiol-inducible promoter. Induction of CEP5pPro was sufficient to negatively affect the auxin-mediated degradation of YFP:IAA7 and YFP:IAA28 in the presence of a functional TIR1 within 100 minutes, while this was unaffected by mCEP5Pro *, $p < 0.05$ according to Student's *t*-test compared to mock (medium with water as used to dissolve CEP5p) or Col-0. All graphs show average ± standard error.

## DISCUSSION AND CONCLUSIONS

Taken together, our results suggest that CEP5 modulates auxin-regulated AUX/IAA stability, which – in this way – impacts on auxin-mediated processes, such as lateral root initiation. Previously, a role for CEPs in regulating aspects of root architecture, namely nitrate-dependent lateral root elongation, was proposed. Specifically, that CEPs act as root-derived ascending N-demand signals to the shoot, where their perception by CEPRs leads to the production of a putative shoot-derived descending signal that up-regulates nitrate transporter genes in the roots (Delay *et al.*, 2013; Mohd-Radzman *et al.*, 2015; Ohyama *et al.*, 2008; Tabata *et al.*, 2014). In addition, CEP3 and CEP5 were shown to regulate lateral root initiation (Delay *et al.*, 2013; Roberts *et al.*, 2016). However, the downstream mechanism remained largely elusive and other potential mechanisms have not been explored. Here, our genetic, biochemical and pharmacological studies have revealed that CEP5 is involved in (locally) attenuating auxin response through stabilising AUX/IAAs. While not each developmental and molecular read-out related to auxin is individually strongly affected by CEP5, there is a clear trend in all experiments, supporting an unmistakable impact on auxin response. The antagonistic relationship between auxin and CEP5 could be important in regulating auxin response thresholds and fine-tuning (very sensitive) auxin responses during growth and development through stabilising AUX/IAAs. It remains, however, to be investigated how CEP5 acts on the auxin signalling components. It is intriguing that CEP5 affects both full length AUX/IAAs and the DII:VENUS reporter, which only contains the degron of IAA28 and no other portions of the protein (Brunoud *et al.*, 2012). This suggests that CEP5 affects the degron itself or affects the TIR1/AFB part of the pathway at the protein level (*e.g.* by phosphorylation). Interestingly, increased CEP5 levels leads to slightly increased expression of *TIR1*/*AFB*, which might be due to an endogenous mechanism trying to reduce the accumulation of stabilized Aux/IAA proteins. At the moment it is unclear if CEP5 acts directly on components of the auxin-mediated ubiquitination complex or works through some intermediates to mediated AUX/IAA levels and/or auxin response. In this context, the recent identification of likely CEP receptors, XIP1/CEPR1 and CEPR2 (Tabata *et al.*, 2014), and the involvement of XIP1 in lateral root initiation (Roberts *et al.*, 2016) support the latter. However, in contrast to the effect of TDIF (Cho *et al.*, 2014), we have – up to now – not been able to detect phosphorylation of, for example, ARF7, suggesting the involvement of another mechanism. In addition, CEP5 seems to be able to stabilize AUX/IAAs in a heterologous yeast system likely not containing the signalling components identified in *Arabidopsis*. This further supports a direct effect of CEP5 on the $SCF^{TIR1/AFB}$ machinery. In case of a direct interaction with, for example, AUX/IAAs and/or $SCF^{TIR1/AFB}$, CEP5 would be expected to localize in the nucleus, but – so far – this could not be demonstrated. Intriguingly, there are (non-plant) examples of receptors that chaperone their ligand into the nucleus (Arnoys and Wang, 2007), which indicates that a similar mechanism might exist for the CEP5−XIP1/CEPR1 or CEPR2 pair. Given the expression patterns of the *CEP* family (Roberts *et al.*, 2013), and especially *CEP5* (Roberts *et al.*, 2016), which appears to mirror areas of increased auxin response, the regulation of auxin response may prove to be a general mechanism for these small signalling peptides throughout growth and development. However, our data suggest that – at least with respect to stabilizing DII:VENUS – CEP1 is less potent, so there are possibly differences between family members. This is likely due to subtle differences in their mature peptide sequence, as single amino acid changes can impact on bioactivity and/or specificity. In conclusion, our results support a new mechanism of regulating AUX/IAA stability during growth and development, and future studies are required to expose all the actors involved.

## METHODS

**Plant material**

The following transgenic lines and mutants were described previously: *CEP5*$^{OE}$ and *CEP5*$^{RNAi}$ (Roberts et al., 2013), *p35S::DII:VENUS* (Brunoud et al., 2012), *pDR5:LUC* (Moreno-Risueno et al., 2010), *IAA19:HA* (Cho et al., 2014), *pBDL::BDL:GUS* (Weijers et al., 2006), and *chl1-5* (Tsay et al., 1993).

**Plant growth and treatment conditions.**

Unless mentioned otherwise, seedlings were grown at 22 °C under continuous light (110 µE m–2 s–1 photosynthetically active radiation, supplied by cool-white fluorescent tungsten tubes, Osram) on square Petri plates containing 50 ml solid half-strength MS growth medium supplemented with sucrose (per liter: 2.15 g MS salts, 0.1 g myo-inositol, 0.5 g MES, 8 g sucrose, 8 g plant tissue culture agar; pH adjusted to 5.7 with KOH). For peptide treatments, media was supplemented with CEP5p$^{Pro}$, CEP5p$^{Hyp}$, or mCEP5p$^{Hyp}$ peptide to a concentration as indicated in the text and/or figure legends. *p35::DII:VENUS* seedlings were grown vertically on sugar-free ½ MS media (MS salts 2.15 g/L, Myo-inositol 0.1 g/L, MES 0.5 g/L, plant tissue culture agar 10 g/L, pH adjusted to 5.7) in continuous light at 21°C. For Col-0 x *35S:DII::VENUS*, *CEP5*$^{RNAi}$ x *35S:DII::VENUS*, *CEP5*$^{OE}$ x *35S:DII::VENUS*, the F1 generation was grown vertically on sugar-free ½ MS agar (MS salts 2.15 g/L, Myo-inositol 0.1 g/L, MES 0.5 g/L, plant tissue culture agar 10 g/L, pH adjusted to 5.7) until 5–6 DAG. For overnight *DII:VENUS* +/- IAA/NAA/CEP5 time-lapse experiments, *DII:VENUS* seedlings were grown vertically on sugar-free ½ MS media (see above) in 24 h light at 21°C until 5 DAG. At this time seedlings were transferred to ½ MS media supplemented with CEP5p 5 µM or plain ½ MS media control plates and incubated overnight. For each biological replicate, the next day one seedling was selected for quantification and placed in a coverglass-bottom dish (Iwaki, Japan) and overlaid with squares of sugar-free ½ MS supplemented with either: IAA 1 µM, NAA 1 µM, IAA 1 µM + CEP5 5 µM, NAA 1 µM + CEP5 5 µM, or CEP5 5 µM alone. For non-time lapse comparison of fluorescence (*DII:VENUS* +/- CEP5), *DII:VENUS* seedlings were grown vertically on sugar-free ½ MS media (see above) in continuous light at 21°C until 5 DAG. At this time seedlings were transferred to ½ MS media supplemented with either CEP5 5 µM, or plain ½ MS media control plates and incubated overnight. The next day seedlings were mounted on glass slides. For analyses in Figure 4a-b, *DII::VENUS* seedlings were grown vertically either on sugar-free ½ MS agar (see above), or sugar-free ½ MS agar supplemented with 5 µM CEP5pHyp in 24 h light at 21°C until 5 DAG. For analyses in Figure 4c-h, *DII::VENUS* seedlings were grown vertically on sugar-free ½ MS agar (see above), in continuous light at 21°C until 5 DAG. Seedlings were then treated with sugar-free ½ MS agar supplemented with either NAA 1 µM or NAA 1 µM + CEP5pHyp 5 µM whilst being imaged on a Leica SP5 confocal microscope (Leica, Wetzlar, Germany (514 nm detector: gain value 100%, offset value 28.98). For gravitropism experiments, *DII:VENUS* or Col-0 seedlings were grown vertically on sugar-free ½ MS media (see above) in continuous light at 21°C until 5 DAG in square petri dishes. Seedlings were then transferred to either fresh ½ MS media or to ½ MS media supplemented with 5 µM CEP5pHyp peptide and allowed to grow for a further 24 h. After this time, a gravistimulus was applied by rotating the growth dishes by 90°. Col-0 seedlings were photographed every 30 minutes after application of the gravistimulus and curvature of the root tip measured using FIJI software. For short term CEP5p treatments, *DII:VENUS* seedlings were grown vertically on sugar-free ½ MS media (see above) in continuous light at 21°C until 5 DAG in square petri dishes. After this time seedlings were placed in coverglass-bottom dishes (Iwaki, Japan) and overlaid with squares of sugar-free ½ MS containing either 5 µM CEP5pHyp or mCEP5Hyp, or unsupplemented fresh media as a control. For determination of IAA19 protein stability, homozygous plants expressing *35S::IAA19:HA* were grown in 1/2 B5 media containing DMSO, CHX, 5 µM CEP5p$^{Hyp}$ or mCEP5p$^{Hyp}$ for 10 days or the indicated minutes. Synthetic peptides were obtained from GenScript (www.genscript.com/peptide-services.html?src=home). For auxin inducibility analyses, seedlings were grown on nylon mesh and transferred to auxin-containing medium for 2 or 6 hours.

**Primary and lateral root phenotyping**

At the indicated time, images of plates with seedlings were taken and roots measured using ImageJ (http://rsbweb.nih.gov/ij/index.html) or FIJI software(Schindelin *et al.*, 2012). For detailed staging of lateral roots and for meristem size measurements, samples were cleared as described previously (Malamy and Benfey, 1997) and analysed by differential interference contrast microscopy (Olympus BX51).

**Histochemical GUS assays**

For microscopic analysis, samples were cleared with 90% lactic acid or as previously described (Malamy and Benfey, 1997). Samples were analysed by differential interference contrast microscopy (Olympus BX53) and a stereomicroscope (Leica MZ16). For anatomical analysis (microtome transversal sectioning) of GUS-stained roots, stained samples were processed as previously described(De Smet *et al.*, 2004).

**LUCIFERASE imaging and expression analysis**

The LUCIFERASE images were taken by a Lumazone machine carrying a CCD camera (Princeton instrument). The CCD camera with macro lens is controlled by WinView/32 software, and *LUCIFERASE* expression movies were taken automatically every 10 min with 10 min exposure time for ~ 24 hours. Before imaging, plates containing ½ MS were sprayed with 1 mM D-Luciferin (Duchefa Biochemie). The expression level of *pDR5::LUC* was measured by selecting the region of interest and quantifying the analog-digital units (ADU) per pixel using ImageJ. To quantify the prebranch sites number (static *DR5* expression sites above the oscillation zone), seedlings harboring *pDR5::LUC* were sprayed with D-Luciferin, and imaged by Lumazone with 15 minute exposure.

**DII :VENUS fluorescence quantification**

Seedlings were imaged on a Leica SP5 confocal microscope (Leica, Wetzlar, Germany (514 nm detector: gain value 100, offset value 28.98). Static images of each seedling were taken and fluorescence was quantified by calculating raw integrated density values for each image, measured using FIJI software10. Background fluorescence was removed using a threshold and only fluorescence coming from the nuclei was quantified. A zone just above the root hair initiation zone was used for analyses. Alternatively, seedlings were imaged on an inverted Nikon eclipse Ti-U confocal microscope (Nikon, Japan) with a fixed delay of 2 minutes over a minimum of 12 hours (10 x objective, a 515/30 detector using gain value 110, offset value 127). Background fluorescence was removed using a threshold and only fluorescence coming from the nuclei was quantified. Plots presented show changes in raw integrated density (how many fluorescent pixels FIJI software counted once the background was subtracted.) values over time, measured using FIJI software10. A minimum of 3 seedlings (~80 nuclei) were independently quantified for each condition. For short term CEP5p treatments, seedlings (n = 5-6) were imaged on a Leica SP5 confocal microscope (Leica, Wetzlar, Germany) with a fixed delay of 5 minutes over a maximum of 8 hours (a 514 nm detector using gain value 100%, offset value 28.98, averaged over 4 frames). Fluorescence was quantified as the relative change in raw integrated density values from starting fluorescence over time, measured using FIJI software. For gravitropism experiments, seedlings were imaged at time points at every hour post gravistimulus using a Leica SP5 confocal microscope (Leica, Wetzlar, Germany) over a timeframe of 6 hours (a 514 nm detector using gain value 100%, offset value 28.98, averaged over 4 frames). Total fluorescence was quantified as raw integrated density values, measured using FIJI software10. n ≥ 9 seedlings per timepoint/treatment. Fluorescence ratio in upper vs. lower horizontal sections of roots was calculated as the percentage share of the total root fluorescence.

**Immunoblotting**

The proteins from *p35S::IAA19:HA* expressing seedlings were analysed by 10% SDS–PAGE and visualized with anti-HA (1:2000, Roche) or anti-actin (1:1,000, MP biomedical cat. no. 69100) antibody. To assess CEP5 protein levels, *Arabidopsis thaliana* seedlings (Col-0, $CEP5^{RNAi}$ and $CEP5^{OE}$) were grown vertically on sugar-free ½ MS media (MS salts 2.15 g/L, Myo-inositol 0.1 g/L, MES 0.5 g/L, plant tissue culture agar 10 g/L, pH adjusted to 5.7) in 24 h light at 21°C until ~9 DAG. At this time whole seedlings (n = ≥ 20 seedlings) were pooled and ground in liquid nitrogen. Proteins were extracted using extraction buffer (12% SDS (w/v), 30% glycerol (w/v), 0.05% Coomassie blue, 150 mM Tris/HCl (pH 7.0)). Nuclear protein extracts were made using a CelLytic PN Isolation/Extraction kit (Sigma-Aldrich, St. Louis, MO, USA) according to the manufacturer's instructions. Due to the proline-rich nature and small size of mature CEP5 peptide, (<2 kDa) samples were run on a 16% tricine-SDS-PAGE gel according to the protocol (Schagger, 2006). Proteins were transferred onto a PVDF membrane (Amersham Hybond 0.2, GE Healthcare, Little Chalfont UK) using semi-dry transfer. Membranes were probed with anti-CEP5 IgG raised in rabbit (GenScript, Piscataway, NJ, USA) overnight followed by secondary probing for 1 h using anti-rabbit IgG peroxidase raised in goat, and visualised using Amersham ECL Prime Western Blotting Detection Reagent (GE Healthcare, Little Chalfont, UK).

**Auxin measurements**

500 pg 13C6-IAA internal standard was added to each sample, and extraction and purification was done as previously described (Andersen *et al.*, 2008), with minor modifications. Quantification of free IAA was then performed by gas chromatography - tandem mass spectrometry (GC-MS/MS).

**Real-time qRT-PCR analysis**

For the analysis of CEP5 expression after auxin treatment, RNA was extracted by first performing an RNA extraction with TRI Reagent® from Sigma-Aldrich according to the manufacturer's protocol, followed by a DNAse treatment on the isolated RNA (DNase I recombinant RNase-free from Roche Applied Science) . This was followed by an extra RNA extraction procedure with the Plant RNeasy Mini kit from Qiagen according to the manufacturer's protocol to further clean up the RNA. Next, 1 µg of total RNA was used for cDNA synthesis using the iScript kit from Bio-Rad according to the manufacturer's protocol. The real-time qRT-PCR reaction was carried out on the LightCycler 480 from Roche Applied Science with the LightCycler 480 SYBR Green I Master Mix from Roche Applied Science. The expression of CEP5 (CCATGGACGAACCCTAAAAG and TGCCATCATCGTCTTGCTAT), TIR1 (GCCTCTCTCTATCTGGCCTCTTGAC and AGGGCAGCTCTCTGGTCTCGAGTCC), AFB1 (AGTGATTTGATGCTTCATCACTTGT and CAATGACTTCGACATTGAGCCTTGGCA), AFB2 (TGGCGGCGCATCCATTCTTGTCCCA and AGATGCTCTCCATAGCCTTTGCAGG), AFB3 (AGCTCGAGATGCTTTCGATAGCTTTTG and TCATTCTGTTCCATCCCATTATTCTCA), AFB4 (TCTCATATCCCGTGGAGGCT and CATGCAGTGTACCTGAAGCA), AFB5 (GCTGCAAGGATATTGCACGAG and GCATTCCTCCCAAGTCCCAA), IAA12 (GGTACTACTTGTCGAGAAAAGGTTAAACC and CCCCTTCCTTATCTTCATAAGTGAGTAC), IAA18 (TGATGATTCCACAAGAGAGAAG and CACCAGGTGGTCCAAGC), LBD16 (AGACGTCAGCCGCCGGAGAT and GCGAGCTCTGTGGCGAGACC), LBD29 (GCTAGGCTTCAAGATCCCATC and TGTGCTGCTTGTTGCTTTAGA), ARF19 (TCCAAGTTCCAACGAAGGAG and AAACTAAAGGCCCTGCACAA), PIN1 (TACTCCGAGACCTTCCAACTACG and TCCACCGCCACCACTTCC), NRT1.1 (GCACATTGGCATTAGGCTTT and CTCAATCCCCACCTCAGCTA), NRT2.1 (AACAAGGGCTAACGTGGATG and CTGCTTCTCCTGCTCATTCC) and NRT3.1 (GGCCATGAAGTTGCCTATG and TCTTGGCCTTCCTCTTCTCA) was determined using two or three biological repeats and the reference genes EEF-1α4 (CTGGAGGTTTTGAGGCTGGTAT and CCAAGGGTGAAAGCAAGAAGA) and At2g32170 (GGACCTCTGTTGTATCATTTTGCG and CAACCCTCTTTACATCCTCCAAAC). To assess DII:VENUS levels, RNA was extracted from a pool of at least 5-10 F1 seedlings at 6 DAG using a Plant RNeasy Kit (Qiagen, Germany) according to the manufacturer's instructions. cDNA was subsequently prepared from a minimum of 250 ng RNA (determined by UV spectrophotometry) using a SuperScript II reverse transcriptase kit and Oligo(dT)12–18 primers (Invitrogen, USA), according to the manufacturer's instructions. Quantitative real-time PCR (qRT-PCR) was performed in a 384-well white dish format using a LightCycler 480 (Roche Applied Science, USA) with 40 PCR amplification cycles using SYBR Green I fluorescent dye (Quanta Biosciences, USA) and primers for the N7 nuclear localisation sequence of VENUS (GGACTCTGAGGATGGAAACG and TCAGCTTCTGTGTCGTCAATG) and referenced to ACTIN (CTGGA GGTTTTGAGGCTGGTAT and CCAAGGGTGAAAGCAA GAAGA).

**ACKNOWLEDGEMENTS**

We thank Maria Njo, Sarah De Cokere, Marieke Mispelaere and Darren Wells, for practical assistance, Daniël Van Damme for assistance with image analysis, Catherine Perrot-Rechenmann for useful discussions, Steffen Lau for critical reading of the manuscript, and Philip Benfey, Gerd Jürgens, and Philippe Nacry for sharing materials. This work was supported by a BBSRC David Phillips Fellowship (BB_BB/H022457/1) and a Marie Curie European Reintegration Grant (PERG06-GA-2009–256354) (I.D.S), Vetenskapsrådet and VINNOVA (S.R.), the Knut and Alice Wallenberg Foundation (A.R.), CEPLAS (EXC 1028) (G.K.K. and R.S.), German Research Council (DFG) (Y.S.), the Paul G. Allen Family Foundation and the National Science Foundation (IOS–0919021) (J.L.N.), National Institutes of Health (T32HD007183) (J.M.G.), a BBSRC Professorial Research Fellowship funding (M.J.B.). M.J.B. acknowledges the support of the Biotechnology and Biological Sciences Research Council (BBSRC) and Engineering and Physical Sciences Research Council (EPSRC) funding to the Centre for Plant Integrative Biology (CPIB). E.S. is a Postdoctoral Research Fellows of the Fund for Scientific Research (FWO)-Flanders (Belgium). This work was in part financed by grants of the Interuniversity Attraction Poles Programme (IAP VI/33 and IUAP P7/29 'MARS') from the Belgian Federal Science Policy Office and the Research Foundation Flanders (FWO). S.S. received a Biotechnology and Biological Science Research Council doctoral training grant studentship. I.R. was supported by the Agency for Innovation by Science and Technology (IWT). I.H. was supported by the National Research Foundation of Korea (NRF-2014R1A2A1A10052592). B.D.R. was funded by the Special Research Fund of Ghent University. We acknowledge Roger Granbom for skilful technical assistance, and the Swedish Research Council (VR) and the Swedish Governmental Agency for Innovation Systems (VINNOVA) for funding to K.L.

## REFERENCES


Andersen SU, Buechel S, Zhao Z, Ljung K, Novak O, Busch W, Schuster C, Lohmann JU (2008) Requirement of B2-type cyclin-dependent kinases for meristem integrity in Arabidopsis thaliana. *Plant Cell* **20:** 88-100.

Arnoys EJ, Wang JL (2007) Dual localization: proteins in extracellular and intracellular compartments. *Acta Histochem* **109:** 89-110.

Band LR, Wells DM, Larrieu A*, et al.* (2012). Root gravitropism is regulated by a transient lateral auxin gradient controlled by a tipping-point mechanism. *Proc Natl Acad Sci U S A* **109:** 4668-4673.

Brunoud G, Wells DM, Oliva M, Larrieu A, Mirabet V, Burrow AH, Beeckman T, Kepinski S, Traas J, Bennett MJ, Vernoux T (2012) A novel sensor to map auxin response and distribution at high spatio-temporal resolution. *Nature* **482,** 103-106.

Calderón Villalobos LI, Lee S, De Oliveira C, Ivetac A, Brandt W, Armitage L, Sheard LB, Tan X, Parry G, Mao H, Zheng N, Napier R, Kepinski S, Estelle M (2012) A combinatorial TIR1/AFB-Aux/IAA co-receptor system for differential sensing of auxin. *Nature Chemical Biology* **8:** 477-485.

Cho H, Ryu H, Rho S, Hill K, Smith 4, Audenaert D, Park J, Han S, Beeckman T, Bennett MJ, Hwang D, De Smet I, Hwang I (2014) A secreted peptide acts on BIN2-mediated phosphorylation of ARFs to potentiate auxin response during lateral root development. *Nat Cell Biol* **16:** 66-76.

De Smet I, Chaerle P, Vanneste S, De Rycke R, Inze D, Beeckman T (2004) An easy and versatile embedding method for transverse sections. *J Microsc* **213:** 76-80.

De Smet I, Lau S, Voss U, Vanneste S, Benjamins R, Rademacher EH, Schlereth A, De Rybel B, Vassileva V, Grunewald W, Naudts M, Levesque MP, Ehrismann JS, Inzé D, Luschnig C, Benfey PN, Weijers D, Van Montagu MC, Bennett MJ, Jürgens G, Beeckman T (2010) Bimodular auxin response controls organogenesis in Arabidopsis. *Proc Natl Acad Sci U S A* **107:** 2705-2710.

De Smet I, Tetsumura T, De Rybel B, Frei dit Frey N, Laplaze L, Casimiro I, Swarup R, Naudts M, Vanneste S, Audenaert D, Inzé D, Bennett MJ, Beeckman T (2007) Auxin-dependent regulation of lateral root positioning in the basal meristem of Arabidopsis. *Development* **134:** 681-690.

Del Bianco M, Kepinski S (2011) Context, Specificity, and Self-Organization in Auxin Response. *in Cold Spring Harb Perspect Biol edited by M. Estelle, D. Weijers, K. Ljung and O. Leyser* **3:a001578:** 201-220.

Delay C, Imin N, Djordjevic MA (2013) CEP genes regulate root and shoot development in response to environmental cues and are specific to seed plants. *J Exp Bot* **64:** 5383-5394.

Delker C, Poschl Y, Raschke A, Ullrich K, Ettingshausen S, Hauptmann V, Grosse I, Quint M (2010) Natural variation of transcriptional auxin response networks in Arabidopsis thaliana. *Plant Cell* **22:** 2184-2200.

Dharmasiri N, Dharmasiri S, Weijers D, Lechner E, Yamada M, Hobbie L, Ehrismann JS, Jurgens G, Estelle M (2005) Plant development is regulated by a family of auxin receptor F box proteins. *Developmental Cell* **9:** 109-119.

Havens KA, Guseman JM, Jang SS, Pierre-Jerome E, Bolten N, Klavins E, Nemhauser JL (2012) A synthetic approach reveals extensive tunability of auxin signaling. *Plant Physiol* **160:** 135-142.

Krouk G, Lacombe B, Bielach A, Perrine-Walker F, Malinska K, Mounier E, Hoyerova K, Tillard P, Leon S, Ljung K, Zazimalova E, Benkova E, Nacry P, Gojon A (2010) Nitrate-regulated auxin transport by NRT1.1 defines a mechanism for nutrient sensing in plants. *Dev Cell* **18:** 927-937.

Lau S, Jurgens G, De Smet I (2008) The evolving complexity of the auxin pathway. *Plant Cell* **20:** 1738-1746.

Lavenus J, Goh T, Roberts I, Guyomarc'h S, Lucas M, De Smet I, Fukaki H, Beeckman T, Bennett M, Laplaze L (2013) Lateral root development in Arabidopsis: fifty shades of auxin. *Trends Plant Sci*. **18:** 450-458

Malamy JE, Benfey PN (1997) Organization and cell differentiation in lateral roots of Arabidopsis thaliana. *Development* **124:** 33-44.

Mohd-Radzman NA, Binos S, Truong TT, Imin N, Mariani M, Djordjevic MA (2015) Novel MtCEP1 peptides produced in vivo differentially regulate root development in Medicago truncatula. *J Exp Bot*.

Moreno-Risueno MA, Van Norman JM, Moreno A, Zhang J, Ahnert SE, Benfey PN (2010) Oscillating gene expression determines competence for periodic Arabidopsis root branching. *Science* **329:** 1306-1311.

Murphy E, Smith S, De Smet I (2012) Small signaling peptides in Arabidopsis development: how cells communicate over a short distance. *Plant Cell* **24:** 3198-3217.

Ohyama K, Ogawa M, Matsubayashi Y (2008) Identification of a biologically active, small, secreted peptide in Arabidopsis by in silico gene screening, followed by LC-MS-based structure analysis. *Plant J* **55:** 152-160.

Overvoorde P, Fukaki H, Beeckman T (2010) Auxin control of root development. *Cold Spring Harb Perspect Biol* **2:** a001537.

Roberts I, Smith S, De Rybel B, Van Den Broeke J, Smet W, De Cokere S, Mispelaere M, De Smet I, Beeckman T (2013) The CEP Family in Land Plants: Evolutionary Analyses, Expression studies and Role in Arabidopsis Shoot Development *J Exp Bot*. **64:** 5371-5381

Roberts I, Smith S, Stes E, De Rybel B, Staes A, Van De Cotte B, Njo MF, Dedeyne L, Demol H, Lavenus J, Audenaert D, Gevaert K, Beeckman T, De Smet I (2016) CEP5 and XIP1/CEPR1 regulate lateral root initiation in Arabidopsis. *J Exp Bot* **(accepted)**.

Schagger H (2006) Tricine-SDS-PAGE. *Nat Protoc* **1:** 16-22.

Schindelin J, Arganda-Carreras I, Frise E, Kaynig V, Longair M, Pietzsch T, Preibisch S, Rueden C, Saalfeld S, Schmid B, Tinevez JY, White DJ, Hartenstein V, Eliceiri K, Tomancak P, Cardona A (2012) Fiji: an open-source platform for biological-image analysis. *Nat Methods* **9:** 676-682.

Tabata R, Sumida K, Yoshii T, Ohyama K, Shinohara H, Matsubayashi Y (2014) Perception of root-derived peptides by shoot LRR-RKs mediates systemic N-demand signaling. *Science* **346:** 343-346.

Tan X, Calderon-Villalobos LI, Sharon M, Zheng C, Robinson CV, Estelle M, Zheng N (2007) Mechanism of auxin perception by the TIR1 ubiquitin ligase. *Nature* **446:** 640-645.

Tsay YF, Schroeder JI, Feldmann KA, Crawford NM (1993) The herbicide sensitivity gene CHL1 of Arabidopsis encodes a nitrate-inducible nitrate transporter. *Cell* **72:** 705-713.

Ulmasov T, Murfett J, Hagen G, Guilfoyle TJ (1997) Aux/IAA proteins repress expression of reporter genes containing natural and highly active synthetic auxin response elements. *Plant Cell* **9:** 1963-1971.

Vanneste S, Friml J (2009) Auxin: a trigger for change in plant development. *Cell* **136:** 1005-1016.

Weijers D, Schlereth A, Ehrismann JS, Schwank G, Kientz M, Jurgens G (2006) Auxin triggers transient local signaling for cell specification in Arabidopsis embryogenesis. *Dev Cell* **10:** 265-270.

Xuan W, Audenaert D, Parizot B, Möller BK, Njo MF, De Rybel B, De Rop G, Van Isterdael G, Mähönen AP, Vanneste S, Beeckman T (2015) Root Cap-Derived Auxin Pre-patterns the Longitudinal Axis of the Arabidopsis Root. *Current Biology* **25:** 1381-1388.

## SUPPLEMENTARY FIGURES

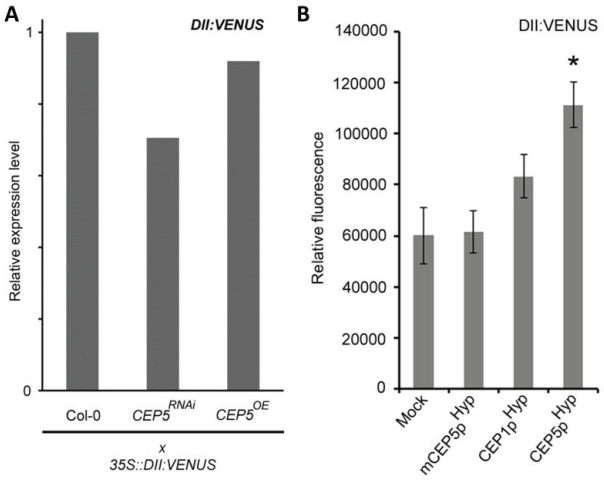


**Figure S1. (A)** *DII:VENUS* transcriptional expression levels in F1 seedlings (pool of 5-10 seedlings at 6 days after germination) of Col-0 x *35S::DII:VENUS*, *CEP5*$^{RNAi}$ x *35S::DII:VENUS*, and *CEP5*$^{OE}$ x *35S::DII:VENUS*. **(B)** Relative DII:VENUS protein fluorescence in *35S::DII:VENUS* reporter line following 18 hrs incubation with 5 µM CEP5p$^{Hyp}$, mCEP5p$^{Hyp}$, and CEP1p$^{Hyp}$ (DFR[HYP]TNPGNS[HYP]GVGH) compared with mock (medium with water as used to dissolve CEPp) treatment at 5-6 days after germination (n = 11). Graph shows average ± standard error. *, $p < 0.05$ according to Student's *t*-test compared to mock and mCEP5p$^{Hyp}$.

# Chapter 7:

## An EMS-mutagenesis screen to identify molecular components controlling root system architecture

**Contributions:**

I.R. was the main author of this work. I.R. conducted all the experimental work, except M.D. performed the initial steps of SHOREmap analysis. I.R. analyzed the data. T.B. and I.D.S. supervised the research. I.R. wrote the manuscript, with contributions from I.D.S. and T.B..

# An EMS-mutagenesis screen to identify molecular components controlling root system architecture

Ianto Roberts[1,2], Marieke Dubois[1,2], Ive De Smet[1,2] and Tom Beeckman[1,2]

[1]Department of Plant Systems Biology, VIB B-9052 Gent, Belgium
[2]Department of Plant Biotechnology and Bioinformatics, Ghent University, B-9052 Gent, Belgium

## ABSTRACT

Plant roots are crucial for water and nutrient uptake from the soil, and thereby have a large impact on plant growth and yield. The efficiency of the root system is determined by its root system architecture (RSA). In this study, molecular components controlling RSA were identified through a classical EMS-mutagenesis screen. Loss-of-function mutations in the *CELLULOSE SYNTHASE 6 (CESA6)*/*PROCUSTE 1 (PRC1)*/*ISOXABEN RESISTANT 2 (IXR2)* gene lead to a shallow dense root system, indicating RSA could at some degree be regulated by altering cellulose synthesis. Loss-of-function mutations in the *CULLIN-ASSOCIATED AND NEDDYLATION-DISSOCIATED 1* (*CAND1*)/*HEMIVENATA* (*HVE*)/*ENHANCER OF TIR1-1 AUXIN RESISTANCE 2* (*ETA2*) gene lead to a narrow dense root system, by inducing supergravitropic lateral roots growing under a steep angle along the primary root axis. This is makes *CAND1*/*HVE*/*ETA2* one of the very few genes known to control the lateral root setpoint angle. A new dominant mutation in the *INDOLE-3-ACETIC ACID INDUCIBLE* (*IAA12*)/*BODENLOS* (*BDL*) gene was identified, which induced a less dense root system with a reduction in lateral roots growing in clusters along the primary root. With the ease of current next-generation sequencing technologies and mapping strategies, EMS-mutant screens are becoming an attractive alternative again compared to transcriptome analyses for identifying genes controlling parameters of RSA.

## INTRODUCTION

With the increase in world population and changes in global climate (*e.g.* drought), the pressure on available arable land becomes more pronounced. It is therefore important to achieve optimal yield from crops. The root system is responsible for the uptake of water and growth-limiting nutrients and represents an important (but often overlooked) part of the plant that could be targeted for improvements (Kong et al, 2014). Engineering the root system might allow designing crops with higher yield under certain environmental conditions. The efficiency of the root system is determined by the root system architecture (RSA). The RSA is dependent on several parameters: 1) root length or growth rate (*e.g.* longer or shorter roots); 2) branching capacity or number of lateral roots (LRs) (*e.g.* more or less LRs); 3) angle of the LRs along the main axis (*e.g.* vertically or horizontally growing LRs); and finally 4) selective positioning and outgrowth of LRs (*e.g.* regions with LR growth arrest) (Lynch, 1995) **(Figure 1)**.

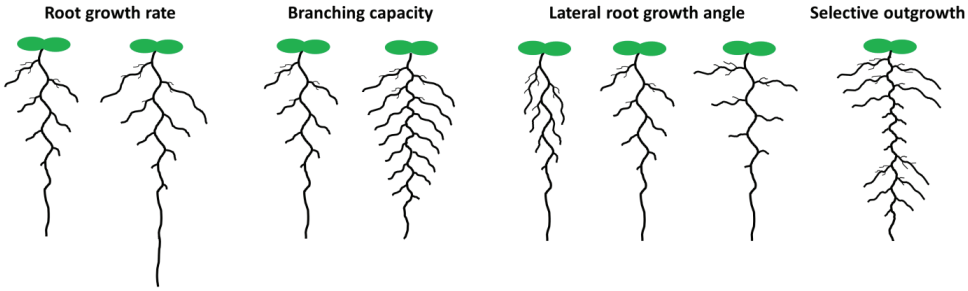


**Figure 1. RSA parameters.** RSA is determined by root growth rate, branching capacity, LR growth angle and selective outgrowth of LRs.

The plasticity of RSA is closely related to the (heterogeneous) nutrient availability (Lopez-Bucio et al, 2003). Some forms of RSA are better suited for certain environmental conditions than others. For example, increased root growth leads to longer roots that are able to penetrate deeper into the soil, which is beneficial for reaching water sources that are located in deeper regions under dry conditions. Longer roots can also scan a larger volume of soil for water and nutrients. An increased number of LRs boosts the potential of the root system to scan the soil more thoroughly and therefore allows for a higher uptake of water and nutrients **(Figure 2A)**. The angle of the lateral roots along the primary root axis also plays an important role in shaping the root system for optimal nutrient uptake. For example, the combination of a long deep primary root with lateral roots that grow under a steep angle alongside the main root ('steep and deep' ideotype), leads to a root system that is better adapted for water and nitrogen uptake, since these are found in deeper regions of the soil (Song et al, 2003; Lynch & Brown, 2012; Lynch, 2013; Uga et al, 2013; Uga et al, 2015) **(Figure 2B)**. In contrast, in the case of a shallow root system with lateral roots that grow almost horizontally near the soil surface, the root system is better adapted for phosphate uptake, since this is mainly found near the soil surface (Lynch, 1995; Hammond et al, 2009) **(Figure 2C)**. Selective positioning or outgrowth of LRs along the main root ensures that the plant only invests energy in lateral root development in regions of nutrient availability **(Figure 2D)**. Thus, adapting the RSA is crucial for optimal uptake of nutrients under different conditions.

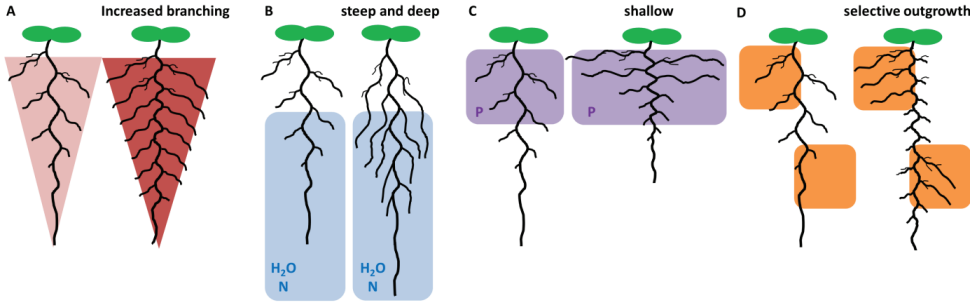


**Figure 2. The plasticity of RSA under different conditions of nutrient availability. (A)** Increased root branching leads to increased uptake of nutrients. **(B)** The steep and deep ideotype is better for water and nitrate uptake deeper in the soil. **(C)** A shallow root system is more suited for phosphate uptake close to the surface. **(D)** Selective outgrowth of lateral roots in regions of high nutrient concentration.

In the past, ethylmethanesulfonate (EMS) mutagenesis was successfully used as a forward-genetics approach to identify mutants that are affected in lateral root formation (Celenza et al, 1995; Rogg et al, 2001; Fukaki et al, 2002; Uehara et al, 2008). However, marker-based mapping of EMS mutations was laborious work (Qu & Qin, 2014), and the emergence of genome-wide transcriptomic analyses, as a reverse-genetics approach, quickly replaced the 'old-school' EMS-mutagenesis approach to identify many novel regulators of the lateral root development process (Himanen et al, 2004; Vanneste et al, 2005; Okushima et al, 2007; De Smet et al, 2008; De Rybel et al, 2012; Xuan et al, 2015). The latter approach has mainly been used on very young seedlings in which LR initiation was induced by hormone treatments, to study the early steps of lateral root development (priming and lateral root initiation). These studies identified a vast amount of potential regulators of the branching capacity of the root system. However, regulators of other parameters of RSA, such as the lateral root growth angle, require another approach for identification. With current next-generation deep sequencing methods (*e.g.* Illumina sequencing technology) and mutant mapping strategies (*e.g.* SHOREmap) (Schneeberger et al, 2009), the use of classical EMS-mutant screens is recently working its way back into developmental studies (Thole & Strader, 2015). The EMS-mutagenesis approach might be more suited for identifying regulators that affect the lateral root growth angle and overall RSA.

EMS produces point mutations throughout the genome with a frequency dependent on the concentration and time of incubation. Its ethyl group reacts with the guanine base in DNA, forming O-6-ethylguanine. During DNA replication, a thymine, instead of cytosine is inserted opposite O-6-ethylguanine. In subsequent rounds of replication, the original G:C base pair becomes an A:T pair, thereby inducing the characteristic G to A or C to T mutation. The outcome of EMS-induced point mutations can be divers: disruption of the ORF by introducing a premature STOP codon, point mutations in crucial residues for catalytic activity or binding sites (besides loss-of-function also potentially leading to gain-of-function or dominant mutants), altered splicing, disruption of an amiRNA recognition site or disruption of an important transcription factor binding site in the promoter region (Maple & Moller, 2007).

In this work, a classical forward EMS-mutagenesis screen was used to identify genes that have a clear impact on RSA by altering LR growth angle and LR spacing. In addition, the RSA phenotypes that were observed under the widely used standard *in vitro* growth conditions on solid ½ MS growth medium, were also shown to be reproducible under more natural growth conditions in soil, using a mini-rhizotron set-up.

## RESULTS

### An EMS-mutagenesis screen identified molecular components affecting RSA

A classical workflow was followed for the EMS-mutagenesis screen **(Figure 3)**. An EMS mutagenesis was performed on approximately 10,000 *Arabidopsis thaliana* seeds. M2 seeds were harvested from a total of 300 pools, with each pool containing seeds from approximately 30 M1 mutant plants. For this study, 100 pools were screened, for which approximately 400 to 500 M2 seeds from each pool were sown on vertically oriented standard petri plates (12 x 12 cm) containing ½ MS growth medium, with 10 seeds per plate. Twelve days after germination, when the M2 seedlings have a root system of sufficient size to score RSA parameters, the seedlings were screened for mutants with a clearly altered RSA (*e.g.* differences in length of the roots, lateral root spacing or lateral root angle).

A total of 455 mutants were selected and transferred to soil for M3 seeds. Only 216 of the 455 M2 mutant plants gave M3 seeds, while the other plants were either sterile or died. The altered RSA phenotype was confirmed in 53 M3 mutant seedlings, from which 24 M3 mutants were retained for their highest differences in RSA **(Supplemental Figure S1)**. From these, 17 M3 mutant lines were used for crossing with Landsberg *erecta* (L*er*) to generate F2 mapping populations. From these, 3 EMS mutant lines were selected for further analysis. Approximately one thousand F2 seedlings from each mapping population were grown for twelve days on ½ MS growth medium, followed by a stringent selection for 180 to 230 F2 seedlings with a clear mutant phenotype that were pooled for deep sequencing and SHOREmapping. Prior to deep sequencing and SHOREmapping, 20 mutant F2 seedlings were sampled separately for 'rough mapping' analysis, in order to have an idea in which region of the genome the causative EMS mutation is localized. For this, 25 insertion-deletion (INDEL) markers, reported in (Hou et al, 2010), were used that are different for Col-0 and L*er* background and are distributed evenly over the five chromosomes. INDEL marker(s) for which all or most of the twenty mutant F2 seedlings are Col-0 background, are most likely associated with the locus of the EMS mutation (EMS mutants are Col-0 background). This allowed us to already have a rough idea where the EMS mutation is potentially located before SHOREmapping.

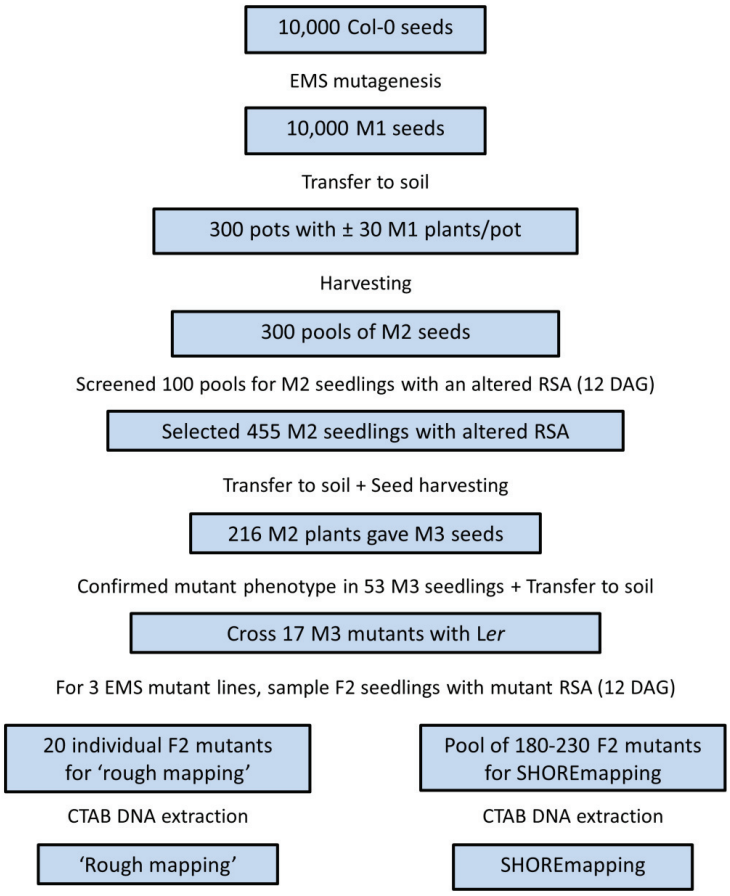


**Figure 3. Overview of the workflow used for the EMS-mutagenesis screen for mutants with altered RSA.**

**A mutant with a shallow root system**

The EMS 24-2 mutant was selected for its shorter primary root and lateral roots that grow more horizontally compared to the root axis and are positioned closer to each other, reminiscent of the shallow root system that is beneficial for phosphate uptake near the soil surface (Lynch, 1995; Hammond et al, 2009) **(Figure 4)**. Rough mapping suggested the causative mutation is situated on the far end of chromosome 5 **(Figure 5A)**. SHOREmap analysis confirmed that the EMS 24-2 mutant contains a G to A mutation at position 25,884,743 on chromosome 5 **(Figure 5B and Supplementary Figure S2A)**, which is located in exon 10 of the *CELLULOSE SYNTHASE 6 (CESA6)/PROCUSTE 1 (PRC1)/ISOXABEN RESISTANT 2 (IXR2)* gene (At5g64740). The *CESA6/PRC1/IXR2* gene belongs to a family of 10 *CESA* genes, which encode membrane-localized Glycosyl-Transferase family 2 (GT-2) enzymes that catalyze cellulose synthesis (Somerville, 2006). The mutation in EMS 24-2 turns a tryptophan (Trp, W) residue into a premature stop codon at position 661 of 1081 (W661stop), leading to a loss-of-function mutant.

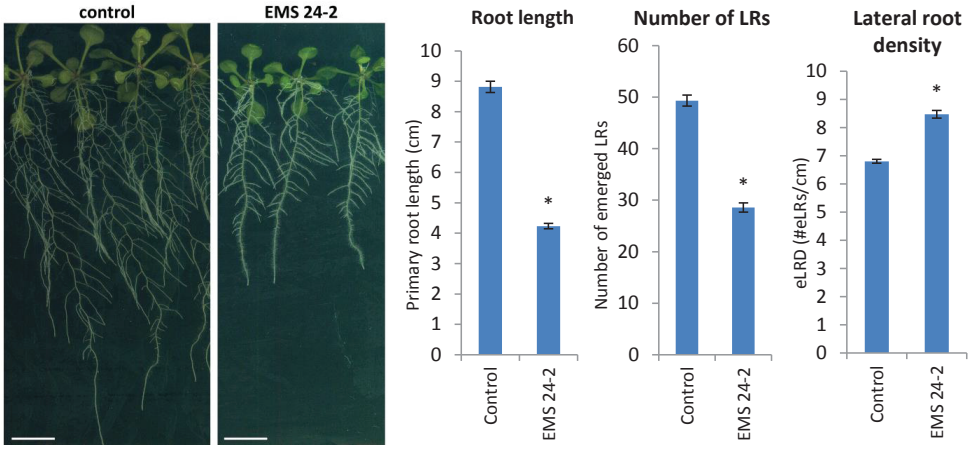


**Figure 4. Phenotype of the EMS 24-2 mutant.** The EMS 24-2 mutant has a shorter primary root and less emerged LRs, which are growing more horizontally and are positioned closer to each other (higher density), compared to control. Seedlings 12 DAG on ½ MS; scale bar = 1 cm; graphs show average ± SE (n≥9); * indicates $p<0.05$ according to Student's *t*-test.

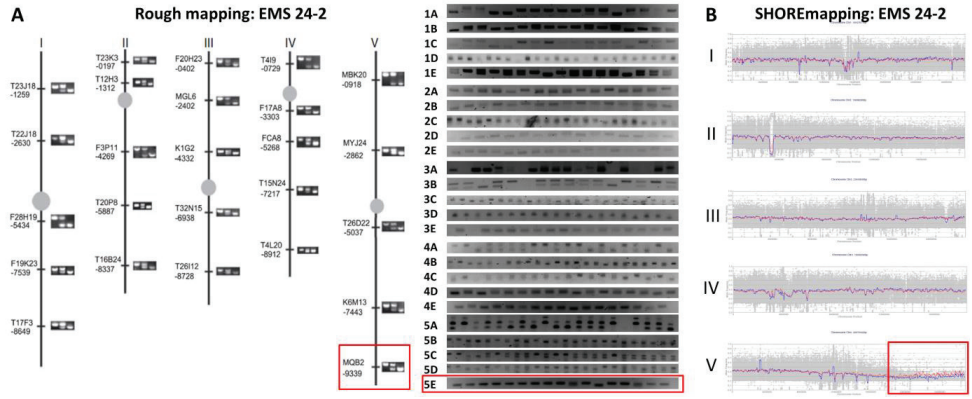


**Figure 5. Mapping the EMS 24-2 mutation.** The mutation associated with the EMS 24-2 mutant phenotype was mapped to chromosome 5 by **(A)** rough mapping and **(B)** SHOREmapping.

To verify that the W661STOP mutation in the *CESA6* gene causes the characteristic phenotype of the EMS 24-2 mutant, two other loss-of-function mutants for the *CESA6* gene were investigated: the SALK_004587 T-DNA insertion line (hereafter *cesa6-1*) with an insertion in the second exon, and the *pcr1-1* (hereafter *cesa6-2*) mutant with a Q720STOP mutation **(Figure 6)**. These mutants showed the same phenotype as the EMS 24-2 mutant (hereafter *cesa6-3*), confirming that a loss-of-function of *CESA6* leads to a shorter and denser root system with more horizontally growing LRs **(Figure 7)**.

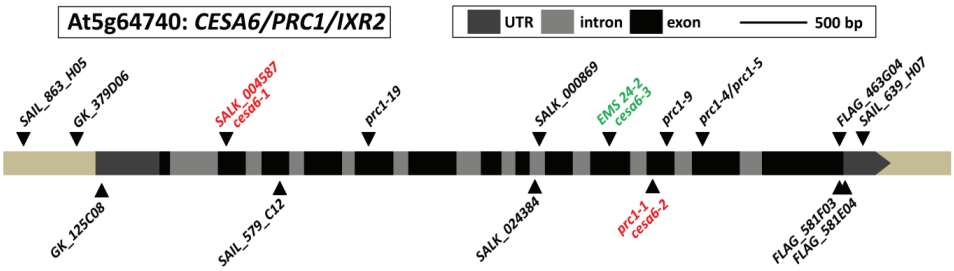


**Figure 6. Overview of *cesa6* mutants.** Overview of the location of mutation sites of publically available mutant lines for the *CESA6/PRC1/IXR2* gene, with two mutant lines used in this study, SALK_004587 (*cesa6*-1) and *prc1-1* (*cesa6-2*), indicated in red , and with the EMS 24-2 mutant (*cesa6-3*) indicated in green.

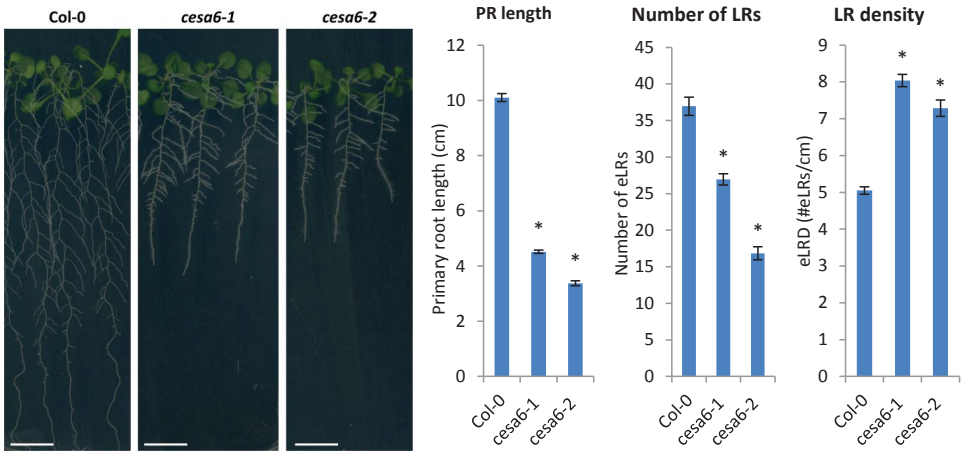


**Figure 7. RSA of *cesa6* mutants.** The *cesa6-1* and *cesa6-2* mutants have a similar RSA as EMS 24-2/*cesa6-3*, a shorter primary root with denser LRs that are oriented more horizontally (seedlings 12 DAG on ½ MS; scale bar = 1 cm; graphs show average ± SE; n≥12; * $p$<0.05 Student's $t$-test).

To have an idea how the root system of the *cesa6* mutants develops over a longer time, seedlings were grown for 15 days on large Petri plates (24 x 24 cm) with ½ MS growth medium, instead of the standard-sized Petri plates (12 x 12 cm). This showed that the *cesa6-1* and *cesa6-2* mutants have a shorter, but denser root system compared to Col-0 control **(Figure 8)**.

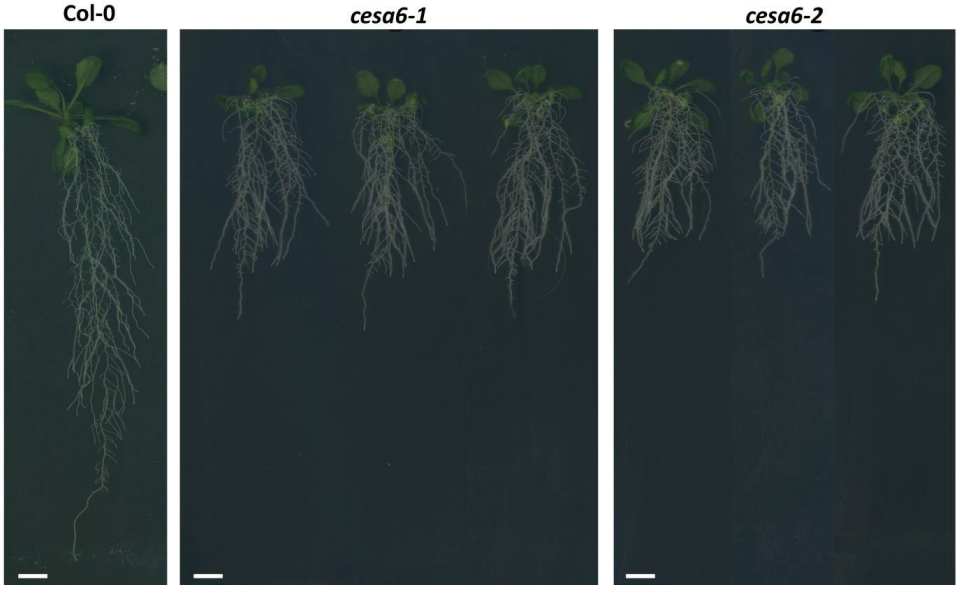


**Figure 8. RSA of *cesa6* mutants.** In a later stage of plant growth, the *cesa6-1* and *cesa6-2* mutants have a more compact and denser shallow root system compared to Col-0 control (seedlings 15 DAG on ½ MS; scale bar = 1 cm).

Until now, most studies on the root system of *Arabidopsis* were performed on young seedlings (usually less than 9 days old) grown on Petri plates with solid ½ MS growth medium. To have an idea whether the root traits observed in these '*in vitro*' growth conditions are still present in more natural 'in soil' conditions, mini-rhizotrons were used to check RSA of the *cesa6* mutant compared to Col-0. Plants were germinated and grown for 43 days, until the inflorescence reached its mature size and stopped growing. RSA was followed over time and revealed that the *cesa6-1* mutant developed a shallower, but much denser root system close to the soil surface in comparison with the deeper and wide spread root system of Col-0 control **(Figure 9)**.

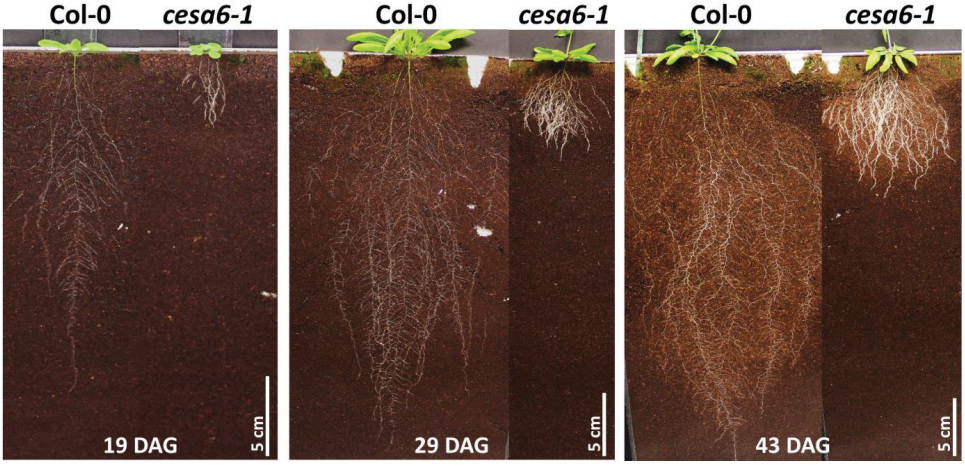


**Figure 9. RSA of *cesa6* in soil.** The *cesa6-1* mutant develops a shallower and much denser root system compared to Col-0, monitored in rhizotrons at 19, 29 and 43 DAG. (scale bar = 5 cm).

**A mutant with a steep lateral root growth angle**

The EMS 48-1 mutant has LRs that grow under a very steep angle along the primary root and are positioned significantly closer to each other **(Figure 10)**. SHOREmap analysis revealed that the causative mutation was located on chromosome 2 with a G to A mutation at position 693,173 in At2g02560 **(Figure 10 and Supplementary Figure S2B)**. This gene encodes CULLIN-ASSOCIATED AND NEDDYLATION-DISSOCIATED1 (CAND1)/HEMIVENATA (HVE)/ENHANCER OF TIR1-1 AUXIN RESISTANCE 2 (ETA2), which regulates the assembly and disassembly of the SCF-complex, consisting of ARABIDOPSIS S-PHASE KINASE-ASSOCIATED PROTEIN1 HOMOLOGUE 1 (ASK1), CULLIN1 (CUL1), an F-box protein, RING BOX1 (RBX1) and an E2 ubiquitin ligase complex (Goldenberg et al, 2004; Dharmasiri et al, 2007; Hotton et al, 2011; Mergner & Schwechheimer, 2014). The mutation in the *CAND1* gene is situated in exon 11 of 27 and leads to the conversion of a tryptophan (Trp, W) residue at postion 419 into a premature STOP codon (W419STOP), leading to a loss-of-function.

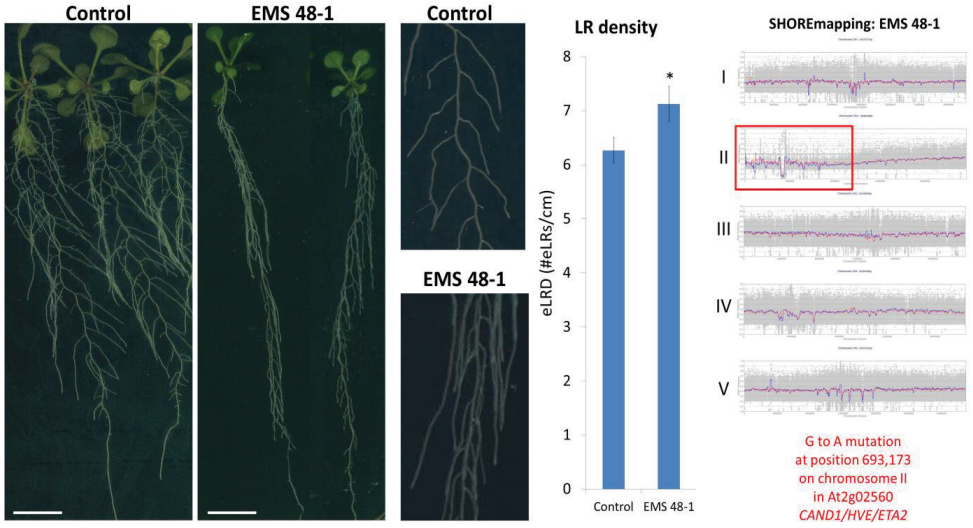


**Figure 10. Phenotype and mapping of the EMS 48-1 mutant.** The EMS 48-1 mutant is not affected in primary root growth, but contains LRs that grow under a very steep angle along the main root axis, and are positioned significantly closer to each other (seedlings are 12 DAG on ½ MS; graph displays average ± SE (n≥9); * $p$<0.05 Student's $t$-test).

CAND1 plays a role in various SCF-dependent signaling pathways, including the auxin, jasmonic acid, strigolactone and gibberellic acid signaling pathways (Perez & Goossens, 2013; Wallner et al, 2016). Its involvement in all these hormone signaling pathways might explain the pleiotropic phenotypes of previously described *cand1* loss-of-function mutants, such as late flowering, aerial rosettes, floral organ defects, low fertility, dwarfism, partial constitutive photomorphogenesis, altered leaf venation, loss of apical dominance and altered plant hormone responses (Chuang et al, 2004; Alonso-Peral et al, 2006). However, an effect on LR setpoint angle was not reported in previous studies. Therefore, in order to verify that the altered RSA phenotype of the EMS 48-1 mutant is due to *CAND1* loss-of-function, three different *cand1* mutant lines were analyzed: SALK_099479/*cand1-2*/*hve-2*/*eta2-79* (hereafter *cand1-2*) with a T-DNA insertion in exon 5, GK_190D07/*cand1-4* (hereafter *cand1-4*) with a T-DNA insertion in exon 18, and Ei-5/*cand1-5*/*hve-1* (hereafter *cand1-5*), which is a natural variation in the Eifel-5 ecotype that leads to missplicing of exon 14 **(Figure 11)**.

When these mutant lines were grown for 12 days on vertical ½ MS growth medium, this revealed that all three showed a steep LR setpoint angle and increased LR density, similar to the EMS 48-1 mutant (hereafter *cand1-6*) **(Figure 12)**. Growing the *cand1* mutants for 15 days on large Petri plates (24 x 24 cm) with ½ MS growth medium, revealed that the steep LR setpoint angle and increased LR density leads to a narrower and denser root system compared to Col-0 **(Figure 13)**.

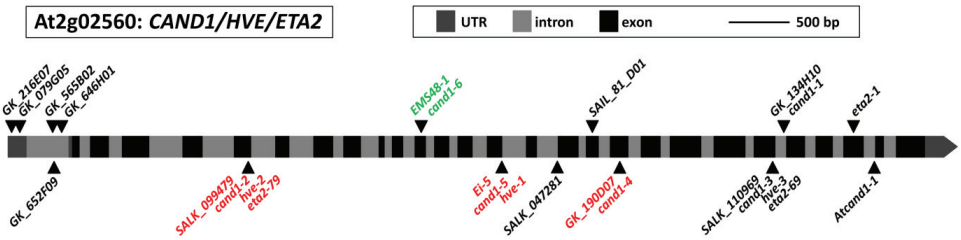


**Figure 11. Overview of *cand1* mutants.** Overview of the location of the mutation sites of publically available mutant lines for the *CAND1/HVE/ETA2* gene, with three *cand1* mutant lines used in this study, SALK_099479/*cand1-2*/*hve-2*/*eta2-79*, GK_190D07/*cand1-4* and Ei-5/*cand1-5*/*hve-1*, indicated in red, and with the EMS 48-1 mutant (*cand1-6*) indicated in green.

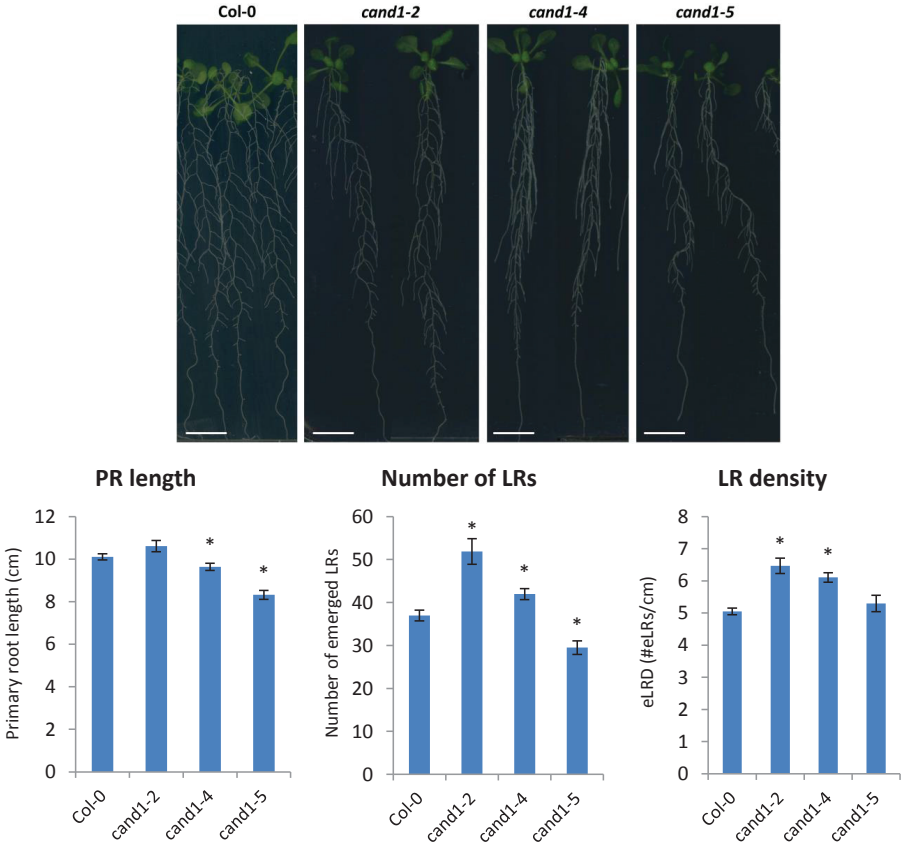


**Figure 12. Phenotype of *cand1* mutants.** Three independent mutant lines of *CAND1* (*cand1-2*, *cand1-4* and *cand1-5*) showed the same steep LR growth angle as the EMS 48-1/*cand1-6* mutant. Differences in primary root length, number of emerged LRs and emerged LR density were observed in the mutant lines compared to Col-0. (seedlings 12 DAG on ½ MS; graphs display average ± SE (n≥8); * $p<0.05$ Student's *t*-test).

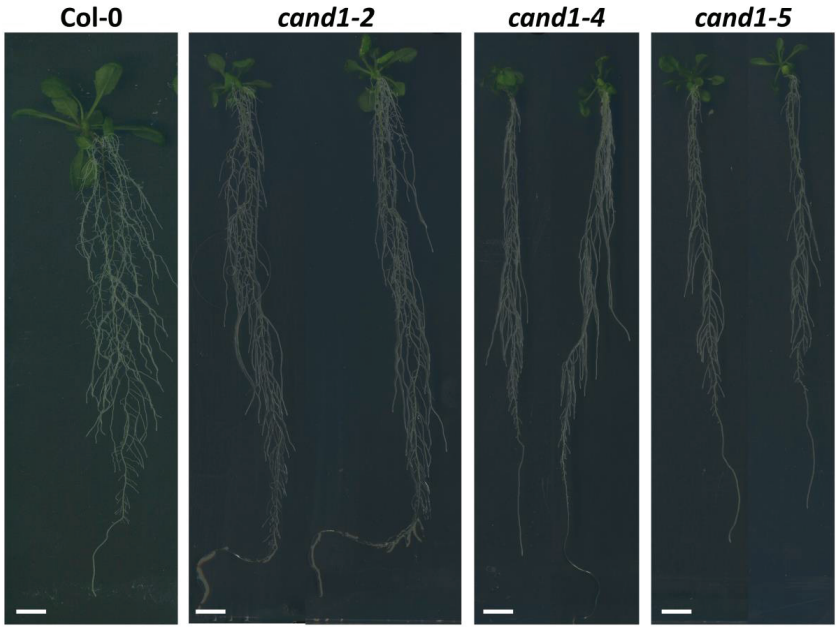


**Figure 13. RSA phenotype of *cand1* mutants.** In a later stage of plant growth, the cand*1-2*, *cand1-4* and *cand1-5* mutants have a narrower and denser root system compared to Col-0 control (seedlings 15 DAG on ½ MS; scale bar = 1 cm).

To check if the RSA phenotype observed under these *in vitro* growth conditions can be translated to more natural conditions, the *cand1-2* mutant was monitored in a mini-rhizotron system, in which the roots were grown in soil in the dark. This revealed that the narrower and denser root system observed on ½ MS plates is retained in soil **(Figure 14)**.

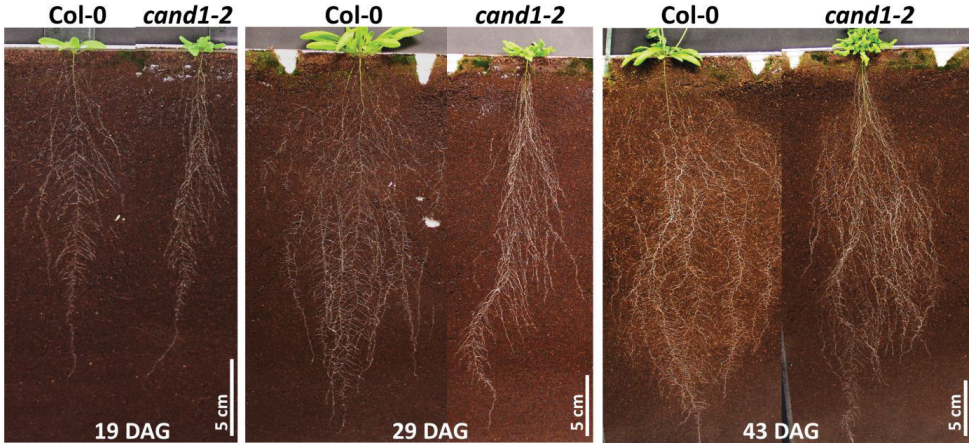


**Figure 14. Rhizotron growth of *cand1*.** The *cand1-2* mutant develops a narrower and denser root system compared to Col-0, monitored in rhizotrons at 19, 29 and 43 DAG. (scale bar = 5 cm).

**A mutant with altered lateral root spacing**

The EMS 42-1 mutant was picked for its drastic reduction in the number of LRs, and for its severely disturbed LR spacing, as it contained regions along the primary root devoid of LRs, as well as regions with dense clusters of LRs next to each other. Genomic sequencing and SHOREmap analysis revealed that the causative mutation was located on chromosome 1 with a G to A mutation at position 1,241,068 in At1g04550 **(Figure 15 and Supplementary Figure S2C)**. This gene encodes INDOLE-3-ACETIC ACID INDUCIBLE 12 (IAA12)/BODENLOS (BDL). The mutation is situated in exon 2 of 5 and leads to the conversion of a glycine (Gly, G) residue at position 72 into a glutamic acid (Glu, E) (G72E).

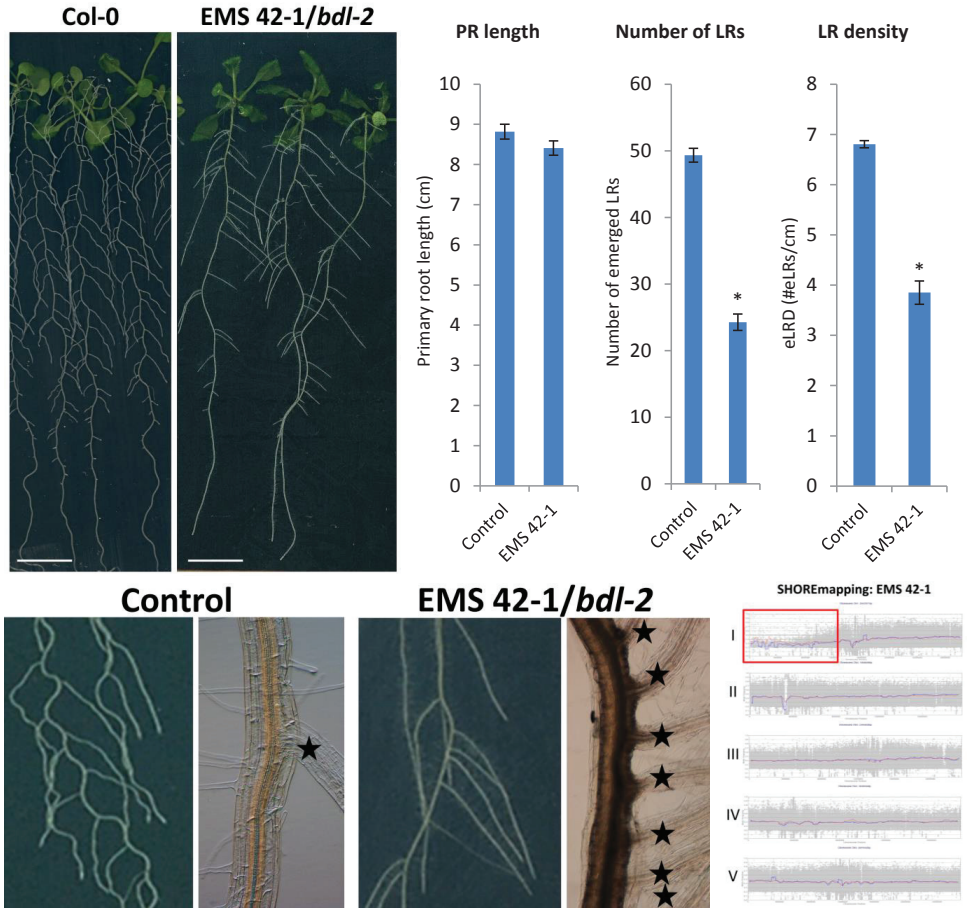


**Figure 15. Phenotype and mapping of the EMS 42-1/*bdl-2* mutant.** The EMS 42-1/*bdl-2* mutant has a drastic reduction in number of emerged LRs, and contains regions with dense clusters of LRs close to each other. Genomic sequencing and SHOREmap analysis revealed that this phenotype was due to a mutation in the *IAA12/BDL* gene. (scale bar = 1 cm; graphs indicate average ± SE (n>8), * $p<0.05$ Student's *t*-test; stars indicate LRs; the red box indicates the region of the causative EMS 42-1/*bdl-2* mutation on chromosome 1).

Previous studies reported that IAA12/BDL is a transcriptional repressor that inhibits the transcriptional activator MONOPTEROS (MP)/ARF5 during primary root embryogenesis and LR initiation (Hamann et al, 1999; Hamann et al, 2002; De Smet et al, 2010). In these studies, the dominant mutant *bodenlos* (*bdl*, hereafter *bdl-1*) was shown to lead to primary root-less seedlings (in homozygous state) and clustered LRs with no obvious effect on primary root length (in hemizygous state). The latter phenotype of clustered LRs is the same as in the EMS 42-1 mutant, confirming that the observed phenotype in EMS 42-1 is caused by the point-mutation in *IAA12*/*BDL* (EMS 42-1: hereafter *bdl-2*) **(Figure 16A-C)**. Noteworthy, the EMS 42-1/*bdl-2* mutant line used in this study is homozygous and dominant, but still leads to relatively normal plants compared to the *bdl-1* homozygous plants. The *bdl-1* mutant contains a point-mutation that generates a proline to serine mutation in residue 74 (P74S mutation), while the *bdl-2* mutant has a G72E mutation. Both mutations are situated in the conserved GWPPV motif in domain II of the IAA protein, similar to many previously described dominant *aux/iaa* mutants **(Figure 16A)**. The importance of the conserved GWPPV motif can be revealed by structural analysis of the auxin binding pocket. The protruding hydrophobic GWPPV residues of an Aux/IAA protein interact with the hydrophobic indole ring and methylene linker of auxin, while the hydrophilic TIR1 auxin binding pocket (formed by H78, R403, S438, S462 and E487) interacts with the hydrophilic carboxyl group of auxin **(Figure 16B)**. In contrast, in the *bdl-1* and *bdl-2* mutants, the hydrophobic residues from the GWPPV motif are mutated into hydrophilic residues (P74S and G72E, respectively), leading to reduced binding affinity of the Aux/IAA protein for the $SCF^{TIR1}$ complex, and thereby reducing/preventing its degradation, and forming a dominant repressor of auxin signaling. Similar mutations in the GWPPV motif in other Aux/IAA proteins were all shown to lead to dominant mutants (Tian & Reed, 1999; Nagpal et al, 2000; Rogg et al, 2001; Fukaki et al, 2002; Tatematsu et al, 2004; Yang et al, 2004; Uehara et al, 2008; Goh et al, 2012) **(Figure 16A)**.

To check how the root system of the EMS 42-1/*bdl-2* mutant copes with the reduced LR formation over a longer time, seedlings were grown for 15 days on large ½ MS plates (24 x 24 cm). This showed that the reduction in formation of LRs is to some degree compensated by increased LR elongation. This leads to a root system with similar contours, albeit less dense compared to Col-0 **(Figure 17)**. Growing the mutant for up to 43 days in mini-rhizotrons revealed that eventually a smaller and less dense root system was formed compared to Col-0 **(Figure 18)**. Thus altogether, the mutated *IAA12*/*BDL* gene leads to a reduction in the overall size and density of the root system.

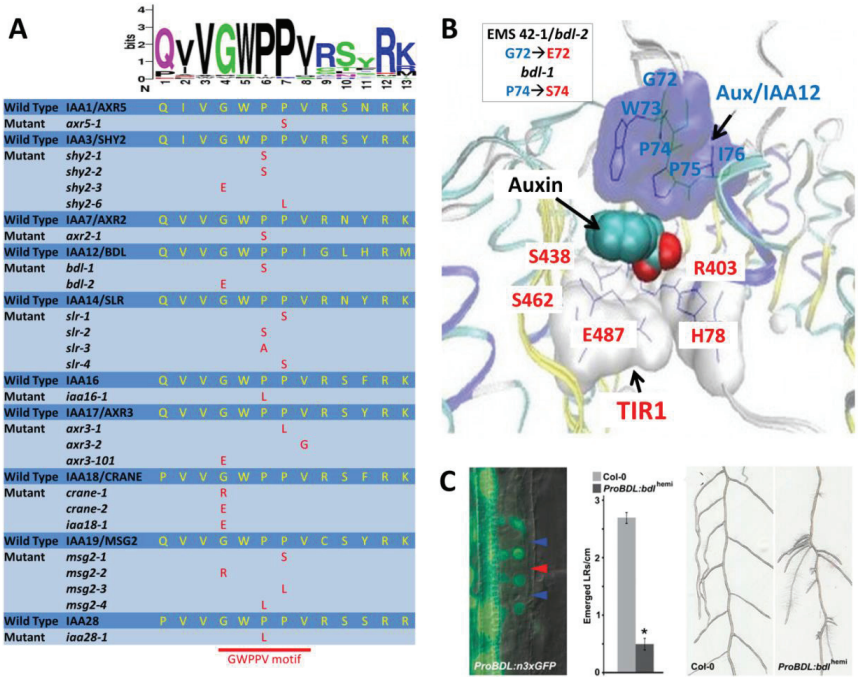


| | | | | | | | | | | | | | | |
|---|---|---|---|---|---|---|---|---|---|---|---|---|---|---|
| Wild Type | IAA1/AXR5 | Q | I | V | G | W | P | P | V | R | S | N | R | K |
| Mutant | *axr5-1* | | | | | | S | | | | | | | |
| Wild Type | IAA3/SHY2 | Q | I | V | G | W | P | P | V | R | S | Y | R | K |
| Mutant | *shy2-1* | | | | | | S | | | | | | | |
| | *shy2-2* | | | | | | S | | | | | | | |
| | *shy2-3* | | | | E | | | | | | | | | |
| | *shy2-6* | | | | | | | L | | | | | | |
| Wild Type | IAA7/AXR2 | Q | V | V | G | W | P | P | V | R | N | Y | R | K |
| Mutant | *axr2-1* | | | | | | S | | | | | | | |
| Wild Type | IAA12/BDL | Q | V | V | G | W | P | P | I | G | L | H | R | M |
| Mutant | *bdl-1* | | | | | | S | | | | | | | |
| | *bdl-2* | | | | E | | | | | | | | | |
| Wild Type | IAA14/SLR | Q | V | V | G | W | P | P | V | R | N | Y | R | K |
| Mutant | *slr-1* | | | | | | | S | | | | | | |
| | *slr-2* | | | | | | S | | | | | | | |
| | *slr-3* | | | | | | A | | | | | | | |
| | *slr-4* | | | | | | | S | | | | | | |
| Wild Type | IAA16 | Q | V | V | G | W | P | P | V | R | S | F | R | K |
| Mutant | *iaa16-1* | | | | | | L | | | | | | | |
| Wild Type | IAA17/AXR3 | Q | V | V | G | W | P | P | V | R | S | Y | R | K |
| Mutant | *axr3-1* | | | | | | | L | | | | | | |
| | *axr3-2* | | | | | | | | G | | | | | |
| | *axr3-101* | | | | E | | | | | | | | | |
| Wild Type | IAA18/CRANE | P | V | V | G | W | P | P | V | R | S | F | R | K |
| Mutant | *crane-1* | | | | R | | | | | | | | | |
| | *crane-2* | | | | E | | | | | | | | | |
| | *iaa18-1* | | | | E | | | | | | | | | |
| Wild Type | IAA19/MSG2 | Q | V | V | G | W | P | P | V | C | S | Y | R | K |
| Mutant | *msg2-1* | | | | | | | S | | | | | | |
| | *msg2-2* | | | | R | | | | | | | | | |
| | *msg2-3* | | | | | | | L | | | | | | |
| | *msg2-4* | | | | | | L | | | | | | | |
| Wild Type | IAA28 | P | V | V | G | W | P | P | V | R | S | S | R | R |
| Mutant | *iaa28-1* | | | | | | L | | | | | | | |

**Figure 16. Domain II mutations in dominant *iaa* mutants. (A)** Overview of the domain II sequence (in yellow) of Aux/IAA proteins revealed a strong conservation of the GWPPV motif (consensus sequence generated with WebLogo3 software). Previously described *aux/iaa* mutants contain mutated residues in the GWPPV motif (in red). **(B)** Overview of the IAA12 – auxin – TIR1 complex at the auxin binding pocket. TIR1/AFB proteins contain a hydrophilic auxin-binding pocket (in TIR1: His78, Arg403, Ser438, Ser462, and Glu 487), which interacts with the hydrophilic auxin carboxyl group. While Aux/IAA proteins contain a hydrophobic GWPPV motif, which interacts with the hydrophobic indole ring and methylene linker of auxin. EMS 42-1/*bdl-2* contains a G72E mutation and *bdl-1* contains a P74S mutation, both changing a conserved hydrophobic residue into a hydrophilic residue, thereby hampering Aux/IAA12 binding to the $SCF^{TIR1}$ complex, and preventing degradation (Image B adapted from www.tetradiscovery.com). **(C)** *IAA12*/*BDL* expression during lateral root initiation and LR phenotype of a hemizygous *bdl-1* mutant (Images in C taken from De Smet et al., 2010).


**Figure 17. RSA of EMS 42-1/*bdl-2*.** In a later stage of plant growth, the EMS 42-1/*bdl-2* mutant develops a root system with similar contours, but less dense, compared to Col-0 (seedlings 15 DAG on ½ MS; scale bar = 1 cm).

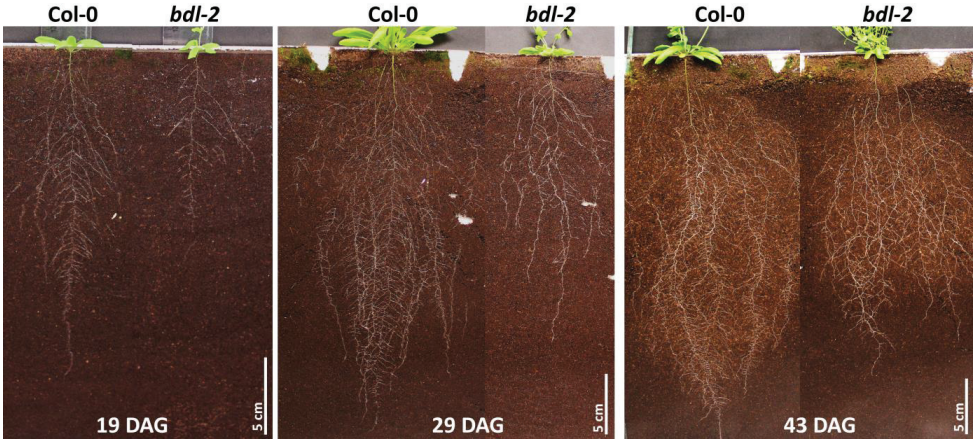


**Figure 18. RSA of *bdl-2* in soil.** The EMS 42-1/*bdl-2* mutant develops a smaller and less dense root system compared to Col-0, monitored in rhizotrons 19 DAG, 29 DAG and 43 DAG (scale bar = 5 cm).

## DISCUSSION AND CONCLUSIONS

In this study, an EMS-mutagenesis screen led to the identification of several mutants with drastically altered RSA phenotypes, from which three were analyzed in more detail.

**CESA6 controls the 'shallowness' of the root system**

We identified the EMS 24-2/*cesa6-3* mutant as a new *cesa6* loss-of-function mutant with reduced primary root growth and a dense network of horizontally growing LRs in seedlings **(Figure 4)**, developing into a dense shallow root system in mature plants **(Figure 9)**.

The *CESA6/PRC1/IXR2* gene belongs to a family of 10 *CESA* genes **(Figure 19A)**, which encode membrane-localized Glycosyl-Transferase family 2 (GT-2) enzymes that catalyze cellulose synthesis (Somerville, 2006). Cellulose is the most abundant biopolymer on Earth and consists of linear (1→4)-β-linked glucan chains that are assembled into cellulose microfibrils by multimeric cellulose synthase complexes (CSCs). Cellulose microfibrils form a major component of the primary and secondary cell walls, which give the plant cell its rigidness. The CSC is formed from three different CESA subunits that are assembled as trimers into a hexameric rosette superstructure, containing in total 18 CESA units that form 18-chain cellulose microfibrils (Vandavasi et al, 2016) **(Figure 19B)**. The CSC for the primary cell wall cellulose synthesis in the plant consists of CESA1, CESA3 and CESA6 subunits (Desprez et al, 2007), while the CSC for secondary cell wall cellulose synthesis consists of CESA4, CESA7 and CESA8 (Hill et al, 2014). While *cesa1* and *cesa3* null mutants are gametophytic lethal, *cesa6* null mutants are viable due to functional redundancy of *CESA6* with *CESA2* and *CESA5* (Desprez et al, 2007). Therefore, it is likely that the phenotype observed in the *cesa6* mutants is due to activity of either CESA2 or CESA5, which leads to different RSA features. In secondary cell wall formation, none of the CESA4, CESA7 or CESA8 subunits can be functionally replaced by another CESA protein. All three were shown to be induced by the master regulator MYB DOMAIN PROTEIN 46 (MYB46) (Kim et al, 2013). It would be interesting to identify a transcriptional regulator of *CESA6* (and *CESA2* or *CESA5*), for modulating their expression to alter RSA in a more controlled manner.

How altered cellulose synthesis leads to altered plant morphology can be explained by the directionality of cellulose microfibril synthesis. CSCs are anchored by the CELLULOSE SYNTHASE INTERACTING 1 (CSI1) protein to cortical microtubules that run just beneath the plasma membrane and are thought to move along these tracks during microfibril synthesis (Bringmann et al, 2012) **(Figure 19C)**. The orientation of extracellular cellulose microfibrils is thus determined by the orientation of the intracellular cortical microtubules. The orientation of the cellulose microfibrils dictates in which direction a cell can expand by turgor pressure (Schopfer, 2006) **(Figure 19D)**. In this manner, CESA proteins control cell shape and size, which translates to altered plant growth.

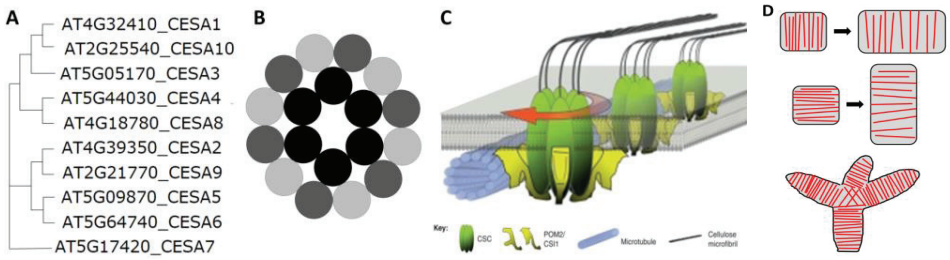


**Figure 19. CESA proteins control cellulose synthesis. (A)** Phylogenetic tree of *CESA1-10* genes in *Arabidopsis*. **(B)** The cellulose synthase complex (CSC) is formed from a hexameric rosette superstructure from trimers of three different CESA proteins. **(C)** The CSC moves along intracellular cortical microtubules and produces extracellular cellulose microfibrils, containing 18 chains of (1→4)-β- glucan (adapted from Bringmann et al., 2012). **(D)** The orientation of the cellulose microfibrils determines cell shape by restricting cell expansion.

In a previous study, mutants of the *CESA8*/*IRREGULAR XYLEM 1*/*LEAF WILTING 2* (*CESA8*/*IRX1*/*LEW2*) gene, *leaf wilting 2-1* (*lew2-1*) and *leaf wilting 2-2* (*lew2-2*), were shown to have enhanced drought and osmotic stress tolerance. The authors suggested this could be due to the observed elevated levels of abscisic acid (ABA), proline and soluble sugars, which are known to increase stress tolerance (Chen et al, 2005). However, based on the altered RSA observed in the *cesa6* mutants in this study, it could be interesting to check whether the enhanced drought and osmotic stress tolerance in the *cesa8* mutants could be due to an altered RSA.

Finally, it would be interesting to see whether the dense shallow root system of *cesa6* mutants performs better growing in low phosphate conditions, since such a RSA has been suggested to be more suited for uptake of phosphate located in the topsoil layers (Lynch, 1995; Hammond et al, 2009). Taken together, engineering RSA through altered cellulose synthesis could potentially lead to a RSA for enhanced drought tolerance and/or enhanced phosphate uptake.

**CAND1 controls the lateral root setpoint angle**

CAND1 is a HEAT (huntingtin-elongation-A-subunit-TOR)-repeat protein folding into a superhelical structure that wraps around the N-terminal domain of the CUL1 subunit from the SCF E3 ligase complex (Goldenberg et al, 2004). Its association with CUL1 depends on the post-translational modification of CUL1 with a conjugated RELATED TO UBIQUITIN/NEURAL PRECURSOR CELL EXPRESSED, DEVELOPMENTALLY DOWN-REGULATED 8 (RUB/NEDD8) protein (= neddylation) at lysine 720 (K720), which occurs in an analogous manner as ubiquitination (Dharmasiri et al, 2007; Hotton et al, 2011; Mergner & Schwechheimer, 2014).

CAND1 is believed to regulate assembly and disassembly of the SCF-complex in a cyclic neddylation-dependent manner. When CUL1 is modified with RUB/NEDD8, the SCF-complex is active and poly-ubiquitinates its substrate protein. After the substrate protein is targeted for proteasomal degradation, the COP9 SIGNALOSOME (CSN) complex de-neddylates CUL1, and the E2 component dissociates from RBX1. As CUL1 is no longer neddylated, CAND1 is able to bind CUL1, and displaces the ASK1 and F-box protein. Next, CUL1 is neddylated again by consecutive AUXIN RESISTANT 1 – E1-C-TERMINAL-RELATED 1 (AXR1-ECR1) or AXR1-LIKE 1 – ECR1 (AXL1-ECR1) and E2 RUB1 CONJUGATING ENZYME 1 (RCE1)-RUB/NEDD8 complex activity, which displaces CAND1. Finally, another ASK1 protein binds to CUL1 and recruits a new F-box protein with a substrate protein, which marks the start of the next cycle (Pierce et al, 2013; Wu et al, 2013) **(Figure 20)**.

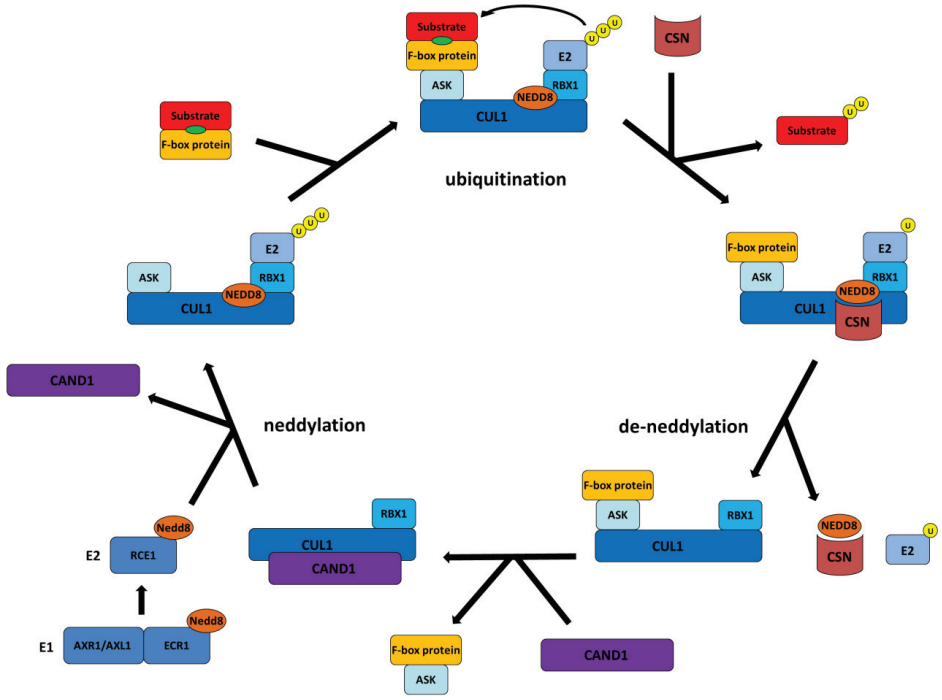


**Figure 20. Role of CAND1 in SCF cycle.** The assembly and disassembly of the SCF complex is dependent on cyclic neddylation/de-neddylation and CAND1 binding. After the substrate is poly-ubiquitinated by the SCF E3 ligase complex, it is targeted for proteasomal degradation. Loss of substrate facilitates recruitment of the COP9 SIGNALOSOME (CSN) protein that triggers de-neddylation of CUL1 and dissociation of the E2 conjugation enzyme from RBX1. After de-neddylation, CAND1 can bind CUL1 and displaces the ASK and F-box proteins. CUL1 is neddylated again by consecutive activity of the E1 AXR1/AXL1-ECR1 and E2 RCE1-NEDD8 complex, which leads to displacement of CAND1. ASK binds CUL1 and recruits another F-box protein and substrate protein targeted for degradation.

In this study, the EMS 48-1/*cand1-6* mutant was identified as a new *cand1* loss-of-function mutant with a dense network of LRs that grow under a steep angle along the primary root axis. This adds CAND1 to the currently very small list of known regulators that play a role in determining the LR setpoint angle. Although the LR growth angle plays such an important role in determining RSA, the factors playing a role in this process remain mostly unknown. LRs are known to partially suppress gravitropic growth in order to radially expand the root system (plagiotropism). In the primary root

tip, gravitropic root growth is mediated in part by the joint activity of the auxin efflux transporters PIN-FORMED 3 (PIN3), PIN4 and PIN7 which are present in the columella cells and upon gravistimulation trigger asymmetric auxin transport towards the lower side of the root tip. The asymmetric auxin flux is further transported by PIN2 and the auxin influx transporter AUXIN RESISTANT 1 (AUX1), from the lateral root cap cells to the lower epidermal cells in the elongation zone. This leads to differential cell elongation in the epidermal cells and eventually triggers root bending towards the gravity vector (Swarup et al, 2005). Interestingly, differential expression of *PIN3*, *PIN4* and *PIN7* is observed in the LRs compared to the primary root tip. In young LRs, PIN3 is present in the columella, while PIN4 and PIN7 are absent. In mature LRs, PIN3 is no longer present in the columella, while PIN4 and PIN7 are now present. These dynamic shifts in the presence/absence of PIN3, PIN4 and PIN7 in LRs generates differences in asymmetric auxin distribution compared to the primary root tip and are suggested to lead to the altered gravitropic response (Guyomarc'h et al, 2012; Rosquete et al, 2013). Besides auxin transport, auxin signaling is also affecting the LR setpoint angle, since reduced auxin signaling in the *tir1-1* mutant leads to more horizontally growing LRs, while enhanced auxin signaling by auxin treatment induces a steep LR setpoint angle (Rosquete et al, 2013). It would therefore be interesting to see if the *cand1* mutants show altered expression of PIN transporters or altered auxin response in the LR tip to induce the steep LR setpoint angle.

The 'steep and deep' narrow root system of the *cand1* mutants is potentially ideal for water and nitrate uptake from deeper regions in the soil (Song et al, 2003; Lynch & Brown, 2012; Uga et al, 2013). However, besides altered RSA, the *cand1* mutants are also drastically affected in the above-ground parts of the plant. The small bushy shoot of *cand1* mutants suggests a disturbance in auxin and/or strigolactone signaling (loss of apical dominance) and gibberellic acid signaling (stunted short shoot). Biochemical analysis showed that *cand1* mutants are less sensitive to auxin, jasmonic acid and gibberellic acid by reducing $SCF^{TIR1/AFB1-5}$, $SCF^{COI1}$ and $SCF^{SLY1}$ activity (Feng et al, 2004). Thus, CAND1 plays a role in various SCF-dependent signaling pathways, such as the auxin, jasmonic acid, strigolactone and gibberellic acid signaling pathways (Perez & Goossens, 2013; Wallner et al, 2016) **(Figure 21)**.

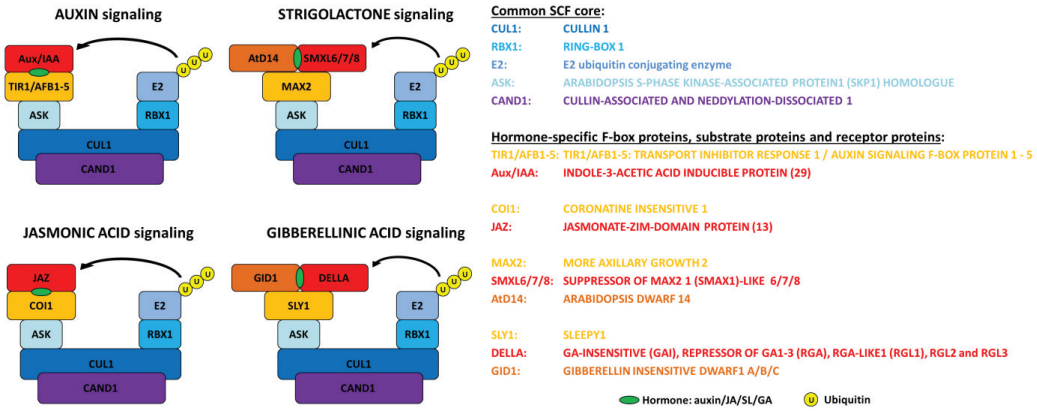


**Figure 21. CAND1 regulates the assembly and disassembly of the SCF-complex that is active during many signaling pathways, such as auxin, jasmonic acid (JA), strigolactone (SL) and gibberellic acid (GA) signaling.**

Besides these phytohormone-related signaling pathways, CAND1 was also implied to regulate the $SCF^{UFO}$ complex (UFO = UNUSUAL FLORAL ORGANS F-box protein) that plays a role during flower development, which might explain the small flowers and low fertility of the *cand1* mutants (Feng et al, 2004). Based on these observations, it seems that CAND1 regulates a wide range of SCF-complexes formed with different F-box proteins. Furthermore, besides interacting with the above-mentioned CUL1-containing SCF-complexes, CAND1 was also shown to interact with CUL4 in the CUL4-RBX1-CDD complex (CDD = COP10 – DET1 – DDB1a) controlling photomorphogenesis and ethylene signaling (Chen et al, 2006). Thus, it could be hypothesized that CAND1 might be a general regulator controlling assembly and disassembly of all SCF-complexes that can be formed from the 21 ASK proteins, 5 CUL proteins, 1 RBX1 protein, 41 E2 ubiquitin conjugating enzymes and more than 700 F-box proteins present in *Arabidopsis* (Risseeuw et al, 2003; Kraft et al, 2005). This explains the pleiotropic *cand1* mutant phenotypes, and necessitates a tissue-specific knock-down of *CAND1* to avoid the undesirable shoot phenotypes (*e.g.* small bushy shoot and low fertility/seed yield), while retaining the desired steep and deep RSA trait. If this approach could be successfully applied to crops in a controlled manner, the steep RSA might be beneficial for water and nutrient uptake in deeper soil regions (Song et al, 2003; Lynch & Brown, 2012; Uga et al, 2013).

**BDL controls lateral root spacing**

The EMS 42-1/*bdl-2* mutant was picked up for its altered LR spacing and LR clustering phenotype, which were shown to be due to a mutation in *IAA12/BDL* **(Figure 15)**. Previous studies already showed that the IAA12/BDL protein plays an important role in asymmetric cell divisions during embryonic root development and during lateral root formation (Hamann et al, 2002; De Smet et al, 2010). In these studies, it was shown that the copy number of the $BDL^{bdl-1}$ allele/transgene determines the phenotypical outcome, with two copies of the $BDL^{bdl-1}$ leading to drastically affected embryonic primary root growth, while one copy generates viable plants with a bushy shoot and clustered LRs. Thus, in the heterozygous/hemizygous situation, the wild type BDL proteins interacting with ARF proteins are degraded in the presence of auxin, thereby releasing the ARFs to immediately initiate transcription of the primary auxin response genes, while the mutant $BDL^{bdl-1}$ proteins are not (or to much lower extent) degraded and continue exerting their repressing effect on ARFs. Thus, a titration effect of wild type BDL proteins versus mutant $BDL^{bdl-1}$ proteins binding to ARFs determines the degree of auxin signaling. The milder phenotype observed in the homozygous EMS 42-1/*bdl-2* mutant, similar to a heterozygous *bdl-1* mutant, could be explained by the difference in the location of the mutation. The *bdl-1* mutation is situated right in the middle of the GW**P**PV motif that interacts with auxin, while the *bdl-2* mutation is a bit out of center of the **G**WPPV motif **(Figure 16)**. The binding affinity of the $BDL^{bdl-2}$ protein to the TIR1/AFB1-5 proteins might therefore be less drastically affected compared to the $BDL^{bdl-1}$ protein, and might still interact to some degree with the $SCF^{TIR1/AFB1-5}$ complex to become targeted for degradation. It would be interesting to test this hypothesis by measuring differences in binding affinity of BDL, $BDL^{bdl-1}$ and $BDL^{bdl-2}$ proteins to TIR1/AFB1-5 F-box proteins with for example surface plasmon resonance (SPR), isothermal titration calorimetry (ITC) or microscale thermophoresis (MST). It has already been demonstrated that differences in sequence in and around domain II are the main determinants of different binding affinities of members from the Aux/IAA protein family for TIR1/AFB1-5 proteins (Calderon Villalobos et al, 2012; Moss et al, 2015). Altogether, this suggests that site-directed mutagenesis in Aux/IAA proteins might be used in the future for engineering RSA, for example to obtain LR clusters in regions of higher nutrient concentrations in a controlled manner by placing the $BDL^{bdl-2}$ gene under the control of a nutrient-

responsive promoter. Furthermore, considering its milder phenotype compared to *bdl-1*, the *bdl-2* mutant can be used for future studies on IAA12/BDL signaling in post-embryonic lateral root development to study its role in the lateral inhibition mechanism, which determines spacing between LR formation.

**General conclusions**

A classical EMS-mutant screen was shown to be suitable to identify molecular components that have an impact on RSA. This approach has the advantage over genome-wide transcriptome analyses by starting immediately the selection based on an obvious altered RSA phenotype, while the latter approach has the advantage to pick candidate regulators from a list without risking ending up with a gene that was already characterized before. In this study, two out of three of the characterized mutants are linked to auxin signaling, which once more underscores the importance of auxin for shaping the root system. The remaining un-characterized EMS-mutants from this screen still provide a valuable resource for identifying other molecular components that affect RSA. Future targeted engineering of transgenic lines containing the altered RSA traits described above (shallow, steep and deep, local LR clusters), without the negative side-effects on shoot growth, will allow to use these lines as tools to study the performance of a specific RSA under various environmental conditions (*e.g.* drought stress, low phosphate or nitrate content). The mini-rhizotron set-ups used in this study, showed that results obtained through *in vitro* lab work can be translated to phenotypes that are retained in more natural growth conditions in the soil and provides a new approach to study RSA under the aforementioned various environmental conditions, bringing our research again one step closer to the field.

**ACKNOWLEDGEMENTS**

We thank Davy Opdenacker and Ana Rita Mendes Leal for help with the rhizotron set-ups. I.R. was supported by the Agency for Innovation by Science and Technology (IWT).

## MATERIAL AND METHODS

**Plant material**

*Arabidopsis thaliana* ecotype Col-0 was used as a control and for transformations in this study. SALK_004587/*cesa6-1* (N685082), *prc1-1* (N297), SALK_099479/*cand1-2*/*hve-2* (N599479), GK_190D07/*cand1-3* (N418187) and Ei-5/*hve-1* (N28225) were requested from the Nottingham Arabidopsis Stock Centre (NASC) collection. The SAIL_240_B04/*acr4-2* line (De Smet et al., 2008) was used for EMS-mutagenesis.

**EMS-mutagenesis**

Approximately 10,000 dry seeds (250 mg) are put in a 50 ml falcon tube overnight in water, gently shaking, for imbibition (better uptake of EMS). Replace the water with 15 ml 0.05% Triton X, vortex for 5 min, and then wash three times with 50 ml water. Replace with 0,3% EMS solution, which contains 30 µl ethyl methanesulfonate (EMS) diluted in 10 ml 0.1 M potassiumphosphate buffer pH 7.5 (17,42 g $K_2HPO_4.3H_2O$ + 13,61 g $KH_2PO_4$ in 1 liter water), and gently shake for 7.5 hours. Discard the EMS solution in 5 M NaOH and wash two times 15 min with 15 ml 100 mM $Na_2S_2O_3$, followed by washing four times with 30 ml water. Finally, transfer the T1 seeds to a new falcon tube with 30 ml water and gently shake overnight at 4 °C. General remark: Work in a fumehood (EMS is volatile) covered with absorbant benchcoat paper, and wrap up all lab material (*e.g.* pipetman) in parafilm at all time when handling EMS, and rinse everything in 5 M NaOH for two days after use before discarding.

**Plant growth conditions**

After the EMS-mutagenesis, T1 seeds should be sowed immediately in soil, with approximately 30 seeds per pot (dimensions: 15 cm diameter x 20 cm height) in 300 pots. Make sure you spray the topsoil with water and cover the pots with transparent plastic foil until the T1 seedlings are of sufficient size, then remove the foil but keep watering the pots until the T1 plants have set seed. Harvest the T2 seed for screening mutants with altered RSA.

For phenotypic analysis of the root system from the mutant lines, seedlings were grown at 21 °C under continuous light (110 µE $m^{-2}$ $s^{-1}$ photosynthetically active radiation, supplied by cool-white fluorescent tungsten tubes, Osram) on vertically oriented square petri plates containing 50 ml solid ½ MS growth medium supplemented with 1% sucrose (per liter: 2.15 g MS salts, 0.1 g myo-inositol, 0.5 g MES, 10 g sucrose, 8 g plant tissue culture agar; pH adjusted to 5.7 with KOH). For propagation and crossings, plants were grown on the Jiffy-7® pellets (www.jiffypot.com) in a greenhouse at 21 °C under long-day conditions (16/8 light/dark).

**Root phenotyping**

Seedlings were grown in the conditions described above for the number of days indicated in figure legends. Emerged lateral roots were counted using a stereo-microscope (CETI, Belgium). A high resolution scan was made from the seedlings with a tabletop flatbed scanner. Primary root length measurements were performed on the scanned images using ImageJ software (http://rsbweb.nih.gov/ij/index.html). Data were analyzed using Microsoft Office Excel software.

**Rhizotron**

To assemble the rhizosheets, take a white PVC plate (24 x 48 x 0.4 cm, Ispa Plastics) and a transparent plexi plate (24 x 48 x 0.4 cm, Ispa Plastics) with mousse spacers (48 x 2 x 0.4 cm) sandwiched in between at the side edges, and tape along the side edges and bottom with two layers of Micropore™ tape (2.5 cm wide) to hold them together. Then, fix everything together with slide binders over the side edges (A4 15 mm, Pavo, Fiducal catalog), keeping the top and bottom free. Use a sieve with mesh holes of 2.8 mm to sieve dried universal potting soil (AVEVE), and use a funnel to pour the sieved soil in the rhizosheet. Always fill the rhizosheet to the top and then gently tap the rhizosheet on the floor until the soil doesn't compact anymore. Repeat this process until 170 g of dry soil fills the rhizosheet completely in a homogenous manner. Seal the top with two layers of Micropore™ tape (2.5 cm wide) and place the rhizosheets overnight submerged in a waterbath (Overtoom transportbox RK906) supplemented with 2 mL WUXAL 8-8-6 solution (AVEVE) per liter of water. Place the soaked rhizosheets tilted at 45 degrees in a plastic box (30 x 40 x 30 cm, Overtoom) with the transparent plexi side facing downward (4 rhizosheets per box, separated by small spacers, such as caps of BD Falcon 5 mL tube) and cover place a cardboard sheet around the rhizosheets to keep the roots in the dark. Remove the Micropore™ tape at the top and sow 5 stratified seeds in the center of the rhizosheet. Cover with transparent Saran foil for 6 days to prevent the top layer from drying out during germination. After that, remove the foil and select one of the germinated seedlings to continue growing in the rhizosheet. Water the rhizosheet every two days with 5 mL water supplemented with 2 mL WUXAL 8-8-6 per liter solution at the top in two indents. After the desired amount of time, the rhizosheets can be taken out the box to take pictures of the root system through the transparent plexi sheet.

**CTAB DNA extraction**

Harvest plant material in a 2 ml microcentrifuge tube (50 ml falcon tube for SHOREmapping samples), freeze on liquid nitrogen, and grind material with two 3 mm metal balls for 1 min using a Retscher-machine at a frequency of 25 Hz (or grind manually with a mortar for SHOREmapping samples). Add 400 µl CTAB solution (10 ml CTAB solution for SHOREmapping samples) to grinded material and mix well [CTAB solution: 2% cetyltrimethylammonium bromide (CTAB), 100 mM Tris-HCl pH 7.5, 0.7 M NaCl, 20 mM EDTA, diluted in water]. Incubate the samples at 60°C for 30 minutes. Cool samples on ice to room temperature. Add 250 µl $CHCl_3$/IAA solution (6.25 ml $CHCl_3$/IAA solution for SHOREmapping samples) [$CHCl_3$/IAA solution: 96% chloroform ($CHCl_3$)/4% iso-amylalcohol (IAA)], mix for 1 min, and centrifuge for 10 min at 8,000 g (20 min at 4,000 g for SHOREmapping samples). Transfer 300 µl supernatant (7,5 ml supernatant for SHOREmapping samples) to a new 1.5 ml microcentrifuge tube (50 ml falcon tube for SHOREmapping samples) together with 300 µl isopropanol (7.5 ml isopropanol for SHOREmapping samples), mix well and incubate for 30 min on ice. Centrifuge 20 min at 10,000 g (30 min at 4,000 g for SHOREmapping samples) and discard the supernatant by decanting. Wash the remaining white pellet with 500 µl 70% ethanol (10 ml 70% ethanol for SHOREmapping samples). Centrifuge 5 min at 10,000 g (10 min at 4,000 g for SHOREmapping samples) and discard the supernatant by decanting. Dry the pellet for 20 min at 60°C to evaporate the remaining ethanol, and resuspend the DNA in 100 µl TE-buffer (2 ml TE-buffer for SHOREmapping samples) [TE-buffer: 10 mM Tris-HCl pH 8, 0.1 mM EDTA, diluted in water].

**Illumina sequencing and SHOREmapping**

Genome sequencing was performed with an Illumina Hiseq platform from VIB Nucleomics Core service facility (Leuven, Belgium), using 15 million paired-end reads of 50 nucleotides per sample. Mapping was performed by SHOREmap analysis according to the protocol documented by Schneeberger et al. (2008).

**Rough mapping**

PCR reaction mixture: 19,8 µl milliQ water, 3 µl 10x PCR buffer (Taq DNA Polymerase, recombinant kit, Invitrogen), 1.4 µl 50 mM MgCl2 (Taq DNA Polymerase, recombinant kit, Invitrogen), 0.2 µl Taq DNA polymerase (5U/µl) (Taq DNA Polymerase, recombinant kit, Invitrogen), 0.5 µl 10 mM dNTPs (Invitrogen), 1.3 µl 10 µM Fw primer, 1.3 µl 10 µM Rev primer and 2.5 µl CTAB DNA (total = 30 µl) per sample in a PCR-well tube. A list of primers from Hou et al. (2010) that was used for rough mapping can be found in addendum. PCR reaction conditions: 3 min at 95°C, followed by 50 cycles of 25 s at 95°C – 30s at 43-50°C – 50 s at 72°C, and followed by 7 min at 72°C, after which the PCR-samples are cooled and stored at 4°C. For gelelectrophoresis, 6x OrangeG loading dye (0.25% OrangeG in 50% glycerol diluted in 1x TAE buffer) was added to the PCR-sample and used for 3% agarose gel electrophoresis, with SYBR®safe (Invitrogen) for visualization of the bands under blue light.

## REFERENCES


Alonso-Peral MM, Candela H, del Pozo JC, Martinez-Laborda A, Ponce MR, Micol JL (2006) The HVE/CAND1 gene is required for the early patterning of leaf venation in Arabidopsis. *Development* **133:** 3755-3766

Bringmann M, Landrein B, Schudoma C, Hamant O, Hauser MT, Persson S (2012) Cracking the elusive alignment hypothesis: the microtubule-cellulose synthase nexus unraveled. *Trends Plant Sci* **17:** 666-674

Calderon Villalobos LI, Lee S, De Oliveira C, Ivetac A, Brandt W, Armitage L, Sheard LB, Tan X, Parry G, Mao H, Zheng N, Napier R, Kepinski S, Estelle M (2012) A combinatorial TIR1/AFB-Aux/IAA co-receptor system for differential sensing of auxin. *Nature chemical biology* **8:** 477-485

Celenza JL, Jr., Grisafi PL, Fink GR (1995) A pathway for lateral root formation in Arabidopsis thaliana. *Genes & development* **9:** 2131-2142

Chen H, Shen Y, Tang X, Yu L, Wang J, Guo L, Zhang Y, Zhang H, Feng S, Strickland E, Zheng N, Deng XW (2006) Arabidopsis CULLIN4 Forms an E3 Ubiquitin Ligase with RBX1 and the CDD Complex in Mediating Light Control of Development. *Plant Cell* **18:** 1991-2004

Chen Z, Hong X, Zhang H, Wang Y, Li X, Zhu JK, Gong Z (2005) Disruption of the cellulose synthase gene, AtCesA8/IRX1, enhances drought and osmotic stress tolerance in Arabidopsis. *The Plant journal : for cell and molecular biology* **43:** 273-283

Chuang HW, Zhang W, Gray WM (2004) Arabidopsis ETA2, an apparent ortholog of the human cullin-interacting protein CAND1, is required for auxin responses mediated by the SCF(TIR1) ubiquitin ligase. *Plant Cell* **16:** 1883-1897

De Rybel B, Audenaert D, Xuan W, Overvoorde P, Strader LC, Kepinski S, Hoye R, Brisbois R, Parizot B, Vanneste S, Liu X, Gilday A, Graham IA, Nguyen L, Jansen L, Njo MF, Inze D, Bartel B, Beeckman T (2012) A role for the root cap in root branching revealed by the non-auxin probe naxillin. *Nature chemical biology* **8:** 798-805

De Smet I, Lau S, Voss U, Vanneste S, Benjamins R, Rademacher EH, Schlereth A, De Rybel B, Vassileva V, Grunewald W, Naudts M, Levesque MP, Ehrismann JS, Inze D, Luschnig C, Benfey PN, Weijers D, Van Montagu MC, Bennett MJ, Jurgens G, Beeckman T (2010) Bimodular auxin response controls organogenesis in Arabidopsis. *Proc Natl Acad Sci U S A* **107:** 2705-2710

De Smet I, Vassileva V, De Rybel B, Levesque MP, Grunewald W, Van Damme D, Van Noorden G, Naudts M, Van Isterdael G, De Clercq R, Wang JY, Meuli N, Vanneste S, Friml J, Hilson P, Jurgens G, Ingram GC, Inze D, Benfey PN, Beeckman T (2008) Receptor-like kinase ACR4 restricts formative cell divisions in the Arabidopsis root. *Science* **322:** 594-597

Desprez T, Juraniec M, Crowell EF, Jouy H, Pochylova Z, Parcy F, Hofte H, Gonneau M, Vernhettes S (2007) Organization of cellulose synthase complexes involved in primary cell wall synthesis in Arabidopsis thaliana. *Proc Natl Acad Sci U S A* **104:** 15572-15577

Dharmasiri N, Dharmasiri S, Weijers D, Karunarathna N, Jurgens G, Estelle M (2007) AXL and AXR1 have redundant functions in RUB conjugation and growth and development in Arabidopsis. *The Plant journal : for cell and molecular biology* **52:** 114-123

Feng S, Shen Y, Sullivan JA, Rubio V, Xiong Y, Sun TP, Deng XW (2004) Arabidopsis CAND1, an unmodified CUL1-interacting protein, is involved in multiple developmental pathways controlled by ubiquitin/proteasome-mediated protein Degradation. *Plant Cell* **16:** 1870-1882

Fukaki H, Tameda S, Masuda H, Tasaka M (2002) Lateral root formation is blocked by a gain-of-function mutation in the SOLITARY-ROOT/IAA14 gene of Arabidopsis. *The Plant journal : for cell and molecular biology* **29:** 153-168

Goh T, Kasahara H, Mimura T, Kamiya Y, Fukaki H (2012) Multiple AUX/IAA-ARF modules regulate lateral root formation: the role of Arabidopsis SHY2/IAA3-mediated auxin signalling. *Philosophical transactions of the Royal Society of London Series B, Biological sciences* **367:** 1461-1468

Goldenberg SJ, Cascio TC, Shumway SD, Garbutt KC, Liu J, Xiong Y, Zheng N (2004) Structure of the Cand1-Cul1-Roc1 complex reveals regulatory mechanisms for the assembly of the multisubunit cullin-dependent ubiquitin ligases. *Cell* **119:** 517-528

Guyomarc'h S, Leran S, Auzon-Cape M, Perrine-Walker F, Lucas M, Laplaze L (2012) Early development and gravitropic response of lateral roots in Arabidopsis thaliana. *Philosophical transactions of the Royal Society of London Series B, Biological sciences* **367:** 1509-1516

Hamann T, Benkova E, Baurle I, Kientz M, Jurgens G (2002) The Arabidopsis BODENLOS gene encodes an auxin response protein inhibiting MONOPTEROS-mediated embryo patterning. *Genes & development* **16:** 1610-1615

Hamann T, Mayer U, Jurgens G (1999) The auxin-insensitive bodenlos mutation affects primary root formation and apical-basal patterning in the Arabidopsis embryo. *Development* **126:** 1387-1395

Hammond JP, Broadley MR, White PJ, King GJ, Bowen HC, Hayden R, Meacham MC, Mead A, Overs T, Spracklen WP, Greenwood DJ (2009) Shoot yield drives phosphorus use efficiency in Brassica oleracea and correlates with root architecture traits. *J Exp Bot* **60:** 1953-1968

Hill JL, Jr., Hammudi MB, Tien M (2014) The Arabidopsis cellulose synthase complex: a proposed hexamer of CESA trimers in an equimolar stoichiometry. *Plant Cell* **26:** 4834-4842

Himanen K, Vuylsteke M, Vanneste S, Vercruysse S, Boucheron E, Alard P, Chriqui D, Van Montagu M, Inzé D, Beeckman T (2004) Transcript profiling of early lateral root initiation. *Proc Natl Acad Sci U S A* **101:** 5146-5151

Hotton SK, Eigenheer RA, Castro MF, Bostick M, Callis J (2011) AXR1-ECR1 and AXL1-ECR1 heterodimeric RUB-activating enzymes diverge in function in Arabidopsis thaliana. *Plant Mol Biol* **75:** 515-526

Hou X, Li L, Peng Z, Wei B, Tang S, Ding M, Liu J, Zhang F, Zhao Y, Gu H, Qu LJ (2010) A platform of high-density INDEL/CAPS markers for map-based cloning in Arabidopsis. *The Plant journal : for cell and molecular biology* **63:** 880-888

Kim WC, Ko JH, Kim JY, Kim J, Bae HJ, Han KH (2013) MYB46 directly regulates the gene expression of secondary wall-associated cellulose synthases in Arabidopsis. *The Plant journal : for cell and molecular biology* **73:** 26-36

Kong X, Zhang M, De Smet I, Ding Z (2014) Designer crops: optimal root system architecture for nutrient acquisition. *Trends Biotechnol* **32:** 597-598

Kraft E, Stone SL, Ma L, Su N, Gao Y, Lau OS, Deng XW, Callis J (2005) Genome analysis and functional characterization of the E2 and RING-type E3 ligase ubiquitination enzymes of Arabidopsis. *Plant Physiol* **139:** 1597-1611

Lopez-Bucio J, Cruz-Ramirez A, Herrera-Estrella L (2003) The role of nutrient availability in regulating root architecture. *Curr Opin Plant Biol* **6:** 280-287

Lynch J (1995) Root Architecture and Plant Productivity. *Plant Physiol* **109:** 7-13

Lynch JP (2013) Steep, cheap and deep: an ideotype to optimize water and N acquisition by maize root systems. *Ann Bot* **112:** 347-357

Lynch JP, Brown KM (2012) New roots for agriculture: exploiting the root phenome. *Philosophical transactions of the Royal Society of London Series B, Biological sciences* **367:** 1598-1604

Maple J, Moller SG (2007) Mutagenesis in Arabidopsis. *Methods in molecular biology* **362:** 197-206

Mergner J, Schwechheimer C (2014) The NEDD8 modification pathway in plants. *Frontiers in plant science* **5:** 103

Moss BL, Mao H, Guseman JM, Hinds TR, Hellmuth A, Kovenock M, Noorassa A, Lanctot A, Villalobos LI, Zheng N, Nemhauser JL (2015) Rate Motifs Tune Auxin/Indole-3-Acetic Acid Degradation Dynamics. *Plant Physiol* **169:** 803-813

Nagpal P, Walker LM, Young JC, Sonawala A, Timpte C, Estelle M, Reed JW (2000) AXR2 encodes a member of the Aux/IAA protein family. *Plant Physiol* **123:** 563-574

Okushima Y, Fukaki H, Onoda M, Theologis A, Tasaka M (2007) ARF7 and ARF19 regulate lateral root formation via direct activation of LBD/ASL genes in Arabidopsis. *Plant Cell* **19:** 118-130

Perez AC, Goossens A (2013) Jasmonate signalling: a copycat of auxin signalling? *Plant, cell & environment* **36:** 2071-2084

Pierce NW, Lee JE, Liu X, Sweredoski MJ, Graham RL, Larimore EA, Rome M, Zheng N, Clurman BE, Hess S, Shan SO, Deshaies RJ (2013) Cand1 promotes assembly of new SCF complexes through dynamic exchange of F box proteins. *Cell* **153:** 206-215

Qu LJ, Qin G (2014) Generation and identification of Arabidopsis EMS mutants. *Methods in molecular biology* **1062:** 225-239

Risseeuw EP, Daskalchuk TE, Banks TW, Liu E, Cotelesage J, Hellmann H, Estelle M, Somers DE, Crosby WL (2003) Protein interaction analysis of SCF ubiquitin E3 ligase subunits from Arabidopsis. *The Plant journal : for cell and molecular biology* **34:** 753-767

Rogg LE, Lasswell J, Bartel B (2001) A gain-of-function mutation in IAA28 suppresses lateral root development. *Plant Cell* **13:** 465-480

Rosquete MR, von Wangenheim D, Marhavy P, Barbez E, Stelzer EH, Benkova E, Maizel A, Kleine-Vehn J (2013) An auxin transport mechanism restricts positive orthogravitropism in lateral roots. *Current biology : CB* **23:** 817-822

Schneeberger K, Ossowski S, Lanz C, Juul T, Petersen AH, Nielsen KL, Jorgensen JE, Weigel D, Andersen SU (2009) SHOREmap: simultaneous mapping and mutation identification by deep sequencing. *Nat Methods* **6:** 550-551

Schopfer P (2006) Biomechanics of plant growth. *Am J Bot* **93:** 1415-1425

Somerville C (2006) Cellulose synthesis in higher plants. *Annual review of cell and developmental biology* **22:** 53-78

Song R, Wu C, Ma L, Guo J, Xing F (2003) [Comparison of roots distribution in different maize plant type cultivars in the Songnen Plain]. *Ying yong sheng tai xue bao = The journal of applied ecology / Zhongguo sheng tai xue xue hui, Zhongguo ke xue yuan Shenyang ying yong sheng tai yan jiu suo zhu ban* **14:** 1911-1913

Swarup R, Kramer EM, Perry P, Knox K, Leyser HM, Haseloff J, Beemster GT, Bhalerao R, Bennett MJ (2005) Root gravitropism requires lateral root cap and epidermal cells for transport and response to a mobile auxin signal. *Nature cell biology* **7:** 1057-1065

Tatematsu K, Kumagai S, Muto H, Sato A, Watahiki MK, Harper RM, Liscum E, Yamamoto KT (2004) MASSUGU2 encodes Aux/IAA19, an auxin-regulated protein that functions together with the transcriptional activator NPH4/ARF7 to regulate differential growth responses of hypocotyl and formation of lateral roots in Arabidopsis thaliana. *Plant Cell* **16:** 379-393

Thole JM, Strader LC (2015) Next-generation sequencing as a tool to quickly identify causative EMS-generated mutations. *Plant signaling & behavior* **10:** e1000167

Tian Q, Reed JW (1999) Control of auxin-regulated root development by the Arabidopsis thaliana SHY2/IAA3 gene. *Development* **126:** 711-721

Uehara T, Okushima Y, Mimura T, Tasaka M, Fukaki H (2008) Domain II mutations in CRANE/IAA18 suppress lateral root formation and affect shoot development in Arabidopsis thaliana. *Plant Cell Physiol* **49:** 1025-1038

Uga Y, Kitomi Y, Ishikawa S, Yano M (2015) Genetic improvement for root growth angle to enhance crop production. *Breeding science* **65:** 111-119

Uga Y, Sugimoto K, Ogawa S, Rane J, Ishitani M, Hara N, Kitomi Y, Inukai Y, Ono K, Kanno N, Inoue H, Takehisa H, Motoyama R, Nagamura Y, Wu J, Matsumoto T, Takai T, Okuno K, Yano M (2013) Control of root system architecture by DEEPER ROOTING 1 increases rice yield under drought conditions. *Nat Genet* **45:** 1097-1102

Vandavasi VG, Putnam DK, Zhang Q, Petridis L, Heller WT, Nixon BT, Haigler CH, Kalluri U, Coates L, Langan P, Smith JC, Meiler J, O'Neill H (2016) A Structural Study of CESA1 Catalytic Domain of Arabidopsis Cellulose Synthesis Complex: Evidence for CESA Trimers. *Plant Physiol* **170:** 123-135

Vanneste S, De Rybel B, Beemster GT, Ljung K, De Smet I, Van Isterdael G, Naudts M, Iida R, Gruissem W, Tasaka M, Inze D, Fukaki H, Beeckman T (2005) Cell cycle progression in the pericycle is not sufficient for SOLITARY ROOT/IAA14-mediated lateral root initiation in Arabidopsis thaliana. *Plant Cell* **17:** 3035-3050

Wallner ES, Lopez-Salmeron V, Greb T (2016) Strigolactone versus gibberellin signaling: reemerging concepts? *Planta*

Wu S, Zhu W, Nhan T, Toth JI, Petroski MD, Wolf DA (2013) CAND1 controls in vivo dynamics of the cullin 1-RING ubiquitin ligase repertoire. *Nature communications* **4:** 1642

Xuan W, Audenaert D, Parizot B, Moller BK, Njo MF, De Rybel B, De Rop G, Van Isterdael G, Mahonen AP, Vanneste S, Beeckman T (2015) Root Cap-Derived Auxin Pre-patterns the Longitudinal Axis of the Arabidopsis Root. *Current biology : CB* **25:** 1381-1388

Yang X, Lee S, So JH, Dharmasiri S, Dharmasiri N, Ge L, Jensen C, Hangarter R, Hobbie L, Estelle M (2004) The IAA1 protein is encoded by AXR5 and is a substrate of SCF(TIR1). *The Plant journal : for cell and molecular biology* **40:** 772-782

## SUPPLEMENTAL DATA

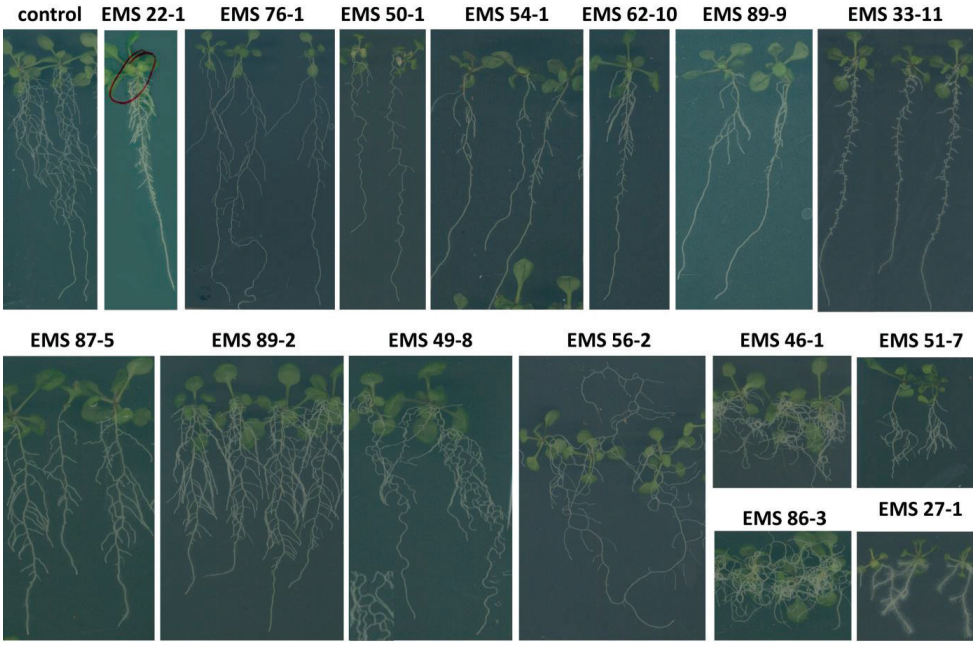


**Figure S1. Overview of other EMS-mutant with altered RSA.** EMS 22-1, EMS 76-1, EMS 50-1, EMS 54-1, EMS 62-10 and EMS 89-9 were affected in LR spacing. The EMS 33-11 mutant showed stunted LRs that undergo growth arrest. EMS 87-5 and EMS 89-2 showed a similar RSA as the EMS 24-2 (*cesa6*) mutant. EMS 49-8 showed extremely wavy primary root. EMS 56-2, EMS 46-1 and EMS 86-3 showed non-gravitropic roots. EMS 51-7 showed a very short branched root system. And EMS 27-1 showed a short root full of root hairs.

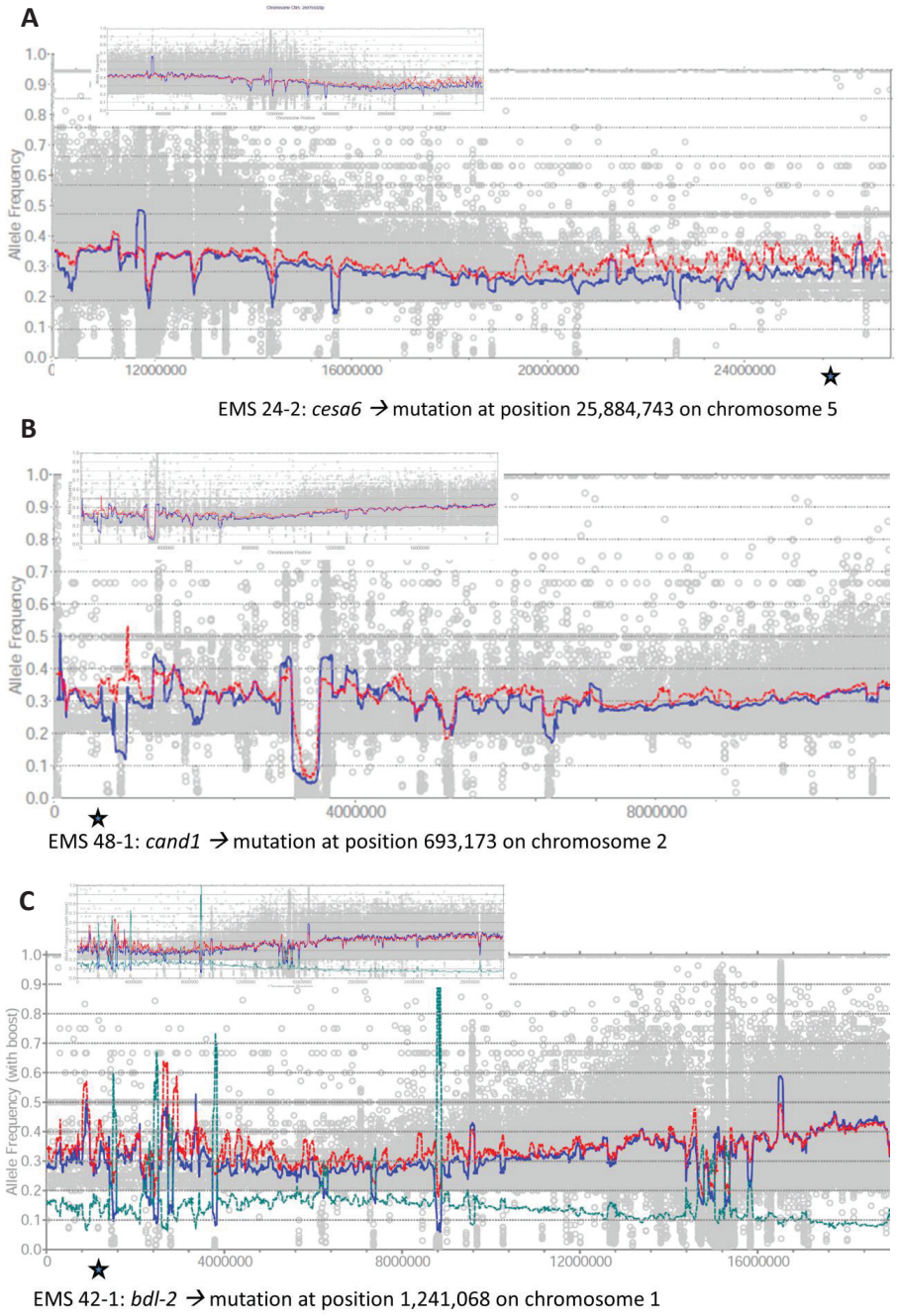


**Figure S2. Detailed view of location of causative mutation in the EMS-mutants through SHOREmap analysis. (A)** Location of EMS 24-2 mutation in CESA6 gene. **(B)** Location of EMS 48-1 mutation in CAND1 gene. **(C)** Location of EMS 42-1 mutation in BDL/IAA12 gene. (*Note:* no clear peaks were found at these sites on the SHOREmap pictures, although further analysis clearly showed that the location of the mutations was situated in these genes)

# PART III:
# General conclusions and perspectives

# GENERAL CONCLUSIONS AND PERSPECTIVES

In this part, some general conclusions from this study will be discussed, along with questions that arose and potential approaches to answer these questions in future studies.

**The evolutionary need for the diversification of (CEP) signaling peptides**

The formation of novel plant structures with ever-increasing complexity during plant evolution required novel signaling molecules for cell-to-cell communication to ensure a strict coordination between cell division and differentiation. Evolution answered this need with the emergence of many different families of signaling peptides.

Our evolutionary analysis ***(Chapter 3)***, together with that from the group of Michael Djordjevic, revealed that *CEP* genes only emerged at the point of seed plants divergence: they are present in angiosperms and gymnosperms, but absent in lycophytes (*e.g. Selaginella moellendorffii*), bryophytes (*e.g. Physcomitrella patens*) and green algae (Delay et al, 2013; Roberts et al, 2013; Ogilvie et al, 2014). A sequenced genome of pterophytes is currently lacking, making it impossible to tell if *CEPs* already originated at that point or not. Similarly to CEP genes, the closely related *IDA/IDL* family also appeared from the seed plant lineage onwards (Vie et al, 2015). In contrast, *RALF* genes can be phylogenetically traced back to lycophytes and bryophytes (Cao & Shi, 2012), while *CLE* genes already originated in Charophyta green algae, from which land plants evolved (Oelkers et al, 2008) **(Figure 1)**.

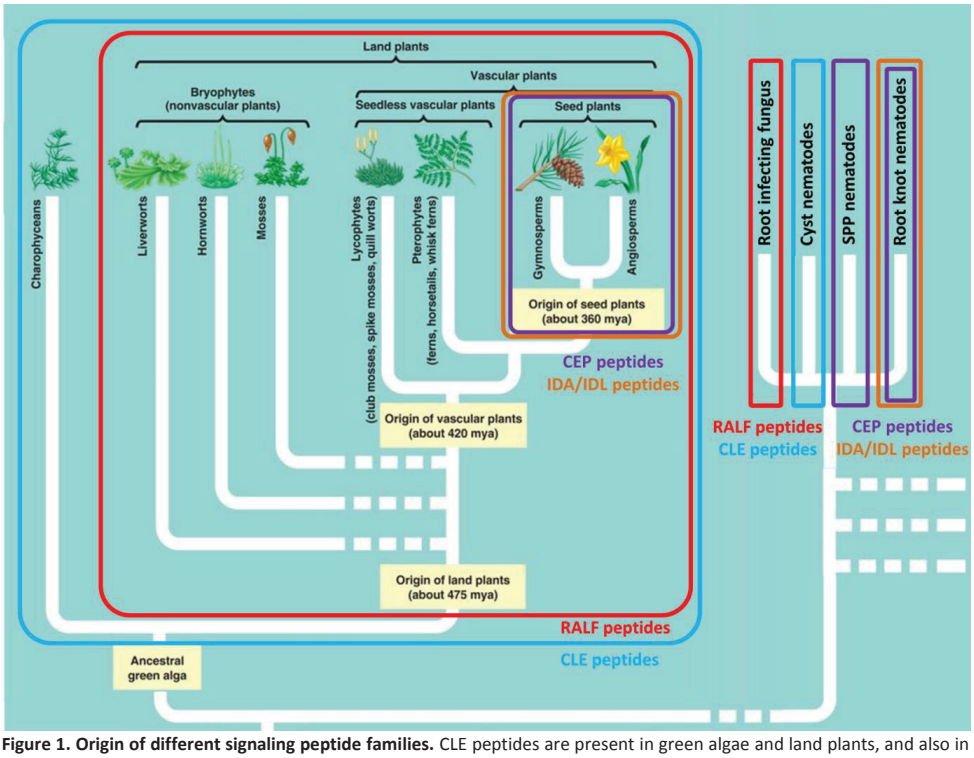


**Figure 1. Origin of different signaling peptide families.** CLE peptides are present in green algae and land plants, and also in cyst nematodes. RALF peptides are present in all land plants. CEP and IDA/IDL peptides are present in seed plants, and also in root knot nematodes and sedentary plant-parasitic (SPP) nematodes (image adapted from kaiserscience.wordpress.com).

This is further corroborated by expression patterns of *CEP* genes that can be correlated with the formation of evolutionary novel plant structures, such as seed development, flower development, nodule formation and lateral root formation from the pericycle ***(Chapter 3, 4 and 5)*** (Imin et al, 2013; Roberts et al, 2013).

Sequence analysis of mature CEP peptides during plant evolution revealed that the C-terminal part (GHSPGI/VGH) is highly conserved, whereas the N-terminal part showed more variation, especially in the *Solanaceae* from the Asterids group (Ogilvie et al., 2014) **(Figure 2)**. From this study, it is highly likely that an arginine (R) at the crucial position 3 is the default residue, while other residues at this position (*e.g.* threonine (T) in *Pinaceae*, aspactic acid (D) in *Poaceae*, lysine (K) in *Fabaceae* or alanine (A) in *Brassicaceae*) probably emerged later during further diversification events. These differences in amino acid residues might lead to altered activity of the CEP peptide ***(Chapter 4)***, or binding to different receptors (remains to be determined in future experiments).

A phylogenetic analysis of CEP receptor proteins in the plant lineage might reveal if all seed plants contain two CEP receptors, similar to CEPR1/XIP1 and CEPR2 from *Arabidopsis*, or whether older plant lineages (gymnosperms) only contain one CEP receptor, from which (an) additional CEP receptor(s) later originated through duplication events in younger plant lineages (eudicots). And, it might reveal if the diversification of CEP peptides in the Asterids is accompanied by a corresponding diversification of CEP receptor proteins. Such an evolutionary analysis has been performed for the HAESA (HAE)/HAESA-LIKE receptor family (Stø et al., 2015).

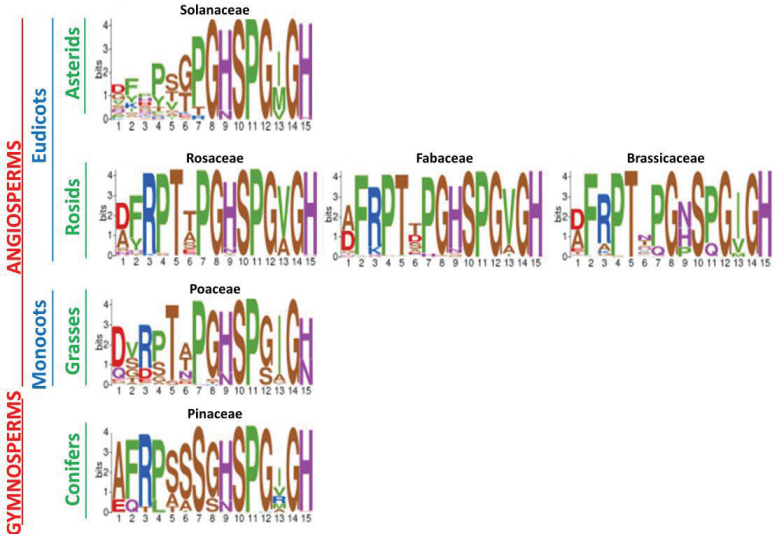


**Figure 2. Evolutionary analysis of CEP peptides in the plant lineage.** CEP peptides are present in seed plants, represented by gymnosperms and angiosperms. The C-terminal part of the CEP peptides contains a higher sequence conservation, whereas the N-terminal part shows more diversity. There are some noteworthy differences between the plant groups/families. Gymnosperms (represented by *Pinaceae* from the conifers) contain a serine (S) at position 7, whereas angiosperms (represented by monocots and eudicots) generally contain a proline (P) residue at position 7. Gymnosperms generally contain an alanine (A) at position 1, monocots generally contain an aspartic acid (D) at position 1, while rosids generally contain either an alanine (A) or an aspartic acid (D) residue at position 1, and asterids show a high level of diversification. At position 3 in the CEP peptides, generally an arginine (R) residue is found, with some differences in alternative residues for each plant groups/families: a threonine (T) in *Pinaceae*, an aspartic acid (D) in *Poaceae*, a lysine (K) in *Fabaceae*, and an alanine (A) in *Brassicaceae*, while a large diversification occurred in *Solanaceae*. (Figure adapted from Ogilvie et al., 2014)

Furthermore, our sequence analysis in *Arabidopsis thaliana* revealed that some *CEP* genes are organized in tandem repeats on the genome, and that some *CEP* genes code for prepropeptides with multiple CEP domains, from which separate mature CEP peptides are derived (***Chapter 3)***. Thus, sequence duplication events occurred at two levels: complete gene tandem duplications and intragenic peptide domain tandem duplications. These duplication events contributed significantly to the diversification of the CEP peptide family and resulted in a wide array of mature CEP signaling peptides specific for many different biological processes (***Chapter 3 and 4)***. Notably, bioinformatics analysis revealed that *CEP* genes with multiple CEP domains only occur in angiosperms, and that the CEP domain sequence diversity significantly increased in angiosperms compared to gymnosperms (Ogilvie et al, 2014).

Intriguingly, secreted CEP-mimic peptides also originated independently in root-knot nematodes and sedentary plant parasitic nematodes (Bobay et al, 2013; Eves-van den Akker et al, 2016), while IDA/IDL-mimic peptides were also identified in root-knot nematodes, and some cyst nematodes were found to produce CLE-mimic peptides (Guo et al, 2011; Wang et al, 2011; Tucker & Yang, 2013; Chen et al, 2015). These mimic-peptides are used to hijack the plant machinery to establish a suitable feeding environment during parasitic infection. Novel plant organs (root knots or cysts) are induced by these parasitic nematodes, suggesting that these secreted elicitors probably play a role in *de novo* organ formation in plants.

In conclusion, the CEP peptide family originated in seed plants as a relatively young peptide family associated with the formation of novel plant structures. But CEP peptides also evolved outside plant species, in plant-parasitic root knot nematodes, either through convergent evolution or through horizontal gene transfer, and are also associated with the formation of novel plant structures.

**A heterogeneous CEP family**

In our study, in parallel with the group of Michael Djordjevic, an additional ten *CEP* genes were identified on top of the originally five-member *CEP* family in *Arabidopsis* (Ohyama et al, 2008; Delay et al, 2013; Roberts et al, 2013). Based on the sequence of the mature CEP peptides, we initially divided the CEP family into two groups: group I (CEP1 to CEP12) and group II (CEP13 to CEP15), in which group I members typically contain three prolines (at position 3, 7 and 11), whereas group II members only have two prolines (at position 9 and 11) ***(Chapter 3)***.

Through a gain-of-function analysis using overexpression lines for all 15 *CEP* genes, clear differences in the effect on plant growth were found between group I and group II members. Furthermore, group I CEP peptides could be subdivided into three functional subgroups based on a correlation between gain-of-function phenotypes and the amino acid at position 3 in the mature CEP peptides. Subgroup Ia CEP peptides, encoded by *CEP2*, *CEP9* and *CEP10*, generally contain a hydrophobic alanine residue at position 3, and their overexpression has no drastic impact on root and shoot growth. Subgroup Ib CEP peptides, encoded by *CEP1*, *CEP3*, *CEP4*, *CEP5*, *CEP7*, *CEP8*, *CEP11* and *CEP12*, all contain a positively charged hydrophilic arginine residue at position 3, and their overexpression leads to a drastic reduction in root and shoot growth. Subgroup Ic only consists of the CEP6a and CEP6b peptides, which contain a hydrophobic glycine and a negatively charged hydrophilic glutamic acid residue at position 3 respectively, and their overexpression leads to intermediate reduced root and shoot growth. This suggested that the amino acid at position 3 might possibly be an important contributor to different activity in the CEP I subgroups. On the other hand, group II CEP

peptides, encoded by *CEP13*, *CEP14* and *CEP15*, contain multiple differences in conserved amino acid residues at the N-terminal part compared to group I CEP peptides, and their overexpression leads to an increase in the size of the root system, opposite to most group I members. Another difference between group I and group II members is the response to auxin, as most group I *CEP* genes are downregulated by auxin treatment, whereas group II members are upregulated. Altogether, this suggests that group II CEP peptides form a separate functional class compared to group I CEP peptides, and group I CEP peptides can be subdivided into three functional subgroups ***(Chapter 4)***.

Ligands with small differences in sequence but an overall similar structure can sometimes still bind to the same receptor, but could have opposing effects on activation or inactivation of the receptor. Such ligands binding to the same receptor with opposing functional activity are known as agonistic and antagonistic ligands, respectively, and have been shown to naturally occur in organisms to control developmental processes (Hruby, 2002; Tolbert et al, 2007; Gabay & Towne, 2015). For the CLE peptide family, it has been described how a single mutation of glycine at position 6 into a threonine residue in the mature CLV3 peptide could turn it into an antagonistic ligand for its receptor (Song et al, 2013). This observation even served as the base for developing the 'antagonistic peptide technology' (Song et al, 2013), although it has been suggested that this technology doesn't always work and requires some structural knowledge (Czyzewicz et al, 2015). Another recent study in stomata development illustrated a naturally occurring competitive binding between the closely related agonistic EPIDERMAL PATTERNING FACTOR (EPF2) peptide ligand and the antagonistic STOMAGEN/EPF-LIKE9 peptide ligand for the same receptor, the LRR-RLK ERECTA (ER). Binding of the antagonistic STOMAGEN/EPFL9 to ER prevents EPF2 from binding to ER, and thereby prevents activating a downstream MITOGEN ACTIVATED PROTEIN KINASE (MAPK) signaling cascade, which is only triggered by the agonistic EPF2 ligand (Lee et al, 2015). Future studies on CEP peptide signaling might reveal if the different (sub)groups of CEP peptides, with small differences in sequence but different functional activity, could potentially bind as agonists and antagonists to their receptors. At the molecular level, an antagonistic CEP peptide ligand could potentially be explained by still being able to bind the receptor protein, but not with the co-receptor, and therefore does not lead to receptor activation.

Interestingly, the CEP members that show no, or less drastic, reduced root growth and delay in flowering, happen to be *CEP* genes that code for prepropeptides with multiple CEP domains: CEP2, CEP9 and CEP10 from subgroup Ia, and CEP6 from subgroup Ic ***(Chapter 3)***. Therefore, one might believe that overexpression of these *CEP* genes has no, or a less drastic, effect on plant growth because they might not lead to the production of functional mature CEP peptides. However, it has been shown that overexpression of *CEP6* and *CEP9* leads to the production of mature CEP peptides from each of the two and five CEP domains in their prepropeptides respectively (Tabata et al., 2014), suggesting that these multi-CEP-domain-prepropeptides undergo correct proteolytic processing into functional mature CEP peptides. Also, it has been shown that application of relatively low concentrations (nanomolar range) of synthetic CEP peptides already leads to significant effects on plant growth ***(Chapter 5)***. Therefore, it is reasonable to assume that these overexpression lines, with more than 1000-fold increased expression levels ***(Chapter 4)***, would lead to sufficiently increased levels of the mature CEP peptides to have an effect on plant growth. Since, no phenotype is observed for these members, it is more likely that this is due to differences in their structure than processing.

**Expression analysis suggests distinct roles in CEP signaling**

Expression analysis of all 15 *CEP* genes showed that some members have very specific expression patterns (*e.g.* leaf hydathodes, stipules, trichome socket cells or epidermal cells overlaying an emerging lateral root primordium), but in most cases there were large overlaps in expression of *CEP* genes from each (sub)group, mainly in the flower organs, in the shoot apical meristem region, in the leaf- and root vasculature, in the pericycle and during lateral root development. Interestingly, only *CEP14* showed expression in the primary- and lateral root apical stem cell niche ***(Chapter 4)***.

Noteworthy, in most cases, there was usually one representative from each functional subgroup present in each expression domain **(Figure 3)**. It remains to be determined if these overlapping CEP peptides all bind and activate the same receptor in a similar manner, or if they compete and act as agonists and antagonists, or if they bind different receptors. It would be interesting to check what happens after co-treatments of synthetic CEP peptides from different subgroups. Would the different CEP peptides compete for the same receptor, or would they bind a different receptor to activate another developmental process? For the CLE peptide family, it was previously shown that members from different functional classes, surprisingly, could act synergistically to induce proliferative cell division during vascular development (Whitford et al, 2008). Finally, it remains to be determined whether CEPR1/XIP1 and CEPR2 are the only receptors for the CEP peptides, since only members from subgroup Ib have been suggested to bind CEPR1/XIP1 and CEPR2 (Tabata et al, 2014), but it is not known if group II CEP peptides also bind to these receptors or to some other receptor. One potential candidate CEP receptor is the LRR RLK protein HAIKU2 (IKU2) (see below). Future analysis is required to answer these burning questions.

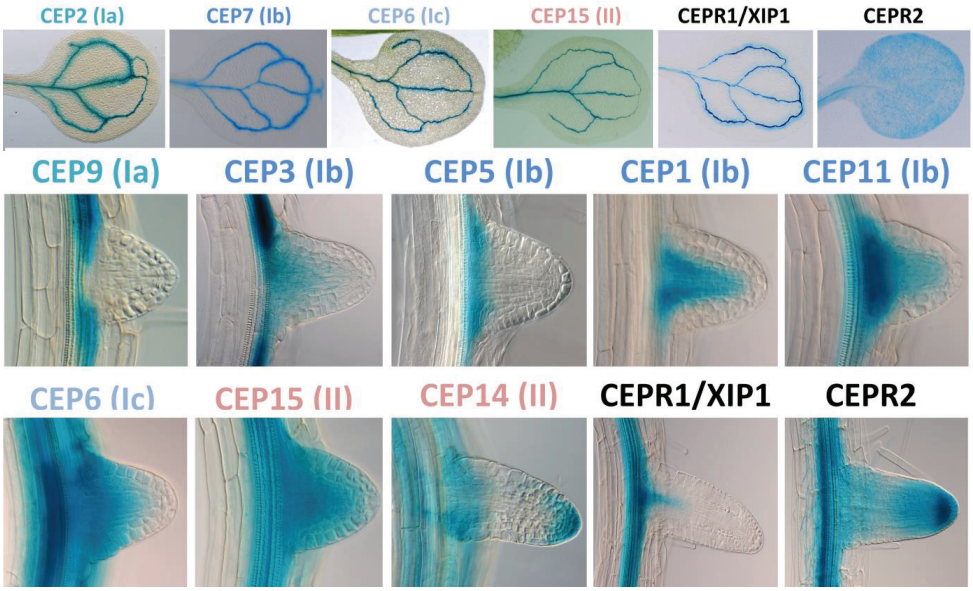


**Figure 3. Overlapping expression of *CEP* genes from different (sub)groups and their receptors. (A)** Expression pattern of *CEP2* (Ia), *CEP7* (Ib), *CEP6* (Ic), *CEP15* (II), *CEPR1/XIP1* and *CEPR2* genes in the cotyledon, visualized through *promoter::nls-GFP/GUS* reporter lines. **(B)** Expression pattern of *CEP9* (Ia), *CEP3* (Ib), *CEP5* (Ib), *CEP1* (Ib), *CEP11* (Ib), *CEP6* (Ic), *CEP15* (II), *CEP14* (II), *CEPR1/XIP1* and *CEPR2* genes during lateral root development, visualized through *promoter::NLS:GFP:GUS* reporter lines.

Expression analysis of *CEPR1*/*XIP1* and *CEPR2* revealed that the receptors are expressed in tissues overlapping with *CEP* expression; however, the two receptors themselves are never expressed in the same tissues. *CEPR1*/*XIP1* is expressed in the flower receptacle and petal veins, in the leaf venation, in the basal meristem in the phloem pole-associated pericycle cells, and in the phloem companion cells in the differentiation zone of the root. In contrast, *CEPR2* is expressed in the pistil and stamen of the flowers, in the shoot apical meristem, in the leaves, in the metaxylem, in the (xylem pole-associated) pericycle cells, and in the primary- and lateral root tips in the apical stem cell niche and columella ***(Chapter 4)***. Considering the non-overlapping expression patterns of the CEP receptors, they probably regulate different developmental processes and are likely not functionally redundant.

**CEP peptide signaling controls root system architecture**

Mutant analysis suggested that CEP signaling plays a role in shaping root system architecture. In agreement with the non-overlapping expression patterns of the receptors, loss-of-function mutants for *CEPR1*/*XIP1* and *CEPR2* showed different root phenotypes. The *xip1-1* mutant showed a drastic reduction in primary root length and number of lateral roots, while the *cepr2* mutants showed no drastic differences in the primary root length and number of lateral roots. For the *CEP* genes, gain-of-function analysis showed that overexpression of *CEP* Ib genes drastically reduces the size of the root system through a gradual consumption of the root apical meristem, whereas higher-order loss-of-function mutants of the *CEP* Ib genes showed an increase in the size of the root system. This suggests that these CEP Ib peptides might function as negative regulators of the size of the root system. On the other hand, overexpression of group II members led to an increase in size of the root system, suggesting that these act as positive regulators of the size of the root system. Altogether, CEP peptides function as root growth control regulators ***(Chapter 4)***.

Unfortunately, no T-DNA insertion lines are available for *CEP6* and *CEP15,* which are the two most abundantly expressed *CEP* genes throughout the plant. One might wonder if the reason for not having an available mutant line for these members is due to a possible vital function in plant development, or is merely by coincidence. It would be interesting to see how mutants for these members would affect plant development. Recent progress in the field of site-directed mutagenesis with CRISPR technology, might allow obtaining knock-out mutants for all *CEP* genes, also for CEP genes for which no mutant lines are available (Feng et al, 2013; Li et al, 2013; Fauser et al, 2014; Zhang et al, 2015). This would also allow knocking-out multiple *CEP* genes at once, including those that are arranged in tandem duplications on the genome, which are impossible to obtain by crossing. This novel molecular approach will revolutionize the way for future studies in peptide signaling.

**A case study: CEP5 negatively regulates lateral root initiation by altering the auxin response**

The CEP5 peptide, belonging to subgroup Ib, was shown to be expressed during the entire lateral root developmental process, from lateral root priming in the basal meristem to lateral root emergence. However, CEP5 is not expressed in the xylem pole-associated pericycle cells, from which lateral root are formed, but instead is expressed specifically in the phloem pole-associated pericycle cells that are associated with the sites (along the longitudinal axis) of lateral root formation. Synthetic CEP5 peptide treatments and *CEP5* overexpression lead to reduced lateral root initiation, while a *CEP5* RNAi knock-down line showed an increase in lateral root initiation, suggesting that CEP5 negatively regulates lateral root initiation. Expression of *CEPR1*/*XIP1* was shown to overlap with *CEP5* expression, and was proposed to function as its receptor. The *xip1-1* mutant showed a reduction in LR initiation, similar to *CEP5* overexpression or CEP5 synthetic peptide treatment ***(Chapter 5)***.

The latter observation might suggest that CEP5 negatively regulates CEPR1/XIP1 activity, possibly explained by an antagonistic role of CEP5 for CEPR1/*XIP1*. Alternatively, CEP5 could signal as an agonist through CEPR2, which is expressed at the sites of lateral root initiation in the xylem pole-associated pericycle cells, and for which the *cepr2* mutant phenotype suggests a repressing function of CEPR2 on (lateral) root growth. To determine which receptor functions as the receptor CEP5, further analysis is necessary. At one hand, this requires to perform *in vitro* binding studies, to determine the binding affinity (Kd values) of the CEP5 peptide to both receptors, for example through microscale thermophoresis. And on the other hand, *in planta* confirmation is required. For example, the availability of the *pCEPR1::CEPR1-GFP* and *pCEPR2::CEPR2-GFP* lines can be used to check internalization of the receptors upon CEP5 peptide application to determine if they act as receptors, since receptor endocytosis is known to occur upon ligand binding. In combination, the applied CEP peptide could be fluorescently labeled (checked for bio-activity first) to visualize the CEP5-induced internalization of the receptor, similar to studies on AFCS-labeled brassinosteroid and BRI1 internalization (Irani et al, 2012). Furthermore, it remains to be determined *in planta* if the CEP5 peptide remains at the phloem pole to bind the local CEPR1/XIP1 receptor, or migrates to the xylem pole to bind the CEPR2 receptor. However, this is a challenging task to handle, since currently no straightforward method is available to check this. C-terminal or N-terminal eGFP translational fusion to CEP peptides is not an option, since it is removed during proteolytic processing of the mature peptide, and it would be unlikely that a 15 amino acid mature peptide still reflects a natural situation when a bulky 32.7 kDa GFP protein is attached. Thus, alternative labeling methods are required in future studies, such as for example attaching a much smaller tetracysteine-containing motif (CCPGCC) to the peptide, which can selectively react with fluorescein-containing biarsenical helix binder (FlAsH-$EDT_2$), or attaching tetraserine motifs to the peptide that bind rhodamine-derived bisboronic acid reagent (RhoBo) (Griffin et al, 1998; Lang & Chin, 2014). Future technological advances in this field of peptide labeling will greatly serve the peptide signaling community.

Further analysis on the mode-of-action of CEP5 activity on lateral root initiation revealed that it might be caused by a reduced auxin response in the basal meristem during the priming event. Several lines of evidence (DII-VENUS, IAA19:HA and BDL-GUS) showed that CEP5 signaling leads to the stabilization of Aux/IAA proteins, which are known to repress the transcriptionally activating ARF proteins, and thereby reduces the expression of the primary auxin response genes. A yeast system that was engineered to monitor auxin-induced degradation of plant Aux/IAA proteins through the fluorescence of YFP-IAA7 and YFP-IAA28 fusion proteins was also used to show that CEP5 negatively affects the auxin-mediated degradation of the Aux/IAA fusion proteins in the presence of a functional TIR1 protein, while this was not observed for a mutated non-functional CEP5 peptide or a mock treatment ***(Chapter 6)***. The latter observation might raise some questions, since it suggests that the CEP5 peptide might directly act on the TIR1-Aux/IAA complex in the nucleus. This would be in conflict with the assumed CEP5 signaling pathway through binding to the proposed membrane-localized CEPR receptors and activating a phosphorylation cascade. Thus, unless yeast has a CEPR-like receptor that is activated by CEP5 peptide and somehow triggers a phosphorylation cascade that stabilizes Aux/IAA proteins, it suggests that CEP5 might directly bind the Aux/IAA – TIR1 complex to reduce their interaction. Future analysis on the (intra-)cellular localization of the CEP5 peptide will be required to answer these questions.

**A current model for CEP signaling**

Based on the observations mentioned above, a model is proposed in which most CEP peptides from group I are down-regulated by auxin and act as negative regulators of root growth, whereas CEP peptides from II are upregulated by auxin and act as positive regulators of root growth. It is currently still unclear which CEP peptides bind to which receptor, and if the peptides can function as agonists and antagonists. Furthermore, details about the mechanism through which CEP signaling controls root growth is unknown, but might involve fine-tuning the auxin response by stabilization of Aux/IAA proteins **(Figure 4)** ***(Chapters 4, 5 and 6)***.

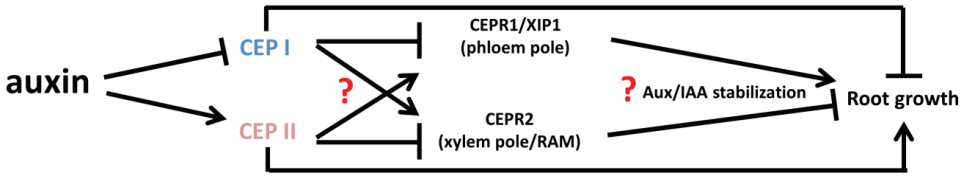


**Figure 4. Model for CEP signaling.** Auxin downregulates group I *CEP* gene expression, while it upregulates group II *CEP* gene expression. Group I CEP peptides reduce root growth, while group II CEP peptides stimulate root growth. It is currently unknown which CEP peptides bind to CEPR1/XIP1 or CEPR2, and how their signaling impacts root growth. One potential mechanism is by finetuning auxin signaling through Aux/IAA protein stabilization (*e.g.* CEP5).

**Future studies on CEP signaling: starting from a structural analysis of the receptor**

CEPR1/XIP1 and CEPR2 are LRR-RLKs from the subfamily XI and contain a short secretory signal peptide (SP) sequence, an N-terminal extracellular LRR receptor domain, a single helical transmembrane region and a C-terminal cytoplasmic serine/threonine kinase domain **(Figure 5-6A)**.

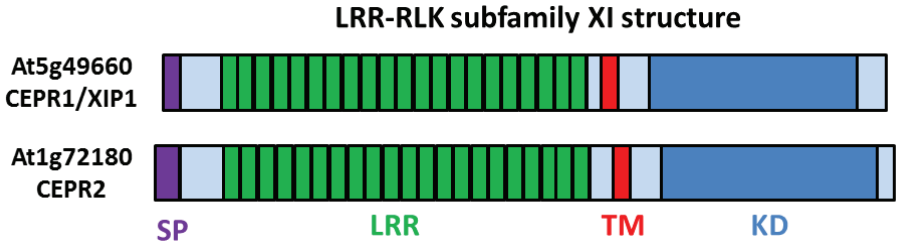


**Figure 5. Structure of CEPR1/XIP1 and CEPR2.** CEPR1/XIP1 and CEPR2 are LRR-RLKs from subfamily XI, with a signal peptide (SP), an N-terminal leucine-rich repeat receptor domain (LRR), a transmembrane region (TM), and a kinase domain (KD).

Nuclear magnetic resonance (NMR) analysis has already been performed to determine the structure of mature CEP peptides. This showed that CEP peptides adopt a β-turn-like-conformation, and illustrated that the proline hydroxylations alter conformational plasticity (Bobay et al., 2013). This structural data on CEP peptide ligands, combined with future detailed 3D-structural information about the CEPR1/XIP1 and CEPR2 receptor proteins might help in determining which residues in the LRR-receptor domain are interacting with each residue of the mature CEP peptides. This might shed more light on the differences in functional activity of CEP peptides towards one of the candidate receptors, or why some CEP peptides might act as agonists, while others might potentially act as antagonists. Furthermore, knowledge about the phosphorylation sites in the intracellular kinase domain might prove useful in studying downstream signaling events. For example, it would be possible to induce the expression of a constitutively activated receptor in a receptor knock-out background, and follow which downstream proteins are phosphorylated over time. Creating such a

constitutively activated receptor could be achieved by substituting a crucial activation-phosphorylation site with a phospho-mimicing aspartic acid residue, and has been used successfully in other studies to identify downstream targets of kinase activity (Dissmeyer & Schnittger, 2011; Lassowskat et al, 2014). To identify such a phosphorylation-site, knowledge about the receptor structure is required.

Detailed structural knowledge of the receptor proteins could be obtained through laborious X-ray crystallography analysis, or alternatively could be predicted using *in silico* structural modeling of the protein based on previously characterized closely-related proteins. The latter approach was followed below to gather some structural knowledge about the CEPR1/XIP1 and CEPR2 receptors. Using iTASSER software, the possible 3D-structure of the LRR-domain of CEPR1/XIP1 was constructed *de novo*. The LRR domain counts 21 LRR unit repeats that fold into an arc shape with an exterior array of alpha helices formed by the variable segments (VS), and an interior beta sheet formed by the highly conserved segments (HCS), which forms the binding pocket for the CEP peptide ligand **(Figure 6B)**. Future *in silico* docking predictions with CEP ligand models could possibly predict which residues in the receptor domain might interact with each residue in the mature CEP peptide ligand.

In a recent study, an interesting alternative approach was used to determine which residues in the LRR receptor domain of the HAESA (HAE), HAESA-LIKE 1 (HSL1) and HAESA-LIKE 2 (HSL2) receptors are potentially important for interacting with the IDA/IDL peptide ligands. A sequence alignment analysis of the HAE and HSL1/2 LRR receptor domain of all the orthologues found in multiple plant species was used to generate a heat map, which revealed conserved residues in LRR units that are most likely important residues interacting with the conserved IDA/IDL peptide ligands (Stø et al., 2015). These results were later confirmed to a large degree with actual X-ray crystallographic analysis of the IDA – HAE ligand receptor complex (Santiago et al., 2016), suggesting that this *in silico* approach is potentially useful for inferring important residues in the LRR receptor domain of CEPR1/XIP1 and CEPR2 proteins that might interact with CEP peptide ligands. Therefore, a phylogenetic study of the CEP receptor proteins in the seed plant lineage would be a useful future analysis, not only for having an idea about the evolutionary origin of this receptor family, but also to identify important residues in the LRR receptor domain that interact with the CEP peptide ligand.

In addition, the iTASSER software was also used to generate a possible 3D-structure of the CEPR1/XIP1 kinase domain, based on its homology with the structurally well-characterized kinase domain from BRASSINOSTEROID INSENSITIVE 1 (BRI1) (Bojar et al, 2014). The intracellular Ser/Thr kinase domain of CEPR1/XIP1 contains a typical N-lobe and C-lobe connected by a flexible hinge region and the ATP-binding pocket sandwiched in between them. The C-lobe contains an activation loop with a predicted threonine activation-phosphorylation site, which is crucial for switching between the active/inactive states of the kinase. In combination with sequence alignments, it was possible to reconstruct the ATP-binding pocket of CEPR1/XIP1 with its corresponding conserved crucial residues **(Figure 6C)**. Knowledge of these critical residues might allow creating a kinase-dead version or a constitutively active kinase version of the receptor for future downstream studies.

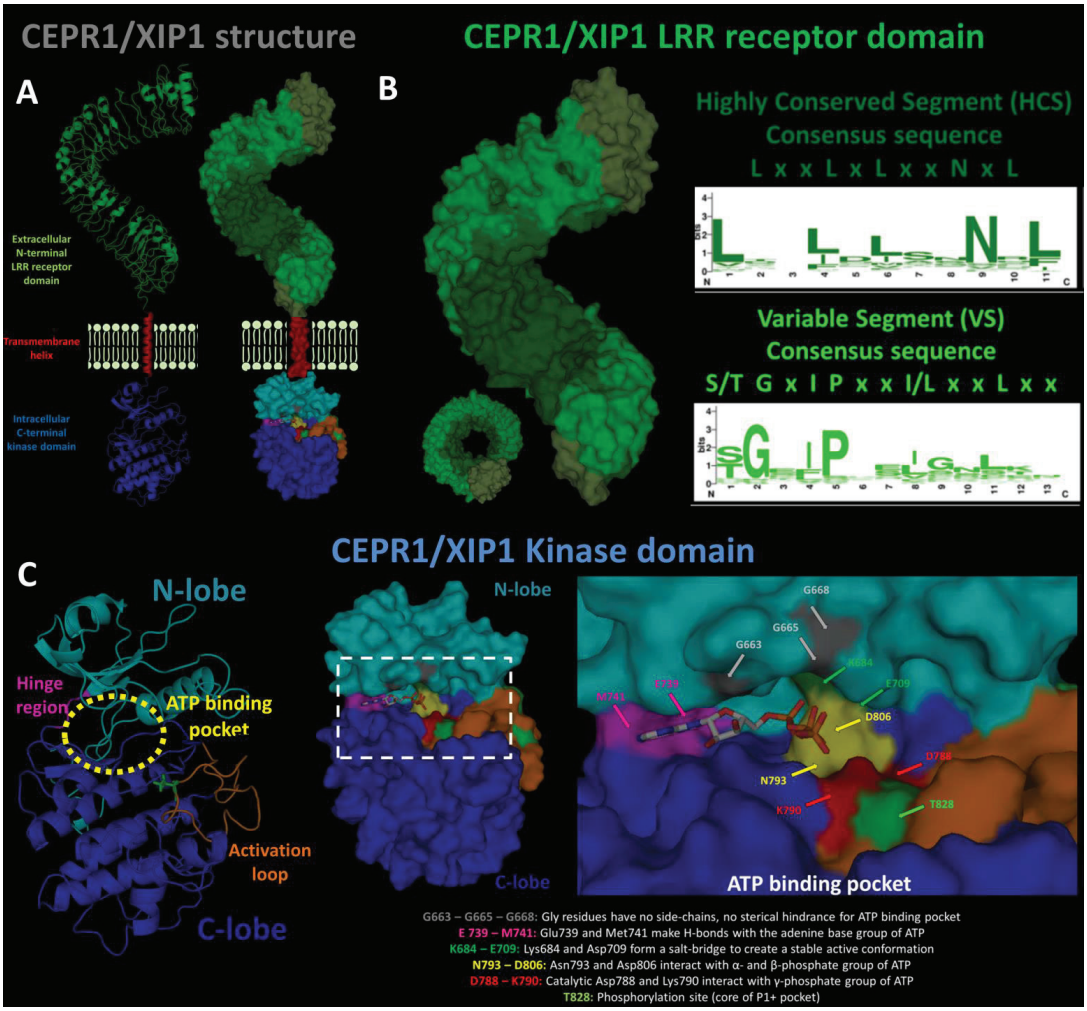


**Figure 6.** ***In silico*** **structure analysis of CEPR1/XIP1. (A)** Overall structure of CEPR1/XIP1. **(B)** The CEPR1/XIP1 LRR receptor domain is composed of 21 LRR-motifs. Each LRR-motif typically counts 23-25 amino acid residues forming a Highly Conserved Segment (HCS) and a Variable Segment (VS). The HCS segments form an interior array of beta-sheets, while the VS segments form an exterior array of alpha-helices. **(C)** The CEPR1/XIP1 kinase domain, with a detailed view of conserved residues in the ATP binding pocket and the activation-phosphorylation site (T828).

Aligning multiple evolutionarily related protein sequences is often used as a fundamental technique for studying protein function, protein structure, protein interactions, mutagenesis analysis and evolution. In *Arabidopsis*, the closest homologs of CEPR1 and CEPR2 are the LRR-RLK proteins RECEPTOR-LIKE KINASE7 (RLK7), HAIKU2 (IKU2), HAESA (HAE), HAESA-LIKE1 (HSL1) and HAESA-LIKE2 (HSL2) **(Figure 7)**. Recently, RLK7 was identified as the receptor for the PAMP-INDUCED SECRETED PEPTIDE (PIP) and PIP-LIKE (PIPL) peptide family (Hou et al, 2014). Although IKU2 is currently not linked to any peptide family, its close relationship to RLK7 suggests that it might also be a receptor for the PIP/PIPL peptides, or alternatively a third receptor for CEP peptides. The receptors HAE, HSL1 and HSL2 are identified as the receptors for the IDA/IDL peptides (Stenvik et al, 2008). These closely related LRR-RLKs bind closely related signaling peptides with a similar structure of the mature

peptide (Vie et al, 2015). Sequence alignment of these LRR-RLKs on one hand reveals the overall conserved regions and strictly conserved crucial amino acid residues important for functionality, and on the other hand regions that differ drastically and are probably responsible for ligand and substrate specificity **(Figure 8)**. Based on sequence alignments of the LRR receptor domain, some differences can be observed between the different LRR-RLKs. CEPR1, CEPR2, RLK7 and IKU2 have 21 LRR-motifs, while HAE, HSL1 and HSL2 have 22 LRR-motifs. LRR motifs closer to the N-terminus show higher variability compared to those near the transmembrane region, which suggests these are probably involved in binding the different peptide ligands. Sequence alignment of the kinase domain of the LRR-RLKs reveals a very strict conservation of the key residues in the ATP binding pocket (highlighted in the same color-code as in **Figure 6**, but also some differences. For example, CEPR1, CEPR2, RLK7 and IKU2 have a conserved threonine (T) activation-phosphorylation site in the activation loop, while HAE, HSL1 and HSL2 have a conserved serine (S) phosphorylation site at the same location. The highly variable regions in the N-lobe and C-lobe are likely involved in binding different interacting proteins. The latter structural information can be helpful to unravel how and which proteins are interacting with the LRR-RLK and study their downstream targets by using site-directed mutagenesis on specific residues crucial for functionality (*e.g.* phosphorylation sites or residues from the ATP binding pocket) (Cao et al, 2013).

In conclusion, structural knowledge about the CEPR1/XIP1 and CEPR2 will likely play an important role in future studies on CEP signaling. *In silico* predictions and multiple sequence alignments are useful to have some ideas about important residues that can be used for designing experiments. However, X-ray crystallography will be necessary to confirm (or reject) these *in silico* predictions and shed light on the mechanisms of CEP ligand binding and accompanied phosphorylation events.

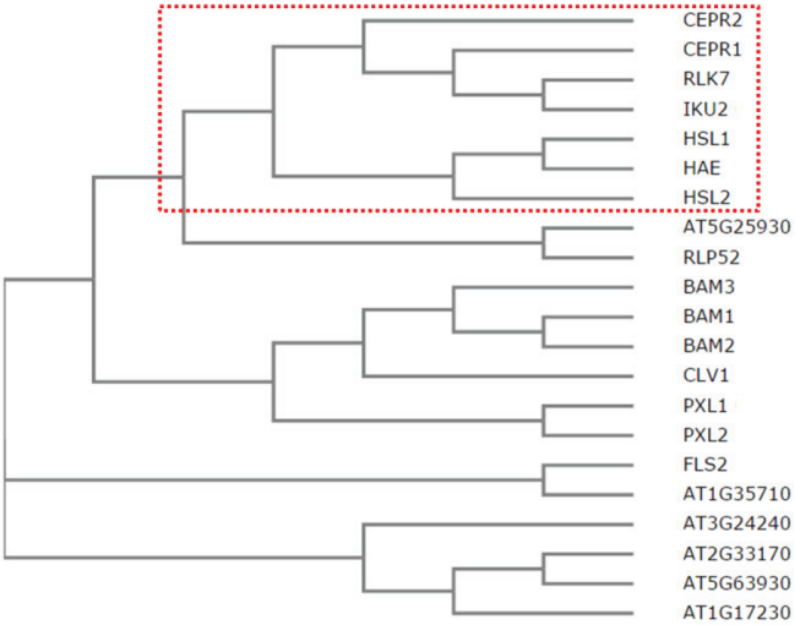


**Figure 7. Phylogeny of LRR-RLKs closely related to CEPR proteins** (closest related members in a red box).

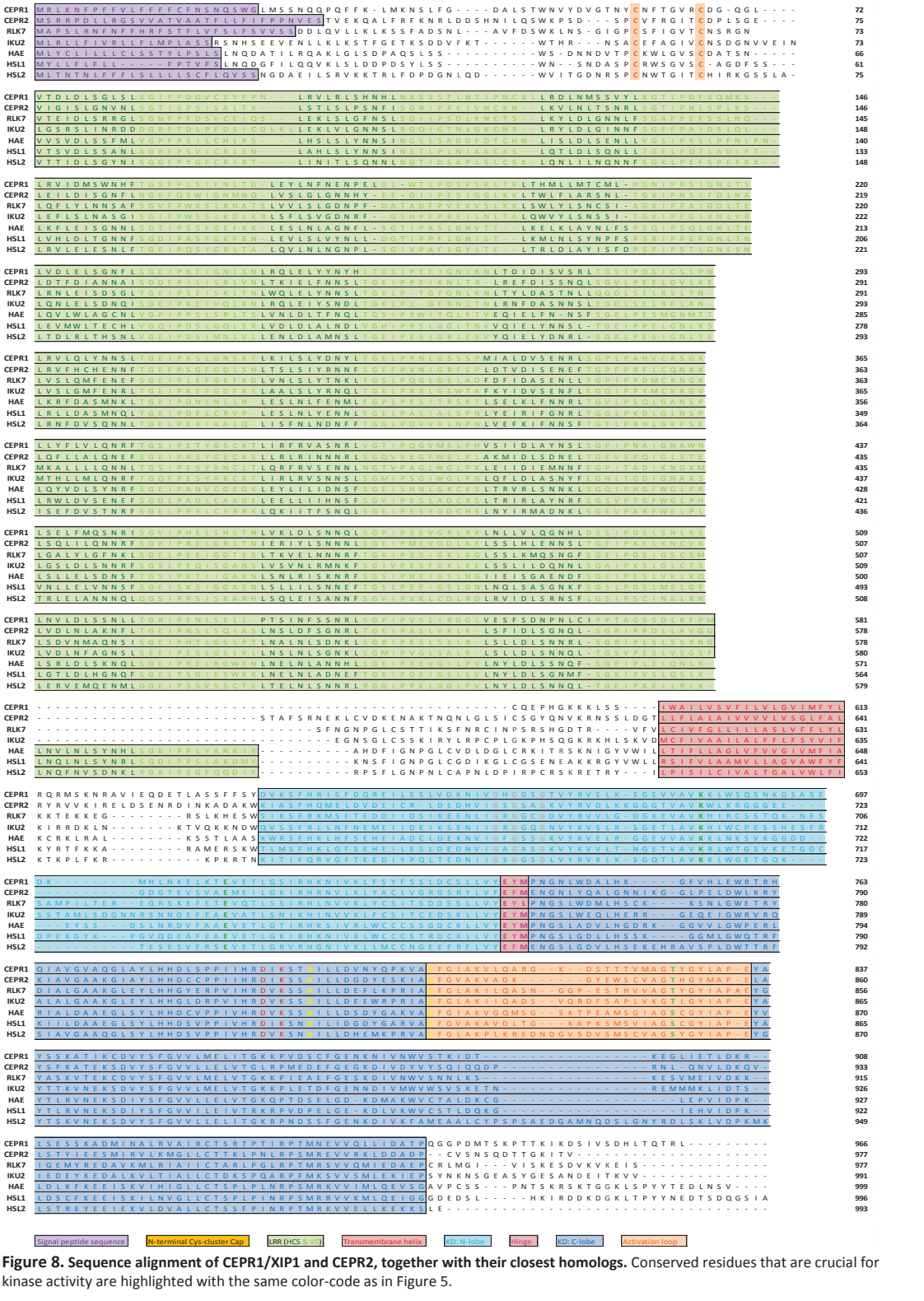


**Figure 8. Sequence alignment of CEPR1/XIP1 and CEPR2, together with their closest homologs.** Conserved residues that are crucial for kinase activity are highlighted with the same color-code as in Figure 5.

**The power of a classical EMS-mutagenesis screen (… and its weaknesses)**

In this study, an EMS-mutagenesis screen led to the identification of three molecular components regulating root system architecture. A loss-of-function mutant in the *CELLULOSE SYNTHASE 6* (*CESA6*) gene was shown to generate a shallow dense root system, by having a shorter primary root with an increased density of more horizontally growing lateral roots. A loss-of-function mutant in the *CULLIN-ASSOCIATED AND NEDDYLATION DISSOCIATED 1* (*CAND1*) gene led to a narrow dense root system, with lateral roots growing under a very steep angle along the primary root. And a new gain-of-function mutant allele for the *IAA12*/*BODENLOS* (*BDL*) gene was identified, which was severely disturbed in lateral root spacing and formed a less dense root system ***(Chapter 7)*** **(Figure 9)**.

The shallow dense root system from the *cesa6* mutant is potentially better suited for the uptake of phosphate, which is mainly situated in the top-soil layer (Lynch, 1995; Hammond et al, 2009). Based on expression analysis, *CESA6* also plays a role in cellulose synthesis in the shoot (Xie et al, 2011), and possibly explains the reduced shoot growth in the *cesa6* mutant. Thus, to obtain a plant with the desired shallow dense root system, but without the unwanted shoot phenotype, a root-specific amiRNA or RNAi knock-down of the *CESA6* gene is required.

The narrow root system from the *cand1* mutant is reminiscent of the steep and deep ideotype, which might be better for water and nitrate uptake in deeper regions of the soil (Lynch, 2013; Uga et al, 2013; Uga et al, 2015). While many regulators have been described for the lateral root development process, very few components are known to regulate the lateral root setpoint growth angle. Considering its involvement in various SCF-dependent signaling pathways, it is difficult to pinpoint exactly how CAND1 regulates the lateral root growth angle. However, altered auxin signaling is likely playing a big role, as this was previously shown to influence the lateral root setpoint angle (Rosquete et al, 2013; Roychoudhry et al, 2013). Therefore, it would be interesting to check if the auxin response is altered in the *cand1* mutant, using *pDR5::GUS* or *pDR5::nls-GFP* reporter lines. While the steep lateral root growth angle could be beneficial, other pleiotropic negative effects, such as reduced fertility and a small shoot/inflorescence, would make a *cand1* knock-out mutant crop less useful in the field. Therefore, a (lateral) root-specific knock-down of *CAND1* is required to generate plants with a steep and deep root system, while keeping normal shoot growth.

Although the overall root system architecture of the *bdl-2* mutant is not producing an efficient root system, the lateral root clustering phenotype from the $BDL^{bdl\text{-}2}$ mutation might potentially be used to engineer plants with induced lateral root clusters in regions of high nutrient content for increased uptake.

This work underscores the importance of controlled protein degradation, through a SCF-dependent process, in regulating RSA, since two mutants with altered RSA are affected in this process (*cand1* in recycling of the SCF-complex and *bdl* in a stabilized SCF-substrate).

The root system architecture phenotypes of these mutants observed on *in vitro* 1/2 MS petri plates, were shown to be retained in more natural conditions in the soil, using mini-rhizotrons. Rhizotrons will likely take on an important role in future studies on root development, bringing our research one step closer to engineering crops with an improved root system in soil and higher yield.

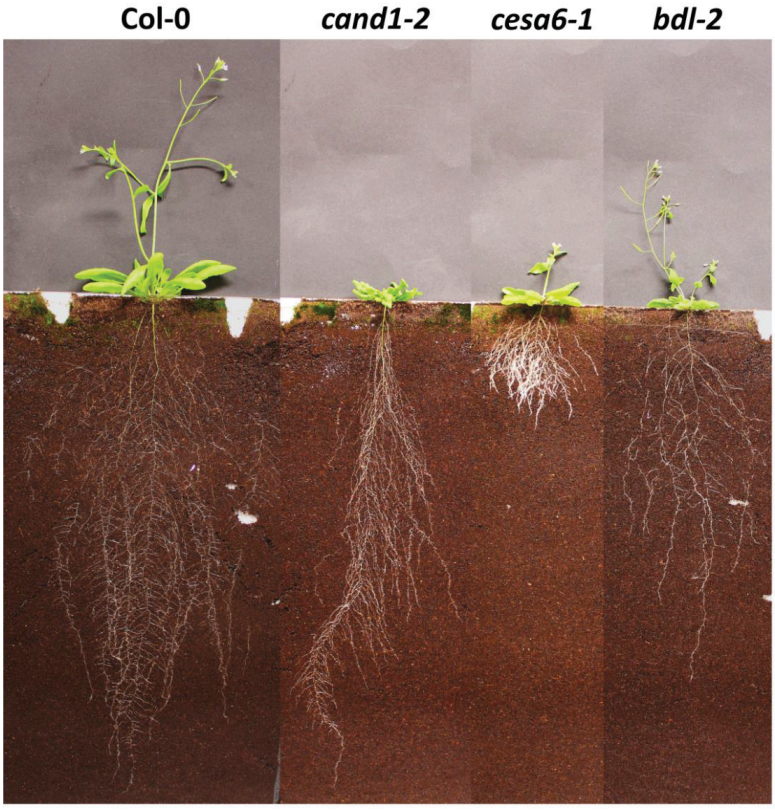


**Figure 9. Overview of the identified mutants with altered root system architecture.**

Over the years, both EMS mutant screens and genome-wide transcriptional analyses led to the identification of regulators of lateral root development. Both approaches have advantages and disadvantages. The EMS mutagenesis screen proves to be useful to identify molecular components that have a drastic impact on the overall root system architecture, since the main benefit of an EMS mutagenesis screen is that you select for a strong phenotype of choice. It was also an approach more suited to identify components that have an impact on the lateral root growth angle, as this is more difficult with a transcriptomics analysis. Over the last couple of years, it became a lot more 'user-friendly' to map the EMS-mutation, considering the drastic price-drops for whole-genome sequencing and the ease of mapping with SHOREmap analysis. However, one disadvantage is that although you select for a phenotype of choice, you do not select for your favorite type of regulator. For example, although the CELLULOSE SYNTHASE 6 protein and the general CAND1 SCF-cycling component have a clear effect on root system architecture, they are not exactly as 'appealing' as a transcription factor or protein kinase to work with. The transcriptomics approach has the advantage to identify regulators that act redundantly in lateral root development, while an EMS-mutation in a functionally redundant regulator would not generate a phenotype. Another advantage of a transcriptomics approach is that it is possible to choose a regulator of interest from a candidate list of potential regulators, such as transcription factors, protein kinases or LRR-RLKs. Thus, both approaches will likely continue to be used in future studies to identify regulators that have an impact on root system architecture.

**A final take home message: avoid comparing apples and oranges**

A final point of interest that I would like to highlight, is the importance to always use the correct controls when phenotyping mutant lines. Very often in research, researchers compare a requested mutant line (*e.g.* T-DNA insertion mutant line or overexpression line) simply with the local 'in-house' Col-0 stock as control. However, many phenotypical differences exist between Col-0 stocks from different labs due to accumulating differences in the genetic background. Two labs could start out with two identical pure genetic lines, but through spontaneous naturally occurring mutations might diverge by fixation of different mutations during several rounds of propagation (Ossowski et al, 2010). Aside from natural mutation rates, contaminated seed stocks and outcrossing are more drastic issues that are probably occurring more frequently than people are aware. For example, a recent report brought the shocking news that many in-house Col-0 'control' stocks in different labs are contaminated by a Wassilewskija-2 (Ws-2) ecotype introgression, suggesting that researchers should always take care handling seed stocks and do sufficient background checks (Bergelson et al, 2016; Shao et al, 2016). Thus, to avoid comparing apples and oranges, researchers should follow the following basic approaches. When generating transgenic lines (*e.g.* overexpression lines), a seed stock from the parental line should be kept as control. For T-DNA insertion mutant lines requested from NASC, the seed stock received usually contain several hemizygous seeds. These should be checked for a single T-DNA locus insertion in the gene of interest, and then the hemizygous lines should be used for propagation. From the next generation, a wild type control and a homozygous mutant should be obtained from the hemizygous parent. In that case, the chance of phenotypical differences between the mutant and the wild type is more likely to depend on the T-DNA insertion in the gene of interest, instead of being caused by other differences in genetic background.

In this study, for the phenotypical analysis of the *cep* single mutants, at first our in-house Col-0 seed stock was used as a control for a quick analysis, and many of the *cep* mutant lines showed promising differences in root length and number of lateral roots compared to the in-house Col-0. However, after comparing mutant lines with the correct wild type lines, in which the T-DNA insert was segregated out of a hemizygous mutant parent, these promising phenotypes in most cases simply disappeared. For example, in **Figure 10**, a wild type Col-0 from one background line was used as a control, and in the other figure a wild type Col-0 from another background line was used as a control. In the first case, it could be concluded that almost every *cep* mutant has a significant increase in primary root length and number of lateral roots. But in the second case, the conclusion would be that *cep* mutants generally have a significant shorter primary root and less lateral roots. In conclusion, researchers should always take care in using correct controls to avoid 'background-induced mutant phenotypes' or 'disappearing phenotypes', such as was recently reported for the *AUXIN BINDING PROTEIN 1* (*ABP1*) gene (Enders et al, 2015; Michalko et al, 2015).

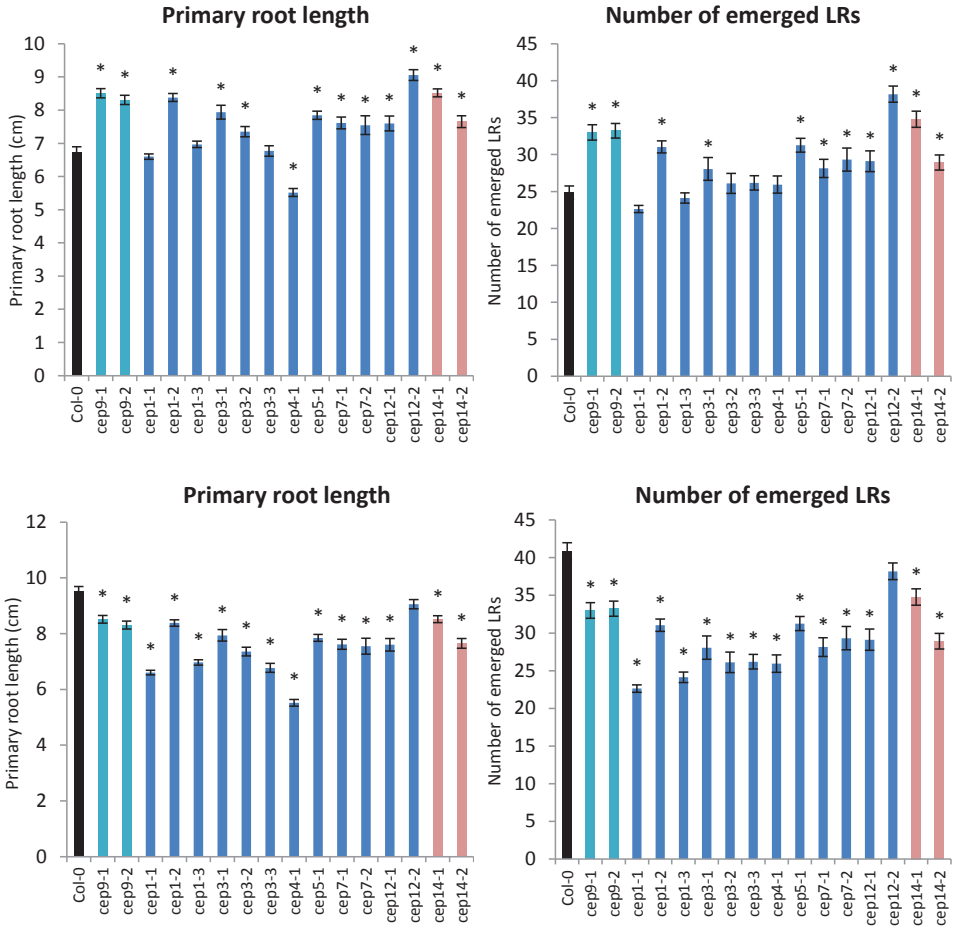


**Figure 10. Using the correct controls.** In the top figures, a Col-0 wild type control from one background was used, while in the bottom figures, a Col-0 wild type control from another background was used. In the first scenario, almost every *cep* mutant seems to have a significantly smaller root system, while in the second scenario, almost every *cep* mutant has a smaller root system compared to the control (graphs show average ± SE, **p*<0.05, Student's *t*-test).

## REFERENCES


Bergelson J, Buckler ES, Ecker JR, Nordborg M, Weigel D (2016) A Proposal Regarding Best Practices for Validating the Identity of Genetic Stocks and the Effects of Genetic Variants. *Plant Cell* **28:** 606-609

Bobay BG, DiGennaro P, Scholl E, Imin N, Djordjevic MA, McK Bird D (2013) Solution NMR studies of the plant peptide hormone CEP inform function. *FEBS Lett* **587:** 3979-3985

Bojar D, Martinez J, Santiago J, Rybin V, Bayliss R, Hothorn M (2014) Crystal structures of the phosphorylated BRI1 kinase domain and implications for brassinosteroid signal initiation. *The Plant journal : for cell and molecular biology* **78:** 31-43

Cao J, Shi F (2012) Evolution of the RALF Gene Family in Plants: Gene Duplication and Selection Patterns. *Evol Bioinform Online* **8:** 271-292

Cao Y, Aceti DJ, Sabat G, Song J, Makino S, Fox BG, Bent AF (2013) Mutations in FLS2 Ser-938 dissect signaling activation in FLS2-mediated Arabidopsis immunity. *PLoS pathogens* **9:** e1003313

Chen S, Lang P, Chronis D, Zhang S, De Jong WS, Mitchum MG, Wang X (2015) In planta processing and glycosylation of a nematode CLAVATA3/ENDOSPERM SURROUNDING REGION-like effector and its interaction with a host CLAVATA2-like receptor to promote parasitism. *Plant physiology* **167:** 262-272

Czyzewicz N, Wildhagen M, Cattaneo P, Stahl Y, Pinto KG, Aalen RB, Butenko MA, Simon R, Hardtke CS, De Smet I (2015) Antagonistic peptide technology for functional dissection of CLE peptides revisited. *J Exp Bot* **66:** 5367-5374

Delay C, Imin N, Djordjevic MA (2013) CEP genes regulate root and shoot development in response to environmental cues and are specific to seed plants. *J Exp Bot* **64:** 5383-5394

Dissmeyer N, Schnittger A (2011) Use of phospho-site substitutions to analyze the biological relevance of phosphorylation events in regulatory networks. *Methods in molecular biology* **779:** 93-138

Enders TA, Oh S, Yang Z, Montgomery BL, Strader LC (2015) Genome Sequencing of Arabidopsis abp1-5 Reveals Second-Site Mutations That May Affect Phenotypes. *Plant Cell* **27:** 1820-1826

Eves-van den Akker S, Lilley CJ, Yusup HB, Jones JT, Urwin PE (2016) Functional C-terminally encoded plant peptide (CEP) hormone domains evolved de novo in the plant parasite Rotylenchulus reniformis. *Molecular plant pathology*

Fauser F, Schiml S, Puchta H (2014) Both CRISPR/Cas-based nucleases and nickases can be used efficiently for genome engineering in Arabidopsis thaliana. *The Plant journal : for cell and molecular biology* **79:** 348-359

Feng Z, Zhang B, Ding W, Liu X, Yang DL, Wei P, Cao F, Zhu S, Zhang F, Mao Y, Zhu JK (2013) Efficient genome editing in plants using a CRISPR/Cas system. *Cell research* **23:** 1229-1232

Gabay C, Towne JE (2015) Regulation and function of interleukin-36 cytokines in homeostasis and pathological conditions. *J Leukoc Biol* **97:** 645-652

Griffin BA, Adams SR, Tsien RY (1998) Specific covalent labeling of recombinant protein molecules inside live cells. *Science* **281:** 269-272

Guo Y, Ni J, Denver R, Wang X, Clark SE (2011) Mechanisms of molecular mimicry of plant CLE peptide ligands by the parasitic nematode Globodera rostochiensis. *Plant physiology* **157:** 476-484

Hammond JP, Broadley MR, White PJ, King GJ, Bowen HC, Hayden R, Meacham MC, Mead A, Overs T, Spracklen WP, Greenwood DJ (2009) Shoot yield drives phosphorus use efficiency in Brassica oleracea and correlates with root architecture traits. *J Exp Bot* **60:** 1953-1968

Hou S, Wang X, Chen D, Yang X, Wang M, Turra D, Di Pietro A, Zhang W (2014) The secreted peptide PIP1 amplifies immunity through receptor-like kinase 7. *PLoS pathogens* **10:** e1004331

Hruby VJ (2002) Designing peptide receptor agonists and antagonists. *Nat Rev Drug Discov* **1:** 847-858

Imin N, Mohd-Radzman NA, Ogilvie HA, Djordjevic MA (2013) The peptide-encoding CEP1 gene modulates lateral root and nodule numbers in Medicago truncatula. *J Exp Bot* **64:** 5395-5409

Irani NG, Di Rubbo S, Mylle E, Van den Begin J, Schneider-Pizon J, Hnilikova J, Sisa M, Buyst D, Vilarrasa-Blasi J, Szatmari AM, Van Damme D, Mishev K, Codreanu MC, Kohout L, Strnad M, Cano-Delgado AI, Friml J, Madder A, Russinova E (2012) Fluorescent castasterone reveals BRI1 signaling from the plasma membrane. *Nature chemical biology* **8:** 583-589

Lang K, Chin JW (2014) Cellular incorporation of unnatural amino acids and bioorthogonal labeling of proteins. *Chem Rev* **114:** 4764-4806

Lassowskat I, Bottcher C, Eschen-Lippold L, Scheel D, Lee J (2014) Sustained mitogen-activated protein kinase activation reprograms defense metabolism and phosphoprotein profile in Arabidopsis thaliana. *Frontiers in plant science* **5:** 554

Lee JS, Hnilova M, Maes M, Lin YC, Putarjunan A, Han SK, Avila J, Torii KU (2015) Competitive binding of antagonistic peptides fine-tunes stomatal patterning. *Nature* **522:** 439-443

Li JF, Norville JE, Aach J, McCormack M, Zhang D, Bush J, Church GM, Sheen J (2013) Multiplex and homologous recombination-mediated genome editing in Arabidopsis and Nicotiana benthamiana using guide RNA and Cas9. *Nature biotechnology* **31:** 688-691

Lynch J (1995) Root Architecture and Plant Productivity. *Plant Physiol* **109:** 7-13

Lynch JP (2013) Steep, cheap and deep: an ideotype to optimize water and N acquisition by maize root systems. *Ann Bot* **112:** 347-357

Michalko J, Dravecka M, Bollenbach T, Friml J (2015) Embryo-lethal phenotypes in early abp1 mutants are due to disruption of the neighboring BSM gene. *F1000Res* **4:** 1104

Oelkers K, Goffard N, Weiller GF, Gresshoff PM, Mathesius U, Frickey T (2008) Bioinformatic analysis of the CLE signaling peptide family. *BMC Plant Biol* **8:** 1

Ogilvie HA, Imin N, Djordjevic MA (2014) Diversification of the C-TERMINALLY ENCODED PEPTIDE (CEP) gene family in angiosperms, and evolution of plant-family specific CEP genes. *BMC Genomics* **15:** 870

Ohyama K, Ogawa M, Matsubayashi Y (2008) Identification of a biologically active, small, secreted peptide in Arabidopsis by in silico gene screening, followed by LC-MS-based structure analysis. *The Plant journal : for cell and molecular biology* **55:** 152-160

Ossowski S, Schneeberger K, Lucas-Lledo JI, Warthmann N, Clark RM, Shaw RG, Weigel D, Lynch M (2010) The rate and molecular spectrum of spontaneous mutations in Arabidopsis thaliana. *Science* **327:** 92-94

Roberts I, Smith S, De Rybel B, Van Den Broeke J, Smet W, De Cokere S, Mispelaere M, De Smet I, Beeckman T (2013) The CEP family in land plants: evolutionary analyses, expression studies, and role in Arabidopsis shoot development. *J Exp Bot* **64:** 5371-5381

Rosquete MR, von Wangenheim D, Marhavy P, Barbez E, Stelzer EH, Benkova E, Maizel A, Kleine-Vehn J (2013) An auxin transport mechanism restricts positive orthogravitropism in lateral roots. *Current biology : CB* **23:** 817-822

Roychoudhry S, Del Bianco M, Kieffer M, Kepinski S (2013) Auxin controls gravitropic setpoint angle in higher plant lateral branches. *Current biology : CB* **23:** 1497-1504

Santiago J, Brandt B, Wildhagen M, , Hohmann U, Hothorn LA , Butenko MA , Hothorn M (2016) Mechanistic insight into a peptide hormone signaling complex mediating floral organ abscission. *eLife*: **5:**e15075

Shao MR, Shedge V, Kundariya H, Lehle FR, Mackenzie SA (2016) Ws-2 Introgression in a Proportion of Arabidopsis thaliana Col-0 Stock Seed Produces Specific Phenotypes and Highlights the Importance of Routine Genetic Verification. *Plant Cell* **28:** 603-605

Song XF, Guo P, Ren SC, Xu TT, Liu CM (2013) Antagonistic peptide technology for functional dissection of CLV3/ESR genes in Arabidopsis. *Plant Physiol* **161:** 1076-1085

Stenvik GE, Tandstad NM, Guo Y, Shi CL, Kristiansen W, Holmgren A, Clark SE, Aalen RB, Butenko MA (2008) The EPIP peptide of INFLORESCENCE DEFICIENT IN ABSCISSION is sufficient to induce abscission in arabidopsis through the receptor-like kinases HAESA and HAESA-LIKE2. *Plant Cell* **20:** 1805-1817

Stø IM, Orr RJ, Fooyontphanich K, Jin X, Knutsen JM, Fischer U, Tranbarger TJ, Nordal I, Aalen RB (2015) Conservation of the abscission signaling peptide IDA during Angiosperm evolution: withstanding genome duplications and gain and loss of the receptors HAE/HSL2. *Front Plant Sci.* **6:**931

Tabata R, Sumida K, Yoshii T, Ohyama K, Shinohara H, Matsubayashi Y (2014) Perception of root-derived peptides by shoot LRR-RKs mediates systemic N-demand signaling. *Science* **346:** 343-346

Tolbert WD, Daugherty J, Gao C, Xie Q, Miranti C, Gherardi E, Vande Woude G, Xu HE (2007) A mechanistic basis for converting a receptor tyrosine kinase agonist to an antagonist. *Proc Natl Acad Sci U S A* **104:** 14592-14597

Tucker ML, Yang R (2013) A gene encoding a peptide with similarity to the plant IDA signaling peptide (AtIDA) is expressed most abundantly in the root-knot nematode (Meloidogyne incognita) soon after root infection. *Experimental parasitology* **134:** 165-170

Uga Y, Kitomi Y, Ishikawa S, Yano M (2015) Genetic improvement for root growth angle to enhance crop production. *Breeding science* **65:** 111-119

Uga Y, Sugimoto K, Ogawa S, Rane J, Ishitani M, Hara N, Kitomi Y, Inukai Y, Ono K, Kanno N, Inoue H, Takehisa H, Motoyama R, Nagamura Y, Wu J, Matsumoto T, Takai T, Okuno K, Yano M (2013) Control of root system architecture by DEEPER ROOTING 1 increases rice yield under drought conditions. *Nat Genet* **45:** 1097-1102

Vie AK, Najafi J, Liu B, Winge P, Butenko MA, Hornslien KS, Kumpf R, Aalen RB, Bones AM, Brembu T (2015) The IDA/IDA-LIKE and PIP/PIP-LIKE gene families in Arabidopsis: phylogenetic relationship, expression patterns, and transcriptional effect of the PIPL3 peptide. *J Exp Bot* **66:** 5351-5365

Wang J, Replogle A, Hussey R, Baum T, Wang X, Davis EL, Mitchum MG (2011) Identification of potential host plant mimics of CLAVATA3/ESR (CLE)-like peptides from the plant-parasitic nematode Heterodera schachtii. *Molecular plant pathology* **12:** 177-186

Whitford R, Fernandez A, De Groodt R, Ortega E, Hilson P (2008) Plant CLE peptides from two distinct functional classes synergistically induce division of vascular cells. *Proc Natl Acad Sci U S A* **105:** 18625-18630

Xie L, Yang C, Wang X (2011) Brassinosteroids can regulate cellulose biosynthesis by controlling the expression of CESA genes in Arabidopsis. *J Exp Bot* **62:** 4495-4506

Zhang Z, Mao Y, Ha S, Liu W, Botella JR, Zhu JK (2015) A multiplex CRISPR/Cas9 platform for fast and efficient editing of multiple genes in Arabidopsis. *Plant cell reports*

# *Curriculum vitae*

## Personal information

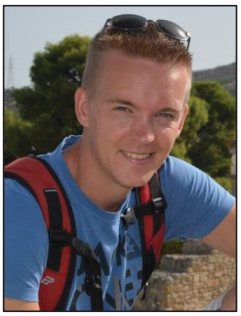


**Name**: Ianto Roberts
**Address**: Kapellen 8
9660 Brakel
**Telephone**: +32 (0) 495 / 35 08 34
**E-mail**: ianto.roberts1987@gmail.com
**Date of Birth**: 11 - 01 - 1987
**Nationality**: Belgian


## Education

**Doctor in Science – Biochemistry and Biotechnology (2011-2016):**

- Department of Plant Systems Biology, from Ghent University/ VIB, Belgium
- Acquired a personal Strategic Basic Research (SBO) funding grant from the Agency for Innovation by Science and Technology (IWT)
- PhD thesis topics:
  - Functional characterization of the CEP peptide family in *Arabidopsis thaliana*
  - Identification of molecular components affecting root system architecture

**Master in Biochemistry and Biotechnology (2008-2010):**

- Ghent University
- Graduated with great honor / *magna cum laude*
- Majors (specialization):
  - Plant Biotechnology
  - Biochemistry and Structural Biology
- Master projects:
  - Characterization of the CRF transcription factors during lateral root initiation
  - Changing the substrate specificity in the glutathione reductase family
- Master thesis:
  - Functional characterization of genes involved in lateral root initiation in *Arabidopsis thaliana* and *Zea mays*

**Bachelor in Biochemistry and Biotechnology (2005-2008):**

- Ghent University
- Graduated with honor / *cum laude*
- Bachelor thesis projects:
  - Genotyping transgenic mice
  - Production of antibodies in transgenic *Arabidopsis* seeds
  - Localization of disulfide bridges in G3DH-enzymes with mass spectrometry

## Experience and skills

**Professional experience:**

- PhD (five years, 2011-2016) in an internationally renowned top-research facility for biotechnology: Plant Systems Biology (Ugent/VIB)
- Summer job (one month, July 2008) in Cropdesign BASF in the Vector Construction Group: Agarose gel electrophoresis, plasmid extraction, bacterial cryo-stocks, …

**Experience with (molecular) techniques:**

- General lab work with plants (*in vitro* growth, hormone treatments, crossings, …), Gateway cloning, restriction digest, plasmid extraction, DNA and RNA extraction, cDNA synthesis, PCR, real-time qRT-PCR, DIC and confocal microscopy, microtome sectioning, phenotyping root/shoot growth parameters with ImageJ software, EMS mutagenesis, SHOREmapping, protein extraction, chromatography, mass spectrometry analysis, enzyme kinetics, …

**Presentation skills:**

- Oral presentations (+ lecturing a workshop) at international symposia
    - **Interuniversitary Attractionpoles (IUAP) meeting: Plant Phenotyping**
      University of Antwerp, Antwerp, Belgium, April 2015
      An EMS-screen to identify regulators that affect the overall root architecture
    - **Interuniversitary Attractionpoles (IUAP) meeting: Plant Phenotyping**
      University of Gent, Gent, Belgium, April 2014
      Oral presentation + supervising a practical workshop on the microscopic study of lateral root development
    - **The 1st European Workshop on Peptide Signaling in Plants**
      University of Oslo, Oslo, Norway, January 2013
      The role of the CEP5 peptide during lateral root development

- Poster presentations at international symposia
    - **The 2nd European Workshop on Peptide Signaling in Plants**
      University of Regensburg, Regensburg, Germany, September 2014
      Title: The CEP5 peptide affects lateral root development by fine tuning the auxin response
    - **Flemish Institute of Biotechnology (VIB) annual seminar**
      Blankenberge, Belgium, February 2013
      Title: The role of the CEP5 peptide during lateral root development
    - **The 1st European Workshop on Peptide Signaling in Plants**
      University of Oslo, Oslo, Norway, January 2013
      Title: The role of the CEP5 peptide during lateral root development
    - **The 6th symposium of the Belgian Plant Biotechnology Association (BPBA)**
      Institute for Agricultural and Fisheries Research (ILVO), Melle, Belgium, November 2012 **Best poster-prize (>30 posters)**
      Title: The role of the CEP5 peptide during lateral root development

**Supervising thesis-students:**

- Master thesis student Biology: University of Gent (2014)
- Master thesis student Biology: University of Gent (2013)
- Bachelor thesis student Biology: University of Gent (2013)
- Bachelor thesis student Biomedical Lab technology: Graduate school of Vesalius (2013)
- Master project student Biochemistry and Biotechnology: University of Gent (2012)
- Bachelor thesis student Biology: University Gent (2012)
- Bachelor thesis student Biomedical Lab Technology: Graduate school Avans (Holland) (2012)

**Supervising practical sessions for student courses:**

- Practicum: Developmental biology – phenotyping root system architecture (2015)
- Practicum: Microscopic analysis of mitotic spindles (2011, 2012, 2013, 2014, 2015)
- Practicum: Confocal Laser Scanning Microscopy (2013)
- Practicum: Plant physiology (2013)

**Additional specialization courses followed during PhD studies:**

- Leadership foundation course (Doctoral Schools Ugent, 2015)
- Introduction to next-generation sequencing technology (VIB, 2014)
- Genome editing with CRISPR/Cas9 workshop (Sigma-Aldrich & IDT, 2014)
- Summer school on advanced microscopy (Doctoral Schools Ugent, 2013)
- Basic bioinformatics concepts, databases and tools (VIB BITS, 2011)
- Perl introduction training (VIB BITS, 2011)
- Protein structure analysis training (VIB BITS, 2011)
- Genevestigator training (VIB BITS, 2011)
- Comparative and intra-species discovery of transcription factor binding sites (VIB BITS, 2011)
- Introductory microscopy training workshop (VIB, 2010)

**IT/Software**

- Microsoft Office (Word, Excel and Powerpoint)
- Endnote
- ImageJ
- Photoshop
- Perl programming (basics)

**Languages**

- Dutch (native)
- English (very good)
- French (moderate)

## Published articles:

- **Roberts I**, Smith S, Stes E, De Rybel B, Staes A, van de Cotte B, Demol H, Lavenus J, Audenaert D, Gevaert K, Beeckman T, De Smet I. (2016) CEP5 and XIP1/CEPR1 regulate lateral root initation in *Arabidopsis*. Journal of Experimental Botany (in press)
- **Roberts I**, Crombez H, Vangheluwe,N, Motte H, Jansen L, Beeckman T, and Parizot B (2016) Lateral Root Inducible System in Arabidopsis and Maize. J. Vis. Exp. (107), e53481
- **Roberts I**, Smith S, De Rybel B, Van Den Broeke J, Smet W, De Cokere S, Mispelaere M, De Smet I, Beeckman T. (2013) The CEP family in land plants: evolutionary analyses, expression studies, and role in Arabidopsis shoot development. J Exp Bot. 2013 Dec;64(17):5371-81
- Jansen L, Hollunder J**, Roberts I**, Forestan C, Fonteyne P, Van Quickenborne C, Zhen RG, McKersie B, Parizot B, Beeckman T. (2013) Comparative transcriptomics as a tool for the identification of root branching genes in maize. Plant Biotechnol J. 2013 Dec;11(9):1092-102
- Lavenus J, Goh T, **Roberts I**, Guyomarc'h S, Lucas M, De Smet I, Fukaki H, Beeckman T, Bennett M, Laplaze L. (2013) Lateral root development in Arabidopsis: fifty shades of auxin. Trends Plant Sci. 2013 Aug;18(8):450-8
- Parizot B, **Roberts I**, Raes J, Beeckman T, De Smet I. (2012) In silico analyses of pericycle cell populations reinforce their relation with associated vasculature in Arabidopsis. Philos Trans R Soc Lond B Biol Sci. 2012 Jun 5;367(1595):1479-88
- Jansen L, **Roberts I**, De Rycke R, Beeckman T. (2012) Phloem-associated auxin response maxima determine radial positioning of lateral roots in maize. Philos Trans R Soc Lond B Biol Sci. 2012 Jun 5;367(1595):1525-33

## Manuscripts in preparation:

- Smith S, **Roberts I**, Stes E, De Rybel B, Xuan W, Cho H, Larrieu A, Dai Vu L, Goodall B, van de Cotte B, Marie Guseman J, Rigal A, Harborough S R, Vanneste S, Kirschner G, Lavenus J, Vandermarliere E, Martens L, Stahl Y, Audenaert D, Friml J, Felix G, Simon R, Bennett M J, Bishopp A, Ljung K, Kepinski S, Robert S, Nemhauser J, Hwang I, Gevaert K, Beeckman T, De Smet I. The small signaling peptide CEP5 attenuates the dynamic AUX/IAA equilibrium (in preparation for submitting to Plant Cell)
- **Roberts I**, De Smet I, Beeckman T. Functional characterization of the CEP peptide family and their proposed receptors in *Arabidopsis* (in preparation)
- **Roberts I**, Dubois M, De Smet I, Beeckman T. An EMS-screen for identification of molecular components controlling root system architecture (in preparation)

## ACKNOWLEDGEMENTS

From childhood onwards, I had always been fascinated by Nature. Therefore, I decided to study 'Biochemistry and Biotechnology' at Ghent University to understand the molecular mechanisms that support Life on Earth. During my studies, the lectures from Tom Beeckman about lateral root development triggered my interest for the 'hidden half' of plants. For my master project, I ended up in his research group, the Root Development Group, under the supervision of Giel van Noorden. This project further stimulated my desire to help in unraveling the underlying molecular mechanisms of lateral root development. Therefore, I decided to do my master thesis in this group, under the supervision of Leen Jansen, to identify and characterize several key regulators of lateral root initiation in maize. Afterwards, I was so fascinated by root development that I started a PhD in this group, with a quest to identify molecular components controlling root system architecture. Now, this quest has come to an end, and resulted in the story written down in this booklet.

Finally, I would like to express my gratitude to the people at work who helped me during my PhD:

- My promoter Tom Beeckman for introducing me to 'the secrets of the underground', giving me the opportunity to do my PhD in his research group and all the help I got during my PhD.
- My co-promoter/supervisor Ive De Smet for all his guidance and substantial contribution to the work documented in this booklet.
- The jury members of my PhD defense: Frank Van Breusegem, Sofie Goormachtig, Bruno Cammue, Danny Geelen, Reidunn Aalen and Bert De Rybel for taking the time to read and evaluate my thesis, and for their helpful suggestions to further improve it.
- Dirk Inzé for creating such a formidable and enjoyable work environment in his department.
- Leen Jansen and Giel van Noorden for introducing me to research on lateral root development and their supervision during my master thesis and master project respectively.
- All the 'roots people' that I have come to know over the years, consisting of the 'adventitious roots' Maria Njo, Davy Opdenacker and Alexa de Knijf, the 'emerged growing lateral roots' Steffen Vanneste, Boris Parizot, Hans Motte, Barbara Möller and Kun Yue, the 'lateral root primordia' Gieljan De Rop, Agnieszka Deja, Ellie Himschoot, Kjell De Vriese, Hanne Crombez, Tao Fang, Fabian Beeckman, Pierre-Mathieu Pelissier, Leandro Martins Ferreira, Ana Rita Mendes Leal, and Hugues De Gernier, and the 'arrested lateral roots' Paul Overvoorde, Valya Vassileva, Wim Grunewald, Lorena Lopez Galvis, Charlotte Van Quickenborne, Philippe Fonteyne, Marleen Verstraelen, Inge Verstraeten, Gert Van Isterdael, Qian Chen, Marlies Demeulenaere and Wei Xuan for all the nice conversations and fun moments together.
- The 'peptide people': Ana Fernandez for all the nice discussions and enjoyable company during the peptide meetings. Nick Vangheluwe for all the nice discussions and fun moments together. Sarieh Ghorbani for the nice chats and enjoyable company at the poker evenings.
- The vasculature people: Bert De Rybel for initiating the work on CEP peptides, and also for the many funny (but often also informative) conversations. Wouter Smet for introducing me to some crazy parties and for all the nice moments we had during your bachelor-thesis and afterwards during your PhD in our group again. Brecht Wybouw for the many funny conversations and interesting discussions about Game of Thrones. And Eliana Mor for being a friendly new neighbor.
- The 'CSF people': Dominique Audenaert for the nice conversations, mostly about triathlon. Long Nguyen for being such a nice neighbor during the first years of my PhD, and for all the

cool evenings we had together playing pool, bowling, board games and poker. Andrzej Drozdzecki for the many crazy/funny conversations and joining the hip-hop course.
- The 'electron microscopy people': Riet De Rycke and Michiel De Bruyne for the help with the electron microscopy work on ACR4 and the informative guided tours in your labs.
- The 'undercover-roots' Wilson Ardiles-Diaz (mi amigo) and Rudy Vanderhaeghen for all the nice conversations in the lab and their mental support over the years.
- Matthias Van Durme for the many funny conversations in the corridors and for the company at several cool parties.
- Marieke Dubois for the help with the SHOREmap analysis and nice chats in the corridors.
- Brigitte van de Cotte for all the help with the CEP project and the nice chats in the corridors.
- The 'greenhouse support team', consisting of Nico Smet, Miguel Riobello and Thomas Farla, for watering my plants, and for the nice chats during my work hours in the greenhouses.
- Nancy Helderwert and Peter Bogaert for preparing the many many liters of growth medium used during my PhD.
- The 'IT support team', mostly Stefaan Vanderkerken and Tim Van De Woestyne, for their help with fixing my computer-related problems and help with the printers.
- The 'administration team', consisting of Diane Hermie, Christine Tiré, Delphine Verspeel, Nathalie Vanden Hautte, Annick Bleys and Bernard Vannasche, for all the help over the years with administrative work.
- Christa Verplancke for the nice conversations in the corridors and for making sure that I always wore my labcoat during benchwork and no gloves in the hallways.
- An Bontinck for always helping me find everything in the product rooms.
- Kristof Verleye for general support and repairing my pipetboys.
- Karel Spruyt for taking the beautiful pictures of my mutant plants.
- Agnieszka Dziegielewska together with several other people for making sure the department was always nice and clean.
- And many other people in the department for the friendly chats in the corridors.

Besides the people at work, I would also like to thank several people at home for their help:

- Dietert De Vos & Caroline Turtelboom and Philip Vandenneucker & Dorien Denayer for the much appreciated recreational time-outs during the weekends over the past years: playing games, paintball, cycling, quiz-evenings, get-together evening …
- Jean-Jacques Vandenneucker & Lutgarde Turtelboom for all the support in the last months.
- My grandmother Nicole De Smedt and Wilfried De Boeck for all the support over the years.
- My parents, Ronald Roberts and Karine Heyvaert, for giving me the opportunity to follow these studies, for always being there for me and for providing me with everything I ever needed. And my brother and sister, Owyn Roberts and Sarah Roberts, for the support and all the fun moments we spent together over the years. I could not wish for a better family and consider myself very lucky to be part of it.
- And finally, my girlfriend Ann Vandenneucker, for her constant support and all the great moments we had together, and also for helping me with measuring the root length of countless seedlings at the end of my PhD.

And now it is time to embark on a new adventure … venturing into the unknown …